NONSTOICHIOMETRY OF CHALCOCITE IN
WATER-XANTHATE SYSTEMS

by

Courtney Alan Young

Thesis submitted to the Faculty of the
Virginia Polytechnic Institute and State University
in partial fulfillment of the requirements for the degree of

MASTER OF SCIENCE

in

Mining and Minerals Engineering

APPROVED:

R. H. Yoon, Chairman   G. T. Adel

J. D. Rimstidt   J. R. Lucas

July, 1987
Blacksburg, Virginia

NONSTOICHIOMETRY OF CHALCOCITE IN WATER-XANTHATE SYSTEMS

by

Courtney Alan Young

Committee Chairman: Roe Hoan Yoon
Mining and Minerals Engineering

(ABSTRACT)

E_h-pH diagrams were constructed from mass-balanced, computer calculations for the copper-sulfur-water system involving different Cu/S ratios that pertain to chalcocite, djurleite, anilite and covellite. Calculations were completed for cases where oxidation of the sulfur proceeded to i) elemental sulfur, ii) thiosulfate, iii) sulfate and iv) destabilized sulfate. Stability regions for each copper sulfide were shown to be dependent on both the Cu/S ratio in the system and the sulfur oxidation state.

E_h-pH diagrams were also constructed for chalcocite oxidation to metastable copper sulfides, both with and without xanthate. Stability regions for copper xanthates were also shown to be dependent on the sulfur oxidation state. As oxidation proceeded from elemental sulfur to sulfate, the copper xanthate stability region extended to lower potentials, directly dependent on the sulfide ion concentration.

IGP experiments at pH 1.1 suggested that chalcocite oxidation produced metastable nonstoichiometric copper sulfides while cyclic voltammetry indicated they formed at pH 1.1, 4.6, 6.8 and 9.2. XPS implied that copper sulfides may be solid solutions of chalcocite with variable amounts of copper disulfide: $Cu_2S \cdot xCuS_2$. The presence of djurleite in the chalcocite samples was confirmed by X-ray diffraction and may be responsible for the reduction reaction which occurred just prior to the reduction of chalcocite to metallic copper.

Reinterpreting cyclic voltammograms from a previous study indicated chalcocite reacted with xanthate to form cuprous xanthate and a nonstoichiometric copper sulfide near 0 mV. Chemisorbed xanthate formed at -295 mV which correlated well with the lower flotation edge determined in this and other studies. The standard free energy of the chemisorbed xanthate was determined to be -13.08 kcal/mole.

ACKNOWLEDGEMENTS

TABLE OF CONTENTS

v

LIST OF FIGURES

ix

.

LIST OF TABLES

CHAPTER I

INTRODUCTION

1.1 <u>General</u>

The separation of valuable minerals from gangue, waste
minerals, in an ore is one major problem facing the mineral
processor. If there is some difference between the physical
or chemical properties of both mineral types, separation can
be accomplished. Numerous processes have been developed to
exploit these differences. For example, physical separation
can be achieved using either magnetic or gravity techniques.
On the other hand, leaching methods exemplify chemical
separation. However, the most commonly employed practice is
the physico-chemical process called froth flotation. In
froth flotation, air is injected into a pulp containing
hydrophobic and hydrophilic particles. Air bubbles attach
to hydrophobic particles which then float to the surface of
the pulp where a froth is developed and removed as a
concentrate. Meanwhile, hydrophilic particles remaining in
suspension are discarded as tailings at the bottom of the
pulp.

Differing from oil and film flotation, froth flotation
was comercially introduced at Broken Hill, Australia in 1904

1

(Sutherland and Wark, 1955). James M. Hyde established the first commercial operation in the United States seven years later at the Montana Basin Reduction Plant to treat 50 tons per day of zinc sulfide tailings from a gravity separator (Fuerstenau, 1962). Since then, froth flotation has grown to treat an excess of two billion tons of ore per year, 95% of which are metal-based, mostly sulfides and oxides. The remainder includes coal, clay, sulfur and other nonmetallic compounds (Kitchener, 1984).

Prior to flotation, and most other processes, the ore is crushed and ground to liberate the valuable minerals from the gangue. During this size reduction process, the ore is mixed with water and treated with various surface-active reagents such as collectors and regulators. Collectors are organic compounds which adhere to the mineral surface to render it hydrophobic. Regulators, any chemical which makes collectors more selective, activate collector adsorption on valuable minerals and/or depress it on gangue. However, some minerals such as molybdenite, graphite and talc exhibit natural hydrophobicity and thus may not require the presence of a collector. In either case, the valuable minerals will be floated and the gangue will not.

Except molybdenite, all sulfide minerals, including pyrite, chalcopyrite, chalcocite, covellite, sphalerite and galena, require collectors to induce hydrophobicity. This,

of course, is disregarding the collectorless flotation which can be performed on several of the sulfides as reviewed by Luttrell (1982). For sulfides, the most widely used collectors are xanthates, which were first used by Keller (1925). Since then, various investigations have shown, often with conflicting results, what xanthate species form at the mineral surface and which regulators control their formation. Regulators include cyanide, sulfide, and most commonly, hydrogen (pH) ions, to name only a few. However, current emphasis is placed on regulators which control the redox potential (E_h) as patented by Cutting et al. (1975). Not only does the redox potential control the formation of xanthate species, it also affects the stabilty of the minerals themselves. In the case of copper sulfides numerous investigations have proven the existence of nonstoichiometric solids, especially during the oxidation of chalcocite, Cu_2S.

Since thermodynamics can predict under what E_h-pH conditions solids will be stable, thermodynamic calculations for the copper-sulfur-water system are carried out in the presence and absence of potassium ethyl xanthate. Nonstoichiometric copper sulfides and metastable sulfur species are considered. The results of the calculations are then compared to experimental data.

1.2 Literature Review

Because ethyl xanthate can react to form derivatives which destroy its hydrophobic nature, copper sulfides exhibit nonstoichiometry, and thermodynamic calculations can predict flotation behavior, the following literature review is divided into three sections: ethyl xanthate derivatives, copper sulfide nonstoichiometry, and computer calculations.

1.2.1 Ethyl Xanthate Derivatives

Ever since Keller (1925) used xanthates for flotation, several theories have arisen to explain the adsorption mechanism of xanthates on sulfides. These theories include 'ion adsorption' (Gaudin, 1927), 'chemical metathesis' (Taggart et al., 1930), 'neutral molecule adsorption' (Cook and Nixon, 1950), and 'mixed potential' (Salamy and Nixon, 1953). The ion adsorption theory states that xanthate ions are simply adsorbed by the mineral surface without reacting. On the other hand, chemical metathesis uses chemical reactions to explain the displacement of other anions with xanthate ions. The neutral molecule theory suggests that uncharged xanthate species must adsorb on the mineral surface to prevent a charge buildup. In the mixed potential theory, various electrochemical reactions, both anodic and cathodic, occur simultaneously on the mineral which possibly partakes in the reactions but, nevertheless, acts as a

source and sink for the transfer of electrons in the reactions. A definition of the mixed potential follows.

When an electrochemical reaction involving only one redox couple (i.e., a half-cell reaction) is at equilibrium, no current exists and the redox potential is at the Nernst potential of the redox couple. However, if the redox potential is not at the Nernst potential, current will flow as illustrated by the voltammogram in Figure 1.1. Including another half-cell reaction in the voltammogram yields a second plot similar to the first but at its own Nernst potential. Since current is additive, a single voltammogram results when the two plots are summed. If the equations of the reactions themselves are also added, a whole-cell reaction is obtained. When there is zero current, the whole-cell reaction will be at the mixed potential which lies somewhere between the Nernst potentials of the two redox couples (see Figure 1.2). However, because the two half-cell reactions occur at separate locations on the electrode, the resulting whole-cell reaction is not at thermodynamic equilibrium. Nevertheless, the redox potential will automatically adjust itself to the mixed potential, a potential where anodic and cathodic currents are equal, and the whole-cell reaction will automatically proceed to the right.

Because numerous investigators have produced direct
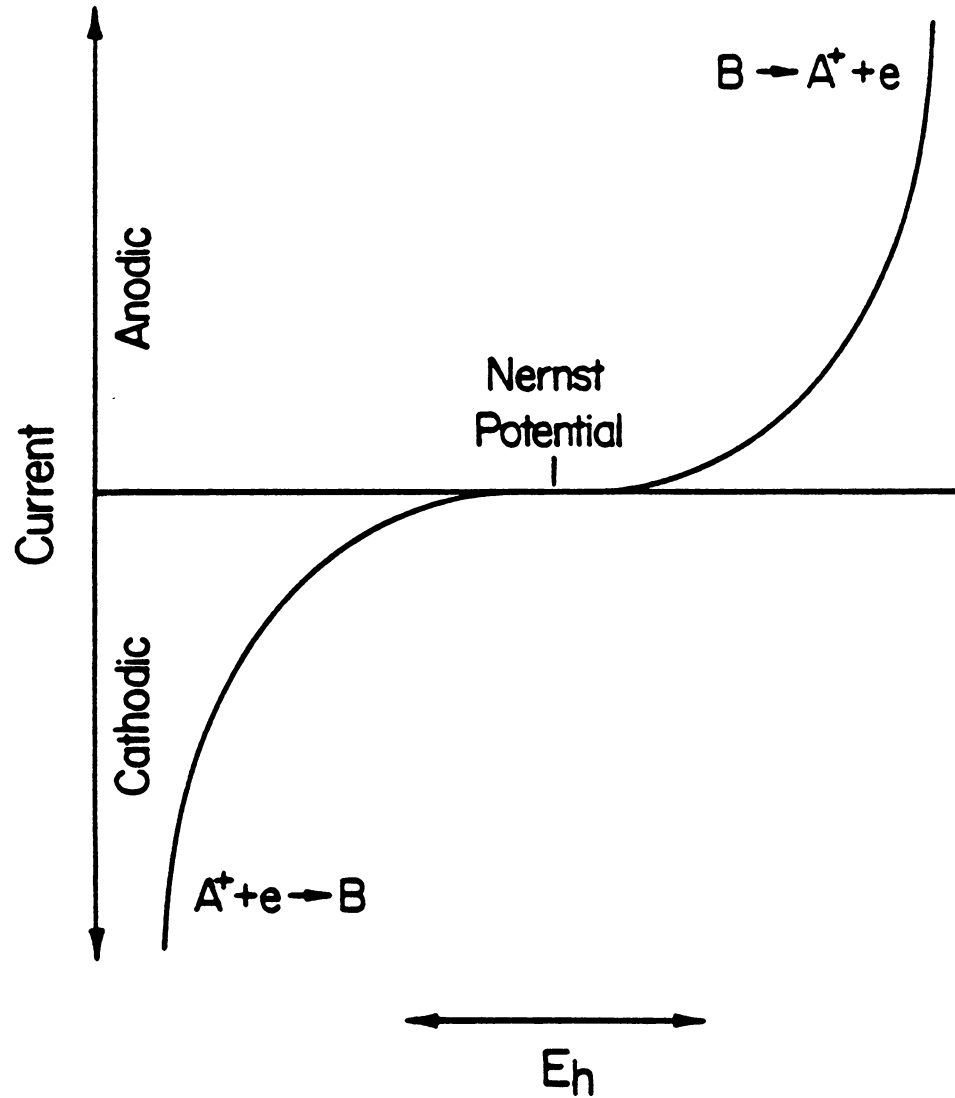
Figure 1.1 Voltammogram of a redox couple showing the effects of current and potential.
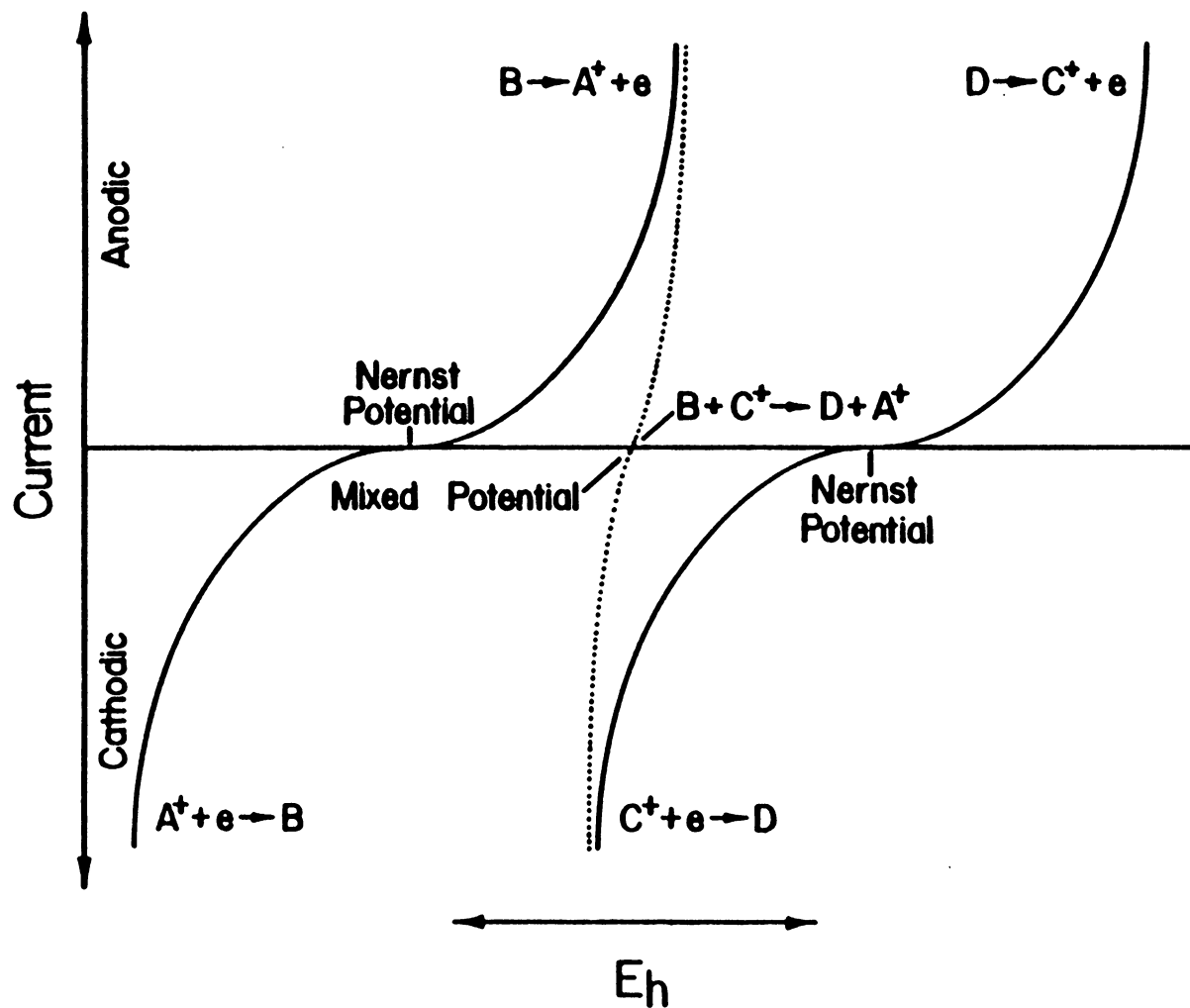
Figure 1.2   Voltammogram of a pair of redox couples establishing a mixed potential at zero current.

evidence in favor of the mixed potential theory, the mixed potential theory best explains xanthate adsorption on sulfides. Using steady-state polarization on galena, lead and platinum electrodes immersed in oxygenated and deoxygenated xanthate solutions, Tolun and Kitchener (1964) concluded that the cathodic reduction of oxygen occurred simultaneously with the anodic oxidation of xanthate which formed lead xanthate and dixanthogen. Toperi and Tolun (1969) came to the same conclusion by showing that the rest potentials of a galena electrode at various pH values of oxygenated xanthate solutions fell within the stability region of lead xanthate and dixanthogen on E_h-pH diagrams. On the other hand, Pomianowski and Czarnecki (1974) observed the anodic oxidation on galena to yield chemisorbed xanthate, not dixanthogen, which subsequently reacted to form lead xanthate. The above investigators, among others (e.g., Plaksin and Bessonov, 1957; Plaksin, 1959; Poling and Leja, 1963; Gaudin and Finkelstein, 1965; Finkelstein, 1970; and Ahmed, 1978), have unanimously agreed that the cathodic reaction in the mixed potential is the reduction of oxygen:

$$1/2O_2 + H_2O + 2e = 2OH^-. \qquad [1.1]$$

However, differences of opinion exist over the anodic oxidation of xanthate, which obviously must occur in order to render the surface hydrophobic. As previously mentioned,

the xanthate ion, X^-, can form chemisorbed xanthate,

$$X^- = X_{ads} + e;$$ [1.2]

dixanthogen according to the following reaction,

$$2X^- = X_2 + 2e;$$ [1.3]
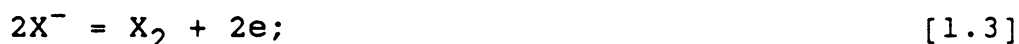
and metal xanthate in the oxidation of the mineral,

$$MS + 2X^- + 4H_2O = MX_2 + SO_4^{2-} + 8H^+ + 8e.$$ [1.4]
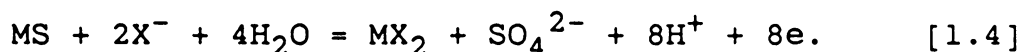
Because sulfide oxidation can be slow, reaction [1.4] may proceed only as far as the formation of thiosulfate or of elemental sulfur. This is shown by the following reactions:

$$2MS + 4X^- + 3H_2O = 2MX_2 + S_2O_3^{2-} + 6H^+ + 8e$$ [1.5]

$$MS + 2X^- = MX_2 + S^O + 2e$$ [1.6]
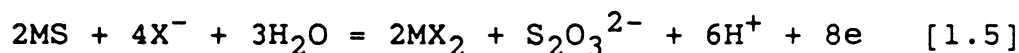
both of which are known to occur (Rolia, 1977; Gardner and Woods, 1979). In defining the mixed potential, Woods (1984) discussed these xanthate oxidation reactions in detail.

Although the following investigations do not provide proof for the mixed potential theory, they do provide evidence that the xanthate oxidation reactions do occur. Cyclic voltammetry on chalcocite electrodes (Kowal and Pomianowski, 1973; Basilio, 1985) and packed-beds of chalcocite particles (Walker et al., 1984; Richardson et al., 1984; O'Dell et al., 1984) in the presence of xanthate

resulted in the formation of three peaks, of which the first two were attributed to chemisorbed xanthate and the third to cuprous xanthate formation. Similarly, Pritzker (1984) showed that chemisorbed xanthate also formed at reducing potentials on galena electrodes. Like cuprous xanthate, lead xanthate formed under oxidizing conditions. Studying the oxidation of xanthate on platinum, gold, copper and galena electrodes, Woods (1971) showed that xanthate ions yielded multilayers of dixanthogen at the electrode surface; however, he proposed that chemisorbed xanthate formed before dixanthogen.

The first metal xanthate to be identified at the mineral surface was cuprous xanthate (Gaudin, 1934) which could not be leached by common solvents (eg. benzene and ether) while other xanthate compounds could. Since then, other techniques, besides voltammetry, have been employed to identify and/or quantify the existence of metal xanthates which, for the purpose of this review, will be restricted to copper xanthates. With potentiometric titration, Kakovskii (1957) and DuRietz (1976) determined the solubility products of cuprous and cupric xanthate respectively. Leja et al. (1963) used infra-red (IR) spectroscopy and showed cuprous xanthate formed on copper in the presence of either xanthate ions or dixanthogen. Contact angle measurements revealed that dixanthogen imparted a more hydrophobic surface,

suggesting that dixanthogen and cuprous xanthate co-existed. On the other hand, Sparrow et al. (1977) used ultraviolet (UV) spectroscopy on aqueous solutions of cupric perchlorate and xanthate, which reacted to form cupric xanthate before immediately breaking down to produce both cuprous xanthate and dixanthogen. Using X-ray photoelectron spectroscopy (XPS), Mielczarski and Suoninen (1984) concluded that the adsorption mechanism of xanthate consisted of a rapid growth of a well-oriented monolayer of xanthate, probably chemisorbed xanthate, followed by a slow accumulation of disordered cuprous xanthate.

Xanthate ions migrate to the mineral surface where they are known to react and form chemisorbed xanthate, dixanthogen, and copper xanthate. Before these products are formed, however, the xanthate ions may yield other xanthate species, either in the bulk of the solution or at or near the mineral surface. In some cases, the three products themselves undergo further reactions and produce other xanthate-derived species. These xanthate derivatives are described below.

Under acidic conditions, the xanthate ion (ROCSS$^-$ or X$^-$) forms xanthic acid (ROCSSH or HX) which decomposes to carbon disulfide (CS$_2$) and alcohol (ROH), where 'R' could represent hydrocarbon chains of any length. Overall, this decomposition takes minutes at pH 2, hours at pH 6, and is

negligible at pH 7 (Iwasaki and Cooke, 1958; Majima, 1961; Tornell, 1966; Hopstock, 1968). Under basic conditions, Tipman and Leja (1975) have demonstrated that dixanthogen also breaks down to form carbon disulfide and alcohol in addition to xanthate ions. This is in direct conflict with Phillip and Fichte (1960) who indicated that, at high pH values, monothiocarbonate (ROCOS$^-$) formed along with hydrogen sulfide ions (HS$^-$). The monothiocarbonate further decomposed to alcohol, hydrogen sulfide ions, and carbonate ($CO_3{}^{2-}$). Harris and Finkelstein (1975) revealed that, at the mineral surface, reactions of metal xanthate and dissolved oxygen yielded monothiocarbonate and elemental sulfur. They also indicated that reactions similar to those proposed by Phillip and Fichte occurred.

Xanthate ions have also been shown to react with hydrogen peroxide (H_2O_2), an intermediate species in oxygen reduction, to produce perxanthate (ROCSSO$^-$) and water (Jones and Woodcock, 1978; Richardson et al., 1984). Jones and Woodcock (1978) also disclosed the presence of perxanthic acid (ROCSSOH) which is stable between pH 2 and 11. Furthermore, Sparrow et al. (1977) concluded that aqueous copper xanthates were present as well. Cupric xanthate cations (CuX$^+$) were shown to react with xanthate ions to form cupric xanthate which immediately decomposed to cuprous xanthate and dixanthogen, as stated earlier. Also, excess

suggesting that dixanthogen and cuprous xanthate co-existed. On the other hand, Sparrow et al. (1977) used ultraviolet (UV) spectroscopy on aqueous solutions of cupric perchlorate and xanthate, which reacted to form cupric xanthate before immediately breaking down to produce both cuprous xanthate and dixanthogen. Using X-ray photoelectron spectroscopy (XPS), Mielczarski and Suoninen (1984) concluded that the adsorption mechanism of xanthate consisted of a rapid growth of a well-oriented monolayer of xanthate, probably chemisorbed xanthate, followed by a slow accumulation of disordered cuprous xanthate.

Xanthate ions migrate to the mineral surface where they are known to react and form chemisorbed xanthate, dixanthogen, and copper xanthate. Before these products are formed, however, the xanthate ions may yield other xanthate species, either in the bulk of the solution or at or near the mineral surface. In some cases, the three products themselves undergo further reactions and produce other xanthate-derived species. These xanthate derivatives are described below.

Under acidic conditions, the xanthate ion (ROCSS$^-$ or X$^-$) forms xanthic acid (ROCSSH or HX) which decomposes to carbon disulfide (CS$_2$) and alcohol (ROH), where 'R' could represent hydrocarbon chains of any length. Overall, this decomposition takes minutes at pH 2, hours at pH 6, and is

negligible at pH 7 (Iwasaki and Cooke, 1958; Majima, 1961; Tornell, 1966; Hopstock, 1968). Under basic conditions, Tipman and Leja (1975) have demonstrated that dixanthogen also breaks down to form carbon disulfide and alcohol in addition to xanthate ions. This is in direct conflict with Phillip and Fichte (1960) who indicated that, at high pH values, monothiocarbonate (ROCOS$^-$) formed along with hydrogen sulfide ions (HS$^-$). The monothiocarbonate further decomposed to alcohol, hydrogen sulfide ions, and carbonate (CO_3^{2-}). Harris and Finkelstein (1975) revealed that, at the mineral surface, reactions of metal xanthate and dissolved oxygen yielded monothiocarbonate and elemental sulfur. They also indicated that reactions similar to those proposed by Phillip and Fichte occurred.

Xanthate ions have also been shown to react with hydrogen peroxide (H_2O_2), an intermediate species in oxygen reduction, to produce perxanthate (ROCSSO$^-$) and water (Jones and Woodcock, 1978; Richardson et al., 1984). Jones and Woodcock (1978) also disclosed the presence of perxanthic acid (ROCSSOH) which is stable between pH 2 and 11. Furthermore, Sparrow et al. (1977) concluded that aqueous copper xanthates were present as well. Cupric xanthate cations (CuX$^+$) were shown to react with xanthate ions to form cupric xanthate which immediately decomposed to cuprous xanthate and dixanthogen, as stated earlier. Also, excess

xanthate ions were suggested to form cuprous xanthate anions (CuX_2^-) from reactions with cuprous xanthate. Leja (1982) and Jones and Woodcock (1984) have also mentioned metal monothiocarbonate and xanthyl thiosulfate ($ROCSS \cdot S_2O_3^-$) as products of xanthate reactions. Because xanthate derivatives can form and thereby destroy the hydrophobic nature of xanthates, their presence could be detrimental to flotation.

1.2.2 Copper Sulfide Nonstoichiometry

Early investigations in the copper-sulfur system suggested there were only two solid phases, covellite (CuS) and chalcocite (Cu_2S), even though chalcocite was known to dissolve enough elemental sulfur to yield a composition of $Cu_{1.80}S$ (Roseboom, 1966). After demonstrating that $Cu_{1.80}S$ was a distinct phase with single-crystal X-ray diffraction, Buerger (1942) named the phase digenite. Since then, five more nonstoichiometric copper-sulfide minerals have been identified: djurleite, $Cu_{1.96}S$; anilite, $Cu_{1.75}S$; geerite, $Cu_{1.60}S$; spionkopite, $Cu_{1.40}S$; and yarrowite, $Cu_{1.12}S$. Because of their similar color to covellite, spionkopite and yarrowite are often referred to as blue-remaining, or 'blaubliebender' covellites. Based on the orientation of the sulfur atoms in the crystal structure of each mineral, these copper sulfides have been divided into three groups

(Goble, 1981). Group 1 minerals (digenite, anilite, and geerite) have approximate cubic close-packed sulfur atoms. Group 2 minerals (spionkopite, yarrowite, and covellite) contain alternating layers of hexagonally close-packed and covalently bonded sulfur atoms. On the other hand, Group 3 minerals (chalcocite and djurleite) are solely comprised of hexagonally close-packed sulfur atoms.

Independently, Roseboom (1962) and Morimoto (1962) established the existence of $Cu_{1.96}S$ using X-ray powder diffraction. They named the mineral djurleite after Djurle (1958) who was the first to recognize that another phase existed between chalcocite and covellite. Continuing the study on djurleite with mineral crystals from the Ani Mine in Japan, Sadanaga et al. (1963) determined the presence of another mineral but could not identify it. Several other investigations (Takeda and Donnay, 1964; Roseboom, 1966; Takeda et al., 1967) also failed to identify the new mineral. Employing electron-probe analysis and microscopy methods, Morimoto et al. (1969) discovered the mineral to be $Cu_{1.75}S$ and termed it anilite after the mine from which it came. During leaching experiments of anilite, Goble (1981) duplicated the crystal structure of a mineral that was initially identified as a copper-deficient anilite although X-ray diffraction patterns said otherwise (Goble and Robinson, 1980). Re-examination of the mineral

then led to its identification as $Cu_{1.60}S$. The mineral was named geerite, in honor of Adam Geer, who collected the first samples.

Natural blue-remaining covellites have been reported as early as 1943 (Ramdohr, 1943) but were attributed to covellite having excess copper. Since natural samples were too small to isolate, only synthetic samples have been studied (Frenzel, 1959; Frenzel, 1961; Moh, 1971; Rickard, 1972; Potter, 1977). It was concluded that only two blue-remaining covellites existed, each in a solid solution series, although no agreement could be reached on their exact compositions. However, using X-ray powder diffraction studies on natural minerals which he managed to isolate, Goble (1980) discovered they were not solid solution series. He determined the stoichiometries to be $Cu_{1.40}S$ and $Cu_{1.12}S$, which were respectively named spionkopite and yarrowite for their places of origin, Spionkop and Yarrow Creeks, Alberta. These values were in complete agreement with Potter (1977), who synthesized samples of blue-remaining covellites as well as the other minerals (except geerite, which was not known to be a mineral at the time) using an electrochemical technique. By controlling the temperature in the cells, Potter also determined standard free energy values for the minerals. Upon evaluation of the thermodynamic data, he demonstrated that digenite and the blue-remaining covellites

were metastable. Later, after conducting leaching tests on anilite, Goble (1981) determined geerite to be metastable as well (see Table 1.1).

Numerous attempts have also been made to verify the existence of nonstoichiometric copper sulfides with the anodic oxidation of chalcocite. Etienne and Peters (1972) used two slightly polarized electrodes and allowed them to relax. Resulting equilibrium potentials were measured and standard free energies of formation were calculated for djurleite, digenite and covellite. Using electrodes constructed of thin films of evaporated chalcocite on glass, Mathieu and Rickert (1972) found that the anodic dissolution of chalcocite in acidic solutions proceeded through three phases before covellite formed: djurleite, a new $Cu_{1.90}S$ phase, and digenite. Because the electrode potential remained constant during the transformation of one phase to another, thermodynamic data was calculated for the four oxidation products. Potter (1977) has since proved that the $Cu_{1.90}S$ phase is not a species at all. However, during acidic ferric sulfate leach tests, Marcantonio (1976) identified the sequence of solid phases to be digenite and a blue-remaining covellite with a $Cu_{1.10}S$ composition. Covellite was never observed to be a reaction product, which is in full agreement with Thomas et al. (1967) who also used acidic ferric sulfate to leach copper from chalcocite.

Table 1.1

Standard Free Energies of Formation (ΔG_f^O) of Copper
Sulfide Minerals as a Function of Temperature (K)

Mineral	ΔG_f^O (kcal·mol^{-1})	T (K)
Chalcocite (Cu_2S)	$-19,226 - 4.112T$	$273.15 - 376.65$
Djurleite ($Cu_{1.96}S$)	$-19,178 - 3.530T$	$273.15 - 363.15$
*Digenite ($Cu_{1.80}S$)	$-18,366 - 1.170T$	$273.15 - 348.15$
Anilite ($Cu_{1.75}S$)	$-18,169 - 2.020T$	$273.15 - 348.15$
*Geerite ($Cu_{1.60}S$)	NA	NA
*Yarrowite ($Cu_{1.40}S$)	$-14,675 - 2.360T$	$273.15 - 423.15$
*Spionkopite ($Cu_{1.12}S$)	$-13,463 - 0.450T$	$273.15 - 423.15$
Covellite (CuS)	$-12,726 - 0.540T$	$273.15 - 388.36$

* metastable

In the most detailed study, Koch and McIntyre (1976) characterized four solid solution phases as thin films of chalcocite anodically oxidized to covellite: $Cu_{1.95-1.91}S$, $Cu_{1.86-1.80}S$, $Cu_{1.68-1.65}S$, and $Cu_{1.40-1.36}S$. They determined the compositions and free energies of the phases from rest potential measurements plotted against the percent of copper removed (see Figure 1.3). Potentials were measured when applied current was stopped but were recorded as rest potentials after equilibrium was attained, usually within minutes. The percentages of extracted copper were determined from both the initial weight of the thin film and the amount of current passed assuming that the only reaction that occurred was the production of the nonstoichiometric copper sulfides and cupric ions at 100% current efficiency. Koch and McIntyre also obtained direct correlation with infra-red absorbance spectra and X-ray diffraction patterns: infra-red spectra at the solid surface exhibited maxima shifting to shorter wavelengths as copper-deficient sulfides were produced, and X-ray patterns of the $Cu_{1.86-1.80}S$ phase corresponded to a natural mineral, $Cu_{1.83}S$ (Clark, 1972). Recently Nowak et al. (1984) revealed that significant errors may result if thermodynamic properties of nonstoichiometric copper sulfides are determined from rest potential measurements on copper electrodes in the presence of cupric ions. However, Koch and McIntyre used the
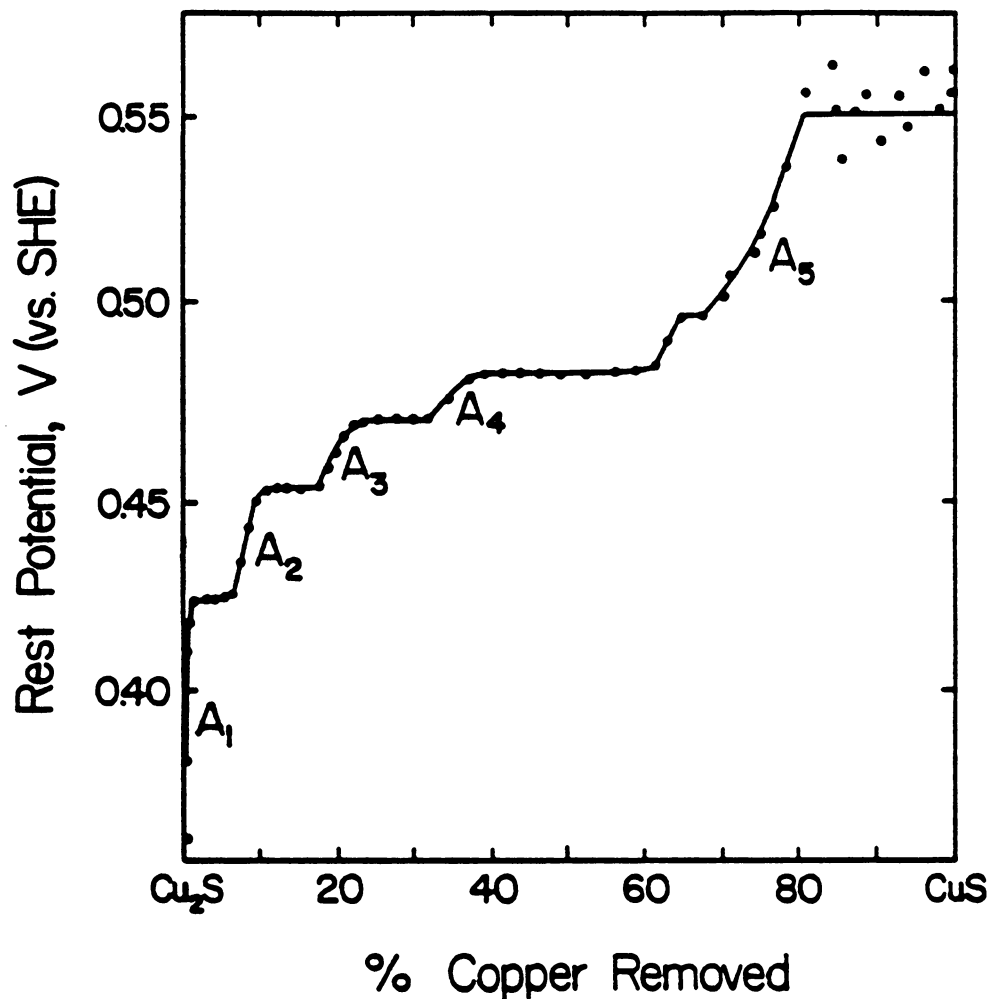
Figure 1.3 Rest potentials observed during the anodic oxidation of Cu_2S to CuS in acid solution. Vertical steps correspond to $Cu_{1.95-1.91}S$, $Cu_{1.86-1.80}S$, $Cu_{1.68-1.65}S$, $Cu_{1.40-1.36}S$. Horizontal steps correspond to their coexistence (from Koch and McIntyre, 1976).

platinum electrode.

Cyclic voltammograms of chalcocite on carbon paste electrodes (Brage et al., 1979; Gerlach and Kuzeci, 1983) have also revealed the existence of nonstoichiometric oxidation products. Brage et al. produced a voltammogram under very acidic conditions and at an extremely slow scan rate. (See Figure 1.4a.) Upon integrating the area under each peak, the six anodic peaks, A_{1-6}, were attributed to the formation of Cu_2S, $Cu_{1.92}S$, $Cu_{1.77}S$, $Cu_{1.60}S$, $Cu_{1.31}S$, and CuS, respectively. Thermodynamic values were then determined from the potentials at which the peaks occurred. Using u-shaped electrodes, so that precipitates would build up on the surface of the electrode rather than fall off, Gerlach and Kuzeci demonstrated the same effect but at a scan rate 1000 times faster (see Figure 1.4b). Taking into account the differences of the reference electrodes (i.e., the saturated calomel electrode used by Brage et al. is 0.241 V vs. SHE and the saturated K_2SO_4/Hg_2SO_4,Hg electrode used by Gerlach and Kuzeci is 0.65 V vs. SHE), the potentials at which the peaks occurred were similar. These potentials also correspond to the data produced by Koch and McIntyre.

The thermodynamic data reported by Etienne and Peters, Mathieu and Rickert, Koch and McIntyre, and Brage et al. are presented in Table 1.2. Because the free energies of the
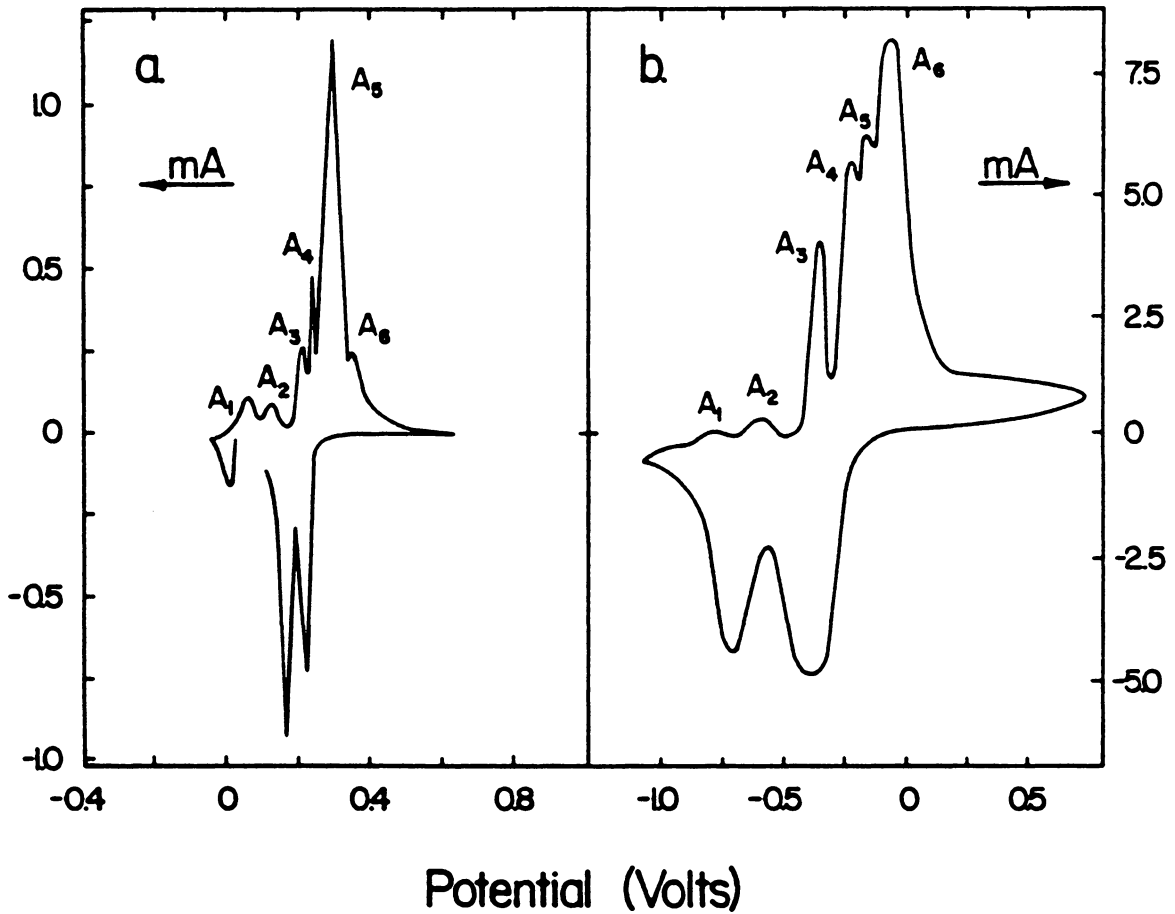
Figure 1.4   Voltammograms of chalcocite on carbon paste
electrodes in acid solutions vs. a) SCE at 0.1
mV/sec (from Brage et al., 1979), and b)
saturated K_2SO_4/Hg_2SO_4,Hg at 100 mV/sec (from
Gerlach and Kuzeci, 1983).

Table 1.2

A Comparison of the Standard Free Energies of Formation
(ΔG_f^o) for Metastable Nonstoichiometric Copper Sulfides
Formed by the Oxidation of Chalcocite (kcal/mole)

$Cu_{2-x}S$ Product	Etienne & Peters	Mathieu & Rickert	Koch & McIntyre	Brage, Lamache & Bauer
$Cu_{1.965}S$	-0.73			
$Cu_{1.96}S$		0.21		
$Cu_{1.95}S$ to $Cu_{1.91}S$			0.45	
$Cu_{1.92}S$				0.32
$Cu_{1.90}S$		0.62		
$Cu_{1.86}S$ to $Cu_{1.80}S$			1.24	
$Cu_{1.77}S$				1.38
$Cu_{1.765}S$	0.83			
$Cu_{1.79}S$ to $Cu_{1.765}S$		1.21		
$Cu_{1.68}S$ to $Cu_{1.65}S$			2.64	
$Cu_{1.60}S$				2.86
$Cu_{1.40}S$ to $Cu_{1.36}S$			5.15	
$Cu_{1.31}S$				6.65
CuS	7.40	7.40	10.10	

oxidation products are greater than that of the stable
minerals reported by Potter (1977), they are considered to
be metastable.

Although most investigations in the copper-sulfur
system have involved chalcocite, other minerals have also
been studied. Thomas et al. (1967) showed that the anodic
dissolution of digenite with acidic ferric sulfate solutions
produced a blue-remaining covellite of $Cu_{1.10}S$, the same as
was observed for chalcocite oxidation. On the other hand,
Whiteside and Goble (1986) observed that digenite formed
only anilite under weak ferric sulfate conditions, but under
stronger conditions the oxidation proceeded through phases
of geerite, yarrowite, spionkopite, and covellite as well.
As discussed earlier, Goble (1981) formed a compound with
the composition of yarrowite and the crystal structure of
geerite during the leaching of anilite. Investigating
geochemical processes involved in weathering of enriched
zones of copper ores, Walsh and Rimstidt (1986) discovered
that the reaction rate for leaching blue-remaining covellite
with ferric ions at pH 2.0 was faster than that for normal
covellite, probably because blue-remaining covellite does
not leach to form covellite (Thomas et al., 1967;
Marcantonio, 1976). This is contradictory to recent
evidence (Whiteside and Goble, 1986) as previously
discussed. Hillrichs and Bertram employed voltammetry to

study the anodic oxidation of several nonstoichiometric

compounds (1983a) as well as covellite (1983b). They

concluded that cupric ions influenced the oxidation and

reduction reactions (recall Nowak et al., 1984), that copper

oxide formation passivated the surface, and that, most

importantly, the composition of the species determined peak

potentials. Even copper-iron-sulfides such as chalcopyrite

(Warren, 1978; Sohn and Wadsworth, 1984) and bornite

(Buckley et al., 1984) oxidize to nonstoichiometric copper

sulfides.

1.2.3 Computer Calculations

Controlling the pH of a mineral slurry has long been

used to activate or depress flotation processes and, as

discussed earlier, the redox potential, E_h, has been shown

to be equally important. Therefore, electrochemical phase

(E_h-pH) diagrams have proven to be a convenient and valuable

tool for presenting thermodynamic information with respect

to mineral processing. Expressing free energy data in this

manner was conceived by Pourbaix (1963). Garrels and Christ

(1965) first applied the method to minerals of geological

interest and geochemical concern. Chander and Fuerstenau

(1975) calculated E_h-pH diagrams to explain the results of

contact angle measurements in both copper- and chalcocite-

dithiophosphate systems. Electochemical phase diagrams

were constructed by Hepel and Pomianowski (1977) for the copper-ethyl xanthate system. However, each of the above authors calculated E_h-pH diagrams in the usual manner: they only considered stable species and assumed soluble species to have constant concentrations. Therefore, mass balance and kinetic effects were ignored. Peters (1984 and 1986), however, at least recognized the effect that kinetics may have on the system: he produced E_h-pH diagrams for sulfur oxidation to thiosulfate and also suggested that sulfate should be destabilized by 75 kcal/mol to account for the hydrometallurgical observation that, at pH = 0, sulfur is not oxidized by Fe^{3+} whereas it is slowly by HNO_3 and rapidly by either OCl^- or Cl_2.

Although E_h-pH diagrams are a convenient and valuable tool, their application to mineral processing systems is limited unless metastable species are considered and mass-balances are maintained. Pritzker and Yoon (1984a), Pritzker et al. (1984), and Basilio et al. (1985) showed mass balanced calculations as sulfur oxidation was allowed to proceed all the way to sulfate for galena-, pyrite-, and chalcocite-ethyl xanthate systems, respectively. Addressing the kinetics of irreversible sulfate formation, Pritzker and Yoon (1984b) further pursued mass-balanced calculations for the galena-ethyl xanthate system by allowing the sulfur to oxidize only as far as either of two metastable species:

elemental sulfur and thiosulfate. In each calculation, the authors solved the mass-balanced equations using the secant method and discovered that the metal sulfide co-existed with the metal. Basilio et al., for example, showed metallic copper was stable at the same time that chalcocite was. Because the authors developed individual programs to perform the mass-balanced calculations, the programs were not flexible to calculate E_h-pH diagrams for any other system. Several flexible programs, however, have been developed to construct E_h-pH diagrams (Brook, 1970; Froning et al., 1976; Williams and Patrick, 1977; Verhulst and Duby, 1977; Bethke, 1978; and Linkson et al., 1979). Although these programs do not maintain a mass balance, they can be used to study the kinetics of a system since a variety of oxidation states can be considered.

Based on the criterion that the total free energy of a system is at a minimum when the system is at equilibrium, a number of mathematical models were developed to first minimize the free energy and then determine equilibrium values. Several of the models were discussed by White et al. (1958), Crerar (1975), Gautam and Seider (1979); and Smith (1980). The free energy equations varied for each model because the derivations of each were based on different assumptions. For example, White et al. derived a model assuming constant pressure rather than, say, constant

volume. All of the models seemed to contain mass balance
considerations, with the exception of Crerar's, which
contained a charge balance.

As the systems being studied became more complex (i.e.,
the number of species under consideration increased ten-
fold), the models were incorporated into computer programs
to ease the tediousness of hand calculations. These
computer programs include HALTAFALL (Ingri et al., 1967),
SOLGAS (Eriksson, 1971); WHITE (Karpov and Kaz'min, 1972);
EQUIL (Ting Po I and Nancollas, 1972); SALT (Wolery and
Walters, 1975); and SOLGASWATER (Eriksson, 1979). Like the
models from which they were developed, the programs can only
consider specific systems. For example, SOLGAS calculates
high temperature equilibria of solids and gases based on the
assumptions that the gases are ideal and are at a constant
total pressure. On the other hand, EQUIL only calculates
equilibria of aqueous species, since solids and gases are
disregarded. SOLGASWATER calculates equilibria of
all types of species, assuming that the gases behave ideally
in a system at standard temperature and pressure.

Although numerous investigators have used SOLGASWATER,
only the most recent are cited. Sjoberg and Ohman (1985)
determined thermodynamic data for the alumina-oxalate system
and used SOLGASWATER to explain the increased weathering of
silicate minerals. After finishing equilibria calculations,

Pettersson et al. (1985a) showed that SOLGASWATER adequately predicted concentrations for the aqueous molybdophosphate system. Bilinski et al. (1985) applied SOLGASWATER to show why thorium preferentially complexes with maleate over hydroxyl groups. Similarly, Lajunen and Sjoberg (1985) explained why cupric ion complexes mononuclearly with the hydroxymethylimidazole at high concentrations but hydroxocomplexes at low concentrations. Investigating the vanadium system under acidic conditions, Pettersson et al. (1985b) found, contrary to previous studies, insignificant vanadic acid concentrations, and confirmed this through the use of SOLGASWATER. Interested in organosilicon processes in living organisms, Sjoberg et al. (1985) used SOLGASWATER to construct distribution diagrams of the silicon-tropolone system. And finally, Slanina et al. (1986) verified with SOLGASWATER that aluminum concentrations are increased in the blood stream when aluminum-citrate complexes form.

By using SOLGASWATER to calculate equilibria in various systems, those and other investigators have successfully demonstrated the reliability and, thereby, the flexibility of SOLGASWATER. However, their calculations did not involve the redox potential because SOLGASWATER was unable to do so. Not until Forssberg et al. (1984) showed the electron concentration to be logarithmically related to the redox potential could the redox potential be calculated. The

electron was considered to be a distinct and separate species in the system (see Appendix I). They applied this scheme to the chalcopyrite-ethyl xanthate system. Palsson and Forssberg (1986) also applied the technique to the galena-ethyl xanthate system. In both cases, the authors simulated actual flotation conditions by including carbonates and by allowing metastable species to form in the systems.

Many investigators have shown SOLGASWATER to be flexible and reliable in computing mass-balanced equilibria in any system, both with and without the inclusion of the redox potential. SOLGASWATER was therefore employed in this investigation.

1.3 Objective

The purpose of this investigation is to further the understanding of copper sulfide systems with specific emphasis placed on nonstoichiometry, especially during the xanthate flotation of chalcocite. Both thermodynamics and kinetics will be examined.

Mass-balanced, thermodynamic calculations determined by the SOLGASWATER program will mostly be presented in the form of E_h-pH diagrams to depict stability regions for aqueous and solid species. Since the calculations are mass-balanced, the concentrations of all aqueous species and

amounts of all solid species will be known. This makes it possible to determine equilibrium reactions among all species and closely examine the co-existence of solid ones. The effect of changing the copper/sulfur ratio in the system to stoichiometries corresponding to chalcocite, djurleite, anilite and covellite will be explored. Furthermore, by allowing the sulfur to oxidize to different oxidation states including elemental sulfur, thiosulfate, destabilized sulfate, and sulfate, the kinetic effect of irreversible sulfate formation will be examined. Never before have nonstoichiometry and destabilized sulfate been considered in thermodynamic calculations of this kind.

Similar calculations will also be performed on chalcocite oxidation to metastable sulfides both with and without xanthate. This too is the first time such calculations have been performed on chalcocite. Particular attention will be paid to the stability regions of copper xanthates: how they are affected by the sulfur oxidation state and how they affect the stability regions of other species. Since the amounts of copper xanthates will be known, the effect of E_h, pH, and sulfur oxidation state can be predicted and compared to flotation results. Data obtained from intermittent galvanostatic polarization, X-ray photoelectron spectroscopy, and cyclic voltammetry will also be used to confirm or contradict the calculations.

CHAPTER II

COMPUTER CALCULATIONS

2.1 Outline of SOLGASWATER

Since the computer program SOLGASWATER is used in this study, the following outline of the computer program is offered. First of all, the program is introduced in a general description which is followed by a short but detailed explanation of the calculation procedure. Lastly, definitions for the input variables to the program are given.

2.1.1 General Desription

SOLGASWATER was developed by Eriksson (1979) at the Department of Inorganic Chemistry, University of Umea, Sweden. It can calculate equilibria compositions of systems by minimizing the total free energy but subject to a mass balance constraint. The calculations are based on the assumption that all reactions are reversible and that the system is homogenous. Thermodynamic calculations are not possible without making this two-fold assumption. The computations can be performed on any combination of solid, liquid, aqueous and gaseous species, whether the species are

stable or metastable. Up to 80 species, including a maximum
of 48 solids, can be handled by the program. A listing of
SOLGASWATER can be found in Appendix II.

The total free energy of a system is equivalent to the
sum of the free energies of all existing species, resulting
in one equation. Often, this one equation is non-linear and
extremely difficult to minimize, especially with mass
balance constraints. However, using the method of
Lagrangian multipliers results in a set of equations which
can be solved by Gaussian elimination. SOLGASWATER employs
both techniques to minimize the free energy and to solve for
the equilibrium compositions. However, the set of equations
changes when a new combination of solids is considered to
exist. Changing the solid phase combination may result in a
lower free energy calculation. Therefore, to minimize the
free energy, SOLGASWATER also employs an iteration process
to add solids to or to withdraw solids from consideration.
When two successive iterations yield the same result, the
iteration process is halted.

2.1.2 <u>Calculation Procedure</u>

SOLGASWATER is modeled after the derivation shown in
Appendix III. The derivation shows, step-by-step, how a
free energy equation can be subjected to mass balance
constraints and result in a set of equations solvable by

Gaussian elimination. The set of equations are:

$$\sum_{k=1}^{m} \pi_k a_{ik} - G_i^o/RT = 0, \text{ and} \qquad [2.1]$$

$$\sum_{k=1}^{m} r_{jk}\pi_k + \sum_{i=n+1}^{nt} a_{ij}x_i = b_j - \sum_{i=1}^{n} a_{ij}\psi_i, \quad j = 1 \text{ to } m, \qquad [2.2]$$

where the Lagrangian multipliers, π_k, are solved for. And then the equilibrium compositions, x_i, are solved for using:

$$x_i = y_i \sum_{k=1}^{m} \pi_k a_{ik} + \psi_i. \qquad [2.3]$$

Nomenclature for the above equations are provided in Table 2.1.

Because it is evident from Equation [2.2] that certain solids will be thermodynamically stable in a given electrochemical environment but not in another, an iteration process is used to determine which solid phase combination minimizes the free energy. The iteration process follows:

1) A solid phase combination is selected.

2) Values for y_i are estimated for the solid phase.

3) Values for π_k are calculated from Equations [2.1] and [2.2] using Gaussian elimination.

4) Values of x_i are calculated from Equation [2.3].

5) When two successive iterations yield the same x_i values, the iteration process is halted.

Table 2.1

Nomenclature of Variables Used in the Equations
Implemented in the SOLGASWATER Program

---

*a_{ij}	Stoichiometry of a component j in species i
*b_j	Molarity concentration of component j in the system
c_i	Activity coefficient of species i
*$G_i{}^o$	Standard free energy of formation of species i
*m	Total number of components in the system
*n	Number of aqueous and gaseous species
*nt	Total number of species including solids
R	Gas constant
r_{jk}	Term defined as $a_{ij}a_{ik}y_i$
T	Temperature
x_i	Unknown equilibrium composition of species i
y_i	Iteration process values which satisfy mass balance
π_k	Lagrangian multiplier, an unknown variable
ψ_i	Term defined as $-y_i[G_i{}^o/RT + \ln c_i + \ln y_i - 1]$

---

* input variable
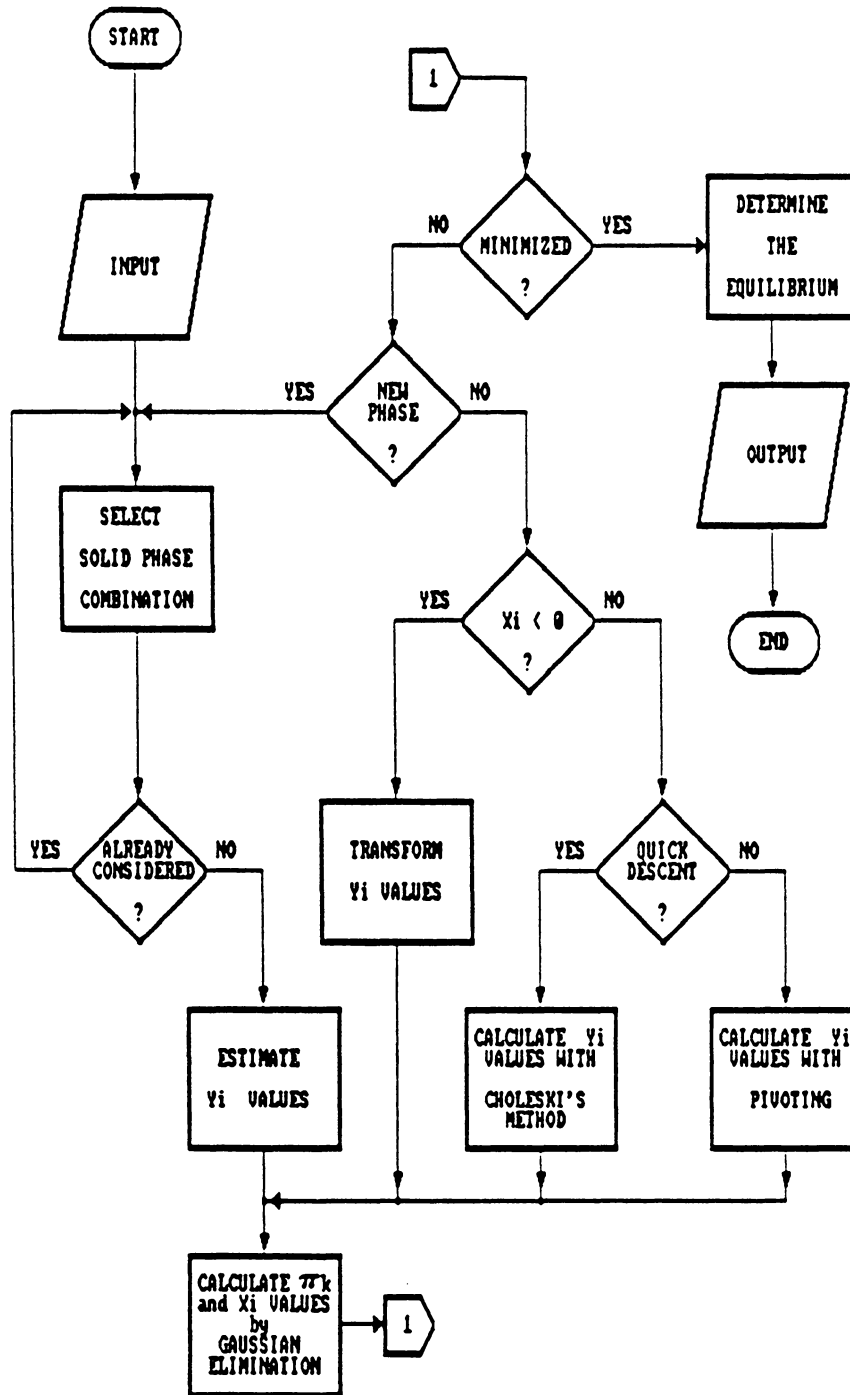
Figure 2.1 Simplified flowsheet for the SOLGASWATER program.

6) Values for y_i are redetermined if

    a. any x_i values are negative, or

    b. any y_i values need changing to provide quick or slow descent to the minimum.

7) A new solid phase combination is chosen and step 2 is repeated when

    a. the solubility of one solid is exceeded,

    b. the amount of a solid is zero or less,

    c. the solid phase has already been considered, or

    d. Gibb's phase rule is violated.

A general flowsheet for the SOLGASWATER program is shown in Figure 2.1.

2.1.3 Input Variables

As shown in Table 2.1, there are six input variables for the SOLGASWATER program: m, n, nt, b_j, G_i^o and a_{ij}. The variables have been described but the latter three are explained in further detail below.

The amount of a component in the system, b_j, is determined from the ratio of copper to water in a pulp containing 30% solids by weight of a chalcocite (Cu_2S) ore which has a 3.0 specific gravity and assays 2% copper. This is equivalent to 0.118 M Cu and 0.059 M S. To simulate flotation pulps of djuleite ($Cu_{1.96}S$), anilite ($Cu_{1.75}S$) and covellite (CuS), the amount of sulfur was kept constant at

0.059 M while the amount of copper was varied accordingly. The amount of one of the remaining components, H^+ and e, was kept constant while the other was incremented after each calculation.

Each species is defined with formation (i.e., reaction) constants based on reactions in which the species are formed from the same components. Therefore, all species are put in terms of the unknown equilibria of the components, thus making the free energy equation easier to solve. Formation constants, K_f, are calculated using Gibbs' free energy change equation,

$$\Delta G = -2.303RTlogK_f, \qquad [2.4]$$

where ΔG is the free energy change. However, if the species being defined are gaseous, 1.39 is subtracted from the value of log K_f (see Appendix IV). For examples, if the components for the copper-sulfur-water system are Cu^{2+}, S^{2-}, H^+ and e, then the following reactions and log K_f's define the Cu^{2+}, $CuSO_4(aq)$, $Cu_2S(s)$ and $H_2S(g)$ species:

$$Cu^{2+} = Cu^{2+} \qquad\qquad 0.00$$

$$Cu^{2+} + S^{2-} + 4H_2O = CuSO_4(aq) + 8H^+ + 8e \qquad 53.04$$

$$2Cu^{2+} + S^{2-} + 2e = Cu_2S(s) \qquad\qquad -31.28$$

$$S^{2-} + 2H^+ = H_2S(g) \qquad\qquad 20.91 - 1.39 = 19.52$$
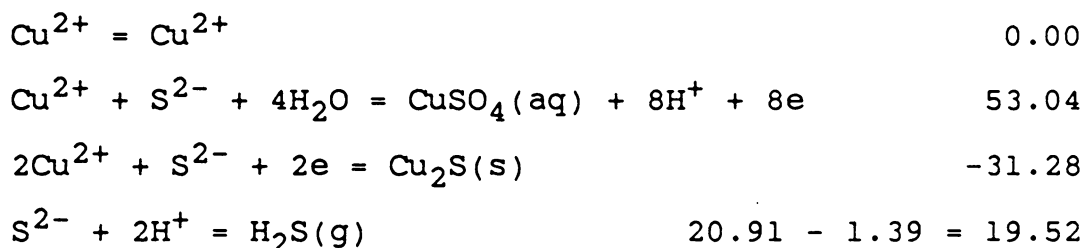
where Table 2.2 lists the standard free energies of species

Table 2.2

Standard Free Energies of Formation (ΔG_f^O) for
the Copper-Sulfur-Water System at 298.15K

Species	ΔG_f^O (kcal·mol^{-1})	Source
Aqueous:		
Cu^+	12.1	1
Cu^{2+}	15.7	1
$CuOH^+$	$-$ 31.0	1
$Cu_2(OH)_2^{2+}$	$-$ 67.0	1
$Cu(OH)_2(aq)$	$-$ 78.26	2
$Cu(OH)_3^-$	$-$118.5	1
$Cu(OH)_4^{2-}$	$-$157.3	1
(a) Stable		
$CuSO_4(aq)$	$-$165.5	1
SO_4^{2-}	$-$177.97	1
HSO_4^-	$-$180.69	1
$H_2SO_4(aq)$	$-$177.97	1
$H_2S(aq)$	$-$ 6.66	1
HS^-	2.88	1
S^{2-}	20.5	1
(b) Sulfate Destabilized by 75 kcal/mole		
$CuSO_4(aq)$	$-$ 90.5	3
SO_4^{2-}	$-$102.97	3
HSO_4^-	$-$105.69	3
$H_2SO_4(aq)$	$-$102.97	3
(c) Thiosulfates		
$Cu(S_2O_3)^-$	$-$129.0	1
$Cu(S_2O_3)_2^{3-}$	$-$259.0	1
$Cu(S_2O_3)_3^{5-}$	$-$388.0	1
$H_2S_2O_3(aq)$	$-$129.9	1
$S_2O_3^{2-}$	$-$127.2	1
$HS_2O_3^-$	$-$129.5	1
(d) Polysulfides		
S_2^{2-}	19.0	1
S_3^{2-}	17.6	1
S_4^{2-}	16.5	1
S_5^{2-}	15.7	1

Table 2.2 (Cont.)

Standard Free Energies of Formation (ΔG_f^O) for
the Copper-Sulfur-Water System at 298.15K

Species	ΔG_f^O (kcal·mol^{-1})	Source
Gaseous:		
$H_2S(g)$	$-$ 8.02	1
Liquid:		
H_2O	$-$ 56.687	1
Solid:		
Cu_2O	$-$ 35.35	1
CuO	$-$ 30.57	1
(a) Stable		
Cu_2S	$-$ 20.45	4
$Cu_{1.96}S$	$-$ 20.23	4
$Cu_{1.75}S$	$-$ 18.77	4
CuS	$-$ 12.89	4
(b) Metastable		
$Cu_{1.93}S$	$-$ 19.99	5
$Cu_{1.83}S$	$-$ 19.19	5
$Cu_{1.67}S$	$-$ 17.79	5
$Cu_{1.38}S$	$-$ 15.09	5
CuS	$-$ 11.24	5

Sources:

1. Duby (1977)

2. Osseo-Asare (1981)

3. Peters (1984 and 1986)

4. Potter (1977)

5. Koch and McIntyre (1976)

in the copper-sulfur-water sytem at 298.15K. Therefore, the free energy of a system is minimized by means of log K_f values.

All copper-water species were considered to be stable. However, all species containing sulfur were grouped into either stable or metastable species. Previously listed in Table 1.1, free energy data for stable solids were determined by Potter (1977). However, thermodynamic data for metastable solids were recalculated from average compositions given by Koch and McIntyre (1976) as shown in Table 1.2. The standard free energy for CuS formed by the anodic oxidation of chalcocite was 1.65 kcal/mole less negative than that for the mineral covellite. This reflects the fact that electrochemically formed CuS is metastable and does not have the same crystal structure as the stable mineral. Aqueous metastability included destabilized sulfates, thiosulfates, and polysulfides. The term 'destabilized sulfate' refers to sulfate species that are 75 kcal/mole higher in free energy than stable sulfate to account for the irreversibility of sulfate formation (Peters, 1984 & 1986).

Referring to the $CuSO_4$ formation reaction given above, water participated in the reaction even though it was not a component of the system. This is because SOLGASWATER was developed under the assumption that the solvent (i.e.,

water, in this case) has unit activity. Therefore, water was not considered to be a component.

The stoichiometry variables, a_{ij}, were also determined from the formation reactions. For example, from the reaction which formed $H_2S(g)$, it took 0 Cu^{2+}, 1 S^{2-}, 2 H^+ and 0 e so the stoichiometries became 0, 1, 2 and 0; however, the stoichiometries for $CuSO_4$ are 1, 1, -8 and -8. The stoichiometries for the H^+ and e components were negative because they appear on the right-hand side of the reaction.

Upon entering the data and running the program, several underflow and overflow errors occurred. Because it was felt that small and large K_f values caused the errors, a scheme was developed in which the log K_f values were minimized (see Appendix V). This scheme took advantage of the facts that 1) the program removes a species from the mass balance calculation if the species is identified with an asterisk, and 2) the differences between free energy terms are significant, not the values of the free energy terms themselves. Therefore, components were invented to minimize the log K_f values and prevent the errors. This scheme was applied throughout this study.

Thermodynamic data for ethyl xanthate species is listed in Table 2.3, where 'X' denotes the xanthate molecule. The free energies were calculated from reaction constants given

Table 2.3

Standard Free Energies of Formation (ΔG_f^O)
for Ethyl Xanthate Species at 298.15K

Species	ΔG_f^O (kcal·mol^{-1})*	Source
HX(aq)	− 2.24	1
X_2(aq)	3.92	2
X_2(l)	− 2.77	3
CuX(s)	−14.20	4
CuX_2(s)	−17.31	5

* free energy values are calculated
from the thermodynamic constants
reported in the sources below

Sources:

1. Iwasaki and Cooke (1958), Majima (1961), Tornell (1966)
   and Hopstock (1968)

2. Tipman and Leja (1975)

3. Mean value reported by DuRietz (1957), Goldstick (1959),
   Tolun and Kitchener (1964), Majima and Takeda (1968)
   and Kakovskii and Arashkevich (1969)

4. Kakovskii (1957)

5. DuRietz (1976)

by the listed authors, assuming that the free energy of the xanthate ion is zero. As stated before, this is a safe assumption because only the differences in free energy values are of any significance. Xanthate-derived species mentioned earlier could not be considered because thermodynamic data were lacking. Therefore, the formation of monothiocarbonate, perxanthate, carbon disulfide and alcohol, for example, are neglected. The amount of xanthate (b_j) was kept constant at 10^{-5} moles.

A typical data file for the SOLGASWATER program is given on the first page of Appendix VI. The input data necessary for the calculation of equilibria of chalcocite oxidation to metastable copper solids, elemental sulfur and polysulfides in the presence of xanthate is shown in the file. Also, all species were defined with invented species, the pH was held constant at 9.5, and the E_h was incremented after each calculation from -0.04 V to 0.031 V.

The results of running the exampled data file are also contained in Appendix VI. Equilibrium compositions are printed out according to specifications. In this case, the logs of all compositions (i.e., amounts of solids and concentrations of solutes) were revealed. The logs of the sum of all solute concentrations for each component were also given.

2.2 E_h-pH Diagrams Without Xanthate

Mass-balanced E_h-pH diagrams have been constructed to depict possible reactions as chalcocite, djurleite, anilite, and covellite oxidize to various oxidation states of sulfur: sulfate, elemental sulfur, thiosulfate, and destabilized sulfate. E_h-pH diagrams have also been developed to show the formation of metastable solids produced during the anodic dissolution of chalcocite. In all cases, aqueous sulfide species were considered.

In the diagrams, long-dashed lines represent equilibria between predominant, aqueous, sulfur-bearing species at equal concentrations; solid lines indicate the appearance and disappearance of solid phases; and short-dashed lines signify the co-existence of the starting mineral (chalcocite, djurleite, anilite, or covellite) with various quantities of a second solid phase. If the quantity of the co-existing solid was determined to be less than 1% of a monolayer where 10^{-5} moles constitutes a monolayer, then the quantity was considered to be negligible. Based on the system under consideration (0.059 moles of mineral per liter of solution), on the surface roughness of a cube-shaped mineral being 4 times the geometric area (Shannon and Trahar, 1986), and on the average particle size of a typical flotation pulp being 50 microns, actual surface coverage would be slightly

greater than 10^{-5} moles per monolayer.

2.2.1 Sulfate

Typical thermodynamic calculations have been performed assuming that sulfide oxidation proceeded to sulfate formation as shown in the works of including Garrels and Christ (1965), Brook (1971), Crerar (1975), Linkson et al. (1979), Pritzker (1985) and Basilio (1985). E_h-pH diagrams for the chalcocite, djurleite, anilite, and covellite oxidation to sulfate have been depicted and are, therefore, shown in Figures 2.2 through 2.5, respectively. It can be seen from these figures that the stability regions of the solid species are dependent on the starting mineral which is to say that the stability regions vary with a change in the copper/sulfur ratio. The diagram for chalcocite, a copper/sulfur ratio of 2 (see Figure 2.2), shows a small region at low pH conditions in which another copper sulfide, djurleite, is stable. However, changing the copper/sulfur ratio to 1.96 (see Figure 2.3) decreases the stability region of chalcocite, increases the stability region of djurleite, and allows anilite to become stable. Similiarly, the stability regions of anilite and covellite are increased as the copper/sulfur ratio is changed to 1.75 in Figure 2.4 and 1.00 in Figure 2.5, respectively.

It can be seen from each figure that the oxidation of
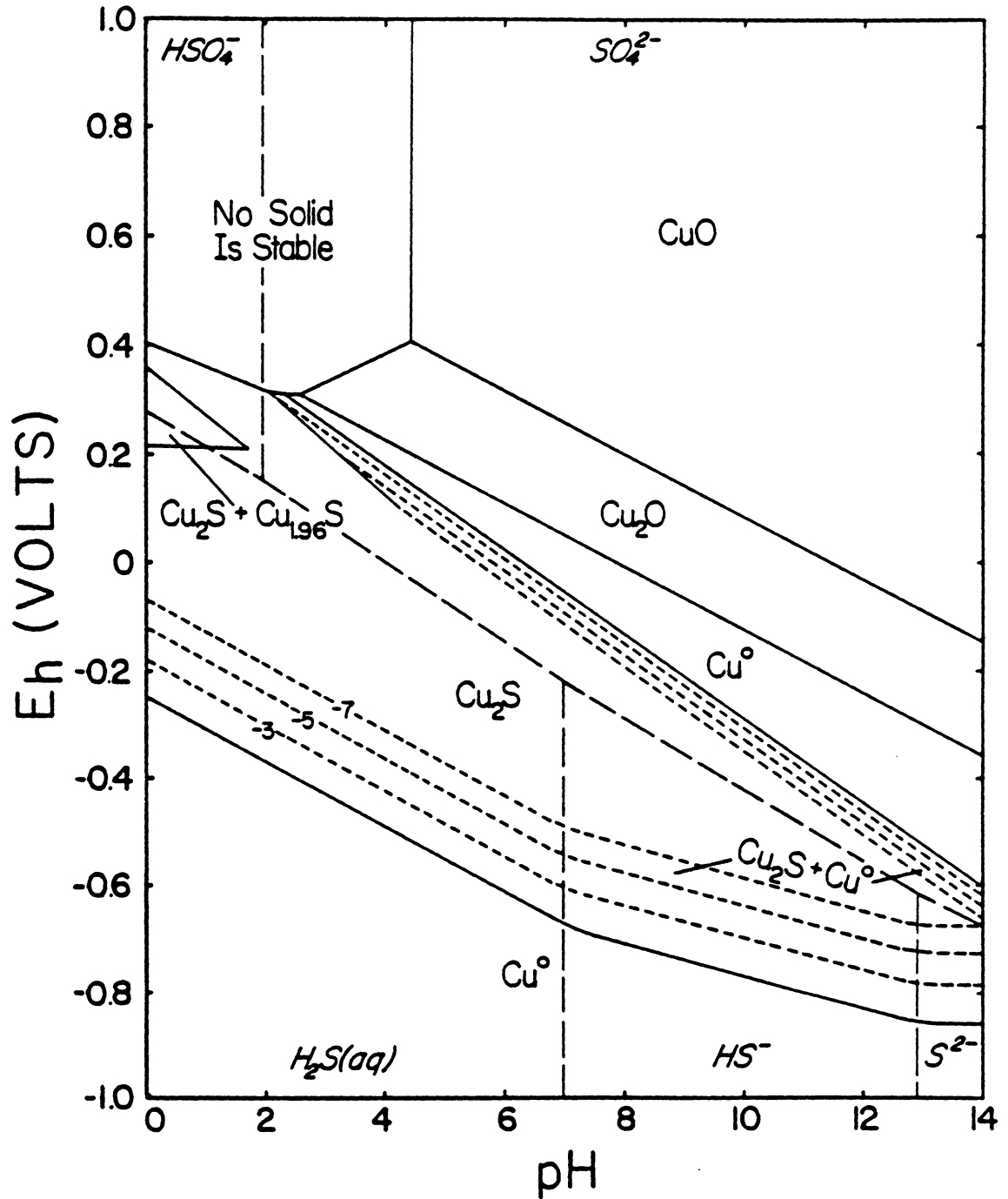
Figure 2.2 E_h-pH diagram depicting chalcocite (Cu_2S) oxidation to sulfate. See text for explanation of dashed lines.
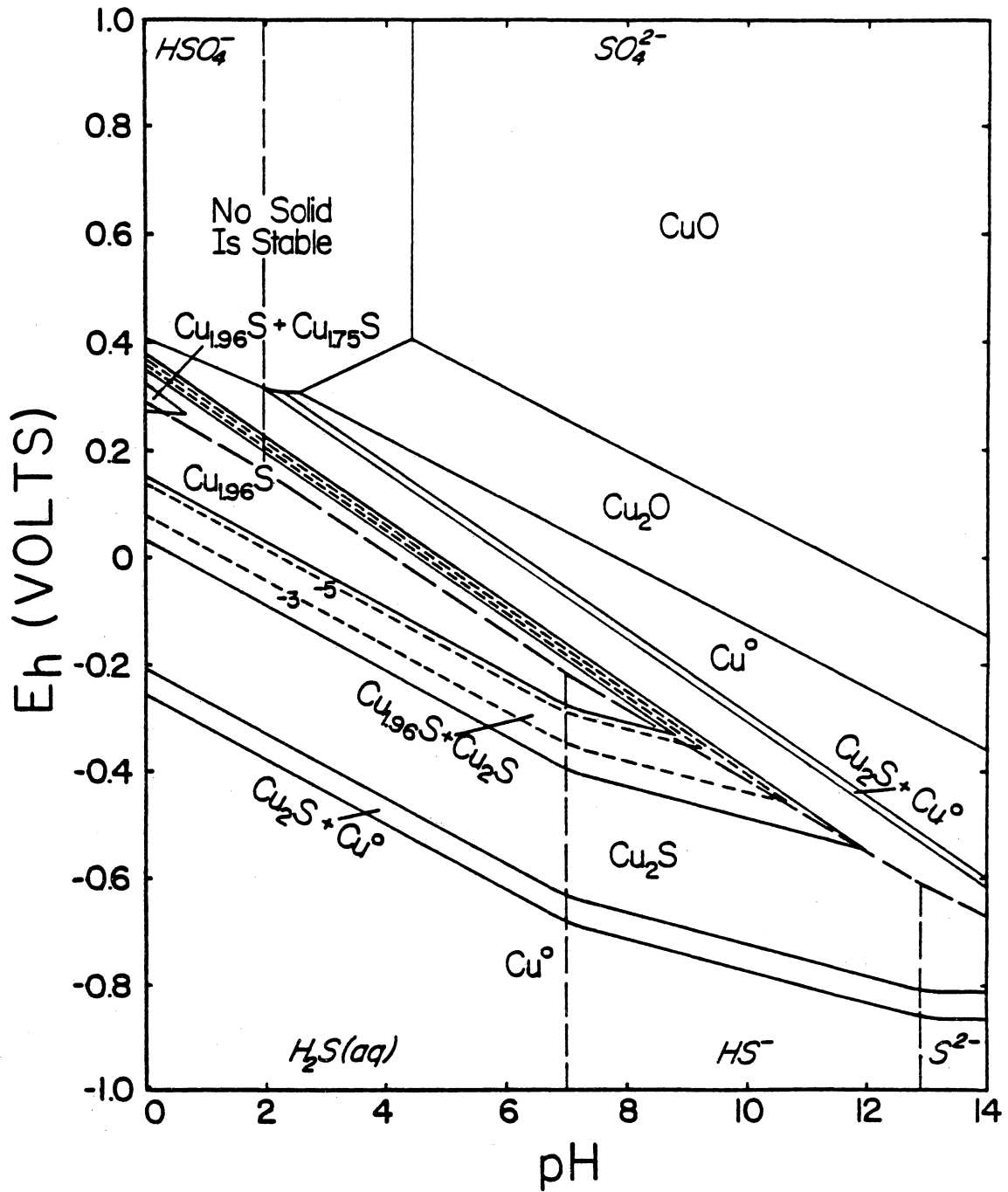
Figure 2.3 E$_h$-pH diagram depicting djurleite (Cu$_{1.96}$S) oxidation to sulfate. See text for explanation of dashed lines.
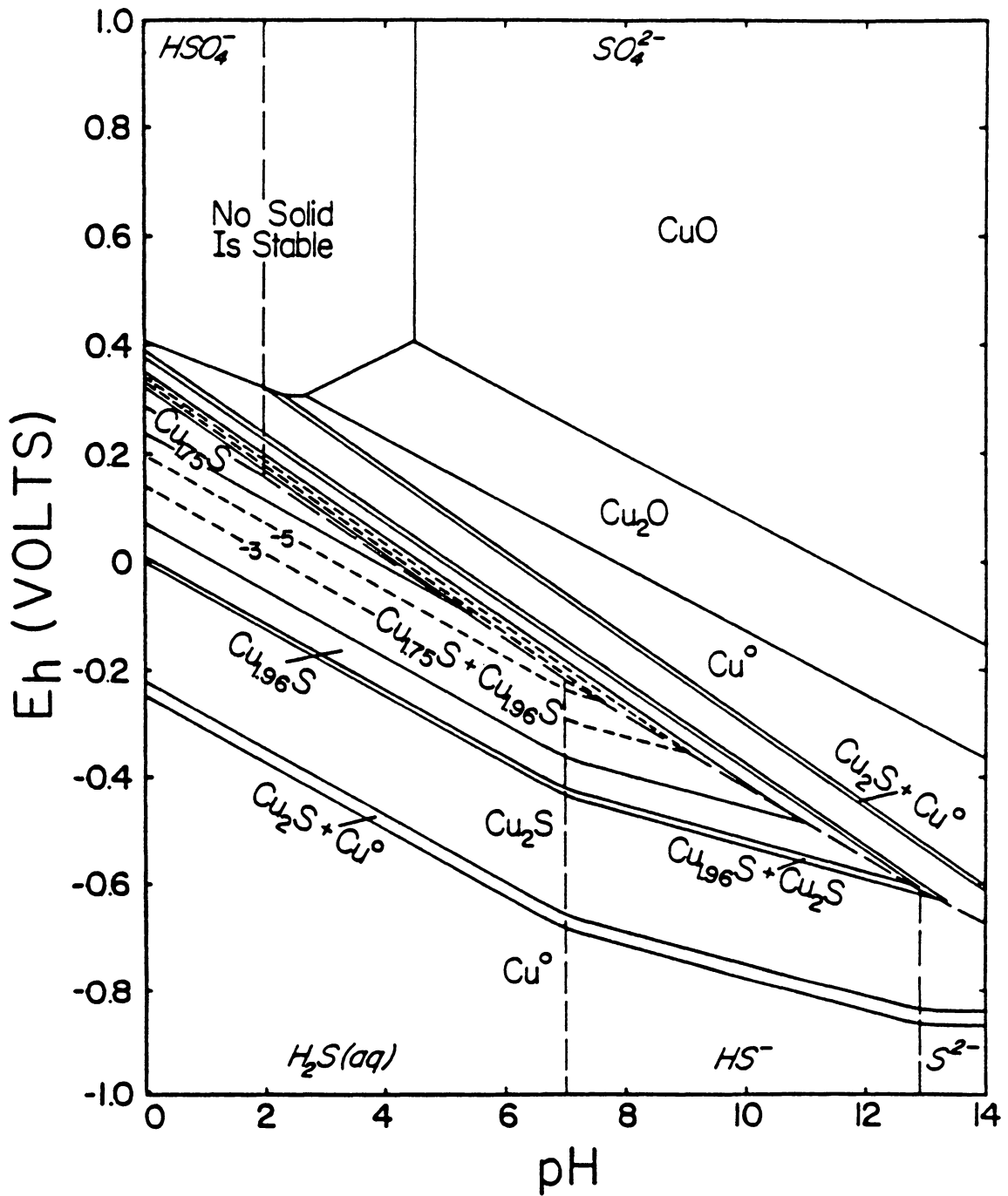
Figure 2.4 Eh-pH diagram depicting anilite ($Cu_{1.75}S$) oxidation to sulfate. See text for explanation of dashed lines.
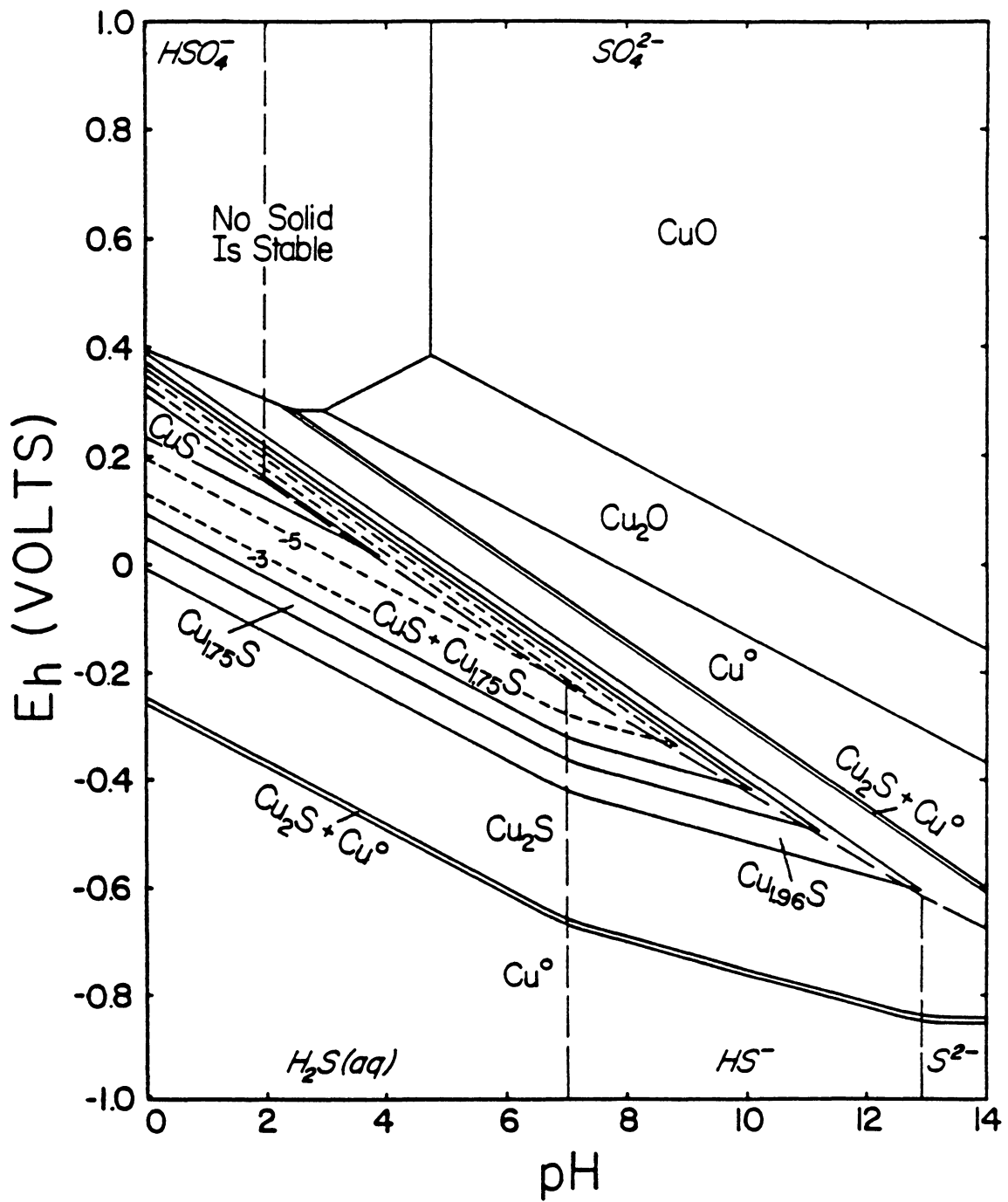
Figure 2.5   E$_h$-pH diagram depicting covellite (CuS)
oxidation to sulfate. See text for explanation
of dashed lines.

the starting mineral eventually leads to the formation of metallic copper from chalcocite via the reaction

$$Cu_2S + 4H_2O = 2Cu^O + SO_4{}^{2-} + 8H^+ + 6e. \qquad [2.5]$$
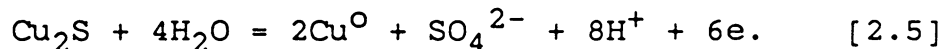
If chalcocite is not the starting mineral in Reaction [2.5], than it can be produced by the following oxidation reaction:

$$(2-x)Cu_{2-x-y}S + 4yH_2O =$$
$$(2-x-y)Cu_{2-x}S + ySO_4{}^{2-} + 8yH^+ + 6ye, \qquad [2.6]$$
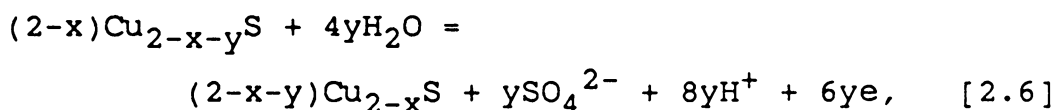
which also encompasses the formation of the other minerals and is therefore known as a general reaction. For example, according to Reaction [2.6], chalcocite can be produced from djurleite if $x = 0$ and $y = 0.04$; however, anilite can be produced from covellite if $x = 0.25$ and $y = 0.75$. Reactions [2.5] and [2.6] could involve any of the other sulfate species as well. Similiarly, the reduction of each sulfide mineral leads to the formation of metallic copper and any of the aqueous sulfide species by the reduction reaction

$$Cu_2S + H^+ + 2e = 2Cu^O + HS^-. \qquad [2.7]$$
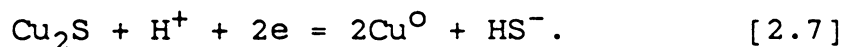
Also, if chalcocite is not the starting mineral, it can be produced by the following general reduction reaction:

$$(2-x)Cu_{2-x-y}S + yH^+ + 2ye = (2-x-y)Cu_{2-x}S + yHS^-. \qquad [2.8]$$
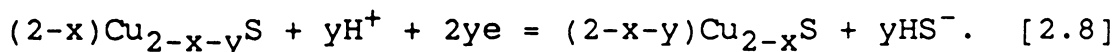
Reactions [2.5] through [2.8] are written as equilibrium

reactions because solid phases co-exist with one another as illustrated in the diagrams.

The co-existence of these solids can be explained using the definition of solubility. If a solid is known to be stable at a specific E_h and pH and if the solubility of the solid gives equilibrium concentrations which exceed the solubility of another solid, the other solid will also be stable. For example, chalcocite solubilizes according to the reaction

$$Cu_2S = 2Cu^+ + S^{2-}. \qquad [2.9]$$

If the resulting concentration of cuprous ions exceeds that in equilibrium with metallic copper, then metallic copper will form. It becomes necessary to know what the E_h and pH are because both cuprous and sulfide ions undergo reduction and oxidation (i.e., effect of E_h) reactions and protonation and hydration (i.e., effect of pH) reactions; hence, Reactions [2.5] and [2.7] will proceed to some extent through the stability domain of chalcocite. Thus, there will be a region where metallic copper co-exists with chalcocite.

Decreasing the copper/sulfur ratio diminishes the region of co-existence, however. For example, in Figure 2.2 the region is large because there is an absence of aqueous sulfate and aqueous sulfide species so both Reactions [2.5]

and [2.7] would proceed to the right. But in Figure 2.5 the co-existence region is small because excess aqueous sulfate produced from Reaction [2.6] hinders Reaction [2.5] from proceeding to the right and excess sulfide produced from Reaction [2.8] hinders Reaction [2.7] from proceeding to the right as well.

The above consideration also explains why the regions of stability for the various stoichiometries differ with changes in the copper/sulfur ratio in the system. Thus, in Figure 2.3, chalcocite oxidizes to djurleite when Reaction [2.8] proceeds to the left. However, chalcocite cannot oxidize to djurleite under the conditions in Figure 2.2 since, in this case, there is no available aqueous sulfide species. Nevertheless, chalcocite does oxidize to djurleite under the conditions in Figure 2.2 but according to the following reaction:

$$Cu_2S = Cu_{1.96}S + 0.04Cu^{2+} + 0.08e. \qquad [2.10]$$
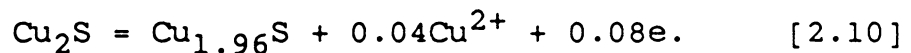
The co-existence of metallic copper and chalcocite was exemplified earlier because it appears in each of Figures 2.2 to 2.5. Furthermore, Figure 2.2 is in agreement with the mass-balanced calulations performed by Basilio (1985) on the starting mineral of chalcocite. In his calculations, the oxidation of the sulfur was assumed to proceed all the way to sulfate and metallic copper was shown to exist

throughout the stability domain of chalcocite, except under acidic and slightly oxidizing conditions. Somewhat similar conclusions can be made from Figure 2.2 which, however, shows a smaller domain. The reason is that amounts of metallic copper less than 10^{-7} moles (i.e., the equivalence of 1% of a monolayer) were considered to be negligible.

2.2.2 Elemental Sulfur

Although thermodynamics dictates that the oxidation of sulfides should produce sulfate, the conditions typical of flotation provide an environment in which sulfide oxidation is very slow, allowing for the formation of metastable products. Voltammetric studies by Gardner and Woods (1979) on galena over a range of pH values suggested that elemental sulfur, a metastable product, was formed. E_h-pH diagrams for chalcocite, djurleite, anilite, and covellite oxidation to elemental sulfur are, therefore, presented in Figures 2.6 through 2.9, respectively. Polysulfides were included since they have oxidation states between those of sulfide (-II) and and elemental sulfur (0). Polysulfides are known to have regions of metastability in neutral and alkaline solutions (Chen and Gupta, 1973) and have been used to explain the collectorless flotation of sulfide minerals (Luttrell and Yoon, 1984). Pritzker (1985) performed similiar calculations on galena, but never before have mass-
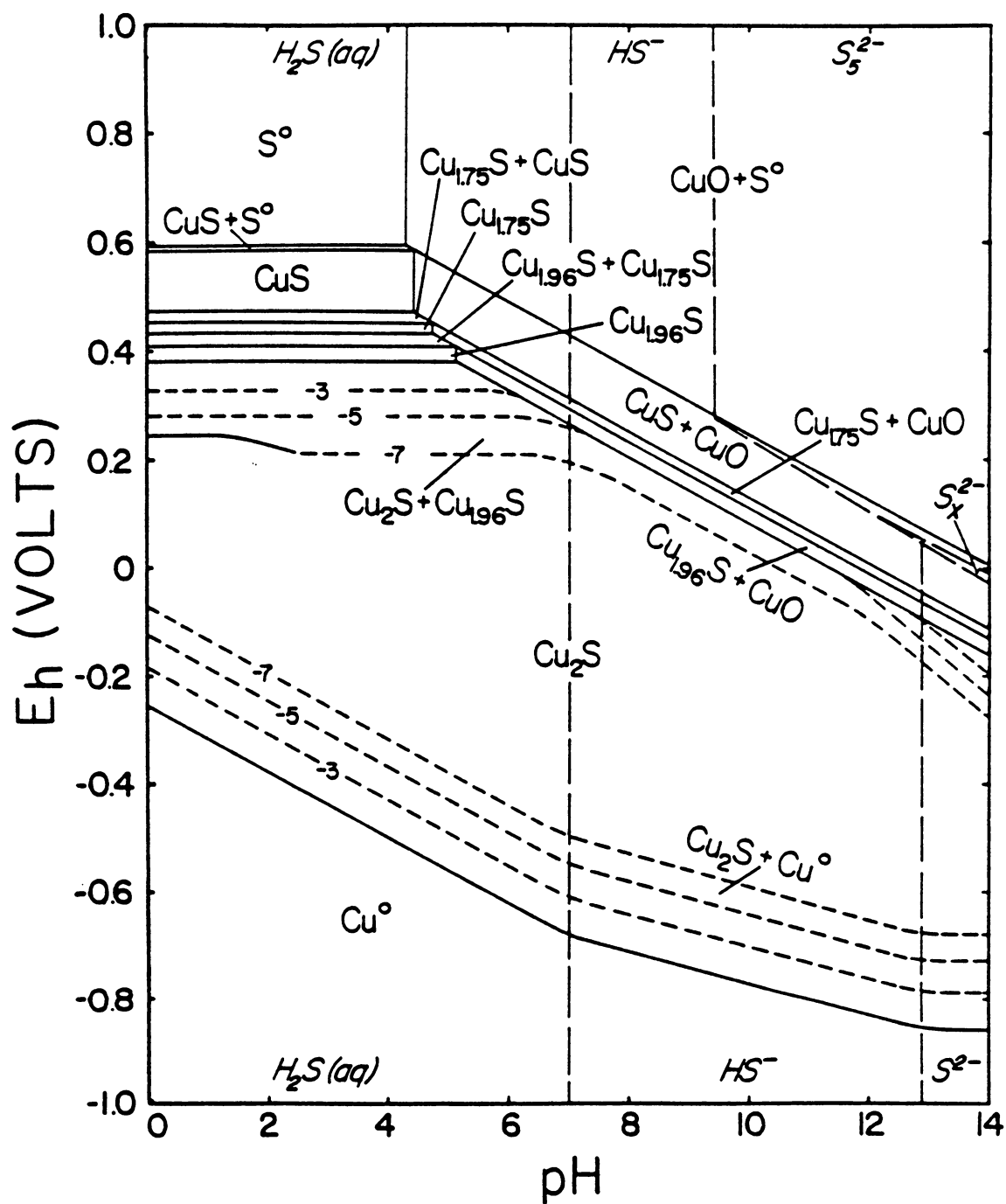
Figure 2.6 E$_h$-pH diagram depicting chalcocite (Cu$_2$S) oxidation to elemental sulfur. See text for explanation of dashed lines.
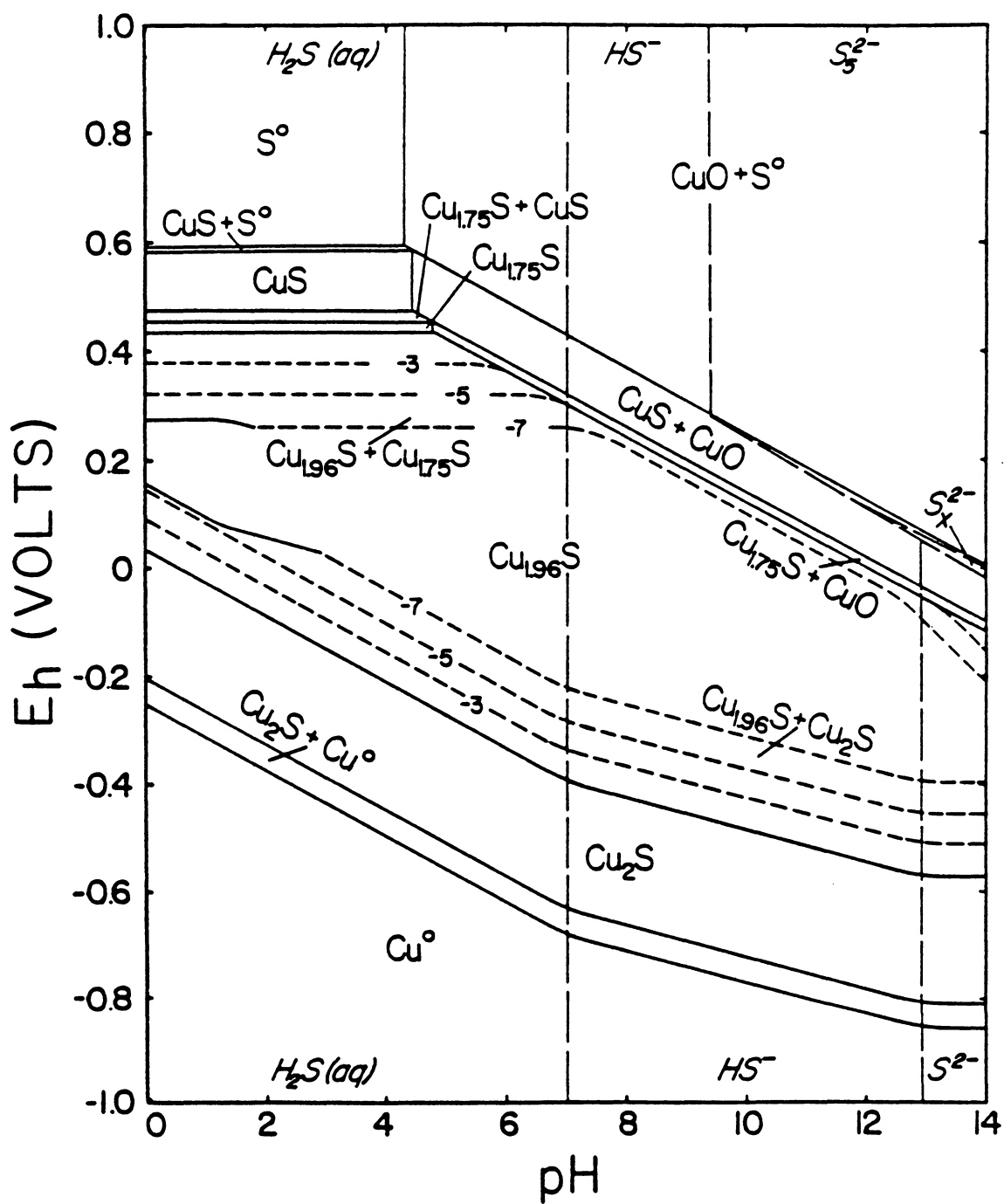
Figure 2.7 Eh-pH diagram depicting djurleite ($Cu_{1.96}S$) oxidation to elemental sulfur. See text for explanation of dashed lines.
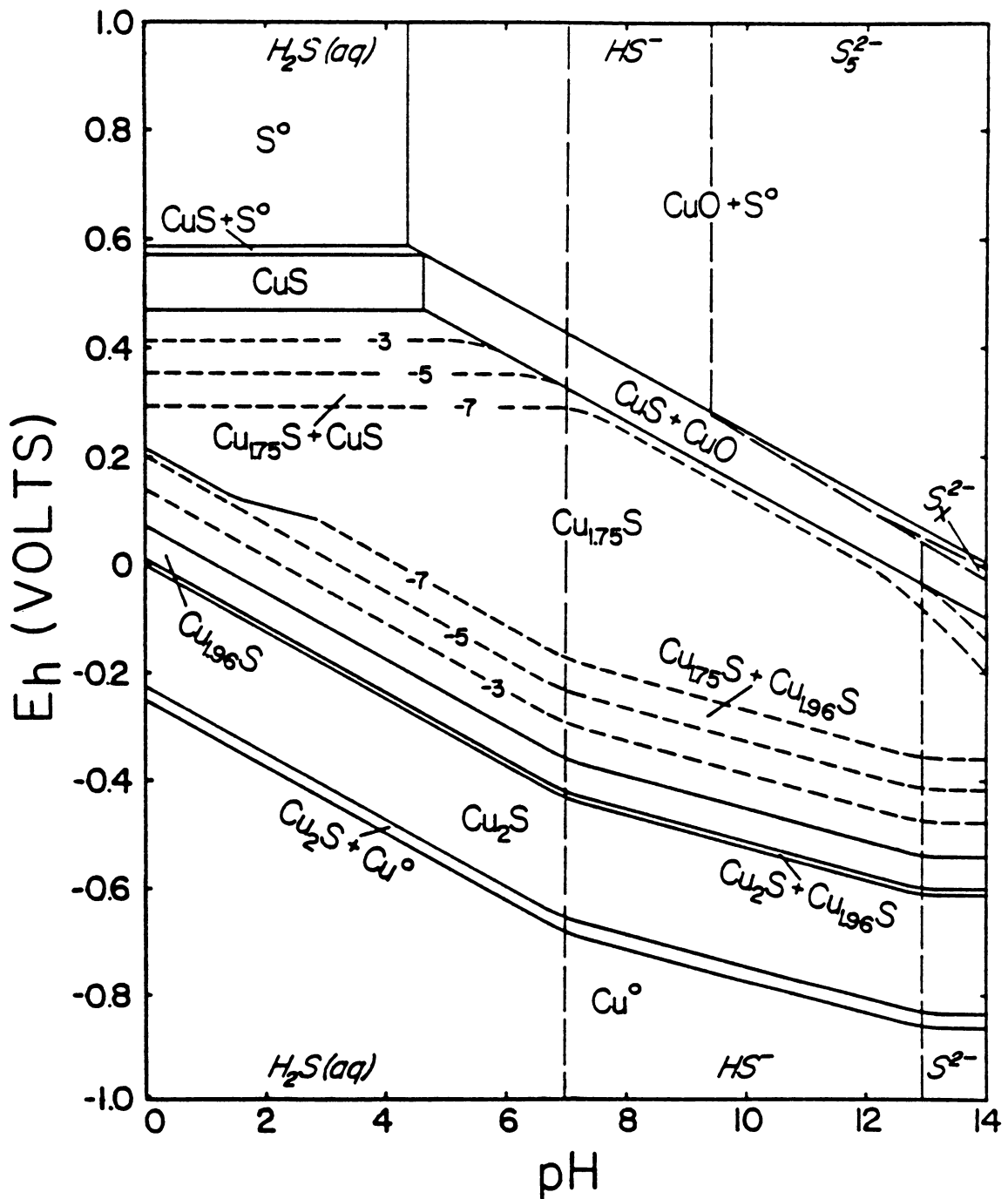
Figure 2.8 E_h-pH diagram depicting anilite ($Cu_{1.75}S$) oxidation to elemental sulfur. See text for explanation of dashed lines.
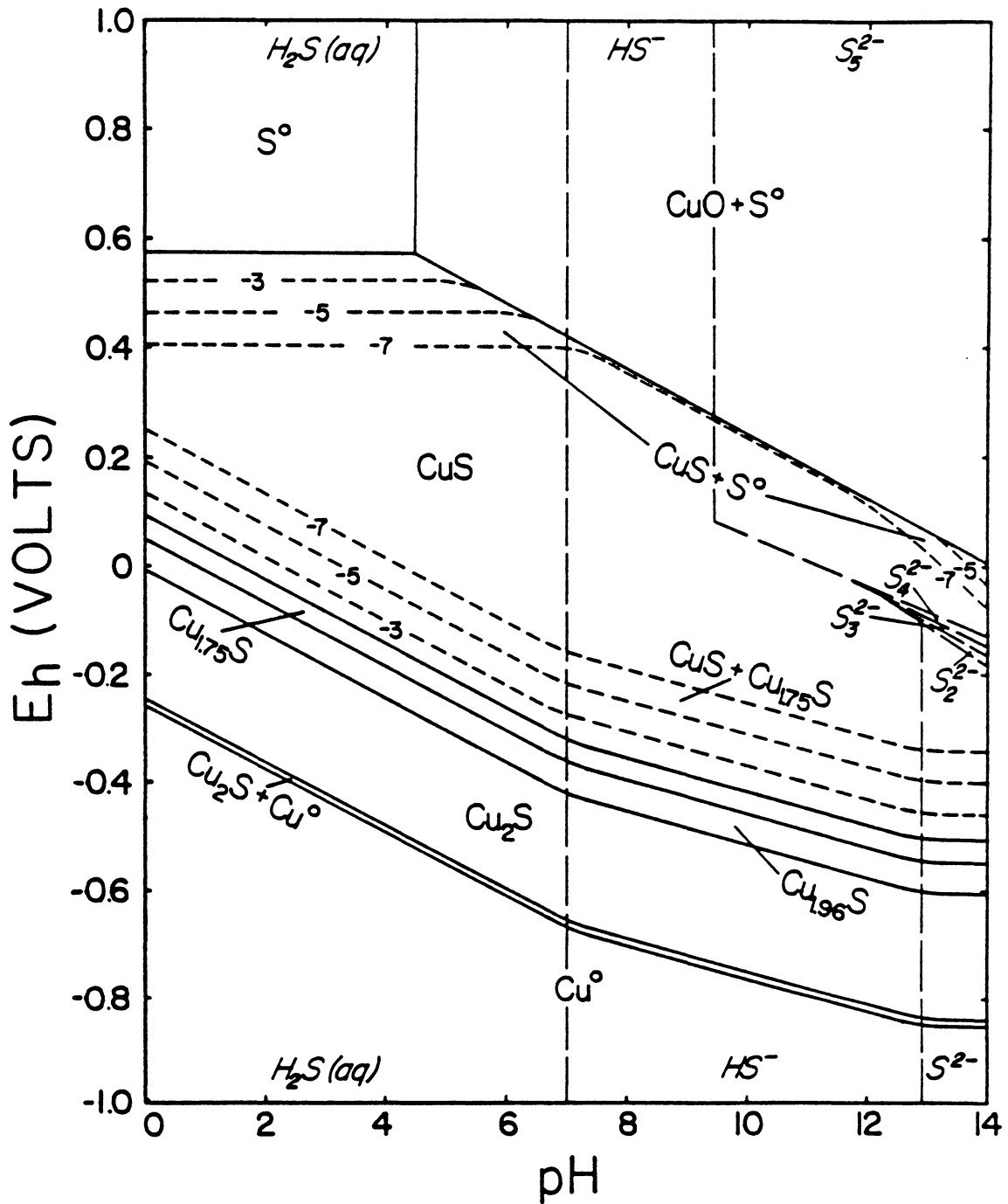
Figure 2.9 E_h-pH diagram depicting covellite (CuS) oxidation to elemental sulfur. See text for explanation of dashed lines.

balanced calculations been carried out on copper sulfide systems as sulfur oxidation proceeded only as far as the formation of elemental sulfur.

Comparing Figures 2.6 to 2.9 with respective Figures of 2.2 through 2.5 reveals that the diagrams remain unchanged at reducing potentials due to the production of aqueous sulfides (see Reactions [2.7] and [2.8]); hence, metallic copper co-exists with chalcocite. Furthermore, by not considering sulfate formation, all copper sulfides become stable, thereby extending their stability regions to higher oxidizing potentials. In all cases, covellite oxidation controls the uppermost potential via the following reaction:

$$CuS + H_2O = CuO + S^o + 2H^+ + 2e. \qquad [2.11]$$
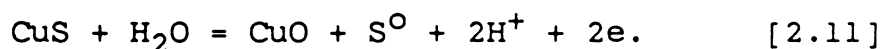
If covellite is not the starting mineral, it can be produced from a second general reaction in the form of

$$Cu_{2-x}S + yH_2O = Cu_{2-x-y}S + yCuO + 2yH^+ + 2ye. \qquad [2.12]$$
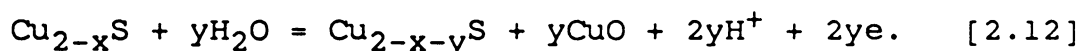
Under acidic conditions, Reactions [2.11] and [2.12] would not involve water allowing for the formation of cupric ions instead of cupric oxide and hydrogen ions (see Reaction [2.10]).

As was the case for the oxidation to sulfate, it is apparent that the stability regions of the copper sulfides shown in Figures 2.6 to 2.9 are dependent on the starting

mineral. In fact, the starting mineral composes the largest stability region of the copper sulfides because Reactions [2.8] and [2.12] never go to completion until significant pH's and E_h's are reached. Therefore, the starting mineral is stable in both oxidizing and reducing environments. However, those minerals with lower copper content than the starting mineral (i.e., compared to the starting mineral, minerals with less copper content are copper-deficient) are stable only under oxidizing conditions (see Reaction [2.12]) and those with higher copper content (i.e., copper-excess) are stable only under reducing conditions (see Reaction [2.8]). For example, the starting mineral djurleite comprises the largest stability region of the copper sulfides in Figure 2.7 and is therefore stable in oxidizing and reducing conditions. However, djurleite is stable only under oxidizing conditions when the system is copper-excess (see Figure 2.6) and stable only under reducing conditions when the system is copper-deficient (see Figures 2.8 and 2.9).

No significant concentrations of polysulfide ions were predicted at any E_h or pH condition. Furthermore, because the insoluble behavior of stable copper sulfide minerals favored the formation of sulfide ions, polysulfide ions were not predominant under neutral conditions as stated by Chen and Gupta (1973). However, the regions of predominance for

the polysulfide ions in Figures 2.6 through 2.9 are exactly the same as predicted by Pritzker (1985) in mass-balanced calculations of galena oxidizing to elemental sulfur.

2.2.3 Thiosulfate

It is well established that reactions in which sulfide species are converted to sulfate species are slow and can, therefore, lead to the formation of metastable products. Gardner and Woods (1979) established through voltammetric studies that metastable sulfur does form; however, they also noted that thiosulfate formed at high pH's and E_h's. Furthermore, investigators like Toperi and Tolun (1969) and Pritzker (1985) recognized the possibility of thiosulfate formation in their construction of E_h-pH diagrams of galena oxidation. After a variety of experimental work, Pritzker (1985) was able to conclude that galena oxidation proceeded to thiosulfate but only after the formation of elemental sulfur. Figures 2.10 to 2.13 show mass-balanced E_h-pH diagrams for chalcocite, djurleite, anilite, and covellite, respectively.

Comparing Figures 2.10 through 2.13 with respective diagrams shown in Figures 2.2 through 2.9 again shows that, under reducing conditions, the diagrams do not change (see Reactions [2.7] and [2.8]), and the co-existence of metallic copper and chalcocite is therefore observed. Further
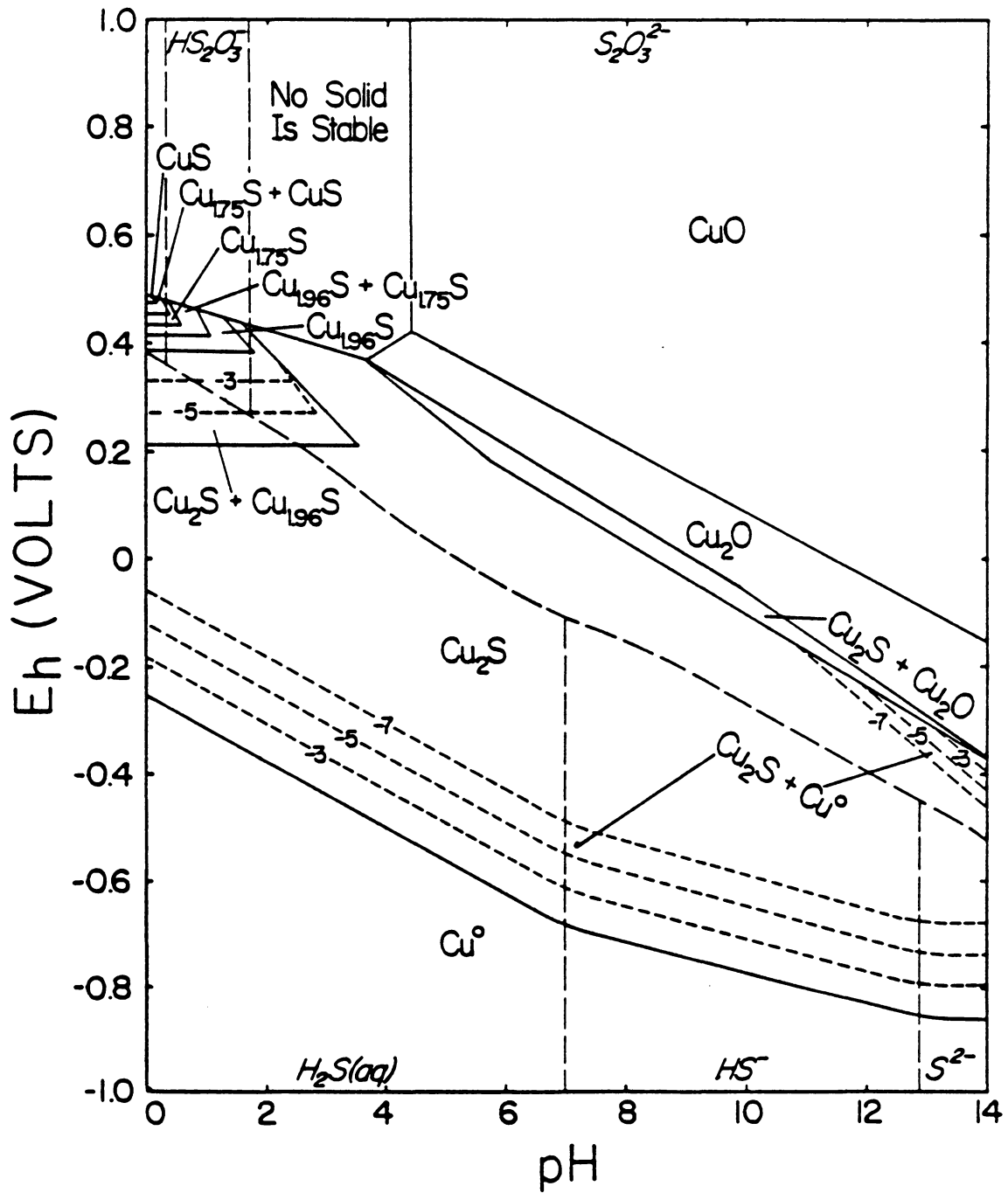
Figure 2.10 E_h-pH diagram depicting chalcocite (Cu_2S) oxidation to thiosulfate. See text for explanation of dashed lines.
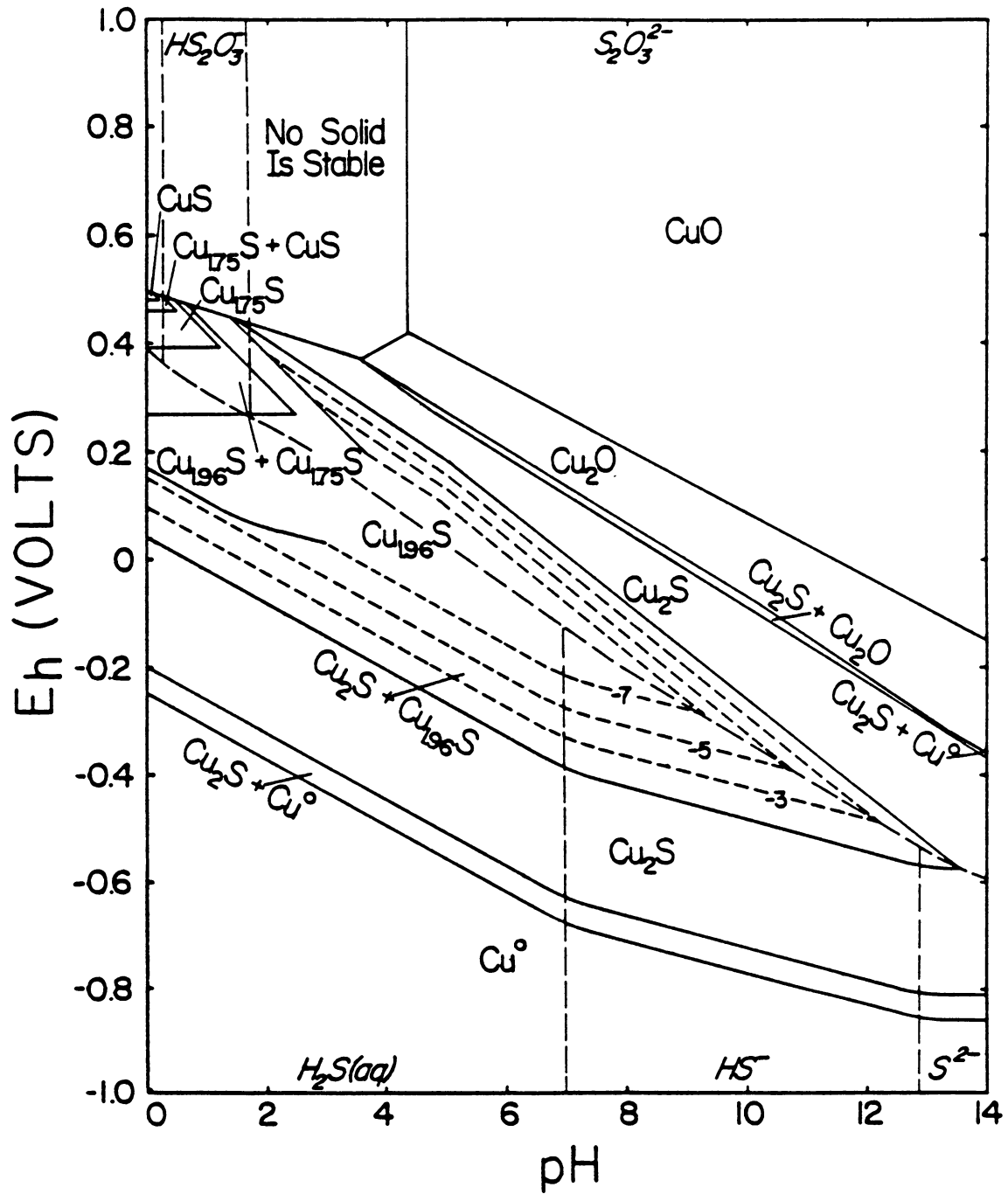
Figure 2.11 E_h-pH diagram depicting djurleite ($Cu_{1.96}S$) oxidation to thiosulfate. See text for explanation of dashed lines.
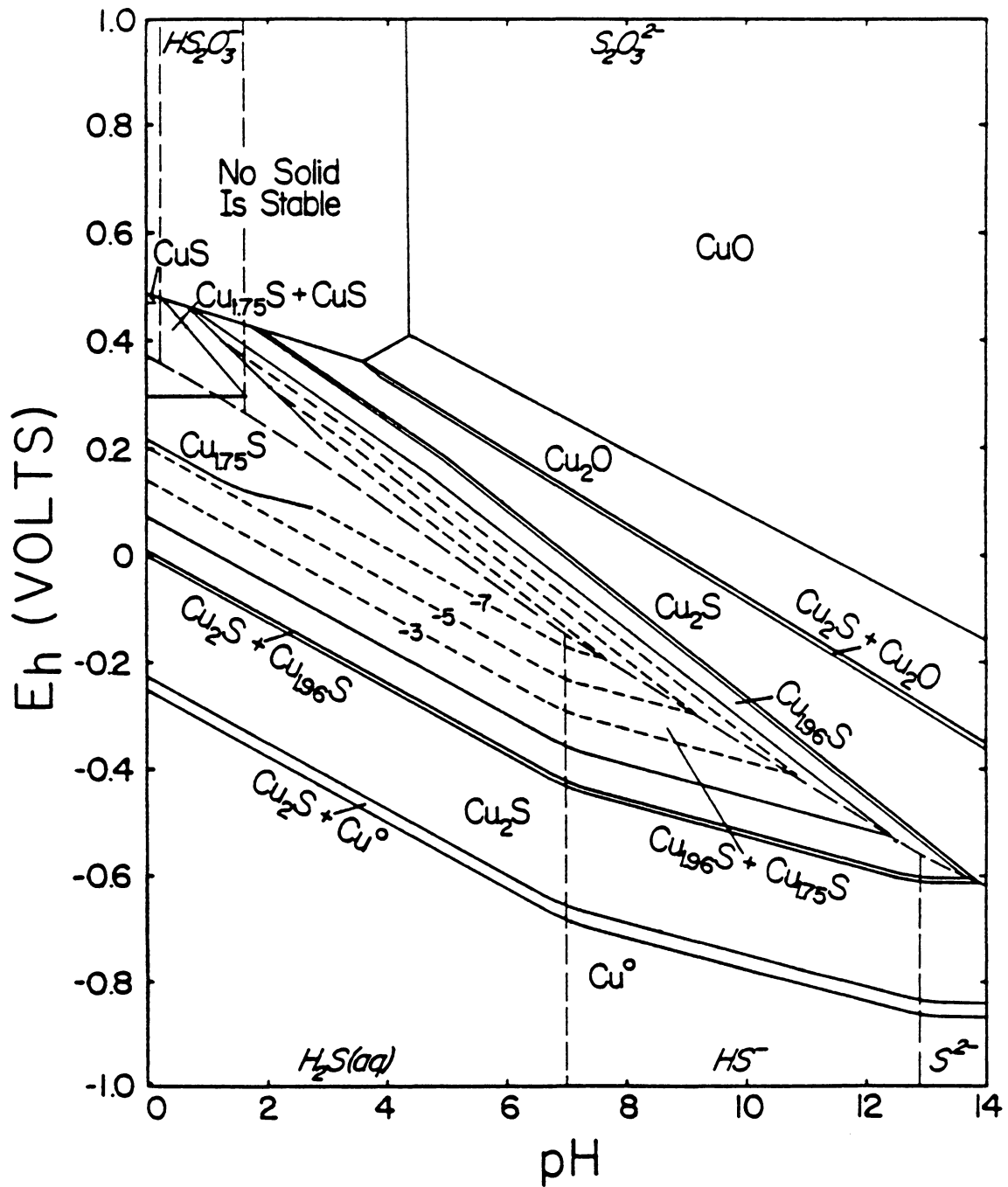
Figure 2.12 E_h-pH diagram depicting anilite ($Cu_{1.75}S$) oxidation to thiosulfate. See text for explanation of dashed lines.
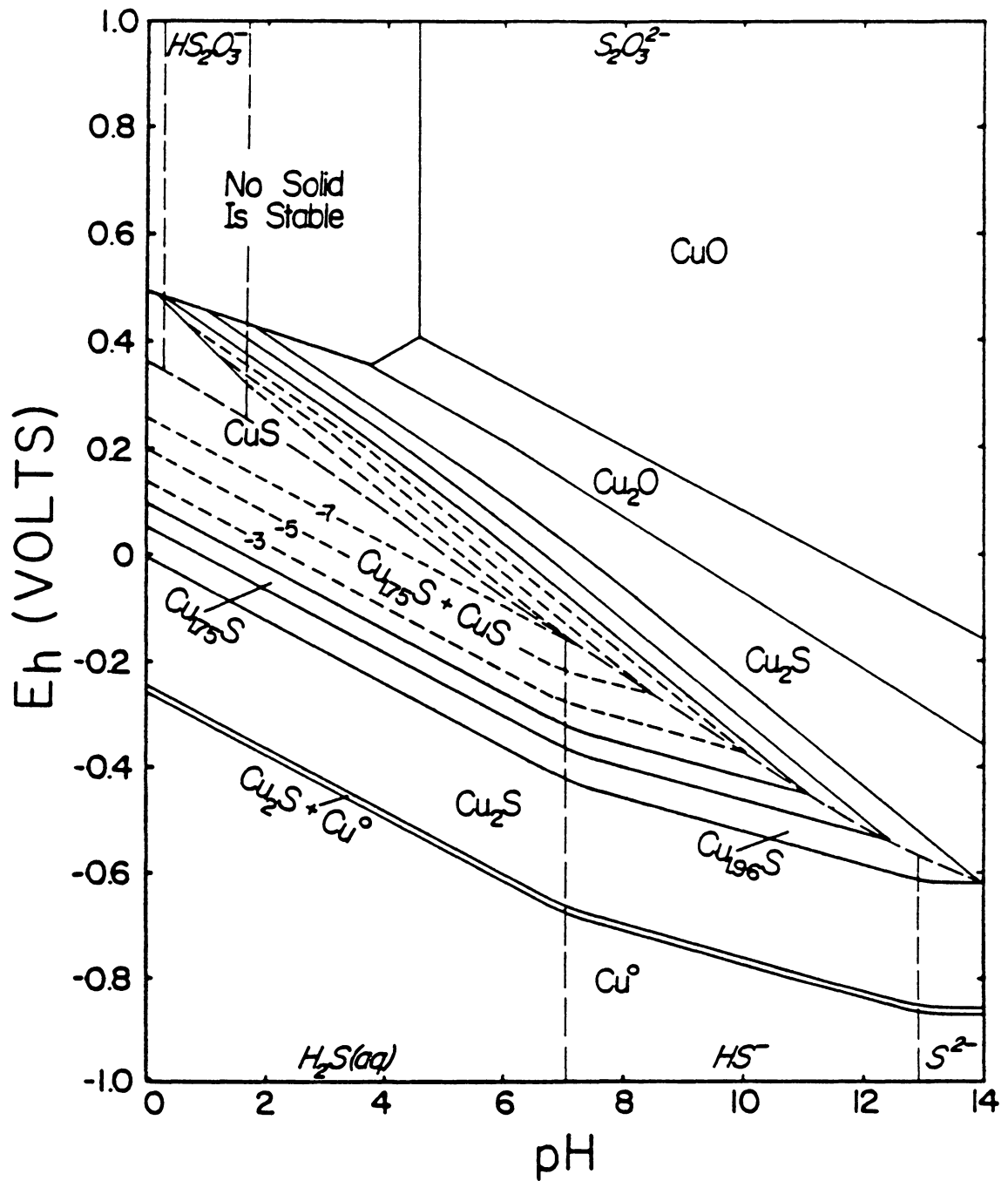
<u>Figure 2.13</u> E$_h$-pH diagram depicting covellite (CuS) oxidation to thiosulfate. See text for explanation of dashed lines.

comparison reveals that the upper potential limit of copper sulfide stability lies between those for sulfate and elemental sulfur as expected. In fact, this upper potential limit is determined by the reaction

$$2Cu_2S + 5H_2O = 2Cu_2O + S_2O_3{}^{2-} + 10H^+ + 8e, \qquad [2.13]$$
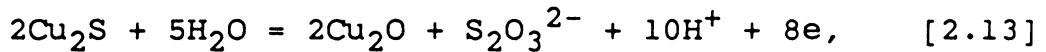
where the chalcocite is either the starting mineral (see Figure 2.10) or is produced by another general reaction:

$$(2-x)Cu_{2-x-y}S + 4yH_2O =$$
$$(2-x-y)Cu_{2-x}S + 0.5yS_2O_3{}^{2-} + 8yH^+ + 7ye. \qquad [2.14]$$
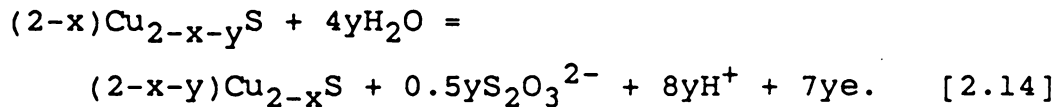
Reaction [2.14] is almost the same as Reaction [2.6] since oxidation to thiosulfate also produces chalcocite. Because the reactions are similiar, the thiosulfate diagrams, Figures 2.10 through 2.13, resemble the sulfate diagrams in Figures 2.2 through 2.5, which further explains why many of the conclusions drawn from the sulfate diagrams can be drawn for the thiosulfate diagrams. For examples, decreasing the copper/sulfur ratio in the system increases the stability regions of the copper-deficient sulfides and oxidation reactions which produce copper-deficient sulfides proceed via the production of cupric ions (see Reaction [2.10]). As stated earlier for the case where oxidation proceeds to elemental sulfur, cupric ions are produced during the oxidation of the copper sulfides (viz. a form of Reaction

[2.12]), which also explains why there is relatively no difference between thiosulfate and elemental sulfur diagrams under acidic conditions (Compare Figures 2.6 to 2.9 with Figures 2.10 to 2.13, respectively).

2.2.4 Destabilized Sulfate

To further explore the irreversibility of sulfate formation, the standard free energies of sulfate species were increased with 75 kcal/mole as suggested by Peters (1984 and 1986). This shift is equivalent to a 406.5 millivolt overpotential for the equilibrium between aqueous sulfide and sulfate species. Mass-balanced E_h-pH diagrams involving destabilized sulfate of any kind have never been developed.

E_h-pH diagrams constructed with destabilized sulfate are shown in Figures 2.14 through 2.17 for the oxidation of chalcocite, djurleite, anilite, and covellite, respectively. Comparing these diagrams with the corresponding diagrams of elemental sulfur formation shows there is no significant influence of destabilized sulfate on copper sulfide equilibria in acid solutions below pH 5. The only difference between the diagrams in this region is shift of the upper stability limit of elemental sulfur caused by its equilibium with destabilized sulfate. In each case, elemental sulfur is only stable below pH 5. Above pH 5, the
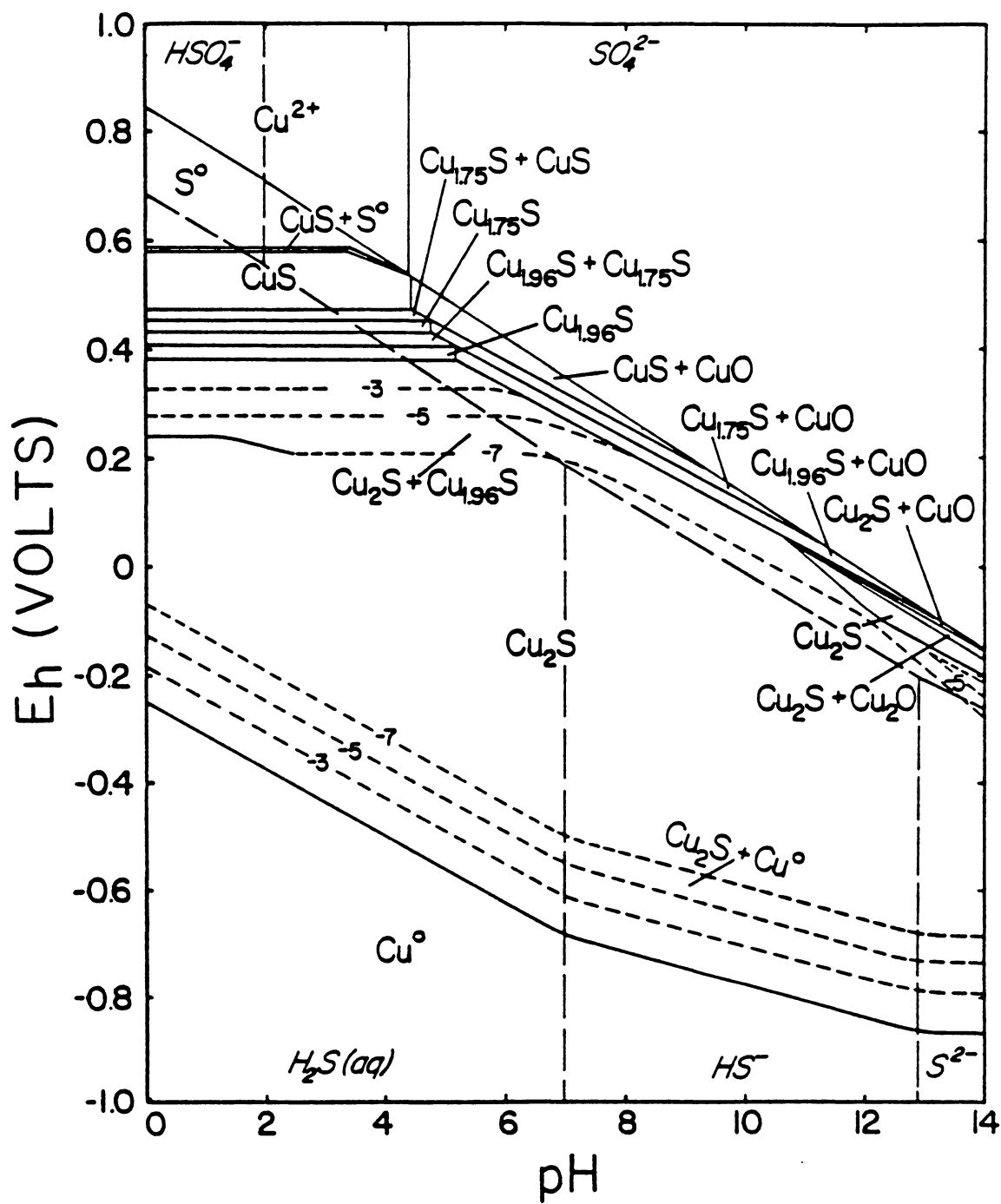
Figure 2.14   E$_h$-pH diagram depicting chalcocite (Cu$_2$S) oxidation to destabilized sulfate. See text for explanation of dashed lines.
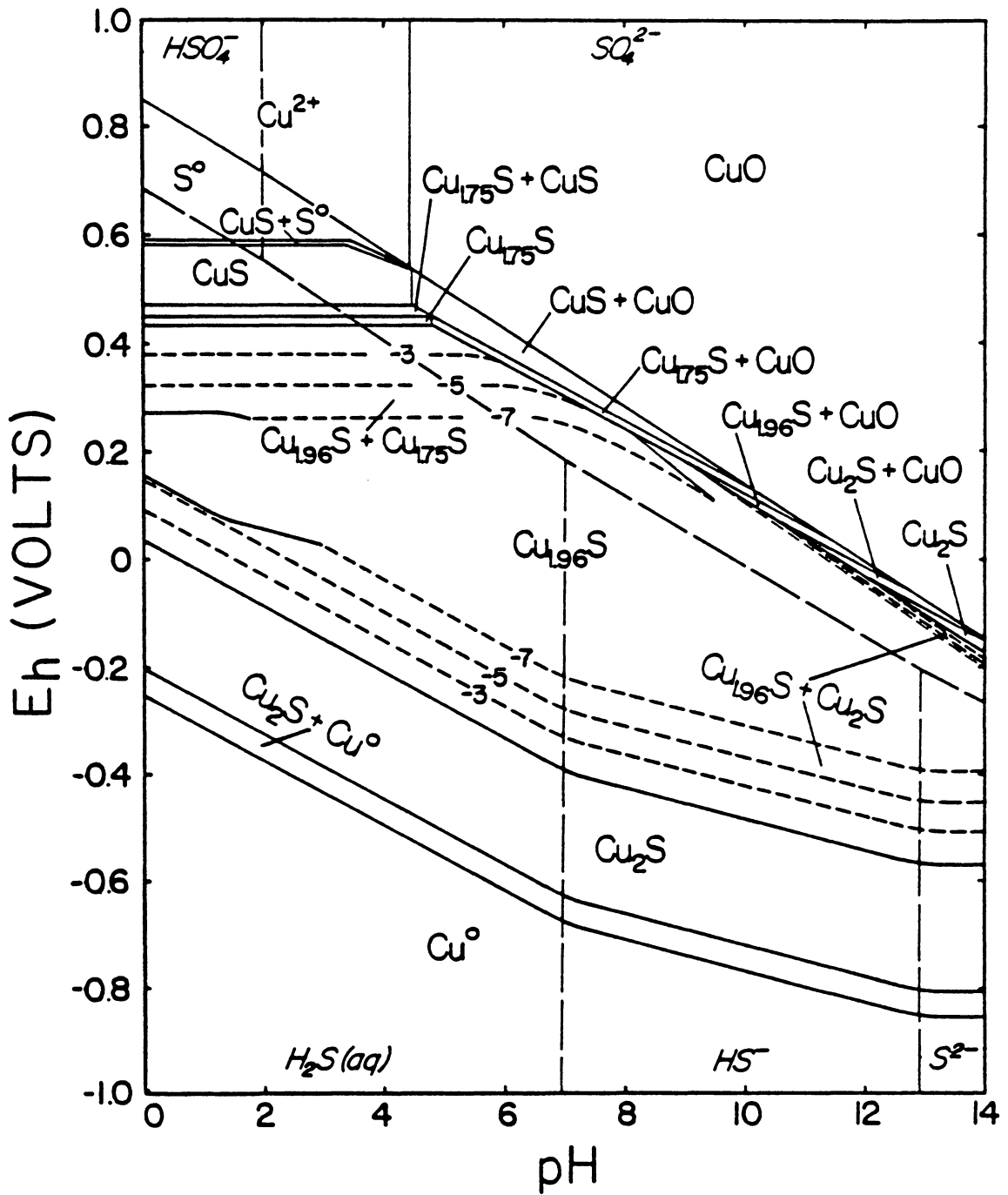
Figure 2.15 E_h-pH diagram depicting djurleite $(Cu_{1.96}S)$ oxidation to destabilized sulfate. See text for explanation of dashed lines.
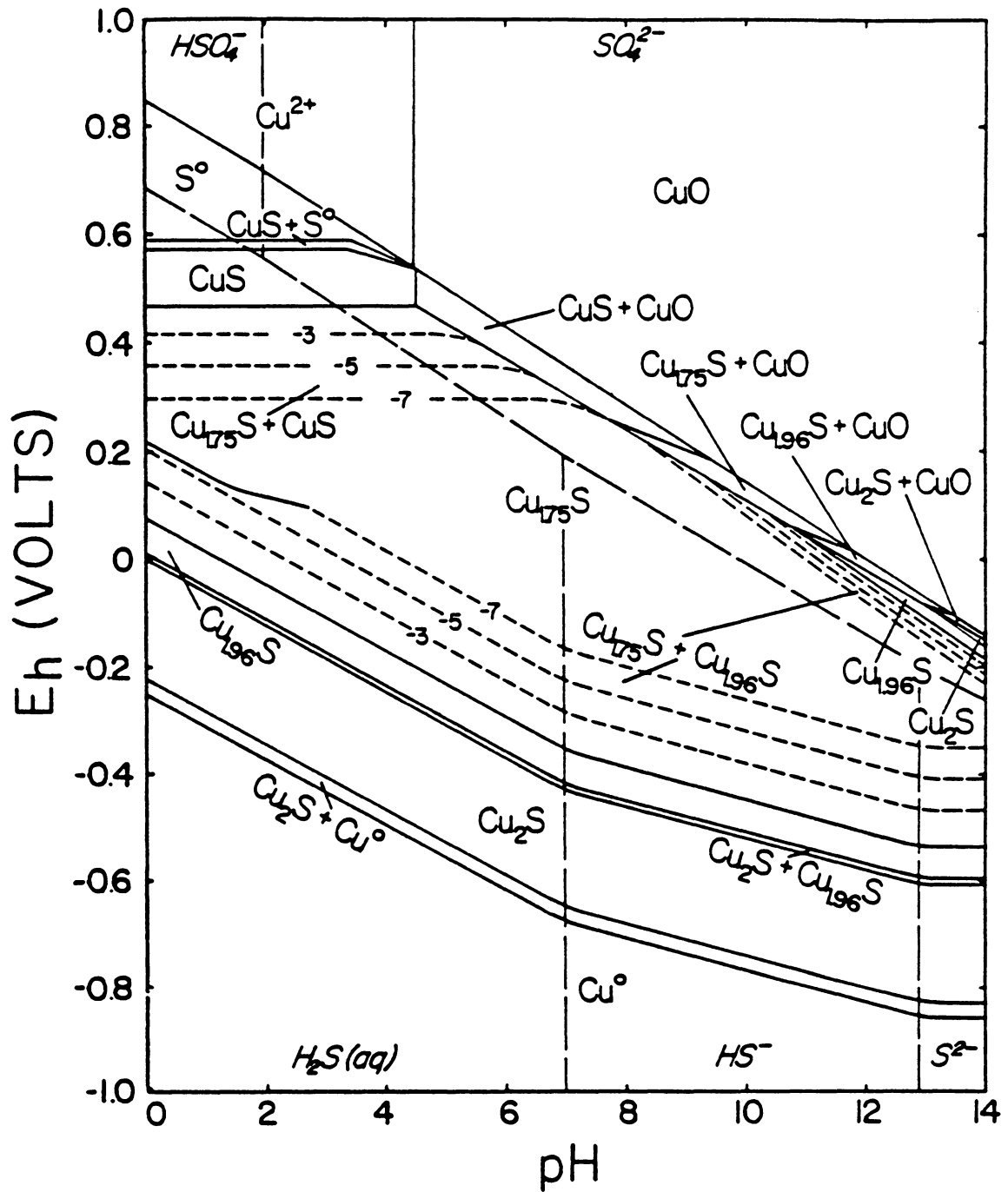
Figure 2.16   Eh-pH diagram depicting anilite ($Cu_{1.75}S$) oxidation to destabilized sulfate. See text for explanation of dashed lines.
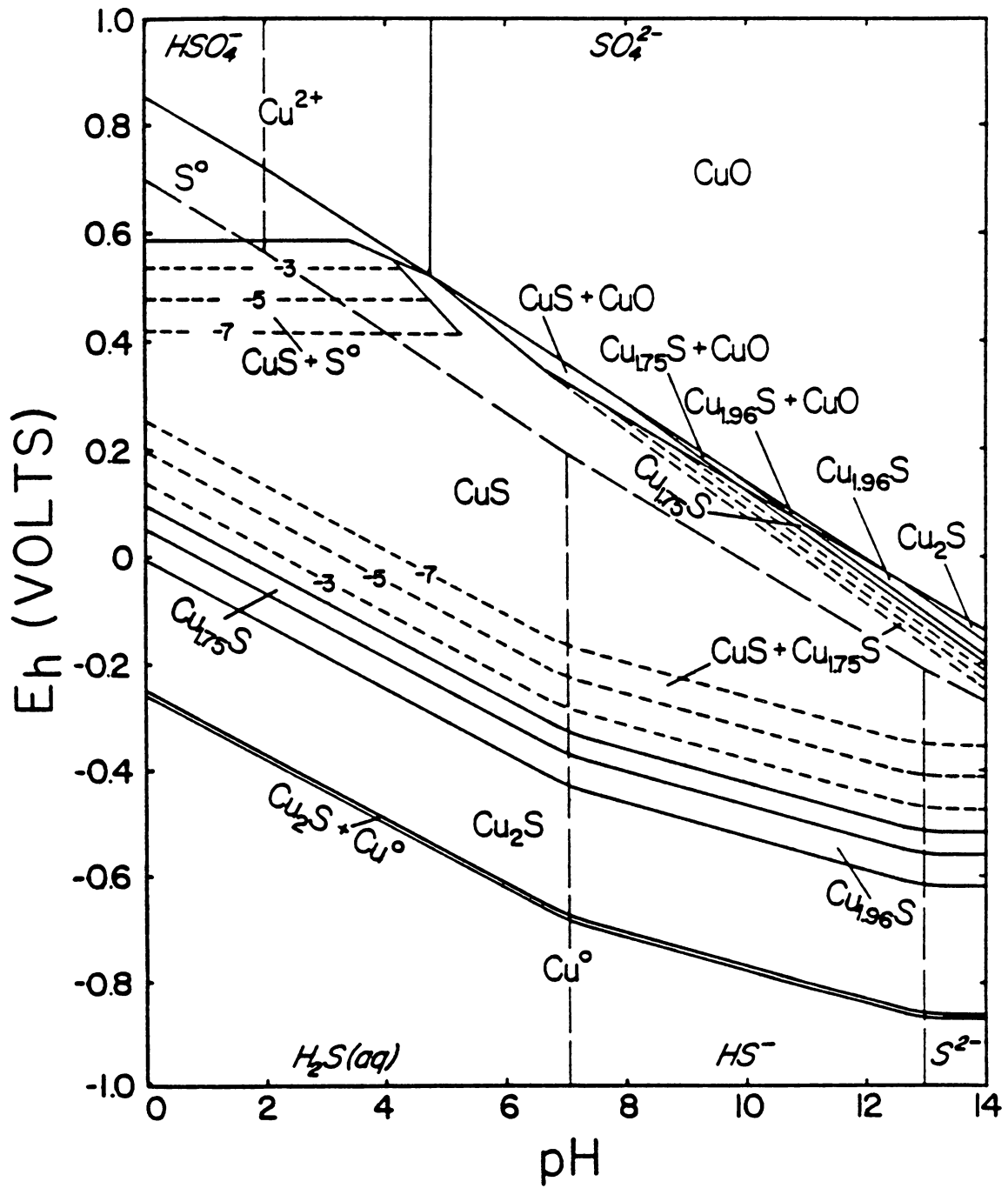
Figure 2.17   E$_h$-pH diagram depicting covellite (CuS)
oxidation to destabilized sulfate. See text
for explanation of dashed lines.

diagrams reveal extremely complex situations in which the starting mineral oxidizes, for the most part, to combinations of cupric oxide and copper sulfides.

These diagrams are in agreement with Eadington and Prosser (1969) who demonstrated that elemental sulfur was the primary oxidation product in acid solutions and that sulfate was in neutral solutions; however, they also showed thiosulfate was the major oxidation product under alkaline conditions. Peters (1986) also points out that other sulfur-oxy species such as thionates are formed. It therefore becomes difficult to assess whether these diagrams are as realistic as previous ones. Nevertheless, diagrams could be constructed to correspond with experimental results by destabilizing sulfur-oxy species that formed since their formation require overpotentials as well.

2.2.5 Metastable Copper Sulfides

From a geological point-of-view, the previous E_h-pH diagrams are important because they reflect how stable copper sulfides (chalcocite, djurleite, anilite, and covellite) are affected by both the copper/sulfur ratio and the final oxidation state of the sulfur. This would explain why one body of ore could have so many different copper sulfides present: localized concentrations within the ore body lead to the formation of individual minerals. However,

geological time scales are required for copper sulfides to oxidize to stable forms (Peters, 1984 and 1986) and so the short time scales encountered in mineral processing may not allow for the copper sulfide to adjust its crystal structure to a more stable form. This can account for the fact that more copper sulfides have been characterized than are known to be stable (see Table 1.1; Potter, 1977; Vaughan and Craig, 1978).

Koch and McIntyre (1976) identified four metastable copper sulfides during the oxidation of chalcocite. Because its crystal structure is not the same as stable covellite and its free energy is less negative, the CuS produced during the oxidation of chalcocite is metastable. E_h-pH diagrams are presented in Figures 2.18 through 2.20 for the oxidation of chalcocite to these metastable copper sulfides as elemental sulfur, thiosulfate, and destabilized sulfate are produced, respectively. Stable sulfate was not considered to be a product because the diagrams contained metastable species. Except the stoichiometries have changed and covellite exhibits a new stability region, there is no difference between these diagrams and those shown earlier.

Figures 2.18 and 2.20 are consistent with the behavior of chalcocite in acid solutions. Plots of the rest potentials observed during the oxidation of chalcocite as
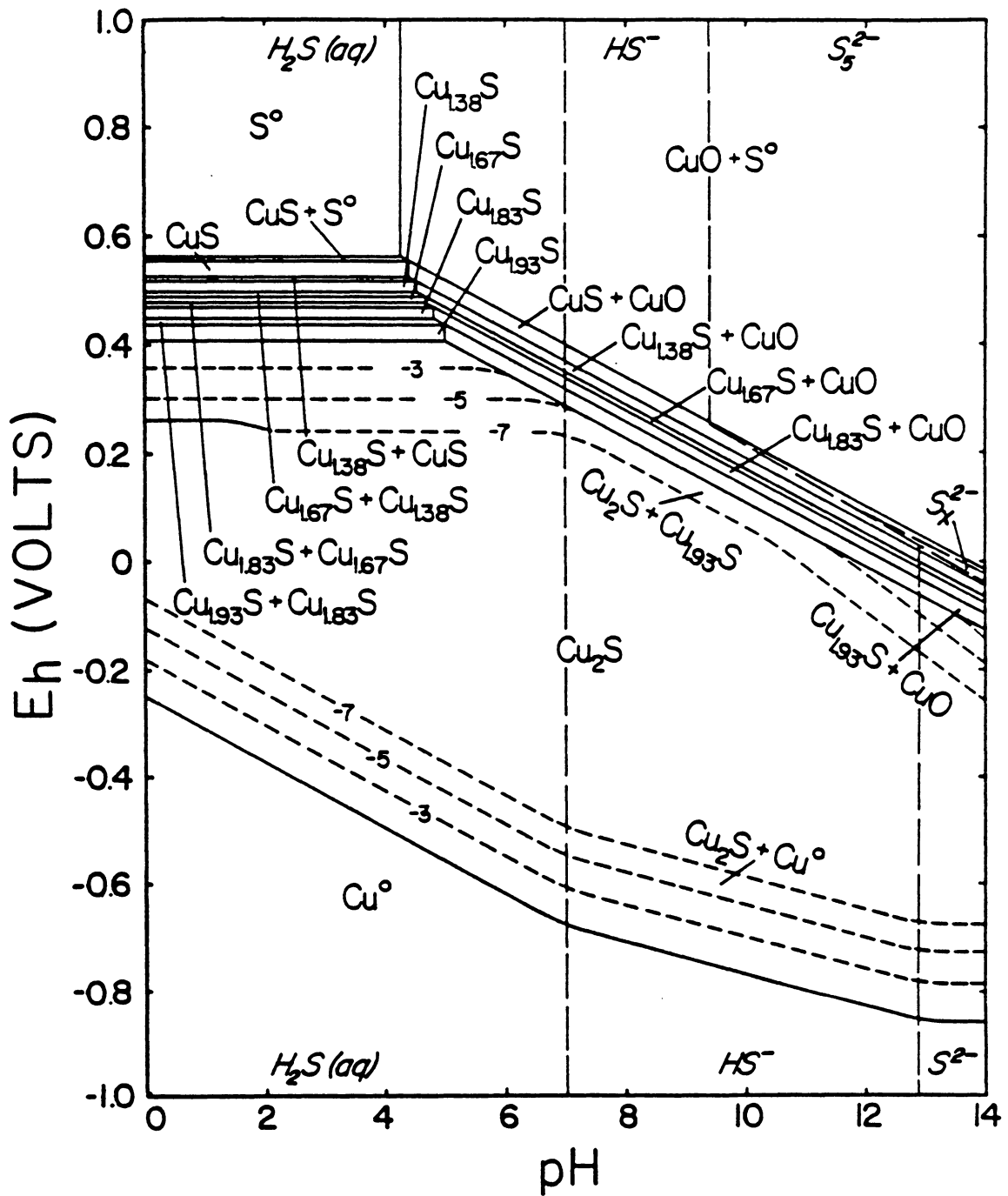
Figure 2.18 Eh-pH diagram depicting chalcocite (Cu₂S) oxidation to metastable copper sulfides and elemental sulfur. See text for explanation of dashed lines.
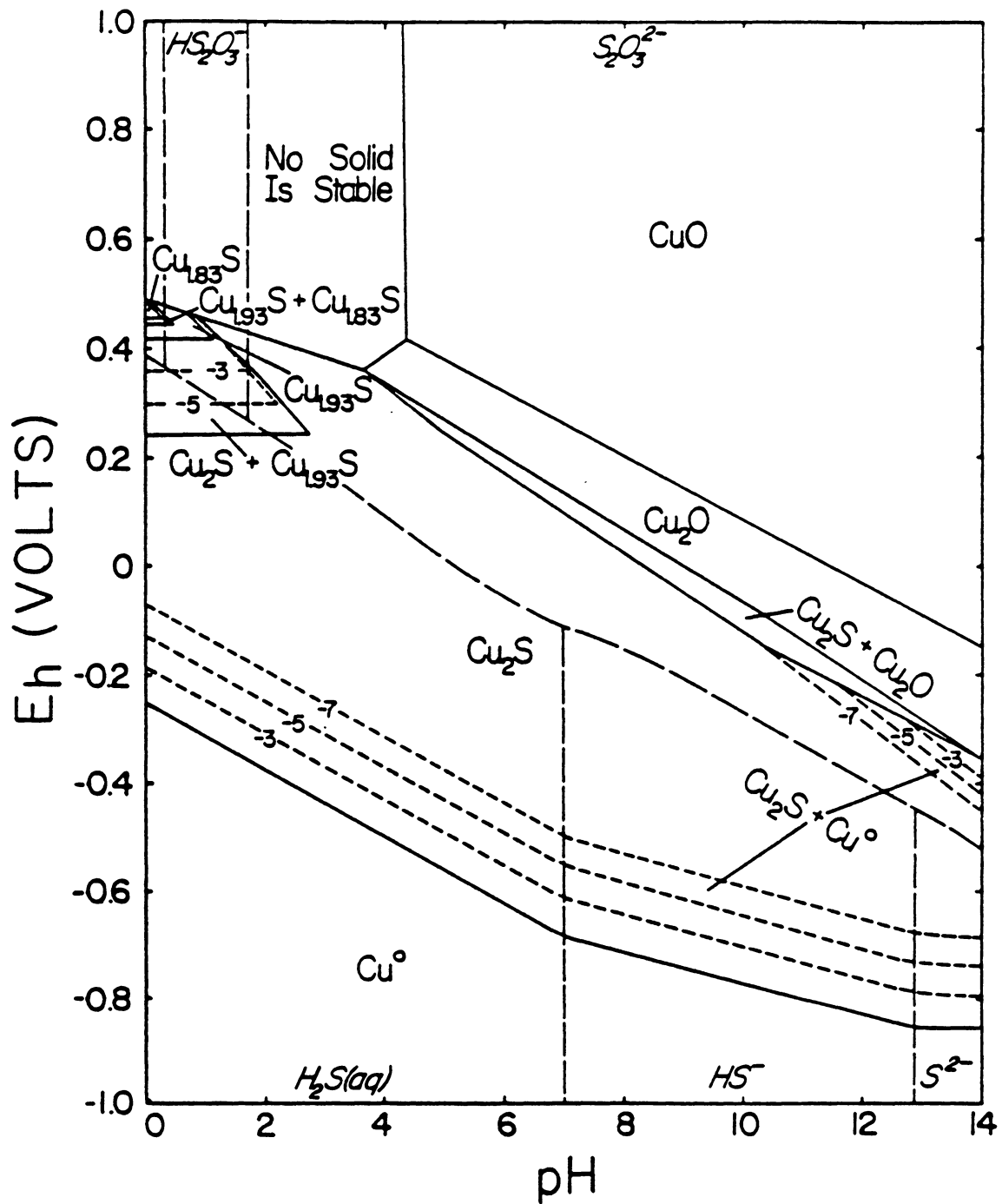
Figure 2.19 E_h-pH diagram depicting chalcocite (Cu_2S) oxidation to metastable copper sulfides and thiosulfate. See text for explanation of dashed lines.
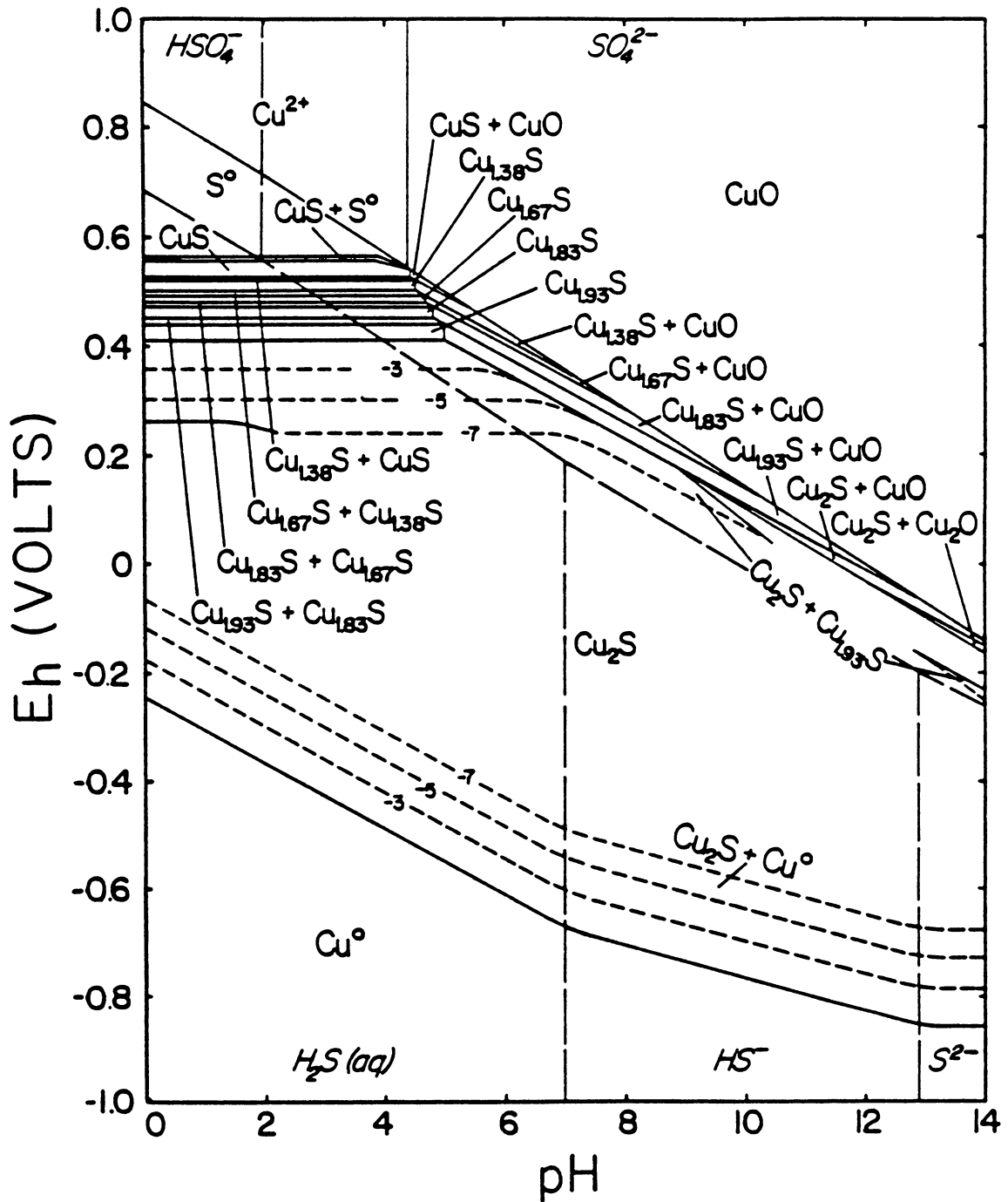
Figure 2.20 E_h-pH diagram depicting chalcocite (Cu_2S) oxidation to metastable copper sulfides and destabilized sulfate. See text for explanation of dashed lines.
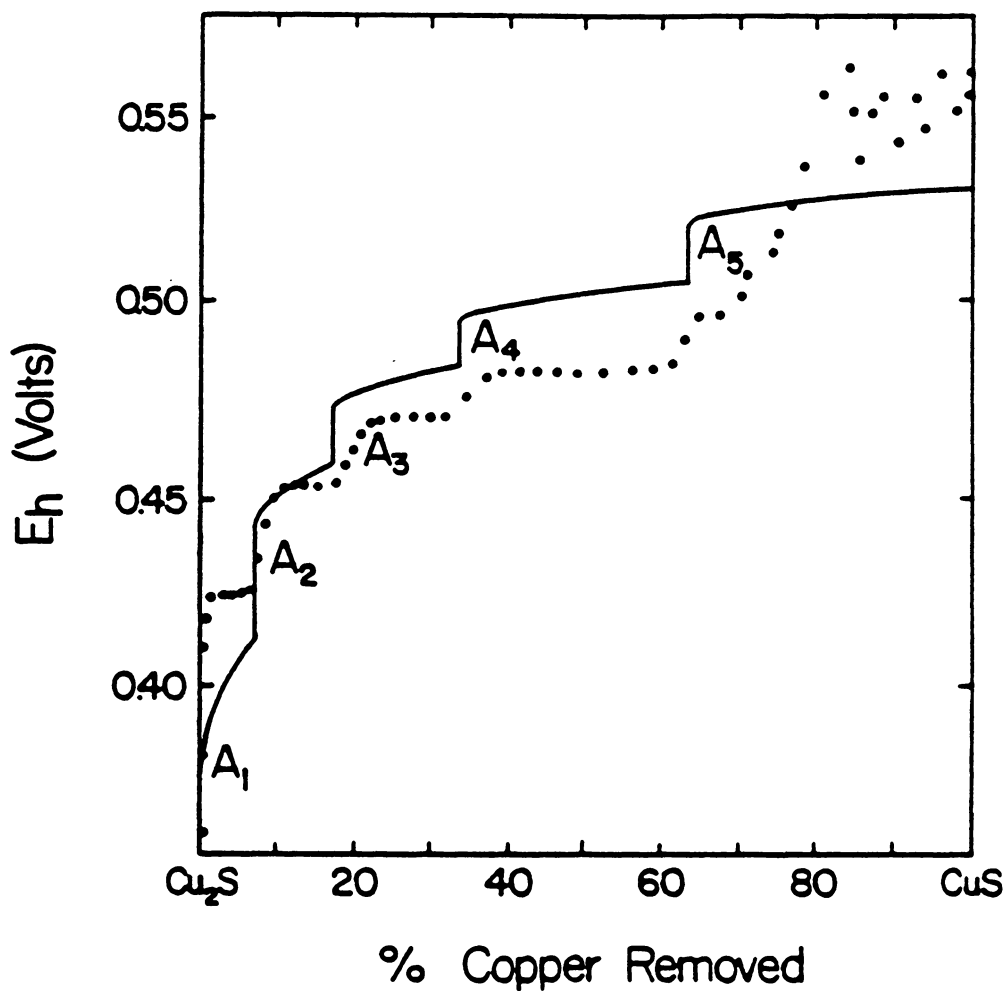
Figure 2.21 Comparison of calculated results obtained from
SOLGASWATER (————) to results obtained by Koch
and McIntyre, 1976 (●●●), as Cu_2S oxidized to
metastable copper sulfides and elemental sulfur.

determined by Koch and McIntyre and as predicted by the thermodynamic calculations are presented in Figure 2.21 to reveal this consistent behavior. The difference between the two plots can be attributed to the fact that Koch and McIntyre kept the cupric ion concentration constant to determine thermodynamic data.

The production of metastable copper sulfides from djurleite, anilite, or covellite have not been studied or have not been studied in detail. Thermodynamic data was therefore lacking so E_h-pH diagrams for these systems were not constructed.

2.3 E_h-pH Diagrams With Xanthate

Mass balanced E_h-pH diagrams have been constructed to depict possible reactions as chalcocite oxidizes to various oxidation states of sulfur: elemental sulfur, thiosulfate, and sulfate. Destabilized sulfate was not considered since it was difficult to assess whether destabilizing sulfate was more realistic. Except in the case for oxidation proceeding all the way to sulfate, only metastable copper sulfides were considered.

As before, solid lines indicate the appearance and disappearance of solid phases and short-dashed lines signify the co-existence of chalcocite and various quantities of a second phase. Because the presence of xanthate did not

affect the equilibrium between aqueous sulfur-bearing species, long-dashed lines shown in earlier E_h-pH diagrams were not used. However, a dotted line is used to show the amount of copper xanthates which, for the purpose of the calculations, is assumed to be solely responsible for the flotation of chalcocite although dixanthogen or chemisorbed xanthate may play a significant role. Because it is not known what amount of copper xanthate is required for flotation, all quantities of co-existing solids, even those less than 1% of a monolayer, were considered. Shaded areas in the diagrams indicate stability regions for the copper xanthates with cuprous xanthate, CuX, stable at lower potentials and cupric xanthate, CuX_2, stable at upper potentials. The lowest and highest potential to which a copper xanthate is stable defines the lower and upper flotation edges, respectively. When it is necessary to distinguish between the copper xanthates, cupric or cuprous xanthate will be stated; otherwise, they will collectively be called copper xanthate.

2.3.1 Elemental Sulfur

An E_h-pH diagram is presented in Figure 2.22 for the oxidation of chalcocite to metastable copper sulfides and elemental sulfur in the presence of 10^{-5} M xanthate. The shape of the copper xanthate stability region is remarkably
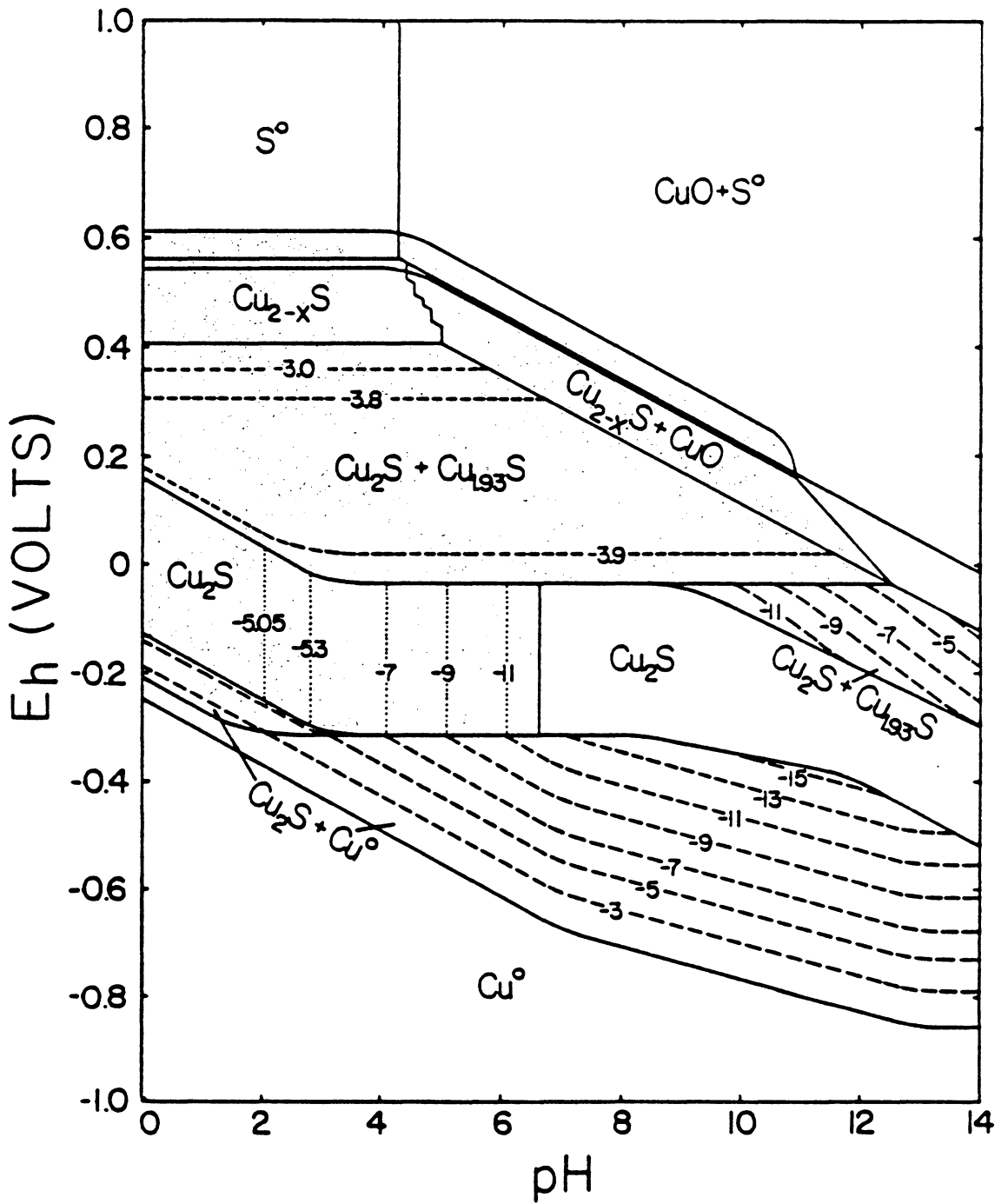
Figure 2.22 E_h-pH diagram depicting chalcocite (Cu_2S) oxidation to metastable copper sulfides and elemental sulfur in the presence of 10^{-5} M xanthate. Shaded region indicates copper xanthate stability regions. See text for explanation of dashed and dotted lines.

similar to the lead xanthate stability region calculated by Pritzker (1985) for galena oxidizing to elemental sulfur. This suggests that xanthate reactions with chalcocite may be like those with galena.

Comparing Figure 2.22 with 2.18 shows that the metallic copper stability region decreases in the presence of xanthate suggesting that the following reaction occurs:

$$Cu^0 + X^- = CuX + e. \qquad [2.15]$$

In fact, the amount of cuprous xanthate formed is exactly equivalent to the amount of metallic copper taken up as illustrated by the intersections of the dotted lines (i.e., amounts of cuprous xanthate) and dashed lines (i.e., amounts of metallic copper). As proposed by Basilio (1985), metallic copper and chalcocite must co-exist in order for Reaction [2.15] to occur (viz. -320 mV vs. SHE is well within the stability domain of chalcocite). Further comparison of the two figures reveals that the stability region of $Cu_{1.93}S$ increases in the presence of xanthate. This indicates the following oxidation reaction takes place:

$$Cu_2S + .07X^- = Cu_{1.93}S + .07CuX + .07e. \qquad [2.16]$$
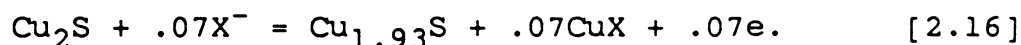
A general reaction comprising Reaction [2.16] was conceived by Paterson and Salman (1968) and later restated by Richardson et al. (1984). Similiar analyses are used to
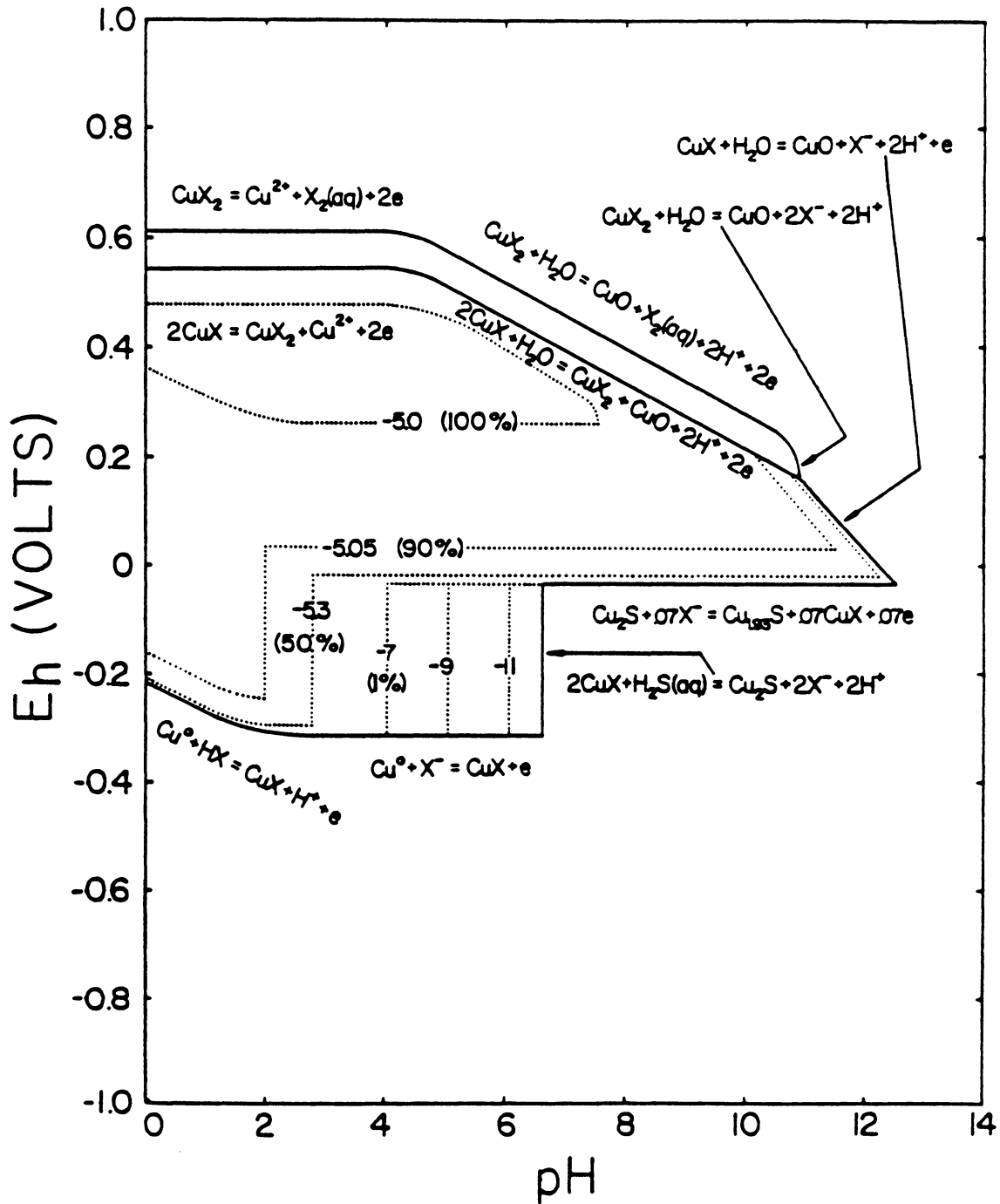
Figure 2.23 E_h-pH diagram showing the amounts of copper
xanthate formed and the reactions controlling
their formation as chalcocite (Cu_2S) oxidizes
to metastable copper sulfides and elemental
sulfur in the presence of 10^{-5} M xanthate.
See text for explanation of dotted lines.

determine what other reactions control copper xanthate formation. At the lower flotation edge, these reactions include Reactions [2.15], [2.16] and the following:

$$Cu_2S + 2X^- + 2H^+ = 2CuX + H_2S(aq).$$ [2.17]
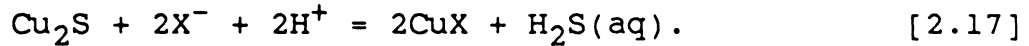
Reactions [2.16] and [2.17] involve sulfur species and should, therefore, be dependent on the sulfur oxidation state. On the other hand, reactions near the upper flotation edge involve only the copper xanthates with, depending on the pH, cupric ions or oxide and are, thus, independent of the sulfur oxidation state.

All of the reactions mentioned above also control the amount of copper xanthate formed. For examples, Reaction [2.17] is the E_h-independent reaction responsible for the amounts of cuprous xanthate shown in Figure 2.22 and, as previously discussed, Reaction [2.15] controls the amount of cuprous xanthate at the lower flotation edge. The cuprous xanthate amounts are better illustrated in Figure 2.23 which also shows the reactions that control the formation of the copper xanthates. Furthermore, the percentage of xanthate which formed the copper xanthates are indicated.

2.3.2 Thiosulfate

Chalcocite oxidation to metastable copper sulfides and thiosulfate in the presence of 10^{-5} M xanthate is depicted

by the E_h-pH diagram in Figure 2.24. As before, the shape
of the copper xanthate stability region is similar to the
lead xanthate stability region calculated by Pritzker (1985)
for galena oxidizing to thiosulfate. Compared to the
oxidation to elemental sulfur, the copper xanthate stability
region is larger for thiosulfate. This is due to the
sulfur-dependent reactions, i.e., Reactions [2.16] and [2.17],
being affected by the formation of the more stable
thiosulfate: under basic conditions, Reaction [2.16] no
longer occurs because chalcocite oxidation proceeds to
thiosulfate instead of nonstoichiometric copper sulfides,

$$2Cu_2S + 4X^- + 3H_2O = 4CuX + S_2O_3^{2-} + 6H^+ + 8e, \qquad [2.18]$$
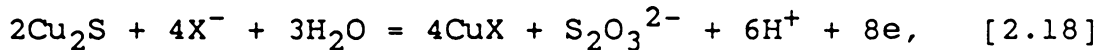
and Reaction [2.17] occurs to a lesser extent because of the
equilibrium between thiosulfate and aqueous hydrogen
sulfide. Thiosulfate formation also leads to the appearance
of cuprous oxide and metallic copper as oxidation products,
both of which react with xanthate to yield cuprous xanthate.
As discussed earlier, metallic copper is the only reactant
to form cuprous xanthate as evidenced by the equal amounts
of the two species along the lower flotation edge. Since
sulfur-dependent reactions only occur at the lower flotation
edge, it was expected and is apparent that only the lower
flotation edge was affected by thiosulfate formation;
however, a very small change did occur at the upper
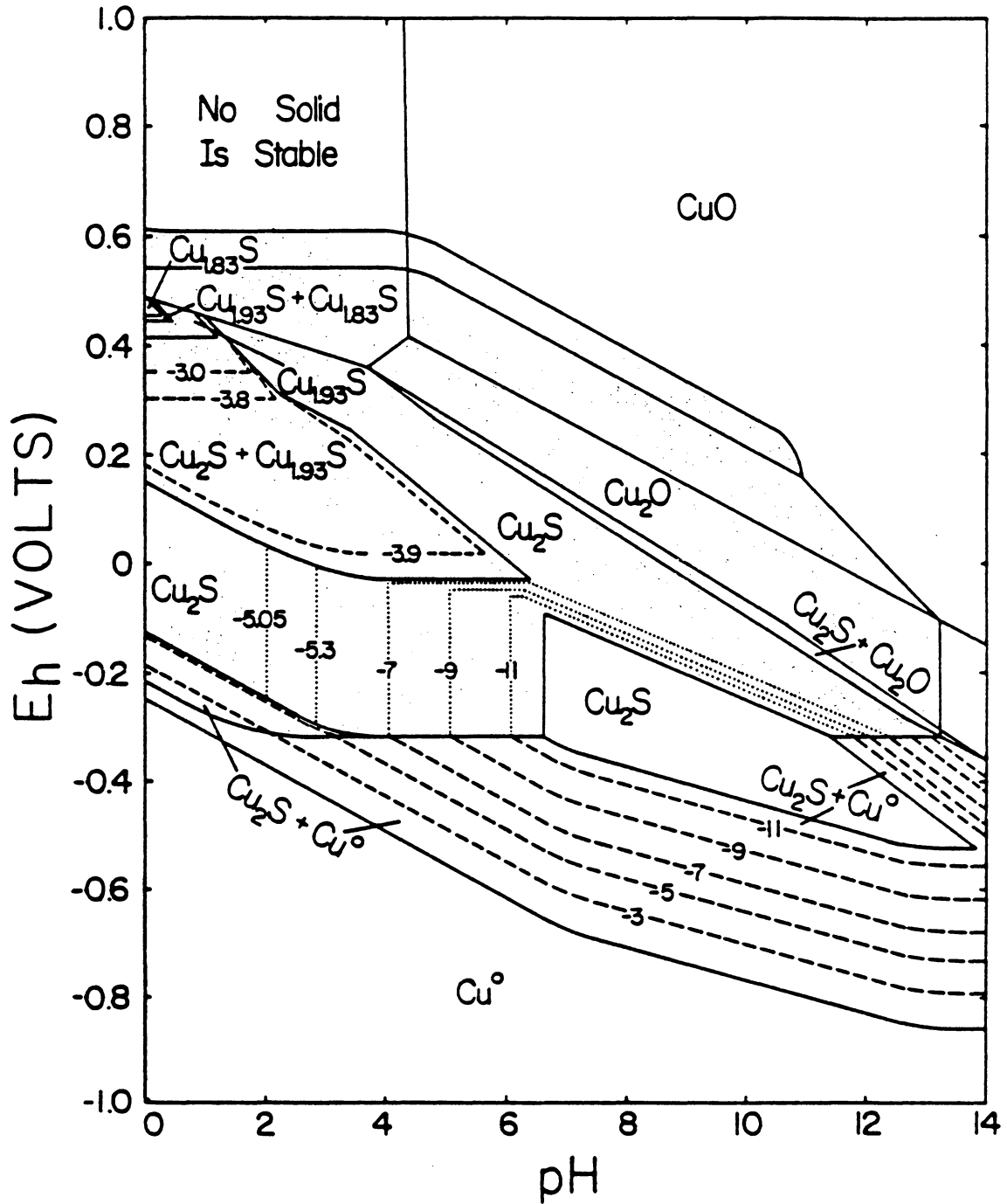
Figure 2.24 E_h-pH diagram depicting chalcocite (Cu_2S) oxidation to metastable copper sulfides and thiosulfate in the presence of 10^{-5} M xanthate. Shaded region indicates copper xanthate stability regions. See text for explanation of dashed and dotted lines.
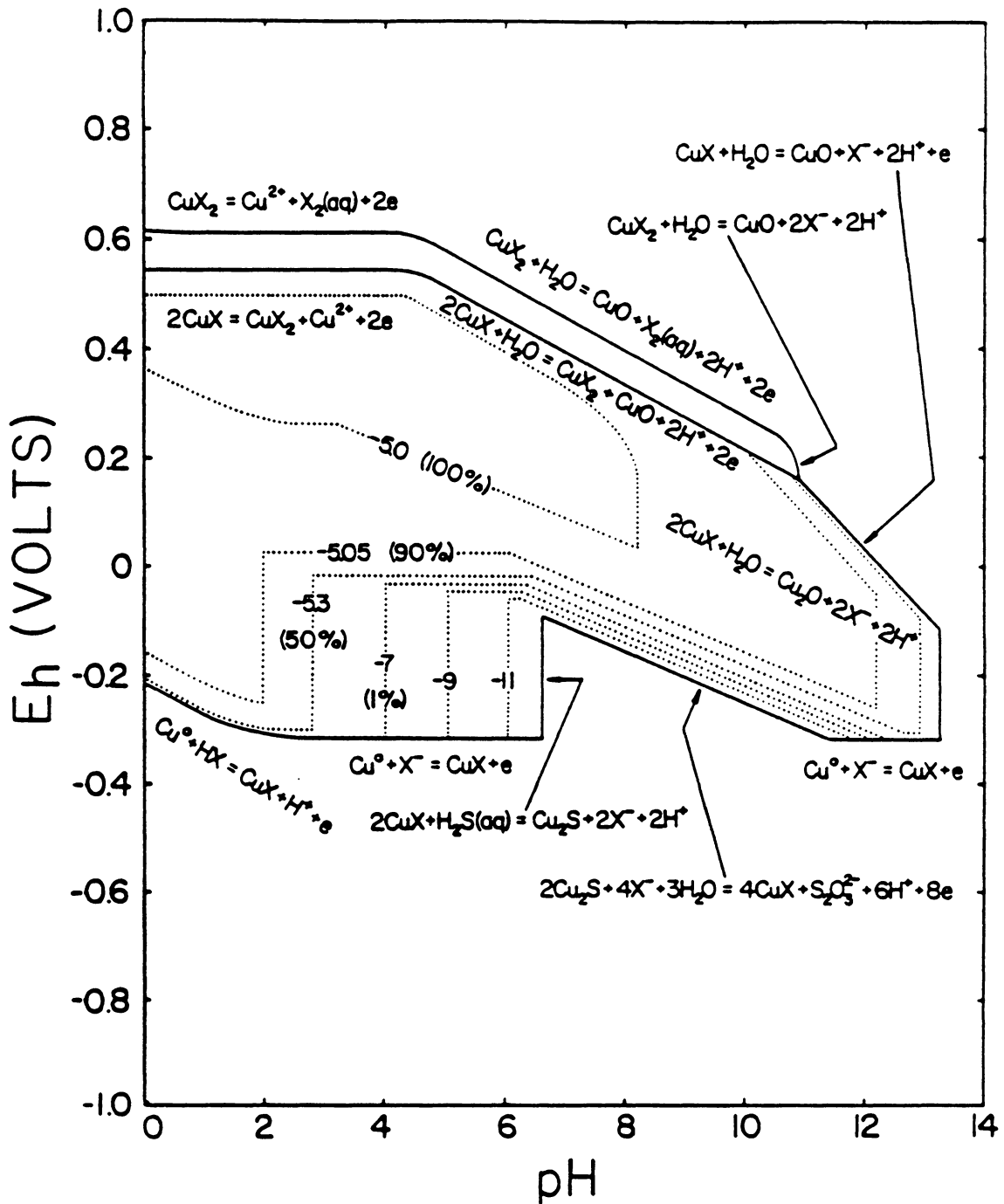
Figure 2.25 Eh-pH diagram showing the amounts of copper
xanthate formed and the reactions controlling
their formation as chalcocite (Cu_2S) oxidizes
to metastable copper sulfides and thiosulfate
in the presence of 10^{-5} M xanthate. See text
for explanation of dotted lines.

flotation edge where, under acidic conditions, cupric ions are in equilibrium with aqueous copper-thiosulfate species. All of these reactions are shown in Figure 2.25 along with cuprous xanthate amounts which were increased due to the change in sulfur oxidation state.

2.3.3 Sulfate

Chalcocite oxidation to sulfate in the presence of 10^{-5} M xanthate is illustrated in Figures 2.26 and 2.27. Metastable copper sulfides were not considered since sulfate is a stable species. Once again, the shape of the copper xanthate stability region is similar to the lead xanthate stability region calculated by Pritzker (1985) for galena oxidizing to sulfate. As before, only the sulfur-dependent reactions are affected by sulfate formation resulting in an enlarged copper xanthate stability region at the lower flotation edge. Oxidation now proceeds to sulfate, the most stable oxidation state of sulfur, according to the reaction

$$Cu_2S + 2X^- + 4H_2O = 2CuX + SO_4^{2-} + 8H^+ + 8e. \qquad [2.19]$$
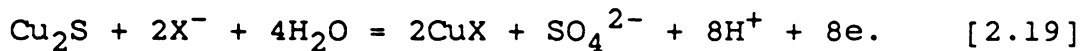
Compared to elemental sulfur and thiosulfate formation, Reaction [2.17] occurs to a lesser extent because of sulfate equilibrium with aqueous hydrogen sulfide. Also, cuprous xanthate amounts are even larger. Basilio (1985) failed to see both Reactions [2.17] and [2.19] in his mass-balanced
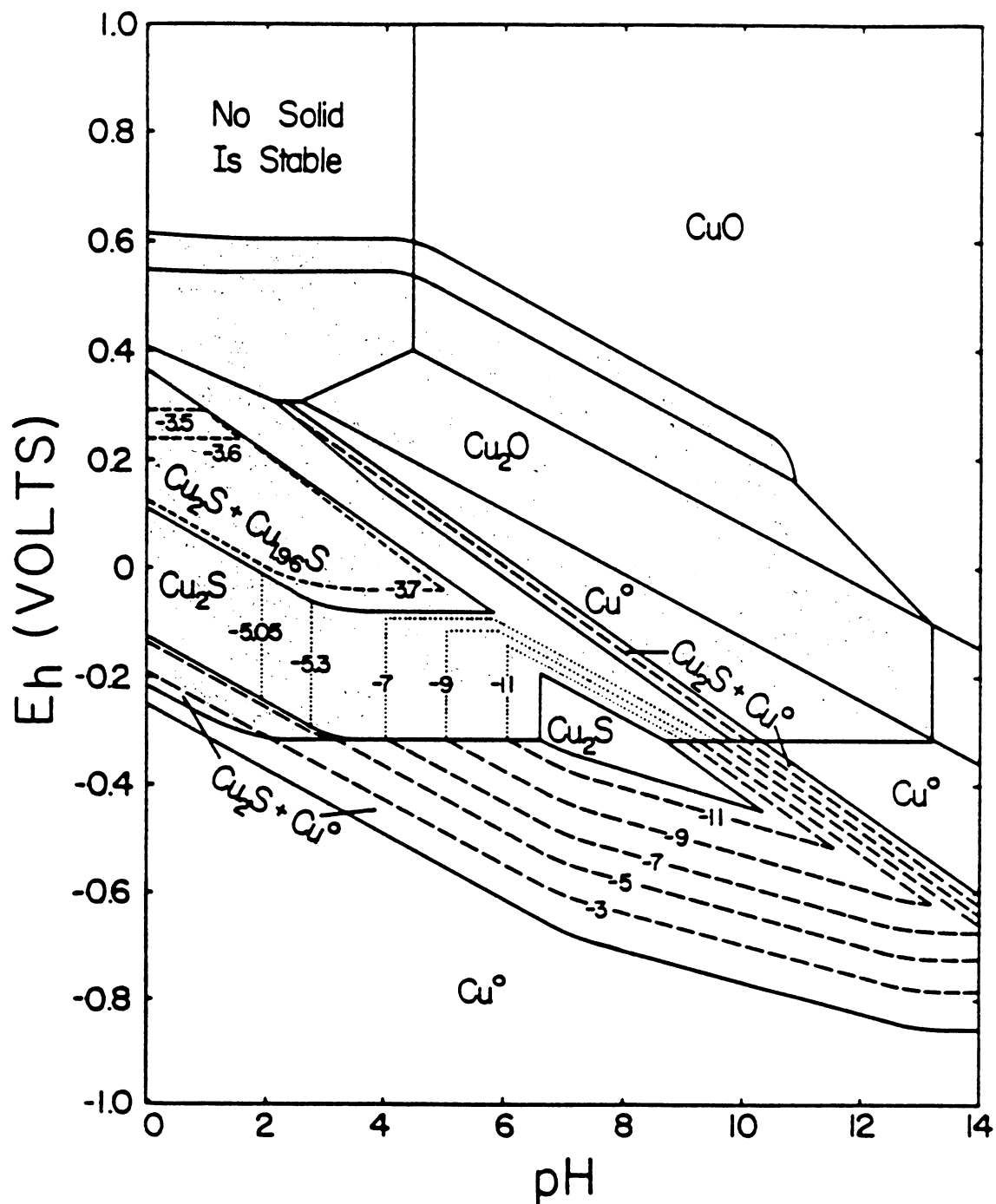
Figure 2.26 E_h-pH diagram depicting chalcocite (Cu_2S) oxidation to stable copper sulfides and sulfate in the presence of 10^{-5} M xanthate. Shaded region indicates copper xanthate stability regions. See text for explanation of dashed and dotted lines.

$CuX_2 = Cu^{2+} + X_2(aq) + 2e$

$2CuX = CuX_2 + Cu^{2+} + 2e$

$CuX_2 + H_2O = CuO + X_2(aq) + 2H^+ + 2e$

$CuX + H_2O = CuO + X^- + 2H^+ + e$

$CuX_2 + H_2O = CuO + 2X^- + 2H^+$

$2CuX + H_2O = CuX_2 + CuO + 2H^+ + 2e$

$2CuX + H_2O = Cu_2O + 2X^- + 2H^+$

-50

(100 %)

-5.05 (90%)

-5.3

(50%)

-7

(1%)

-9

-11

$Cu^0 + HX = CuX + H^+ + e$

$Cu^0 + X^- = CuX + e$

$Cu^0 + X^- = CuX + e$

$Cu_2S + 2X^- + 4H_2O = 2CuX + SO_4^{2-} + 8H^+ + 8e$

$2CuX + H_2S(aq) = Cu_2S + 2X^- + 2H^+$
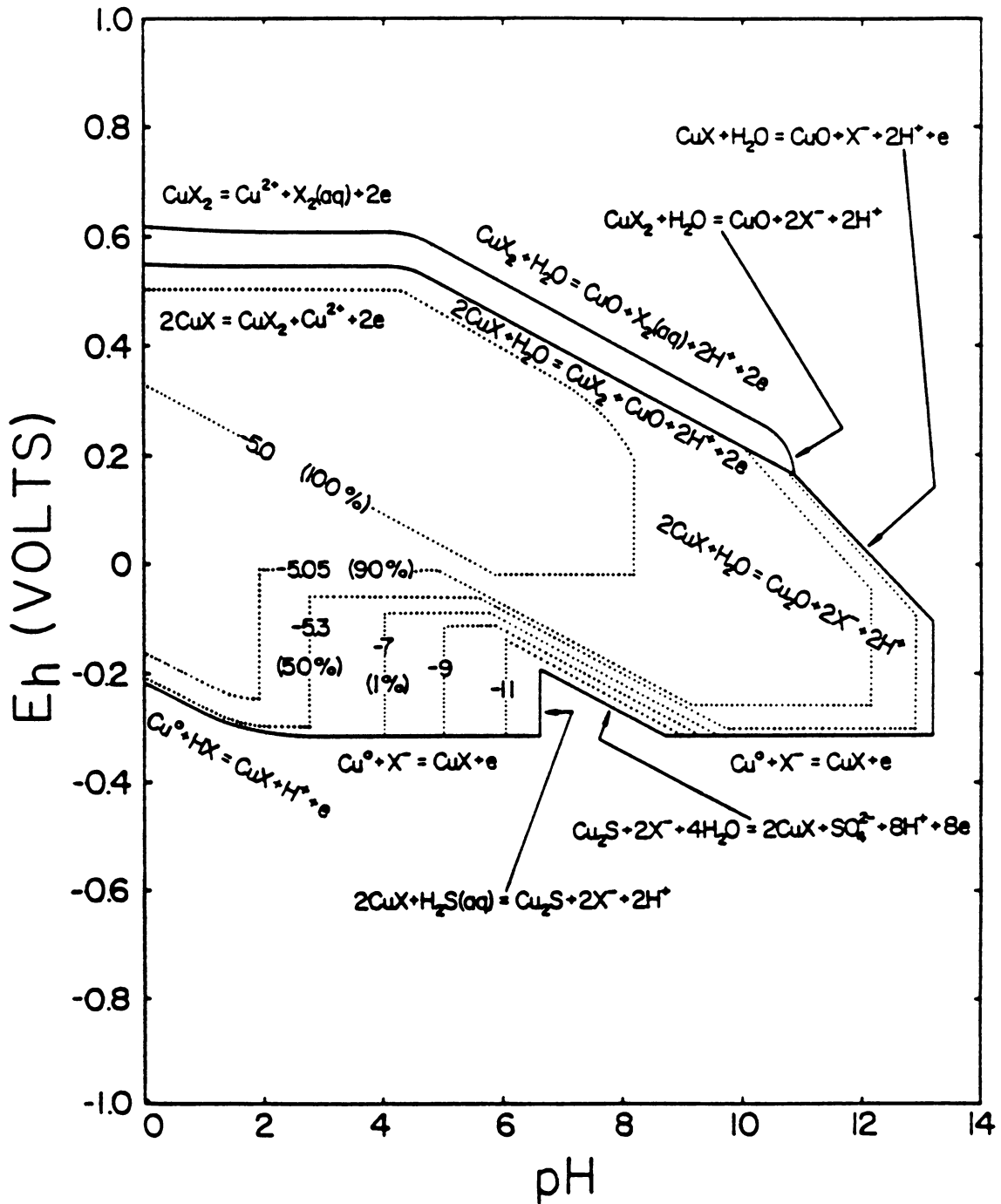
Figure 2.27 E_h-pH diagram showing the amounts of copper
xanthate formed and the reactions controlling
their formation as chalcocite (Cu_2S) oxidizes
to stable copper sulfides and sulfate in the
presence of 10^{-5} M xanthate. See text for
explanation of dotted lines.

calculations. Furthermore, the upper flotation edge remained the same except for a small change, once again, under acidic conditions where cupric ions and aqueous copper sulfate are in equilibrium.

2.3.4 Metallic Copper

Since chalcocite reduces to metallic copper and aqueous sulfide species and since aqueous sulfide species are in equilibrium with gaseous hydrogen sulfide which, when produced, is lost to the system, only metallic copper would exist on the particle surface and, therefore, only metallic copper would be available to the system. In effect, sulfur-dependent reactions become nonexistant and a copper-water system results. Therefore, an E_h-pH diagram for copper in the presence of 10^{-5} M xanthate is presented in Figure 2.28. Compared to previous diagrams, the upper flotation edge is unchanged and the lower flotation edge is totally dependent on Reaction [2.15], uninhibited by aqueous sulfur species. Because there is no sulfur in the system, the cuprous xanthate stability domain has increased. Hepel and Pomianowski (1977) performed similar calculations.

2.4 Further Discussion

Since the calculations are mass-balanced, contour plots showing the effect of E_h, pH, and sulfur oxidation state
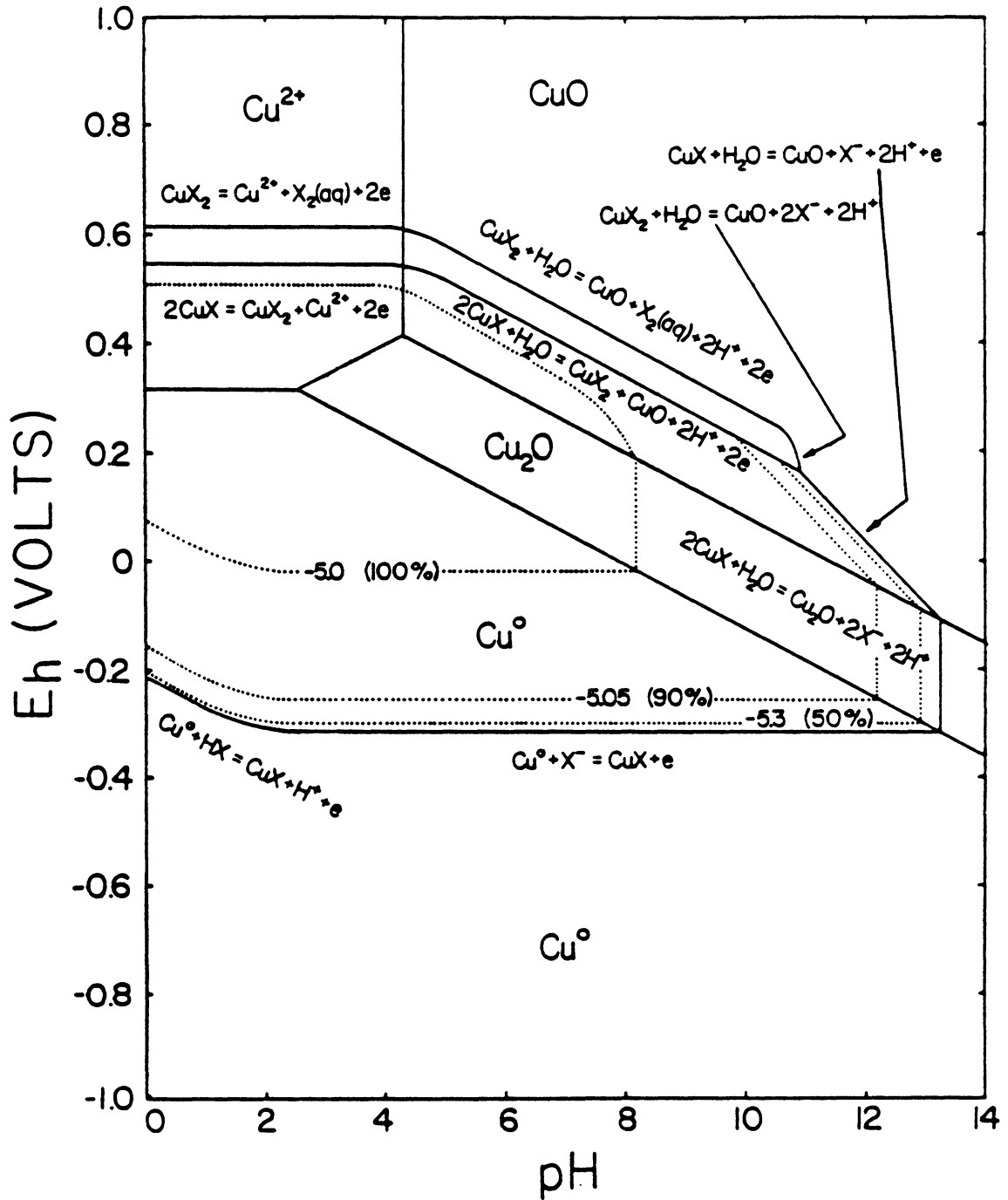
Figure 2.28 E_h-pH diagram showing the amounts of copper
xanthate formed and the reactions controlling
their formation as metallic copper oxidizes in
the presence of 10^{-5} M xanthate. See text for
explanation of dotted lines.

have been shown for the amounts of solids (i.e., co-existence) and can also be determined for aqueous species. Also, the percentage of xanthate which reacted to form copper xanthates can be examined as a function of E_h, pH, and sulfur oxidation state and then compared to actual flotation data.

2.4.1 Contour Plots

If the following reaction proceeded all the way to the right at a xanthate concentration of 10^{-5} M, the sulfide ion concentration would be half that of the xanthate:

$$Cu_2S + 2X^- = 2CuX + S^{2-}. \qquad [2.20]$$

Thermodynamically, however, the reaction can only proceed to the right if the sulfide ion concentration is less than $10^{-19.2}$ M. Protonation and oxidation reactions of the sulfide ion must then occur if any cuprous xanthate is to form. These reactions include the following:

$$S^{2-} + 2Cu^0 = Cu_2S + 2e, \qquad [2.21]$$

$$xS^{2-} + (2-x)Cu_2S = 2Cu_{2-x}S + 2xe, \qquad [2.22]$$

$$S^{2-} + 2H^+ = H_2S(aq), \qquad [2.23]$$

$$2S^{2-} + 3H_2O = S_2O_3^{2-} + 6H^+ + 8e, \text{ and} \qquad [2.24]$$

$$S^{2-} + 4H_2O = SO_4^{2-} + 8H^+ + 8e. \qquad [2.25]$$
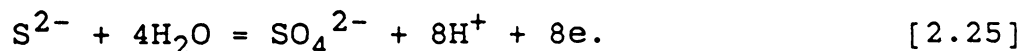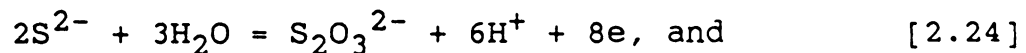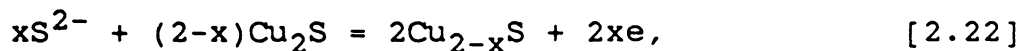
Adding these reactions to Reaction [2.20] results in the

reactions which control the lower flotation edge, i.e., Reactions [2.15] through [2.19]. Reaction [2.20] should then be the key reaction responsible for the formation of cuprous xanthate. Contour plots of the sulfide ion concentration are, therefore, shown in Figures 2.29 to 2.31 for the oxidation to elemental sulfur, thiosulfate, and sulfate, respectively. In each of these plots, the dashed line indicates the maximum concentration of sulfide ions (i.e., $10^{-19.2}$ M) allowable for cuprous xanthate to form. For the most part, this line corresponds exactly with the lower flotation edge in previous diagrams, thereby indicating that Reaction [2.20] controls the formation of CuX at the lower flotation edge. Furthermore, sulfide ions are known to depress xanthate flotation of sulfide minerals.

Obviously, Reaction [2.20] will be affected by changes in xanthate concentrations. Increasing the xanthate concentration will increase the maximum allowable sulfide ion concentration for cuprous xanthate formation which, in effect, will lower the lower flotation edge. For example, increasing the xanthate concentration to 10^{-4} M allows for a maximum sulfide ion concentration of $10^{-17.2}$ M. From the contour plots, $10^{-17.2}$ M occurs at lower potentials than $10^{-19.2}$ M. Therefore, increasing the xanthate concentration will expand the copper xanthate stability region. A decrease will have the opposite effect. In either case, all
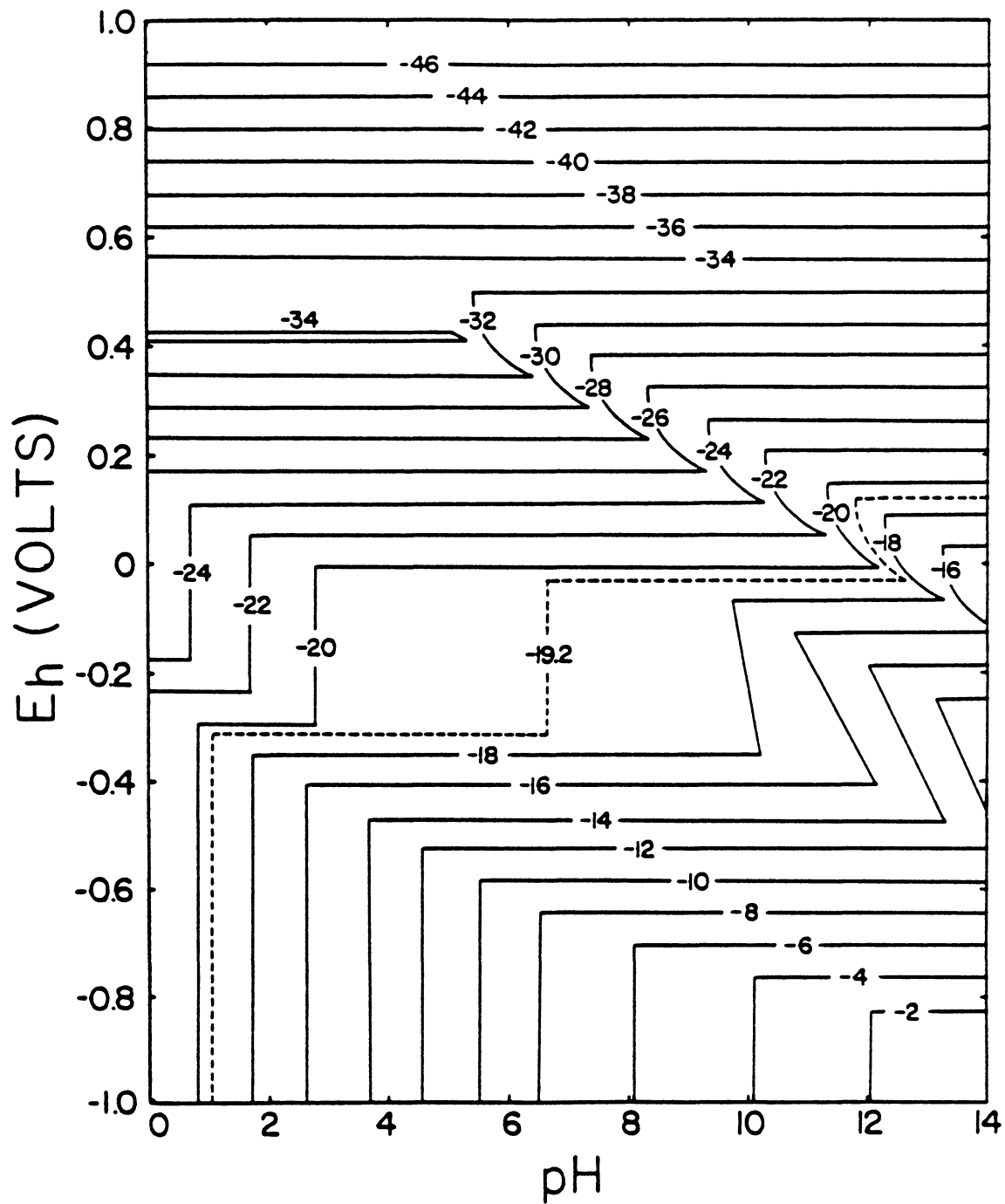
Figure 2.29   Contour plot of [S^{2-}] during chalcocite (Cu_2S) oxidation to metastable copper sulfides and elemental sulfur in the presence of 10^{-5} M xanthate.
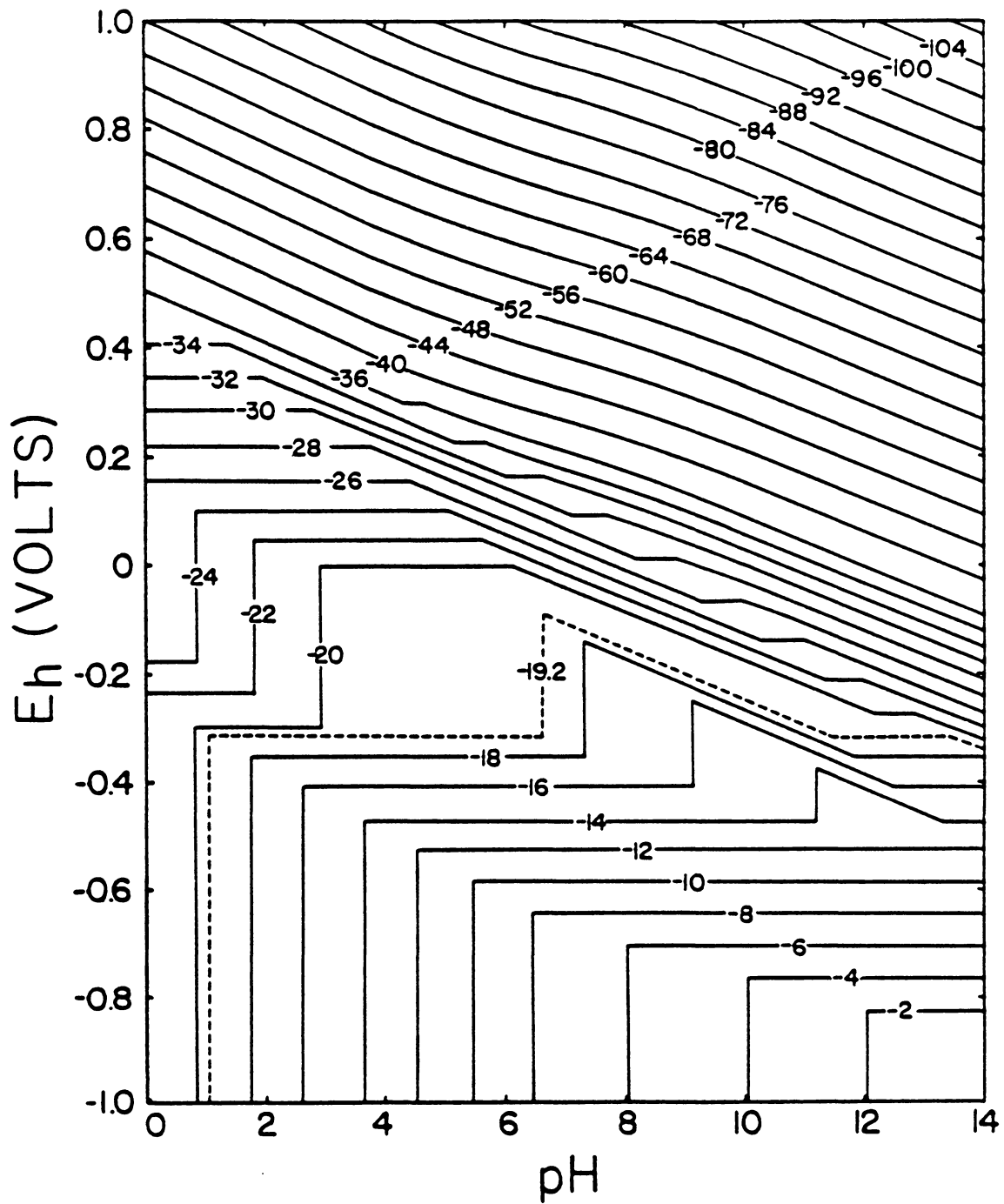
Figure 2.30   Contour plot of [S^{2-}] during chalcocite (Cu_2S) oxidation to metastable copper sulfides and thiosulfate in the presence of 10^{-5} M xanthate.
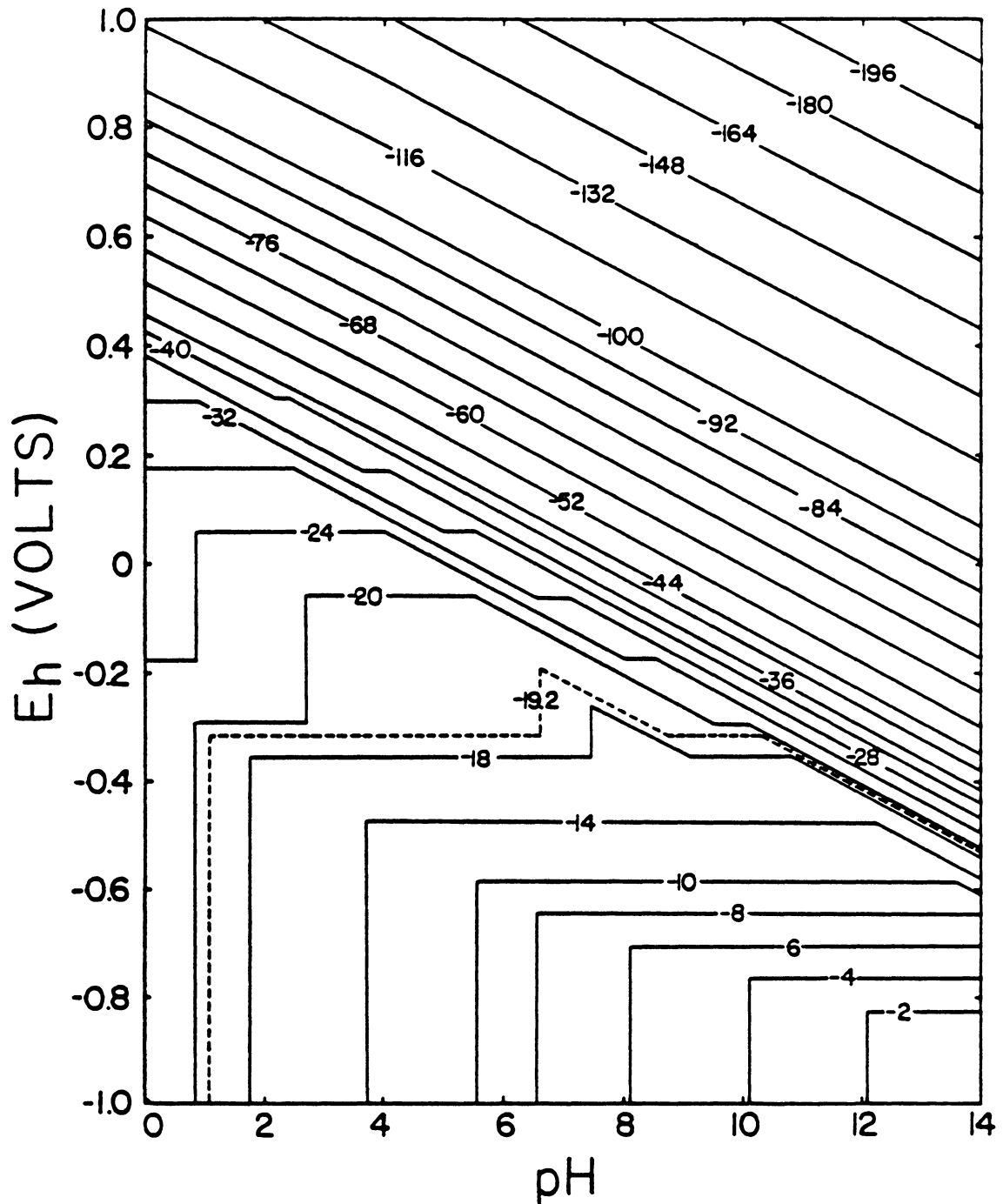
Figure 2.31   Contour plot of $[S^{2-}]$ during chalcocite (Cu_2S) oxidation to stable copper sulfides and sulfate in the presence of 10^{-5} M xanthate.

reactions which limit the formation of copper xanthate should be relatively the same.

It is interesting to note that a contour line changes its slope when a new equilibrium reaction starts to take place; especially equilibrium reactions between co-existing solids. Under acidic and reducing conditions, the sulfide ion concentration is not affected by the sulfur oxidation state. Under basic and oxidizing conditions, however, the contour plots change with the sulfur oxidation state. In Figure 2.29, eventhough polysulfides were stated not to have any significant concentration, polysulfide equilibrium with sulfide ions is recognizable under basic conditions near -0.2 V vs. SHE. In fact, comparing Figures 2.29 and 2.22 reveals that the polysulfides are responsible for the formation of the extremely small amounts of metallic copper (i.e., 10^{-13} and 10^{-15}) which were not found when oxidation proceeded to thiosulfate or sulfate.

2.4.2 Effect of E_h

Figures 2.32 to 2.34 show the effect of E_h on the percents of copper xanthates formed at various pH values for chalcocite oxidation to elemental sulfur, thiosulfate, and sulfate, respectively. The effect of E_h for the oxidation of metallic copper is shown in Figure 2.35. Each of the figures show that the plots begin to rise from the lower
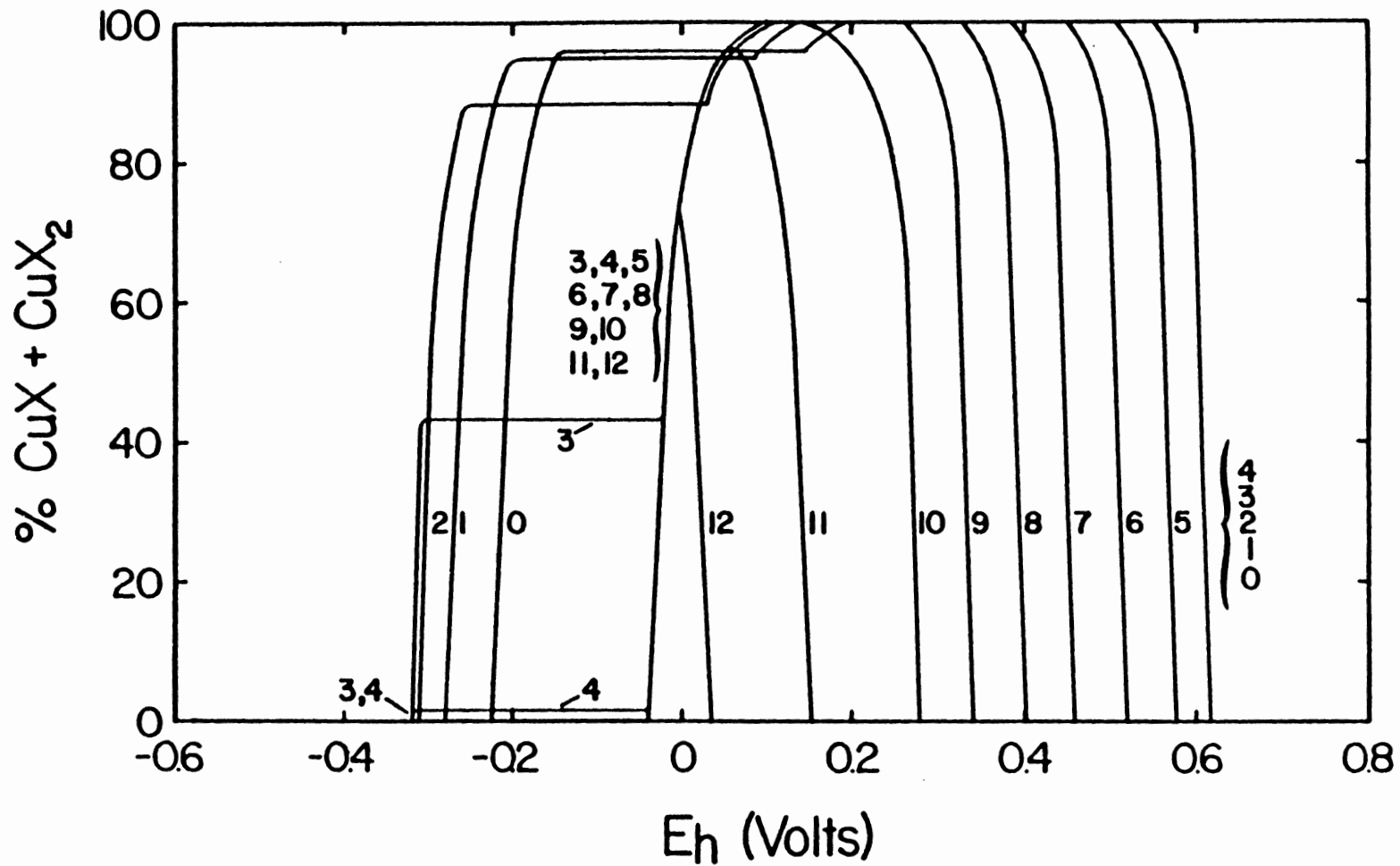
Figure 2.32　Effect of E_h on the percent of copper xanthate formed during chalcocite (Cu_2S) oxidation to metastable copper sulfides and elemental sulfur in the presence of 10^{-5} M xanthate.
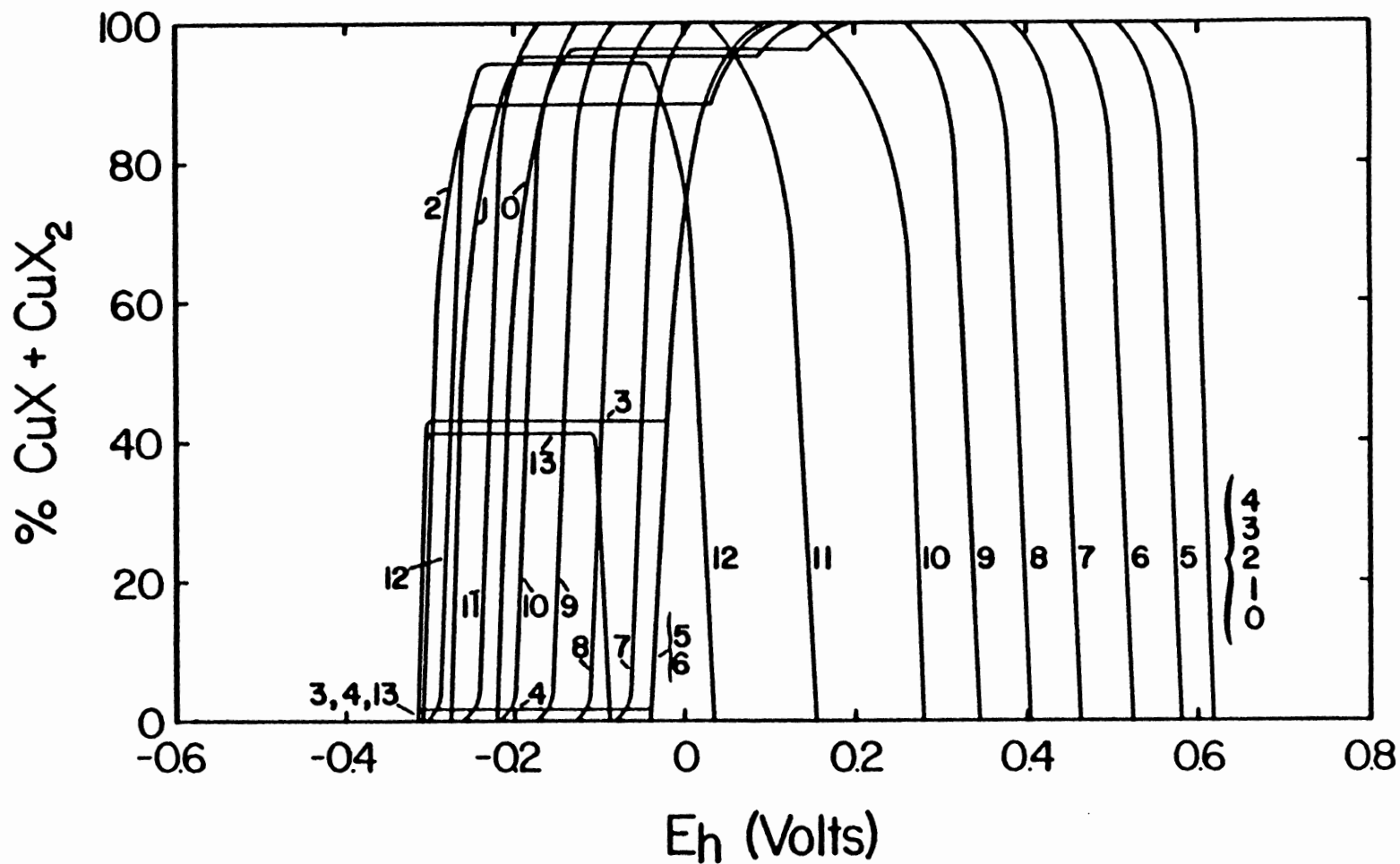
Figure 2.33   Effect of E_h on the percent of copper xanthate formed during chalcocite (Cu_2S) oxidation to metastable copper sulfides and thiosulfate in the presence of 10^{-5} M xanthate.
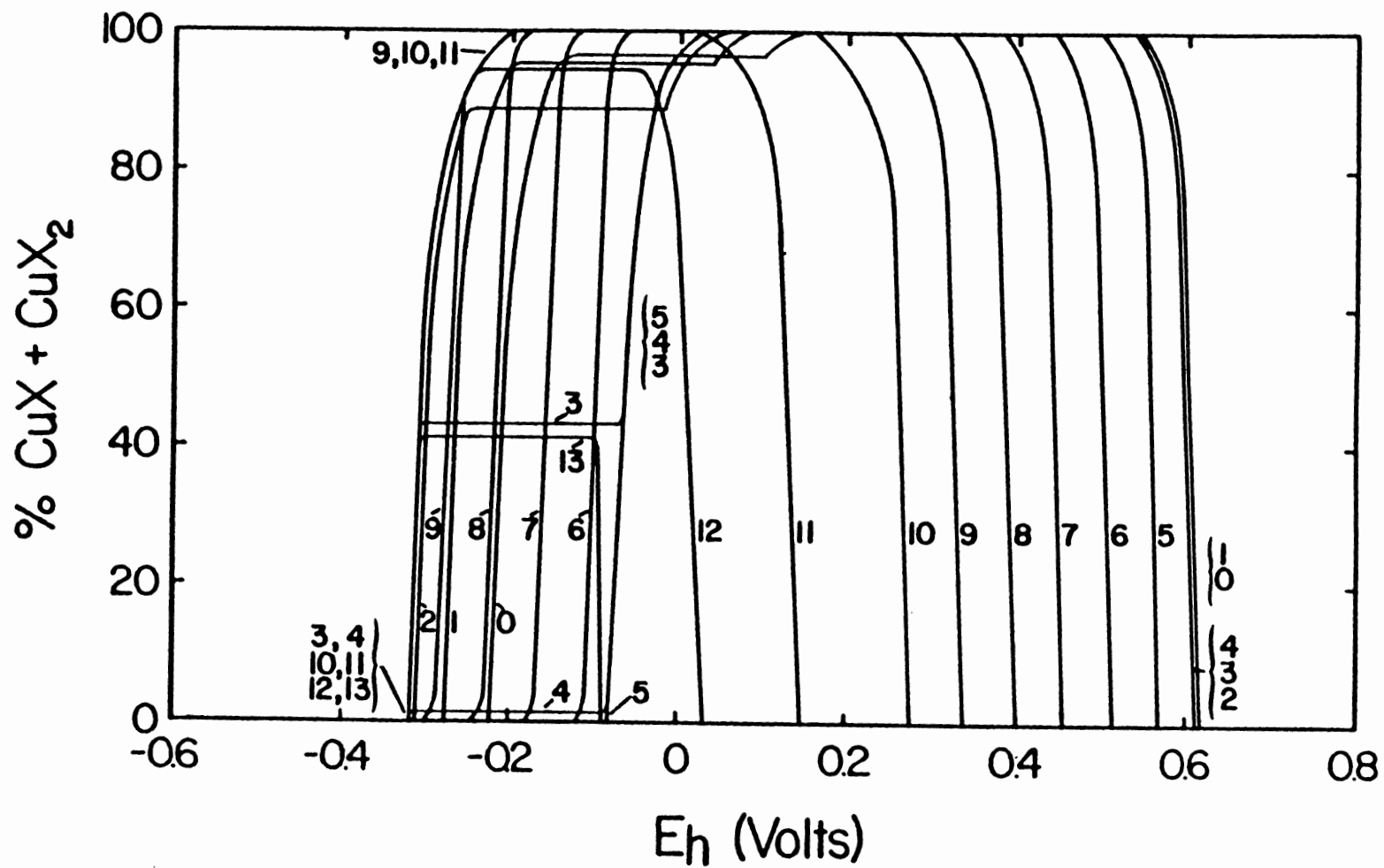
Figure 2.34   Effect of E_h on the percent of copper xanthate formed during chalcocite (Cu_2S) oxidation to stable copper sulfides and sulfate in the presence of 10^{-5} M xanthate.
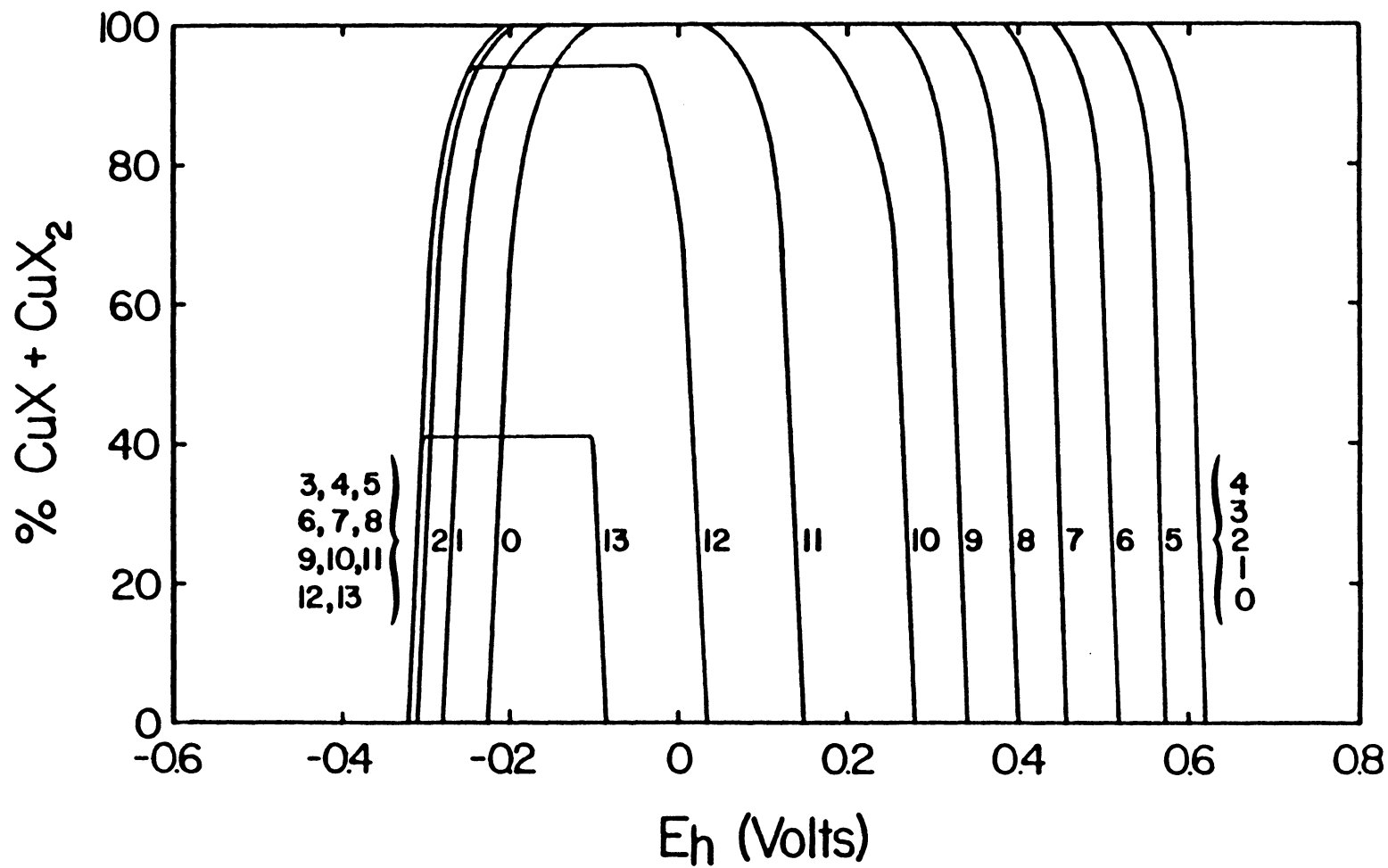
Figure 2.35   Effect of E_h on the percent of copper xanthate formed during
the oxidation of metallic copper in the presence of 10^{-5} M
xanthate.

flotation edge, level off at a maximum percentage, and then drop to form the upper flotation edge. If the pH is less than 5, the plots level off at a maximum due to Reaction [2.17] and then rise to level off at a second maximum due to Reaction [2.16] in Figures 2.32 to 2.34. In fact, at pH's less than 5, the plots remain the same until the E_h becomes greater than 0, at which point Reactions [2.18] and [2.19] take over. At potentials less than 0 and pH's less than 5, the cuprous xanthate amounts do not change with the sulfur oxidation state since Reactions [2.16] and [2.17] control the amounts. This is not true in Figure 2.35 for obvious reasons. However, comparison of all four figures reveals that, at pH 5 and above, the lower flotation edge grows to lower and lower potentials until the limit of -320 mV vs. SHE due to Reaction [2.15] is reached. All four figures also show that there is no difference in the upper flotation edge except under acidic conditions where cupric ions are in equilibrium with a variety of aqueous copper-sulfur species. It is important to note that the difference in potentials for the upper flotation edge between consecutive pH units from 5 to 10 is 60 mV. This is thermodynamically expected since the reaction at the upper flotation edge in the specified pH range involves one electron per hydrogen ion.

2.4.3 Effect of pH

Figures 2.36 to 2.38 illustrate the effect of pH on the percents of copper xanthate formed at various E_h values for chalcocite oxidation to elemental sulfur, thiosulfate, and sulfate, respectively. Figure 2.39 represents the effect of pH for the oxidation of metallic copper. Typically, each plot rises from 0 percent at a certain pH, flattens out at a maximum percentage, and then drops back to 0 at another pH. As was just explained, Figures 2.36 to 2.38 reveal that, less than pH 5 and less than E_h 0, the plots are exactly the same. However, at E_h 0, increasing the sulfur oxidation state and increasing the pH above 5 increases the percentage of copper xanthate. At potentials greater than 0, the plots are duplicated except for an E_h of 600 mV which reflects how increasing the sulfur oxidation state affects equilibrium reactions with cupric ions. Comparing Figures 2.37 and 2.38 to 2.36 shows that, under basic conditions, copper xanthate begins to form at potentials less than 0 indicating the copper xanthate stability region increases with sulfur oxidation state. When oxidation proceeds to elemental sulfur (Figure 2.36), the -300 mV vs. SHE plot only occurs under acidic conditions; however, when thiosulfate forms (Figure 2.37), the -300 mV plot also appears under basic conditions. The -300 mV plot under basic conditions increases in size when sulfate forms (Figure 2.38) and
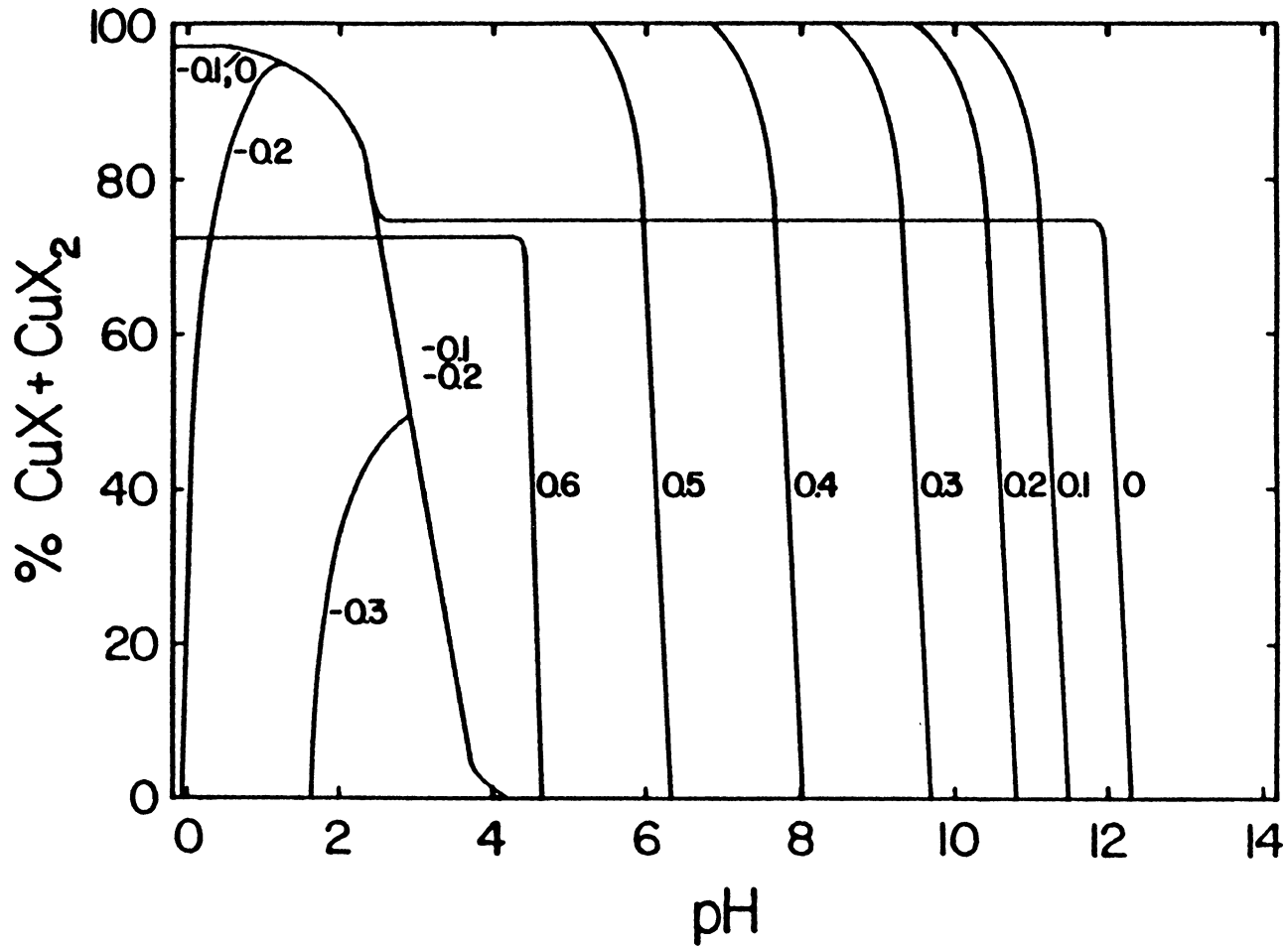
Figure 2.36   Effect of pH on the percent of copper xanthate formed during chalcocite (Cu_2S) oxidation to metastable copper sulfides and elemental sulfur in the presence of 10^{-5} M xanthate.
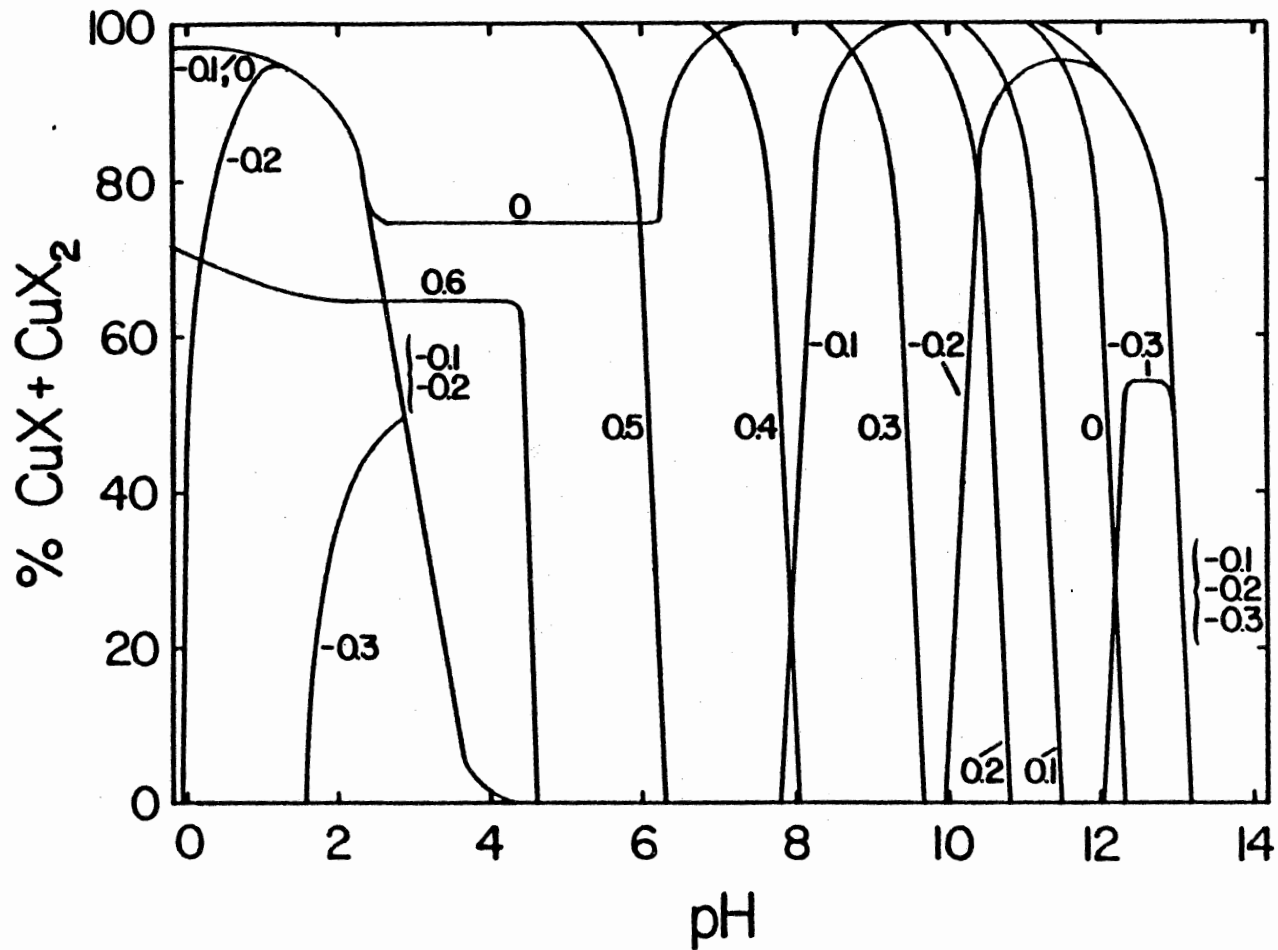
Figure 2.37   Effect of pH on the percent of copper xanthate formed during chalcocite (Cu_2S) oxidation to metastable copper sulfides and thiosulfate in the presence of 10^{-5} M xanthate.
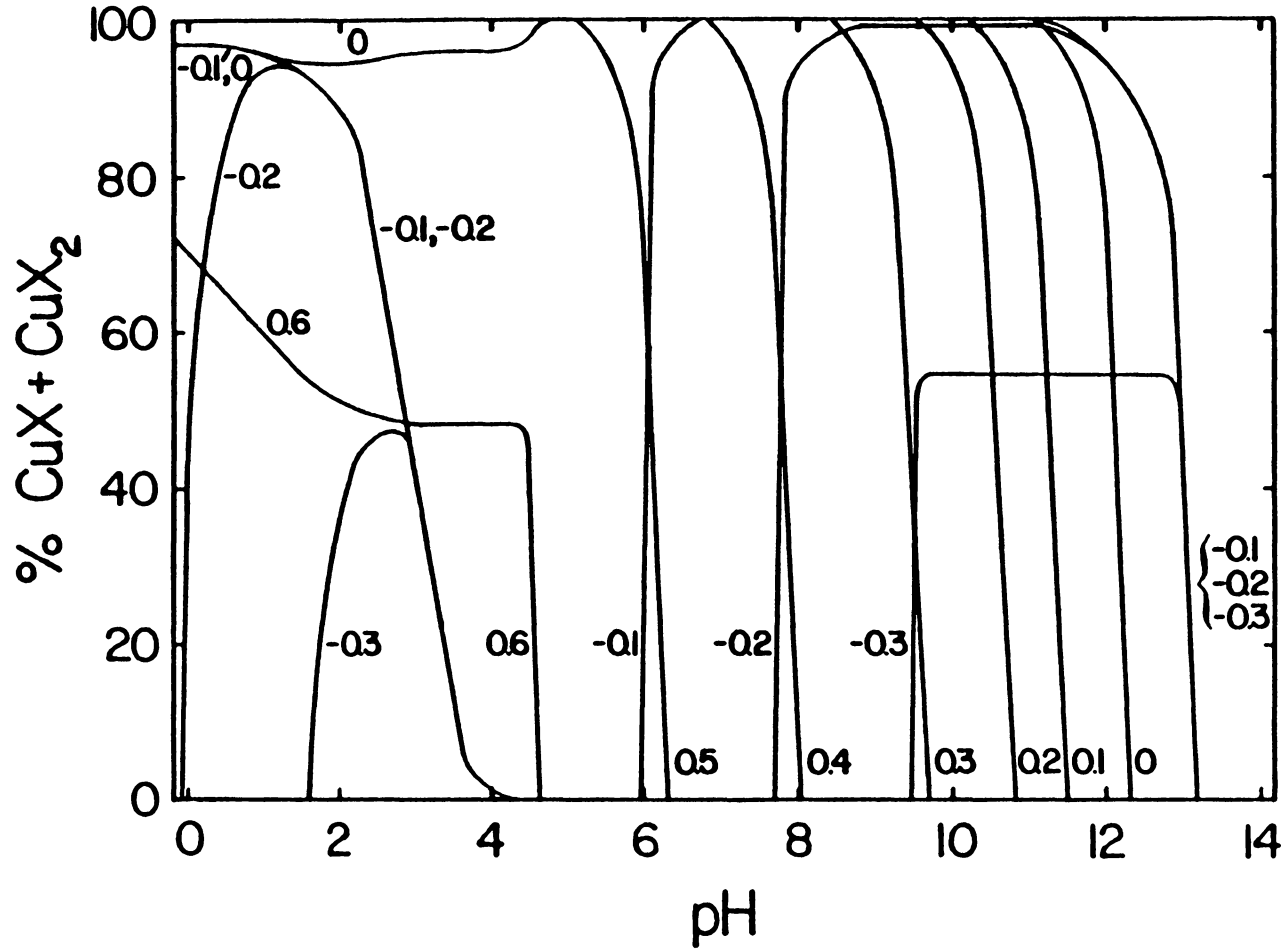
Figure 2.38   Effect of pH on the percent of copper xanthate formed during chalcocite (Cu_2S) oxidation to stable copper sulfides and sulfate in the presence of 10^{-5} M xanthate.
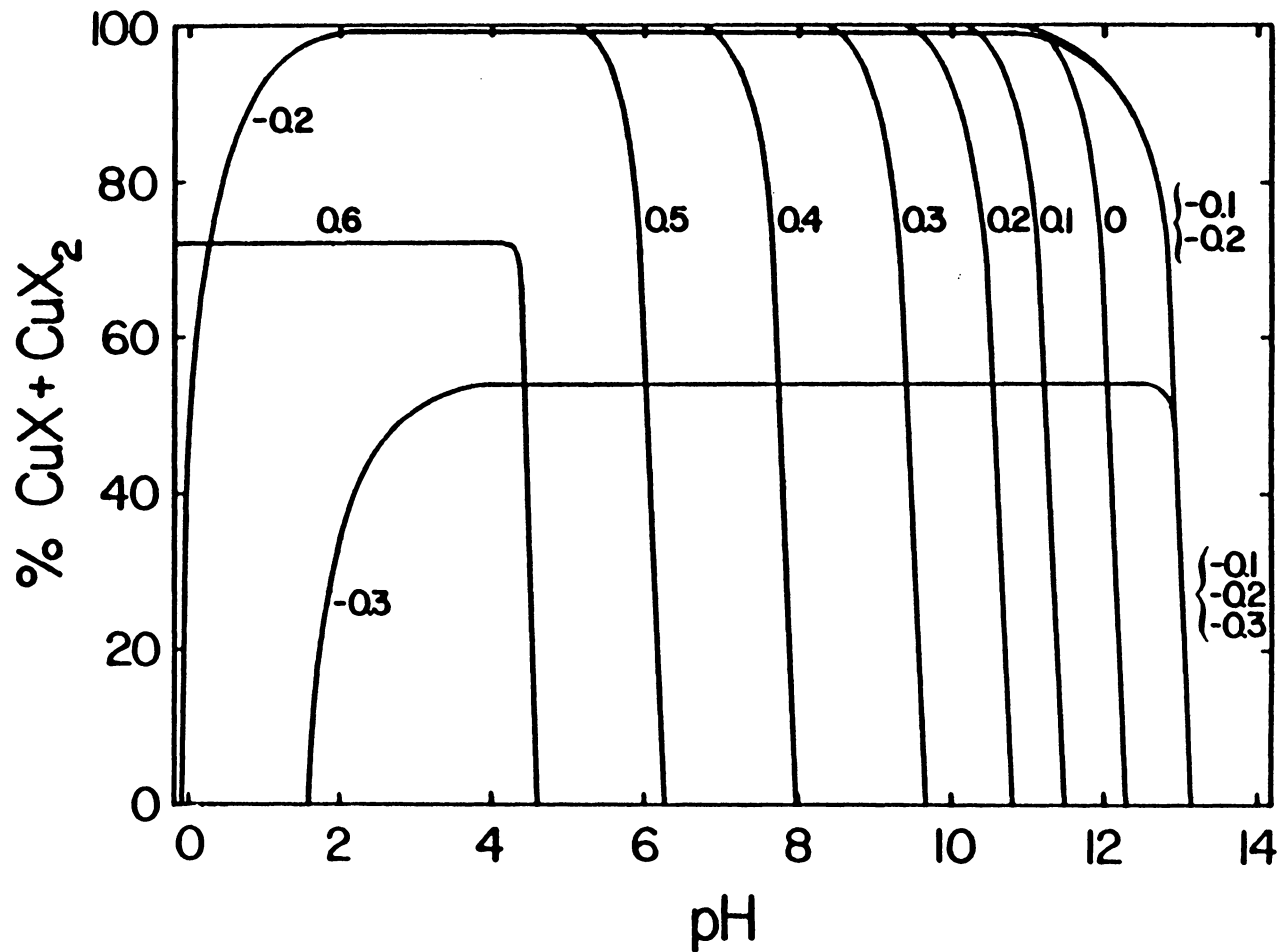
Figure 2.39   Effect of pH on the percent of copper xanthate formed during the oxidation of metallic copper in the presence of 10^{-5} M xanthate.

becomes continuous in the specified pH range when only the oxidation of metallic copper is considered (Figure 2.39).

2.4.4 Co-existence

The co-existence of solids has been explained using the definition of solubility. This co-existence can also be verified using Gibbs' phase rule which states

$$P = C - V + 2, \qquad\qquad [2.26]$$

where P is the number of phases present (i.e., solid, liquid, and gas), C represents the number of independent components in the system (i.e., copper, sulfur, and xanthate), and V stands for the variance or the number of independent ways in which the system can be changed (e.g., temperature, pressure, pH, E_h, and amount of a component).

In order to do the mass-balanced calculations, the temperature and pressure were kept constant at 298.15K and 1 atmosphere, respectively. The amounts of each component were also kept constant. Therefore, the variance is 2 since the only way to vary the system is by changing the pH and E_h. Then from Equation [2.26], the number of phases will be equal to the number of components which obviously varies with the system under consideration. In the copper-water system, copper is the only component (recall that water is the solvent and is not considered as a component) meaning

that only one phase is present. Since the phase cannot be readily interconvertible, the phase must be a solid (i.e., aqueous phases are readily converted into solid phases simply by precipitation). Therefore, in the copper-water system, no solids co-exist because only one solid phase can be present (i.e., metallic copper, cupric oxide, and cuprous oxide), and this is known to be true.

In the copper-sulfur-water, copper-sulfur-xanthate-water, and copper-xanthate-water systems, the number of solid phases which can co-exist is 2, 3 and 2, respectively. A variety of co-existences were shown in Figures 2.2 through 2.20 for the copper-sulfur-water system but at no point did more than two solids co-exist. Three solids, chalcocite and cuprous xanthate with either metallic copper or $Cu_{1.93}S$, were shown to co-exist in the chalcocite-xanthate-water system (see Figures 2.22 to 2.27). Finally, the copper-xanthate-water system represented in Figure 2.28 shows no more than two solids co-existing. Therefore, the E_h-pH diagrams constructed in this present work are in agreement with Gibbs' phase rule which explains the co-existence of solid phases.

CHAPTER III

EXPERIMENTAL STUDIES

3.1 <u>Background and Equipment</u>

In order to gain an understanding of an electrochemical system, it is best to first understand the techniques and instrumentation which give that knowledge. For that reason, background information about the techniques and equipment used in this study are given. They include Intermittent Galvanostatic Polarization, X-ray Photoelectron Spectroscopy, Cyclic Voltammetry, and Microflotation.

3.1.1 <u>Intermittent Galvanostatic Polarization</u>

During Intermittent Galvanostatic Polarization (IGP), a current is repeatedly applied to an electrode for a short time to continually polarize the electrode and then turned off for, typically, an equivalent time to allow the electrode potential to relax to an open-circuit potential (i.e., no current is applied). Potentials must be measured at open-circuit in order to relate them to equilibrium potentials. When the current is applied, the electrode potential will increase in the direction of polarization until the electrode undergoes an electrochemical reaction

which exactly offsets the applied current, thereby forcing the electrode potential to remain constant. However, when a reactant becomes depleted or a product becomes abundant, the electrochemical reaction can no longer keep pace with the applied current and the electrode potential will, once again, begin to increase in the direction of polarization until another reaction occurs. If too large of a current is applied, the electrode potential may skip over the the equilibrium potential of the first reaction and, if too small of a current is applied, the electrode potential may not reach the equilibrium potential of the first reaction within a reasonable time frame. Therefore, recording the potential against time produces a series of plateaus which correspond to the equilibrium potentials of the reactions.

Nagel et al. (1957) first applied the IGP method to study the equilibrium potentials in various metal-water systems. Horvath and Hackl (1965) used it to verify Eh-pH diagrams for metal-sulfur-water systems and compared the results to metal corrosion in aqueous hydrogen sulfide solutions. In combination with cyclic voltammetry, Thornber (1982) used IGP to study two nickel-iron sulfides, pentlandite and violarite, under neutral and acidic conditions. Most recently, Pritzker (1985) showed galena oxidation proceeded to elemental sulfur which further oxidized, possibly to thiosulfate, by increasing the
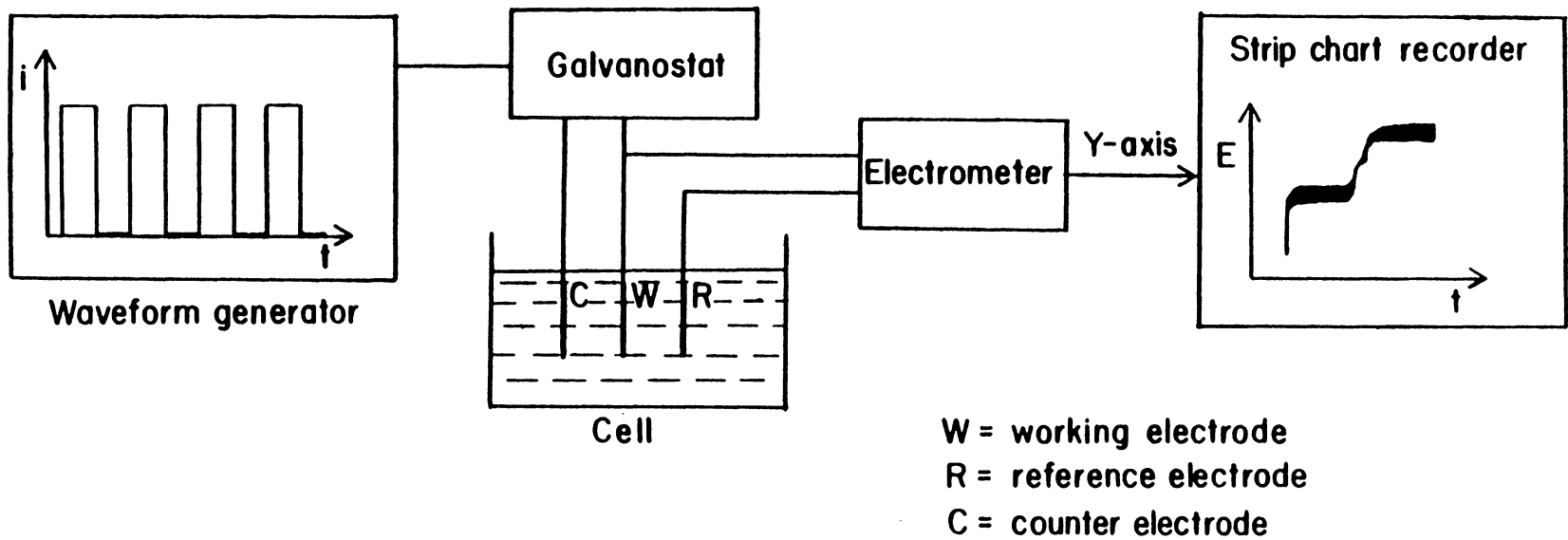
Figure 3.1   Schematic diagram of the equipment used in the intermittent galvanostatic polarization experiments (from Pritzker, 1985).

potential, pH, time, or any combination thereof.

Figure 3.1 illustrates the instrumentation needed for IGP experiments. As can be seen, the conventional three-electrode system is required. Current is pulsed between a counter electrode (platinum) and a working electrode (chalcocite) by means of a waveform generator and a galvanostat which were a PAR Model 175 Universal Programmer and a PAR Model 371 Potentiostat/Galvanostat, respectively. The potentials which develop on the working electrode were measured with respect to a reference electrode (saturated calomel) and recorded on a Houston Instrument Model 4523 X-t recorder.

3.1.2 X-ray Photoelectron Spectroscopy

In X-ray Photoelectron Spectroscopy (XPS), also known as Electron Spectroscopy for Chemical Analysis (ESCA), the surface of a sample is bombarded with soft X-ray photons of constant energy causing a photoelectric effect which results in the emission of electrons called photoelectrons. As illustrated in Figure 3.2a, an atom in the sample absorbs the X-ray photons of energy $h\nu$ and, to minimize the excess energy, simultaneously ejects an electron with a kinetic energy of E_k from an atomic orbital with a binding energy of E_b. Obviously, the kinetic energy cannot exceed the energy of the incident X-rays. From the conservation of energy,
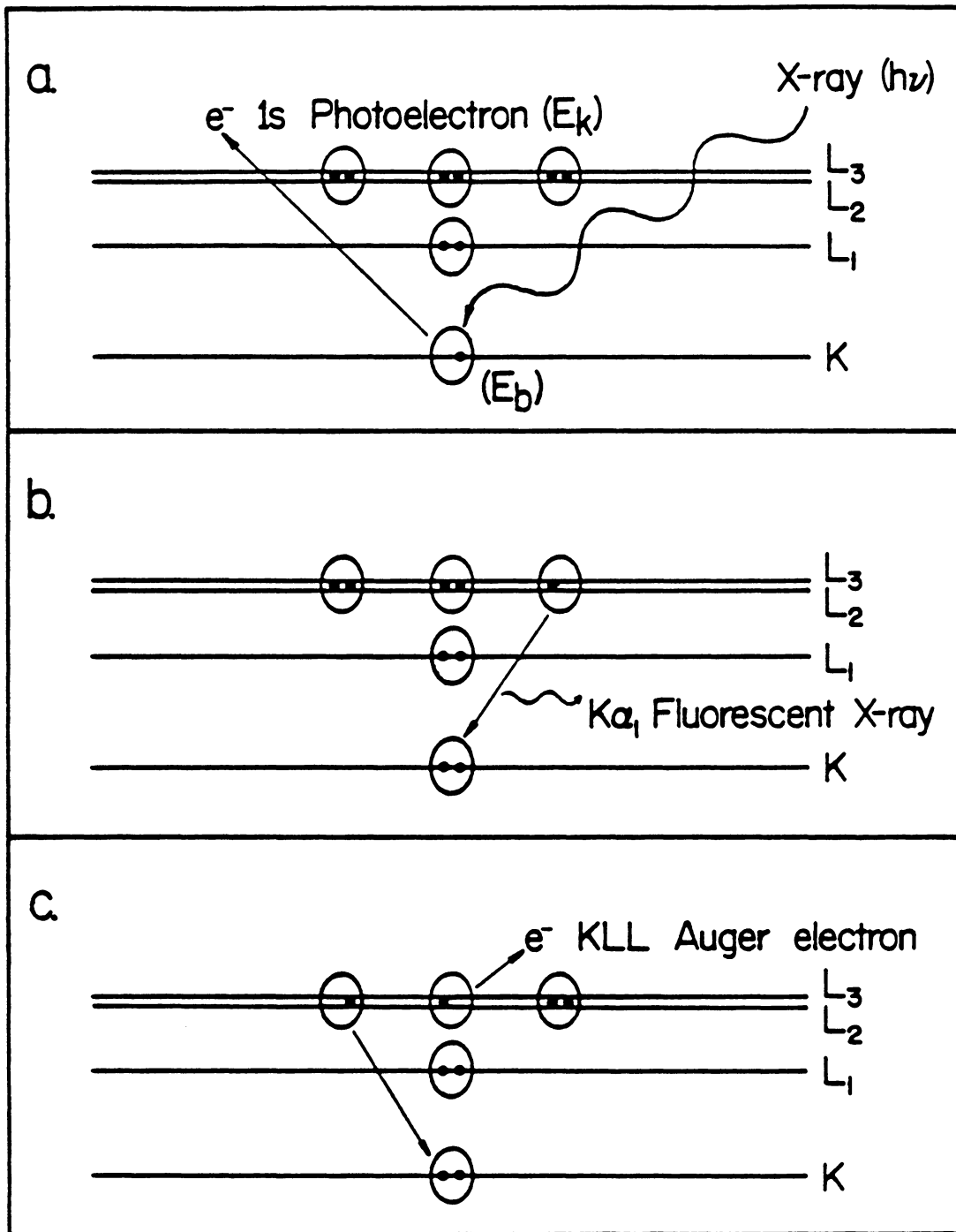
Figure 3.2 Illustration of the photoelectric effect:
a. Excitation by photoelectron emission
b. De-excitation by X-ray fluorescence
c. De-excitation by the Auger process.

one can write:

$$E_k = h\nu - E_b - \phi \qquad [3.1]$$

where ϕ is the work function which is dependent on both the sample and the spectrometer. However, the dependency of the work function on the sample can be eliminated by calibrating the binding energy of the electrons to the Fermi level of the sample which, by definition, corresponds to zero binding energy. The Fermi level is the energy to which atomic energy levels are filled with electrons. All levels of higher energy are vacant.

Typically, the binding energies are referenced to the carbon 1s (C 1s) orbital since adventitious carbon will be present on all surfaces. It is generally accepted that the binding energy of the C 1s electrons of adventitious carbon is 284.8 eV and any deviation from that value is attributed to static charging. Static charging is a balance between electron loss from the surface by emission and electron gain by conduction and is typical of insulators. By subtracting the static charge from all binding energies (or adding the static charge to all kinetic energies), all energies become referenced to adventitious carbon. All XPS spectra can than be compared; however, Swift (1982) expressed caution when using adventitious carbon as the reference source.

Although any electron with a binding energy less than

the incidental X-ray energy can be ejected, the probability is greatest for inner-shell electrons. However, the removal of an electron from an inner-shell creates an excited atomic state. De-excitation of the atom to produce a more stable state occurs either by fluorescence or by the Auger process. During both processes, an outer-shell electron falls to fill the inner-shell vacancy creating excess energy which is released as either fluorescent X-rays (see Figure 3.2b) or as a second electron called the Auger electron (see Figure 3.2c). As shown in Figure 3.2c, for example, the Auger electron was called a KLL electron because the original vacancy was created in the K-shell, an electron fell from the L-shell to fill it, and, subsequentially, an L-shell electron was ejected. Under XPS conditions, fluorescence occurs less than one percent of the time and Auger electron emission occurs within 10^{-14} seconds of the photoelectron emission (Wagner et al., 1979). Both photoelectrons and Auger electrons are therefore ejected during X-ray bombardment in XPS but both must originate within 100 Angstroms of the solid surface since electrons highly interact with matter. Furthermore, a vacuum must be applied to prevent interactions with air. Because of this small sampling depth and its nondestructive nature, XPS is the premiere tool for surface analysis.

Photoelectrons and Auger electrons can only be
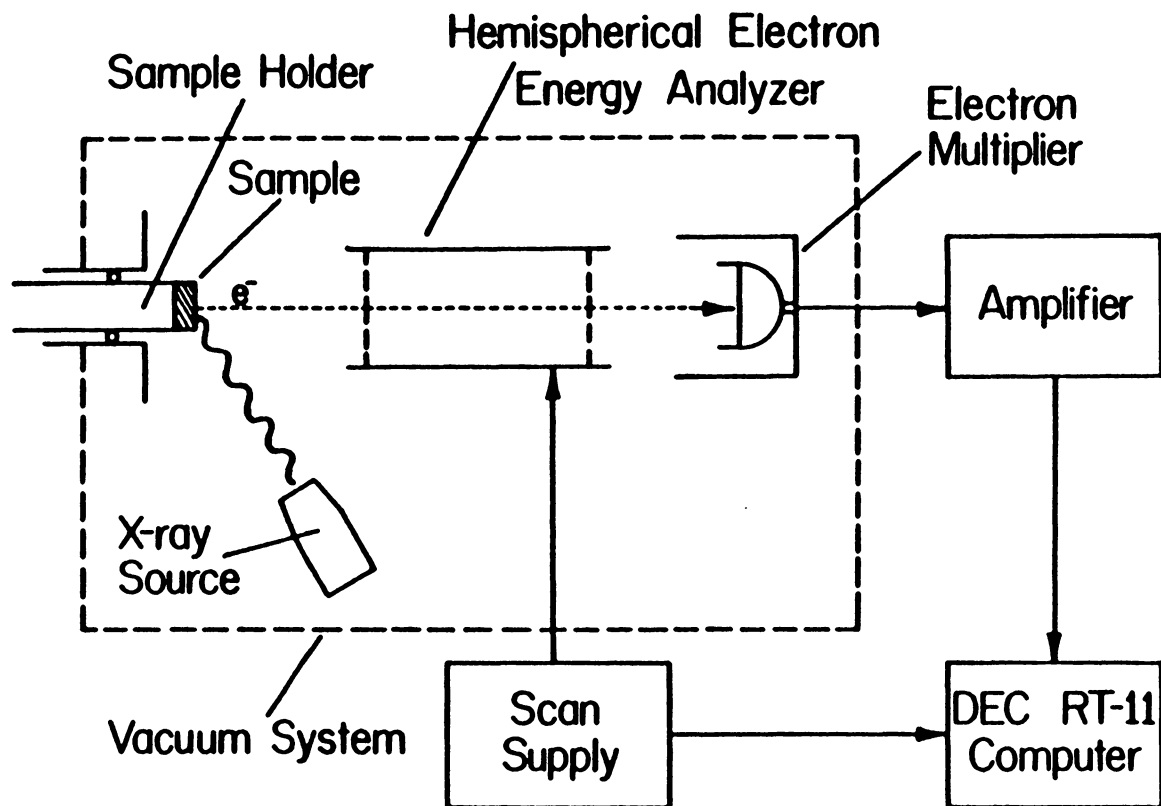
Figure 3.3 Schematic diagram of the equipment used in the X-ray
            photoelectron spectrometer.

distinguished from their kinetic energies as measured by an electron spectrometer. Within the spectrometer, an analyzer, acting as an energy barrier, allows only those electrons with a specific kinetic energy to pass on to an electron multiplier which detects and counts the electrons (see Figure 3.3). By varying an electrostatic field from zero to the incident X-ray photon energy with a scan supply, the spectrometer counts all electrons with any possible kinetic energy. From Equation [3.1] the binding energy for each electron can be determined if the spectrometer work function is known. Because the binding energy of an electron, and hence its kinetic energy, is unique for each atom and its orbitals, all elements except hydrogen can be identified. Therefore plotting the number of electrons against either kinetic or binding energy produces spectral peaks which identify with the elements on the sample surface. Also, because of electronegativity (i.e., the relative attraction of electrons between atoms of different elements), the binding energy of an electron alters when atoms bond together resulting in a shifted peak which enables the chemical state of an element to be identified. As shown in Figure 3.4 and Table 3.1, the chemical state of both copper and sulfur compounds can be detected. For example, metallic copper and chalcocite can not be identified using the Cu $2p_{3/2}$ photoelectron but can be using
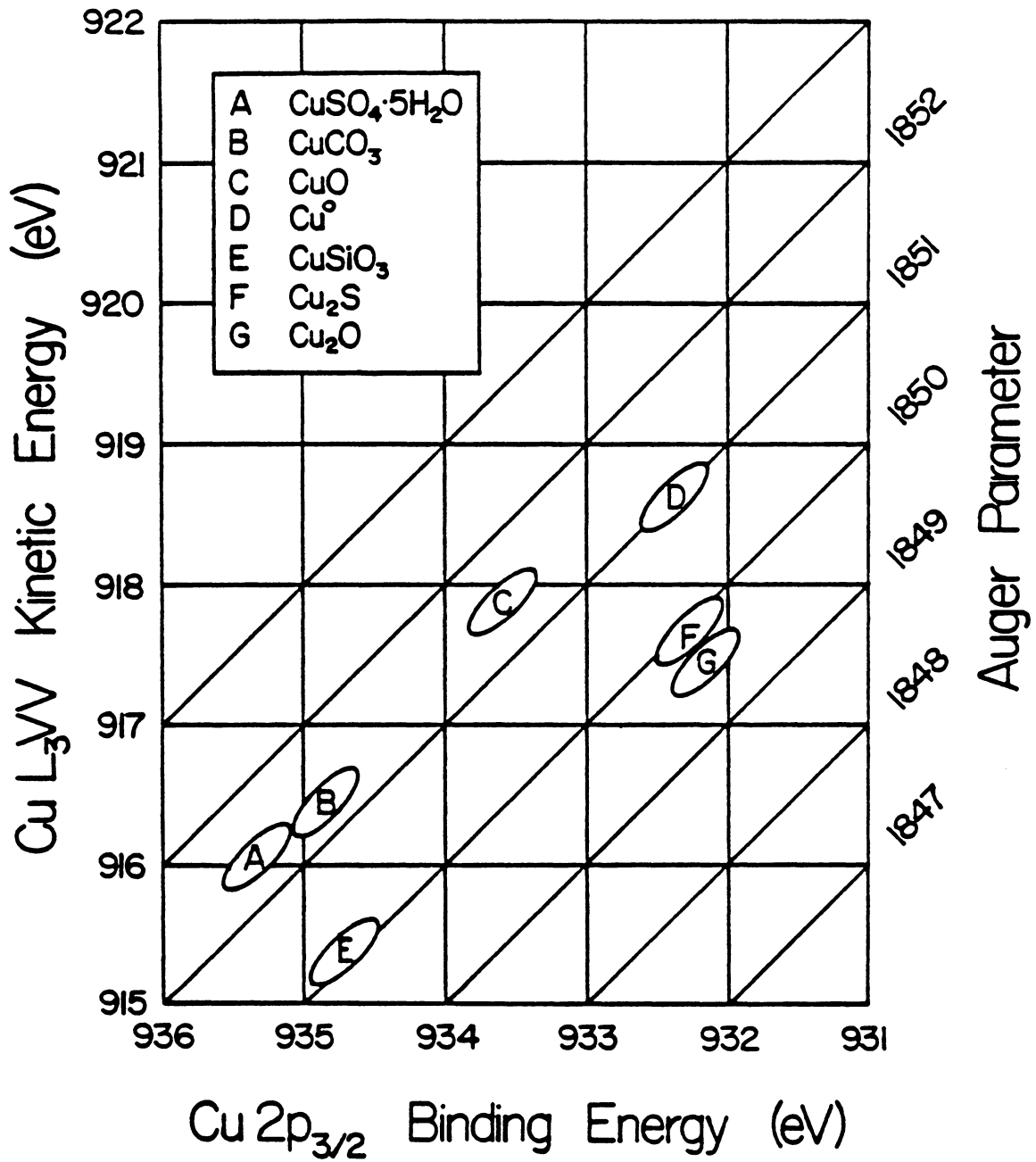
Figure 3.4 Identification of copper compounds with the Cu 2p$_{3/2}$ photoelectron and the Cu L$_3$VV Auger electron.

Table 3.1

Binding Energies of S 2p Electrons in Sulfur-bearing
Compounds (from Wagner et al., 1979)

Compound	Binding Energy (eV)	Compound	Binding Energy (eV)
Na_2S	161.6	S_2N_2	164.3
PbS	160.6	Me_3SI	165.6
FeS	161.2	Ph_2SO	165.8
$KFeS_2$	161.3	BzMeSO	165.8
WS_2	161.9	$PhSO_2Na$	166.1
MoS_2	162.2	Na_2SO_3	166.3
$Na_2\underline{S}\cdot SO_3$	161.5	$Na_2S\cdot\underline{S}O_3$	167.5
$PhSCMe_3$	162.2	$BzMeSO_2$	167.8
Ph_3PS	162.3	SO_2	167.9
PhSH	162.9	$PhSO_3Na$	168.0
Ph_2S	163.0	$PhSO_3Me$	168.3
Ph_2S_2	163.8	Na_2SO_4	168.5
S_8	163.8	$FeSO_4$	168.5
S_n	164.0	$Fe_2(SO_4)_3$	168.9

the Cu L_3VV Auger electron. Adding the energies of these two electrons together yields the Auger parameter which is important because it eliminates static charging and allows for another way to identify a compound. When different chemical states of the same element co-exist, corresponding peaks grow together to form a broadened peak with shoulders unless, of course, the peak shifts were large enough to produce distinct and separate peaks. However, since photoelectrons produce Gaussian-shaped peaks, the broadened peak can be resolved into separate and distinct peaks, provided that the broadened peak was formed solely from photoelectrons. Each peak can then be represented by

$$N(E) = B\exp\{-[(E - E^O)/b]^2\} \qquad [3.2]$$

where B is the peak height, b is the peak width at half the peak height, and E^O is the kinetic or binding energy at which the peak reaches a maximum; all of which are constant. The number of electrons, $N(E)$, is then dependent on the various kinetic or binding energies, E. But because the peaks are additive, the overall response becomes

$$N(E) = \sum_{i=1}^{n} B_i\exp\{-[(E - E_i^O)/b_i]^2\} \qquad [3.3]$$

and is summed over the number of peaks, n, in the spectrum or, in this case, the number of peaks to be resolved in the

broadened peak. Peak resolution has been used by many investigators including Luttrell and Yoon (1984), Craynon (1985), and Termes et al. (1987) on sulfur (S 2p) electrons produced by metal polysulfides.

Once the chemical states of elements present on the sample surface have been identified and all overlapping peaks have been resolved, calculations can be performed to determine the ratios of one chemical state to another:

$$n_1/n_2 = (I_1/S_1)/(I_2/S_2) \qquad [3.4]$$

where I, the intensity, is the number of photoelectrons detected for a given peak and is found by integrating N(E) over the corresponding energy range to give the area under the peak; and S, the sensitivity factor, is the product of the mean free path of the electrons in the sample, the photoelectric cross-section of the orbital from which the electron evolved, and the instrument transmission function. The photoelectric cross-section is the probability of an orbital being ionized when irradiated by a photon and is therefore a fraction of the total number of photoelectrons. The mean free path or escape depth is the distance in a solid that photoelectrons travel before 36.8% (i.e., 1/e) have not suffered enegy loss through collisions. Because the instrument transmission function is the efficiency at which the electrons of a definite kinetic energy are

separated from other electrons by the analyzer, the instrument transmission function, and hence the sensitivity factor, is proportional to the kinetic energy. This proportionality constant remains the same at different energies and therefore cancels out in Equation [3.4] and the sensitivity factor, for all purposes, becomes dependent on the kinetic energy. However, the sensitivity factors vary from one spectrometer to another. Lawson (1984) determined sensitivity factors for each element for the spectrometer described below.

The X-ray photoelectron spectrometer used for surface analysis was the X-SAM 800 manufactured by KRATOS, Ltd., England. The instrument was equipped with a hemispherical electron energy analyzer, a turbo-molecular vacuum pump typically operated at 10^{-8} mm of Hg, and a dual anode X-ray source of which only the Mg K_α source (1253.6 eV) was used at, normally, 13 kV and 20 ma. All spectra were collected using high resolution, an analyzer slit width of 2 mm, and a Fixed Retarding Ratio (FRR) mode to insure maximum detection. Interfaced to the spectrometer, a DEC RT-11 computer system with KRATOS software provided automatic acquisition and manipulation of spectra. Automatically subtracted from Equation [3.1] by the computer to obtain either kinetic or binding energies, the spectrometer work function was constantly found to be 3.4 eV.

3.1.3 Cyclic Voltammetry

In IGP, a current is pulsed to the working electrode and the corresponding potentials are measured; but, in voltammetry, the potential is varied and the corresponding currents are measured. The potential is changed from an initial value, E_i, to a value, E_1. After the E_1 potential is reached, the scan direction is reversed until a second potential, E_2, is obtained. Cyclic voltammetry results when the potential is cycled between the two potential limits, E_1 and E_2. As with IGP, the conventional three-electrode system is required (see Figure 3.5). The potential is applied across the working and the reference electrodes by a waveform generator, a PAR Model 175 Universal Programmer, which programs a potentiostat, a PAR Model 371 Potentiostat/ Galvanostat, to control the initial potential, the two potential limits, the initial scan direction, and the scan rate, v. A voltammogram, a plot of current vs. potential, was made using an X-Y recorder, either a Linseis LY 18100 or a Hewlett Packard 7004B.

If there is an abundance of an aqueous species, A, and the following oxidation reaction occurs at a potential E_r

$$A = B + ne, \qquad\qquad [3.5]$$

then, when the applied potential is below E_r, no reaction will occur and no current will be generated. However, as
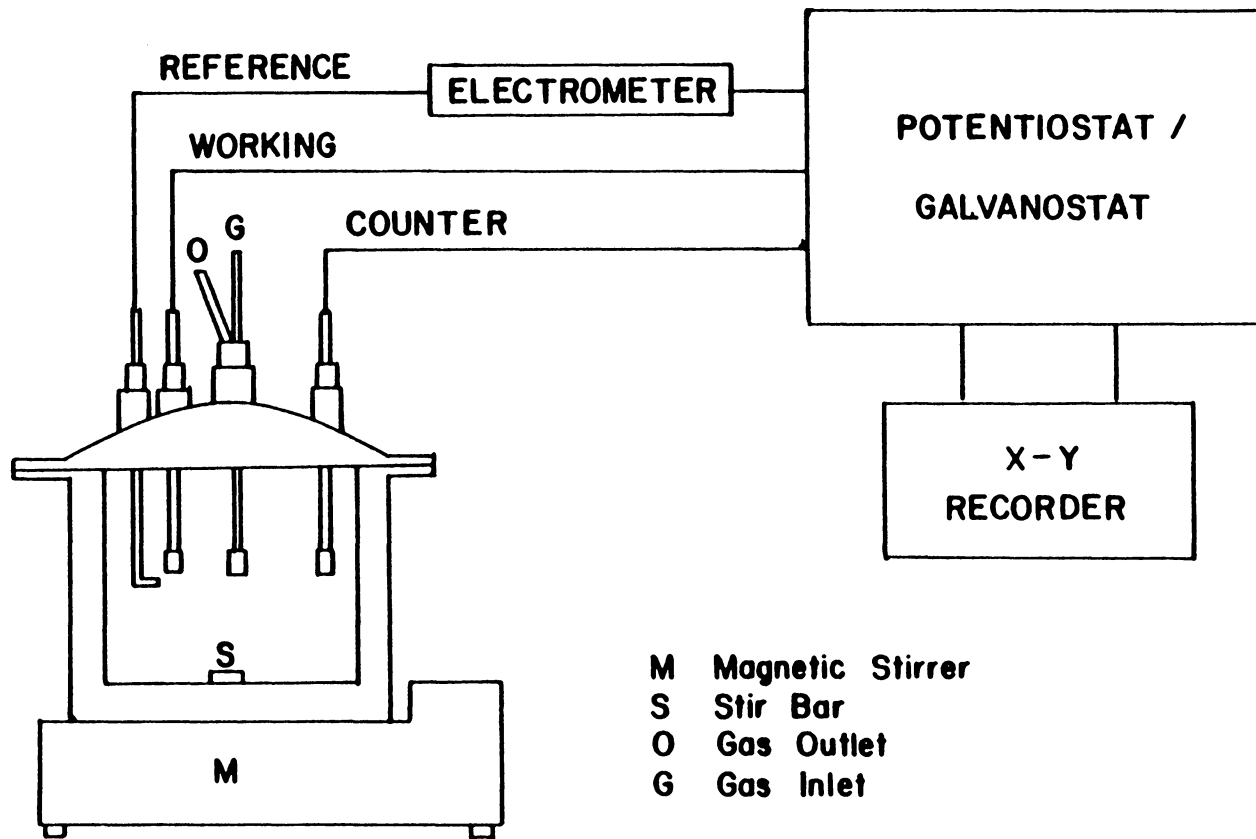
Figure 3.5   Schematic diagram of the equipment used in the cyclic
voltammetry experiments (from Basilio, 1985).

the potential is increased to E_r, current will begin to
flow. Increasing the potentials beyond E_r will increase the
current as long as species A is supplied to the surface of
the working electrode at a pace faster than the kinetics of
Reaction [3.5]. Furthermore, the concentration of A at the
surface continually decreases with increasing potentials and
becomes zero at a potential when the supply of A to the
surface exactly equals its consumption. At this potential,
the current has reached a maximum and is entirely controlled
by the mass transport of A to the surface and through the
diffusion layer. Further increases in potential will
decrease the concentration gradient of A in the diffusion
layer and the current will therefore decrease. An anodic
peak is then produced by increasing potentials. Also,
assuming the product, B, in Reaction [3.5] also undergoes an
oxidation reaction, voltammetry will produce a second peak
which begins at the reversible potential of the second
reaction. Furthermore, reversing the scan direction should
result in a reduction reaction exactly the opposite of
Reaction [3.5] and should produce another peak which, in
this case, would be a cathodic peak. Nevertheless,
reactions can be identified from the potentials at which
each peak begins to form.

Further information about a reaction can be collected
by examining the effect that stirring has on a peak. For

example, as was just mentioned, species B in Reaction [3.5] may undergo further oxidation which results in the formation of a second peak. However, if species B was soluble and the system was stirred, species B would constantly be swept away from the electrode surface. Upon increases in potential, a second peak could not develop since species B is not present to react. If the peak persists then species B must be a solid.

Analysis of the charge corresponding to a peak can also be used to identify a reaction. By noting that the charge, Q, is equivalent to the current multiplied by the change in time and recognizing that the potential is a linear function of time as set by the scan rate, the charge can be determined by multiplying the current with the change in potential and dividing by the scan rate. This is equivalent to the area under a peak. Taking the ratio of charges for a sequence of peaks and comparing to a theoretical charge ratio of proposed reactions will then help identify a reaction. Both Pritzker (1985) and Basilio (1985) used charge-ratioing to help identify reactions for galena and chalcocite, respectively.

3.1.4 <u>Microflotation</u>

The flotation process was briefly described in the Introduction to Chapter I. Shown in Figure 3.6, the
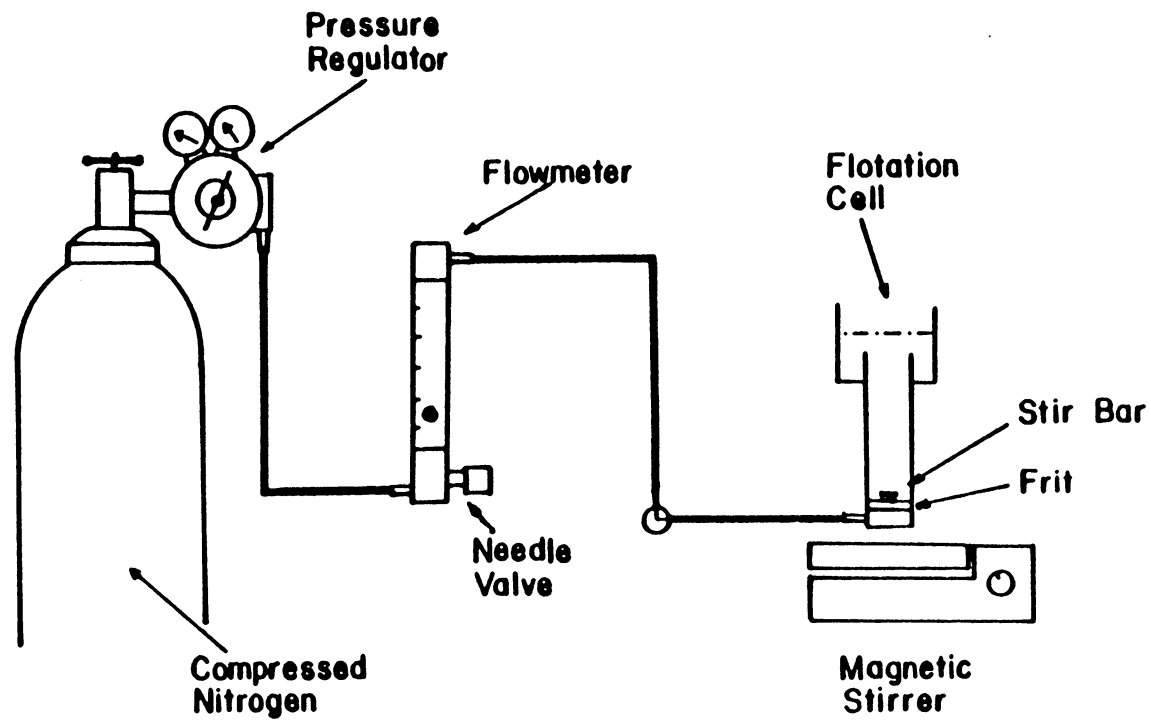
Figure 3.6   Schematic diagram of the equipment used in the microflotation experiments (from Basilio, 1985).

microflotation set-up requires nitrogen gas, a gas flowmeter, a magnetic stirrer, and the flotation cell similar to that first employed by Partridge and Smith (1971). Low-oxygen nitrogen gas was used because it removes dissolved oxygen from the solution and because it is inert. So that all flotation tests were performed at a constant gas flow rate, a micrometer capillary flowmeter made by Gilmont was used. Within the flotation cell, a medium porosity frit was used to produce gas bubbles of an adequate and uniform size. In combination with the magnetic stirrer, a Teflon-coated magnetic stir bar kept the system agitated preventing bubbles from coalescing and particles from flocculating. Pritzker (1985) and Basilio (1985) used the same microflotation set-up; however, in the present case, the set-up was placed inside a glove box and purged with nitrogen gas to provide an atmosphere free of oxygen. Using the microflotation cell drastically reduces the sample size thereby sparing sample and enabling more tests to be performed.

3.2 Procedure and Materials

The best results have been obtained using the following sample preparation procedures for the experimental techniques just described.

3.2.1 Electrochemical Experiments

Both IGP and voltammetry require three electrodes: the working, reference, and counter electrodes. The working electrode, a chalcocite electrode, was prepared from a contaminant-free specimen obtained from Butte, Montana, courtesy of the Smithsonian Institution. The sample was cut with a Buehler Isomet low-speed diamond saw into a rectangular prism, attached to a copper lead with a carbon-based conducting cement called Electrodag 199, and sealed in a glass holder with Buehler epoxy resin (Pritzker, 1985; Basilio, 1985). The surface area of the electrode measured 0.30 cm^2. Before each test run, the chalcocite electrode was wet-polished with 600-grit silicon carbide paper and then rinsed with double-distilled water. The reference electrode, a saturated calomel electrode (SCE), was refilled regularly with saturated KCl solution while the counter electrode, a platinum wire, was cleaned prior to each test with 10% nitric acid solution. By placing both the platinum and saturated calomel electrodes in ZoBell solution (Garrels and Christ, 1965) prior to each test, the electrode pair was checked with an Accumet Model 610A potentiometer. ZoBell solution measures 430 mV vs. SHE and 185 mV vs. SCE at $25^{o}C$ and consists of 1/300 M potassium ferrocyanide, 1/300 M potassium ferricyanide, and 0.1 M potassium chloride.

Prior to each electrochemical experiment, 75 ml of

buffer solution was poured into the cell and deoxygenated
with low-oxygen nitrogen gas (<0.5 ppm O_2) for at least half
an hour. The buffer solutions were pH 1.1 (0.1 M $HClO_4$),
pH 4.6 (0.5 M CH_3COOH/0.5 M CH_3COONa), pH 6.8 (0.1 M KH_2PO_4/
0.1 M NaOH), and pH 9.2 (0.05 M $Na_2B_4O_7$). They were
prepared using A.C.S. reagent grade materials and double-
distilled water. When a test was started, the gas inlet was
raised above the solution but nitrogen was continually
introduced to keep a positive pressure within the cell.

When desired, purified potassium ethyl xanthate was
added to the buffer solutions at concentrations of either
1.0×10^{-3} or 2.5×10^{-5} M. Originally at commercial grade,
the xanthate was purified by dissolving in acetone,
filtering, recrystallizing with petroleum ether, and
filtering once again. After repeating the process three
times, the purified xanthate was stored under the ether.

3.2.2 X-ray Photoelectron Spectroscopy

Because the entrance to the XPS sample chamber is
small, the chalcocite electrode had to be redesigned. Small
disks of chalcocite measuring about 2 mm in thickness and
10 mm in diameter were prepared. The chalcocite specimen
was obtained from Messina, Transvaal, South Africa, this
time courtesy of Ward's Natural Science Establishment. The
sample was cut into a rectangular prism with the Isomet

diamond saw and set directly in Buehler epoxy resin. The diamond saw was then used to cut the sample into the disks, each with a surface area of 0.34 cm^2.

Since XPS is very sensitive, all samples had to be extremely clean. Therefore, prior to each test, a disk was subjected to three polishing stages using the Buehler Ecomet III polishing wheel: 600-grit silicon carbide was first used and followed by canvas and then microcloth. The cleaned disks were then mounted on a Metrohm carbon paste electrode using the Electrodag 199 as an adhesive. When the Electrodag was dry, the electrochemical tests were performed.

When a test was over, the disk was washed with double-distilled water and removed from the carbon paste electrode. Nitrogen gas was then blown on the sample to dry it and prevent as much oxidation as possible. Once dry, the disk was immediately attached to the XPS sample holder with double-stick adhesive tape and introduced into the sample chamber. When the pressure was less than 10^{-7} mm Hg and the temperature was colder than -90^oC, spectra of the Cu $2p_{3/2}$, Cu L_3VV, S 2p, C 1s, and the O 1s were taken and followed by a wide scan. The cool temperatures prevented the photoreduction of copper and were obtained as liquid nitrogen circulated through the sample holder. Also, the Cu spectra were obtained first to insure that, if

photoreduction occurred, it was not significant.

3.2.3 Microflotation

The chalcocite obtained for the XPS studies was also used for the microflotation tests. Although the samples were crushed in the glove box purged with nitrogen, the samples were only crushed prior to each experiment to minimize oxidation. While the sample was being crushed with a porcelain mortar-and-pestle, those samples contaminated with quartz or any other mineral matter were discarded. For each test, 1 gram of hand-screened -100+150 Mesh sample was collected and placed in a beaker containing 100 ml of deoxygenated pH 9.2 buffer solution. The potential of the pulp was adjusted before or after the addition of xanthate which was at a concentration of 10^{-5} M. In either case, the pulp was gently conditioned for 5 minutes, transferred to the flotation cell, and floated for 1 minute using a nitrogen gas flow rate of 40 ml/minute. Both the tailings and the concentrate were collected, filtered, dried, and weighed to obtain the flotation recovery.

CHAPTER IV

RESULTS AND DISCUSSION

4.1 <u>Intermittent Galvanostatic Polarization</u>

The co-existence of solid phases has been shown to
occur in a variety of mass-balanced thermodynamic
calculations and has been explained using both the
definition of solubility and Gibbs' phase rule. More
importantly, metallic copper and chalcocite were found to
co-exist as originally concluded by Basilio (1985).
Furthermore, this co-existence was shown to be independent
of the sulfur oxidation state although the extent to which
it occurred was not. IGP experiments were therefore
employed at pH 9.2 to confirm the co-existence of metallic
copper and chalcocite. IGP experiments were also conducted
at pH 1.1 to detect the presence of the nonstoichiometry.
Acidic conditions were necessary to prevent the passivation
of the surface with copper oxides and hydroxides (see
Section 1.2.2; Koch and McIntyre, 1976; Brage et al., 1979;
and Gerlach and Kuzeci, 1983).

4.1.1 <u>Reduction of Chalcocite</u>
At pH 9.2 (0.05 M $Na_2B_4O_7$), cathodic current pulses of

0.025 mA/cm^2 were applied at 2 Hz to produce reducing potentials on a polished chalcocite electrode for 18 minutes. The results are shown in Figure 4.1 for unstirred (4.1a) and stirred (4.1b) cases. Both plots show that the open-circuit potential quickly dropped to a constant of approximately -700 mV vs. SHE at C_1 which corresponds to the reduction of chalcocite to metallic copper and hydrogen sulfide ion,

$$Cu_2S + H^+ + 2e = 2Cu^O + HS^-, \qquad [4.1]$$
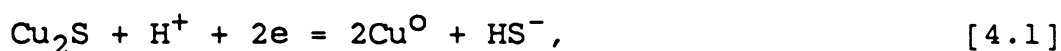
and is in full agreement with each of the E_h-pH diagrams depicted for chalcocite. Two differences between the plots are observed. First, it took 7 minutes for the unstirred case and 2 minutes for the stirred case to reach the -700 mV equilibrium potential. Obviously, the potential of the electrode in the unstirred system was inhibited by the steady accumulation of hydrogen sulfide ions in the diffusion layer. Therefore, with stirring, the potential reached -700 mV faster because the hydrogen sulfide ions were swept away. Second, a small plateau at C_3 developed within the first minute but only for the unstirred case. This indicates hydrogen sulfide ions were also produced at C_3. Furthermore, the reaction at C_3 occurred near -370 mV and thus may be caused by the reduction of djurleite,

$$2Cu_{1.96}S + .04H^+ + .08e = 1.96Cu_2S + .04HS^-, \qquad [4.2]$$
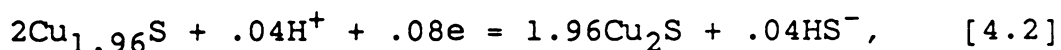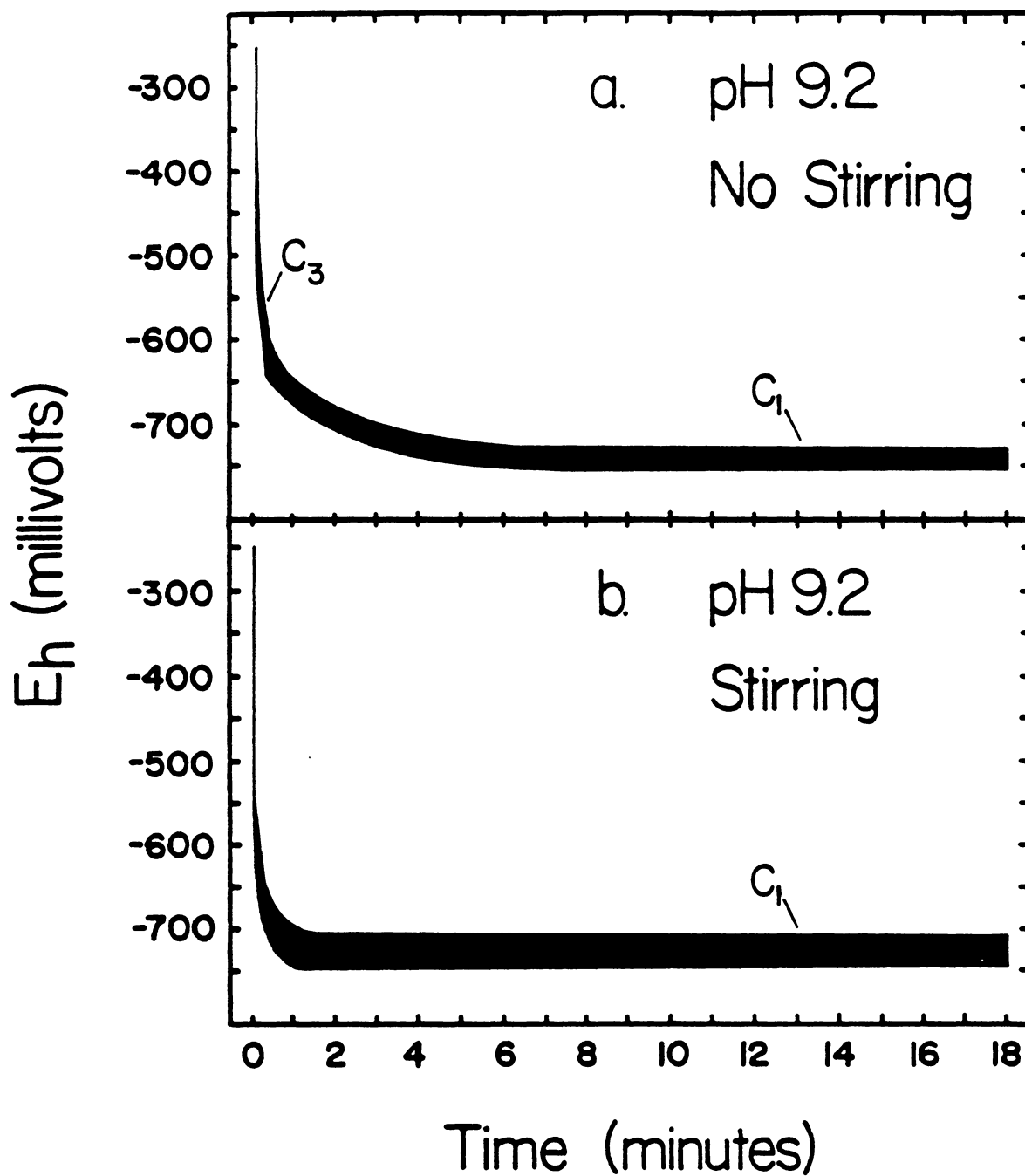
Figure 4.1 IGP diagrams obtained for the reduction of Cu_2S with current density pulses of 0.025 mA/cm^2 at 2 Hz for 18 minutes at pH 9.2 (0.05 M $Na_2B_4O_7$) a) without stirring and b) with stirring.

which suggests there was djureite-contamination in the chalcocite electrode. Both an automated diffractometer and a Gandolfi camera were used to obtain X-ray powder diffraction patterns and both showed djurleite was present (Johnson, 1987) which is typical of chalcocite from Butte, Montana (Craig, 1987).

4.1.2 Oxidation of Chalcocite

Because copper is very mobile, even within a solid, fast current pulses at 2 Hz were applied so that, if metastable nonstoichiometric compounds formed at pH 1.1 (0.1 M $HClO_4$), they would be detected. In Figure 4.2, a chalcocite electrode was oxidized with current pulses of 0.033 mA/cm^2 for 30 minutes. When the system was not stirred (Figure 4.2a), a series of five plateaus resulted. Each are labeled A_2 to A_6 to correspond with the results of the investigators mentioned above and occurred at potentials of approximately 399, 404, 408, 411, and 428 mV vs. SHE respectively. These plateaus are evident but not very distinguishable for two reasons. First, assuming that the products of the reactions which give the plateaus correspond to a solid solution series of copper sulfides such as $Cu_{1.86-1.80}S$ as concluded by Koch and McIntyre (1976) rather than copper sulfides of specific stoichiometry like $Cu_{1.83}S$, then sharp and distinct plateaus will not be
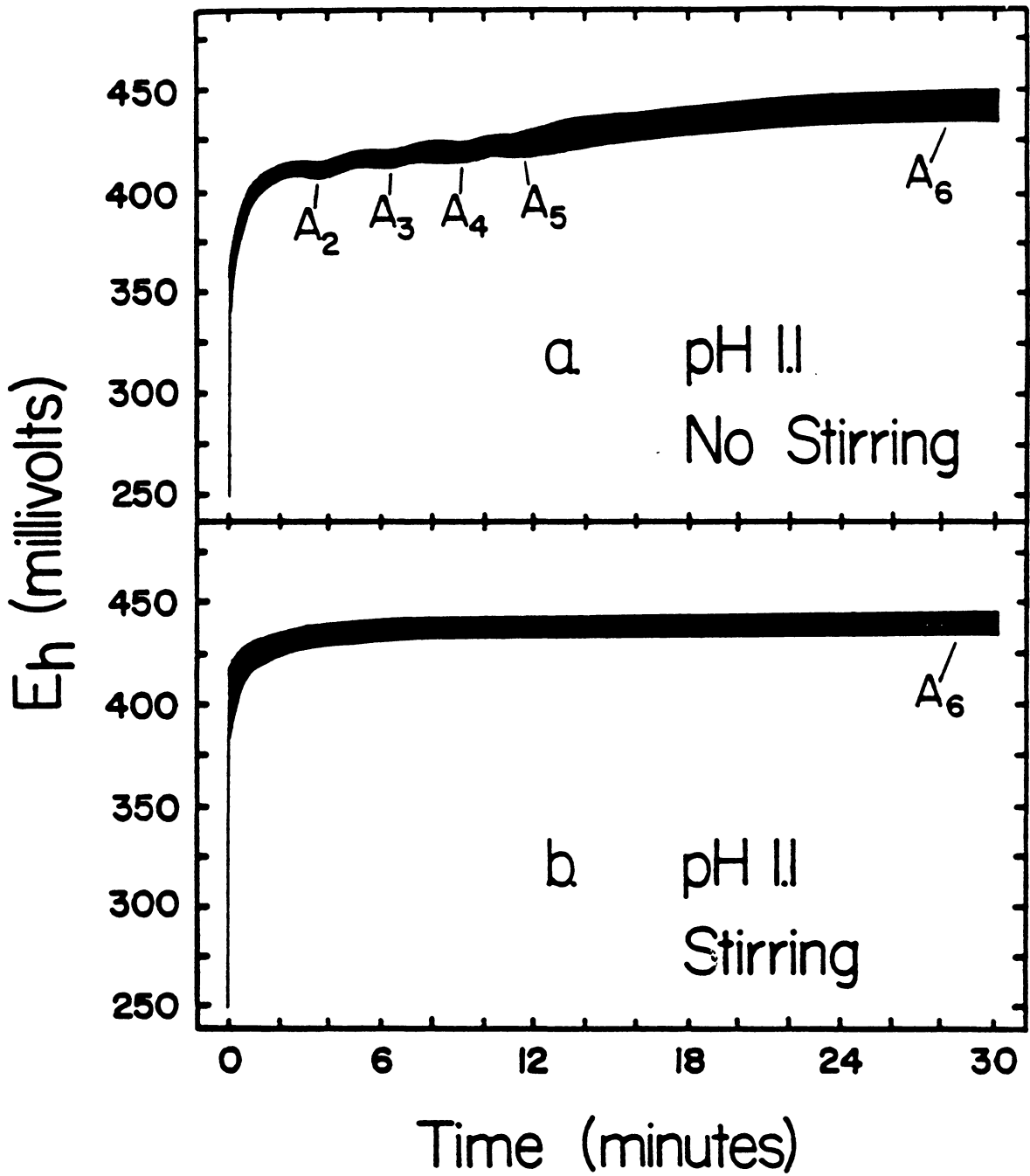
Figure 4.2 IGP diagrams obtained for the oxidation of Cu_2S with current density pulses of 0.033 mA/cm^2 at 2 Hz for 30 minutes at pH 1.1 (0.1 M HClO$_4$) a) without stirring and b) with stirring.

produced. Second, the reaction which produces the nonstoichiometry from chalcocite also produces cupric ions according to the following general reaction:

$$Cu_{2-x}S = Cu_{2-x-y}S + yCu^{2+} + 2ye.$$ [4.3]
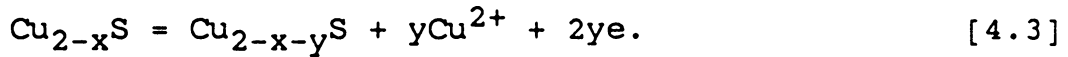
However, the resulting cupric ion concentration changes with time because it is dependent on the rate at which Reaction [4.3] proceeds as well as the mass transport of cupric ions away from the surface and through a continually growing diffusion layer. Therefore, stirring the system should give results similar to when, under reducing condtions, the hydrogen sulfide ions were swept away from the chalcocite surface. As can be seen from Figure 4.2b, stirring the cupric ions away caused the four initial plateaus, A_2 to A_5, to completely disappear and the final A_6 plateau to reach the equilibrium potential of 428 mV in 9 minutes as compared to 24 for the unstirred case. After 30 minutes of polarization for both the stirred and unstirred cases, the chalcocite had developed a blue color meaning that the oxidation proceeded to covellite as concluded by the previously mentioned investigators. However, this blue tint could be caused by the formation of either of the blue-remaining covellites, i.e., yarrowite or spionkopite, of which the latter was shown to be the final oxidation product of chalcocite as concluded by both Thomas et al. (1967) and

Marcantonio (1976) during acidic ferric sulfate leach tests.

IGP tests were also performed in fixed copper concentrations (0.01 M $CuNO_3$) at pH 1.1 so that, if the nonstoichiometric products could be observed, thermodynamic data could be derived for the products. Unfortunately, the plateaus never developed possibly because $CuNO_3$ is a slight oxidizing agent which would affect the current flow as well as the potential measurement.

4.2 X-ray Photoelectron Spectroscopy

IGP experiments have shown that metallic copper co-exists with chalcocite and that the formation of the metastable nonstoichmetric copper sulfides can be detected. Because the amounts of the species produced during the IGP experiments were too small to be analyzed with XPS, attempts failed to confirm both reduction and oxidation cases. Furthermore, the use of three polishing stages to obtain a clean surface produced inconsistent surface areas resulting in different current density pulses being applied and, thereby, giving non-repetitive information. Therefore, in order to produce detectible and consistent amounts of a product, a constant potential was applied to the electrode rather than a constant current density. The set-up required was exactly the same as that for cyclic voltammetry (see Figure 3.5) except that the X-t recorder was used in place

of the X-Y recorder. Current densities were measured as a function of time. These tests are referred to as chronoamperometry experiments and have previously been used to study galena reaction mechanisms (Pritzker, 1985).

4.2.1 Reduction of Chalcocite

To detect the co-existence of chalcocite and metallic copper, chalcocite samples were subjected to constant potentials of 0, -200, -400, -600, -800, -1000, and -1200 mV vs. SHE for five minutes at pH 9.2 (0.05 M $Na_2B_4O_7$). Current flow was monitored during the experiments and recorded as current density (see Figure 4.3). The system was stirred because equilibrium is obtained faster as shown by the previous IGP diagrams. Also, current densities were relatively independent of stirred and unstirred systems. As shown in Figure 4.3, cathodic current flowed at all applied potentials; hence, reduction reactions such as [4.1] or [4.2] occurred at each potential. Decreasing the potential increased the current density but as the potential was lowered to -800 mV or further, the current density changed irregularly with time as compared to the smooth changes for the other potentials. Therefore, the transition from smooth to irregular current flow occurred somewhere between -600 and -800 mV, probably near -700 mV which corresponds to the equilibrium potential of Reaction [4.1] and agrees with both
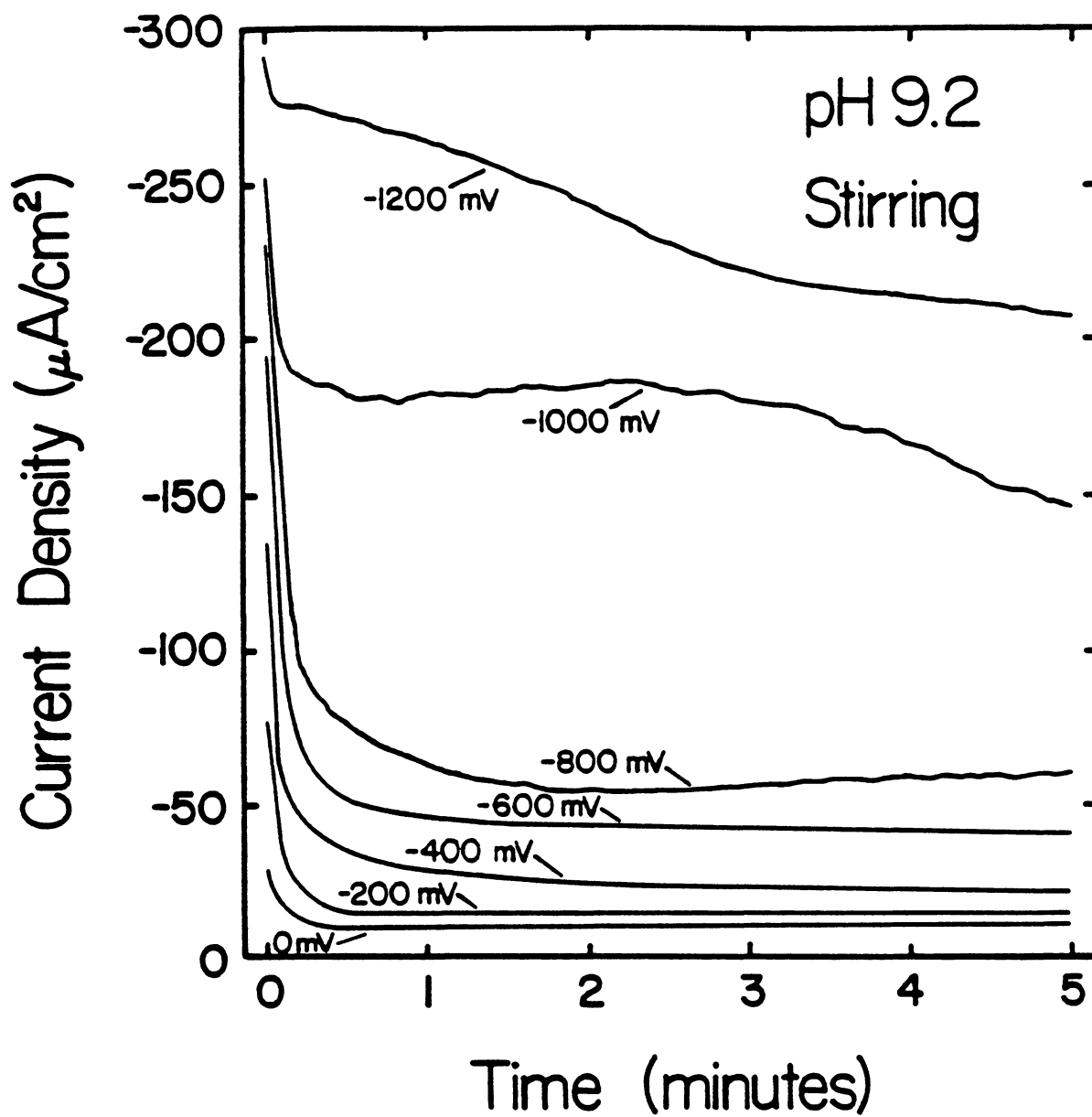
Figure 4.3 Chronoamperometry tests of Cu_2S for 5 minutes at pH 9.2 (0.05 M $Na_2B_4O_7$) with stirring.

the computer calculations and IGP. Furthermore, the
irregular changes in current density can be explained by an
unsteady accumulation of metallic copper on the surface
resulting in a fluctuating surface area. The unsteady
accumulation would be caused by the three-dimensional (e.g.,
dendritic) growth of metallic copper. On the other hand,
layer-by-layer (e.g., platelike) growth would account for an
unchanging surface area and, hence, smooth changes in
current density. Therefore, at potentials above -700 mV,
the accumulation of metallic copper occurs steadily. The
same could be said of the production of chalcocite below
-370 mV according to Reaction [4.2]. Below -700 mV,
metallic copper is produced unsteadily. When metallic
copper is formed by Reaction [4.1], the chalcocite acts like
a shrinking core.

As discussed in Section 3.2.2, the procedure and
materials for XPS, wide scans of the chalcocite samples were
taken following the five narrow scans of the Cu $2p_{3/2}$, Cu
L_3VV, S 2p, C 1s, and O 1s peaks. A typical wide scan of
electrochemically untreated chalcocite (i.e., the standard)
is shown in Figure 4.4 which shows the five narrow scans
occur at binding energies near 933, 337, 162, 285, and 532
eV, respectively. A wide variety of other peaks are also
labeled including the Si 2s (152 eV) and the Si 2p (100 eV)
which appear as a result of using silicon carbide in the
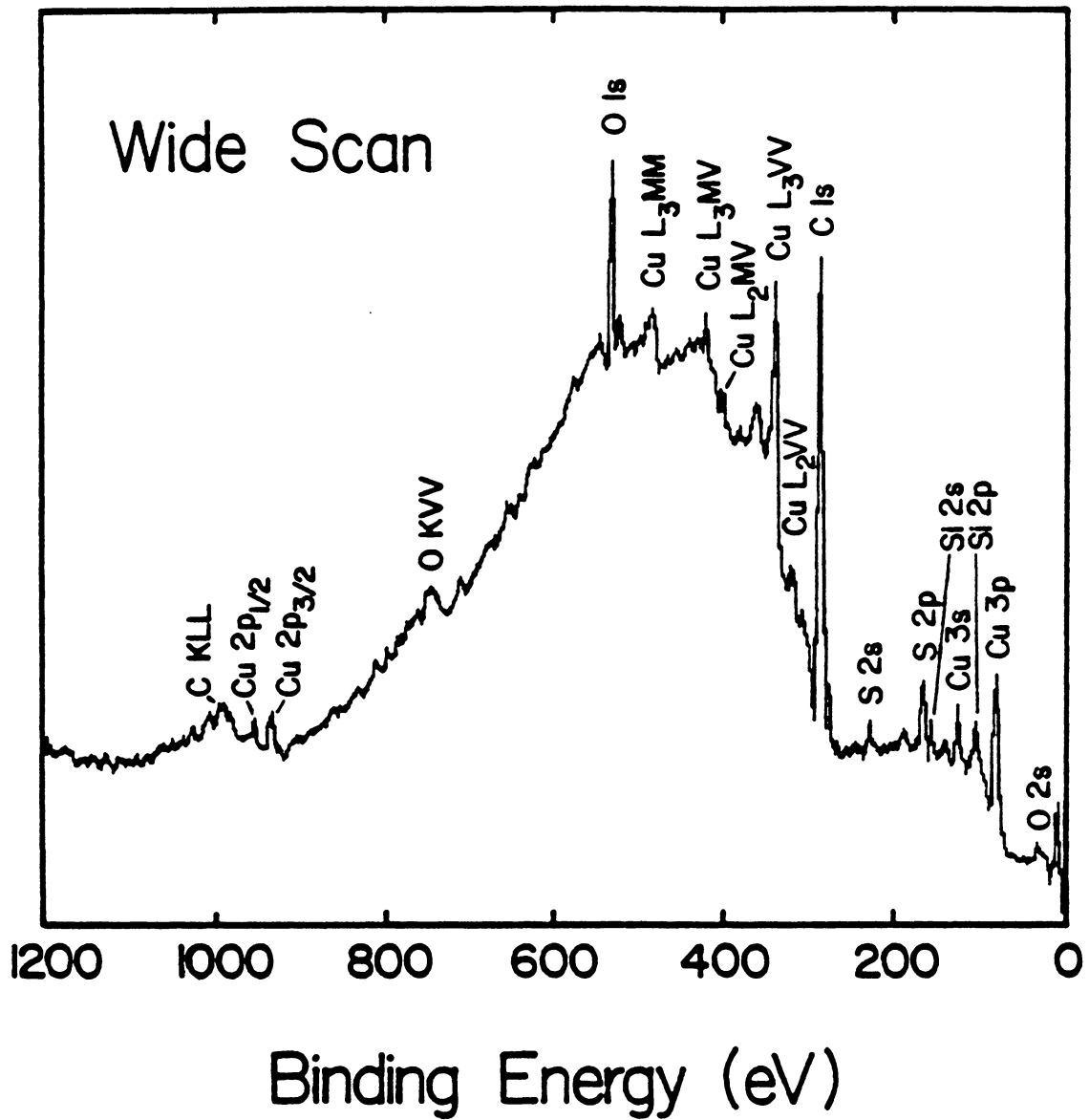
Figure 4.4 Wide XPS scan of polished chalcocite.

first polishing stage. Subsequent polishing stages were
therefore employed to remove the silicon and, hence, its
signal, thereby enhancing the signal of the other peaks.

XPS spectra of the C 1s and O 1s peaks are shown for
each of the samples in Figures 4.5a and 4.5b, respectively.
Because a majority of the signal arises from the epoxy, a
mixture of two hydrocarbons known as triethylenetetramine
and n-butylglycolether each of which contain a variety of
oxygen and carbon atoms, the intensity of each of the peaks
are quite broad. Therefore, the signal for adventitious
carbon at 284.8 eV was masked and could not be referenced
to. However, at the -800 mV potential, two distinct types
of carbon were observed: supposedly, adventitious carbon
with the higher binding energy and epoxy carbon with the
lower. After referencing the suspected adventitious carbon
peak to 284.8 eV, a static charge of 4.1 eV was calculated
which seemed high but indicated that the epoxy was a good
insulator. All peaks were then referenced to the
adventitious carbon peak when the static charge was
substracted from all binding energies (or added to all
kinetic energies). Such calculations were not possible for
the other potentials so their results were merely matched to
the results of the -800 mV potential.

Figure 4.6 shows the results obtained for the narrow
scans of the Cu L_3VV Auger electron. Since the peak was
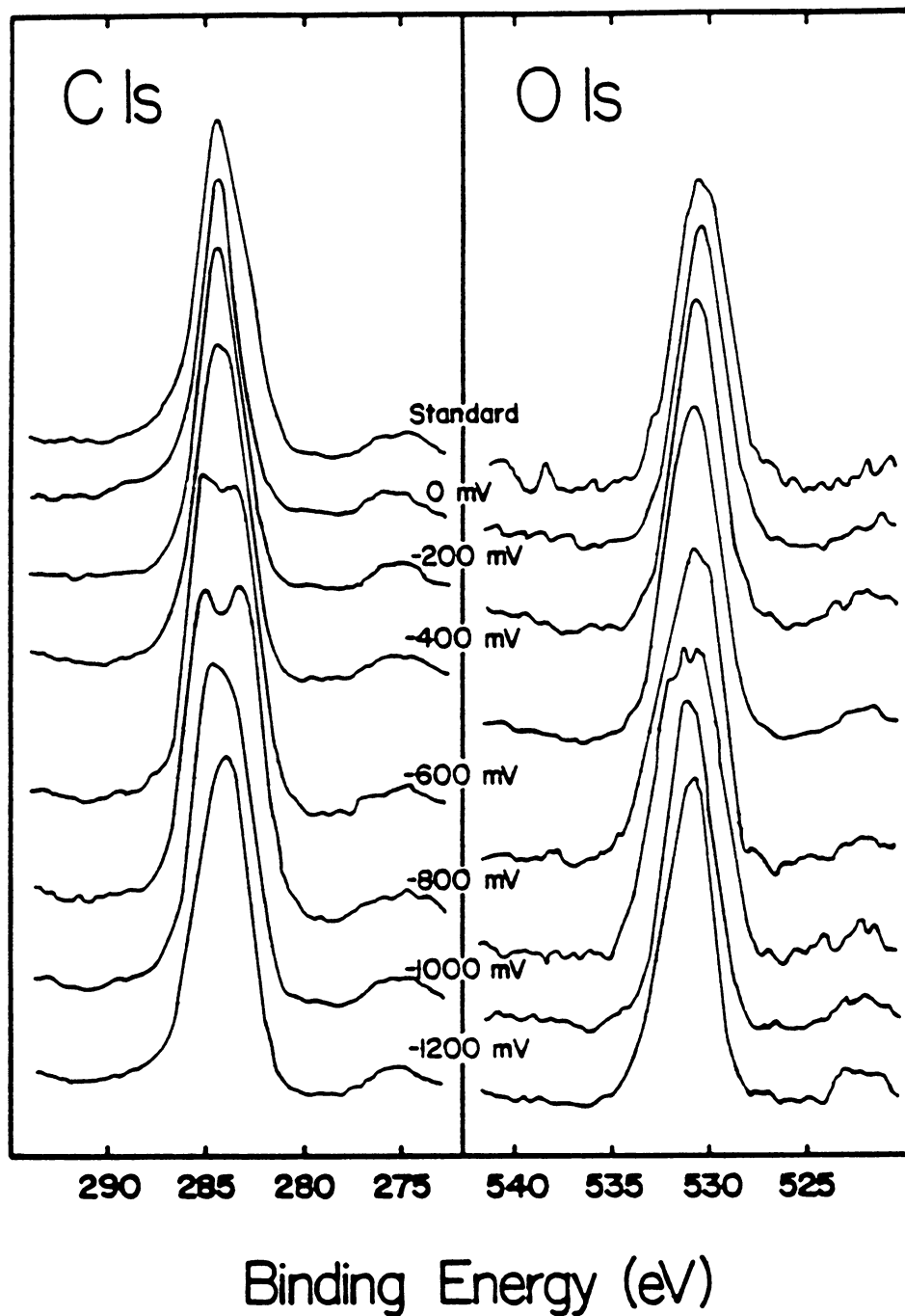
Figure 4.5   Narrow XPS scans of the 1s electrons from carbon and oxygen after 5 minutes of applying the indicated potentials to Cu_2S at pH 9.2 (0.05 M $Na_2B_4O_7$) with stirring.
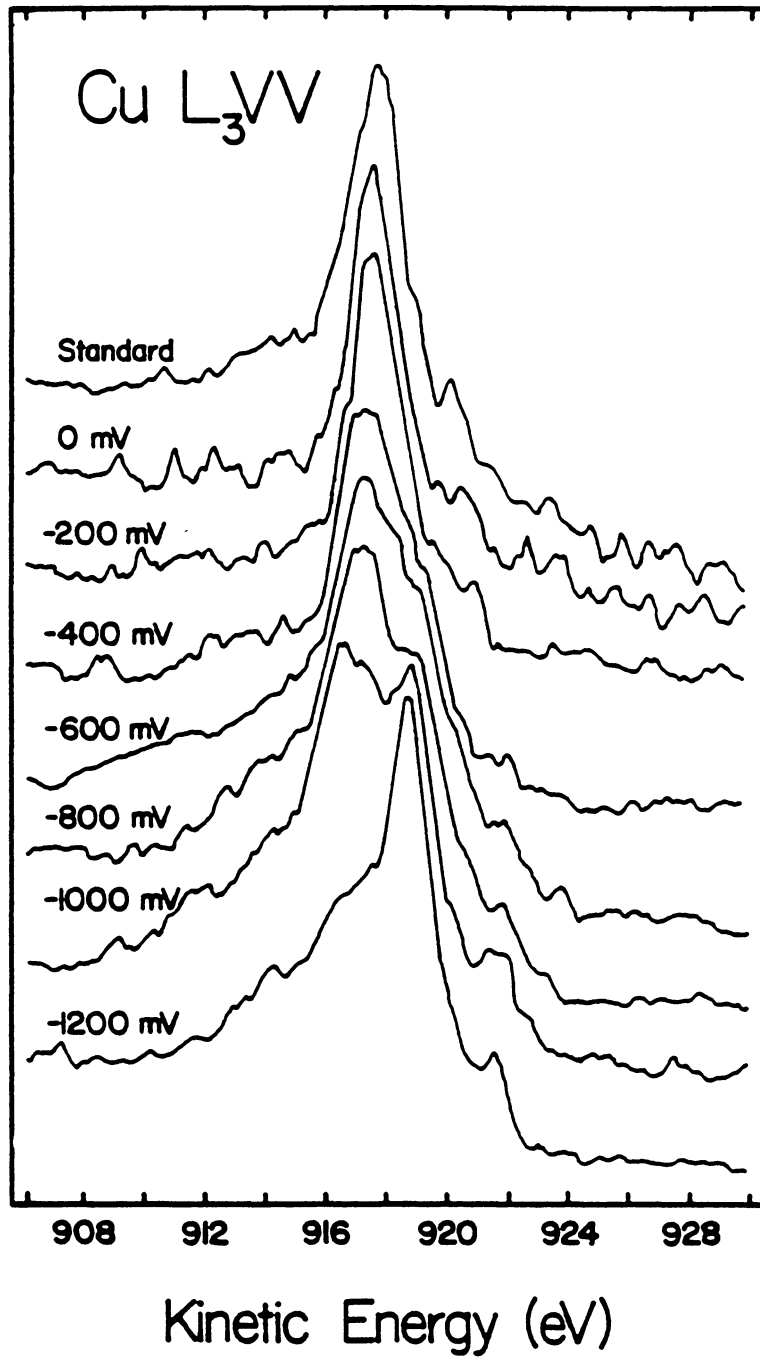
Figure 4.6   Narrow XPS scans of the Cu L_3VV Auger electrons
             after 5 minutes of applying the indicated
             potentials to Cu_2S at pH 9.2 (0.05 M $Na_2B_4O_7$)
             with stirring.

produced by an Auger electron, the kinetic energy scale is provided. The Cu L_3VV for the standard reaches a maximum at a kinetic energy of 917.1 eV (i.e., a binding energy of 336.5 eV). Holding the potentials at 0 and -200 mV vs. SHE did not affect the position or the shape of the peak. However, reducing the potentials further shows that the peak develops a shoulder at 918.7 eV (i.e., a binding energy of 334.9 eV) which corresponds to metallic copper. The shoulder eventually becomes a peak at -1000 mV. Therefore, it can be concluded that, according to XPS, metallic copper and chalcocite co-existence starts between -200 and -400 mV vs. SHE at pH 9.2. Furthermore, photoreduction of chalcocite to metallic copper did not occur since the standard, 0 mV, and -200 mV samples revealed no metallic copper signal at 918.7 eV.

In order to quantify the XPS results, narrow scans of the Cu $2p_{3/2}$ and S 2p peaks were taken as shown in Figures 4.7a and 4.7b, respectively. Eventhough chalcocite and metallic copper cannot be distinguished from the Cu $2p_{3/2}$ peak (932.7 eV), the signal appears to get stronger as the potential was decreased. Similiarly, the S 2p peak at 161.5 eV seemed to get weaker as the potential was decreased suggesting that hydrogen sulfide ions formed and were stirred away. The appearance of S 2p peaks at 168 eV are caused by sulfate, the presence of which can not be
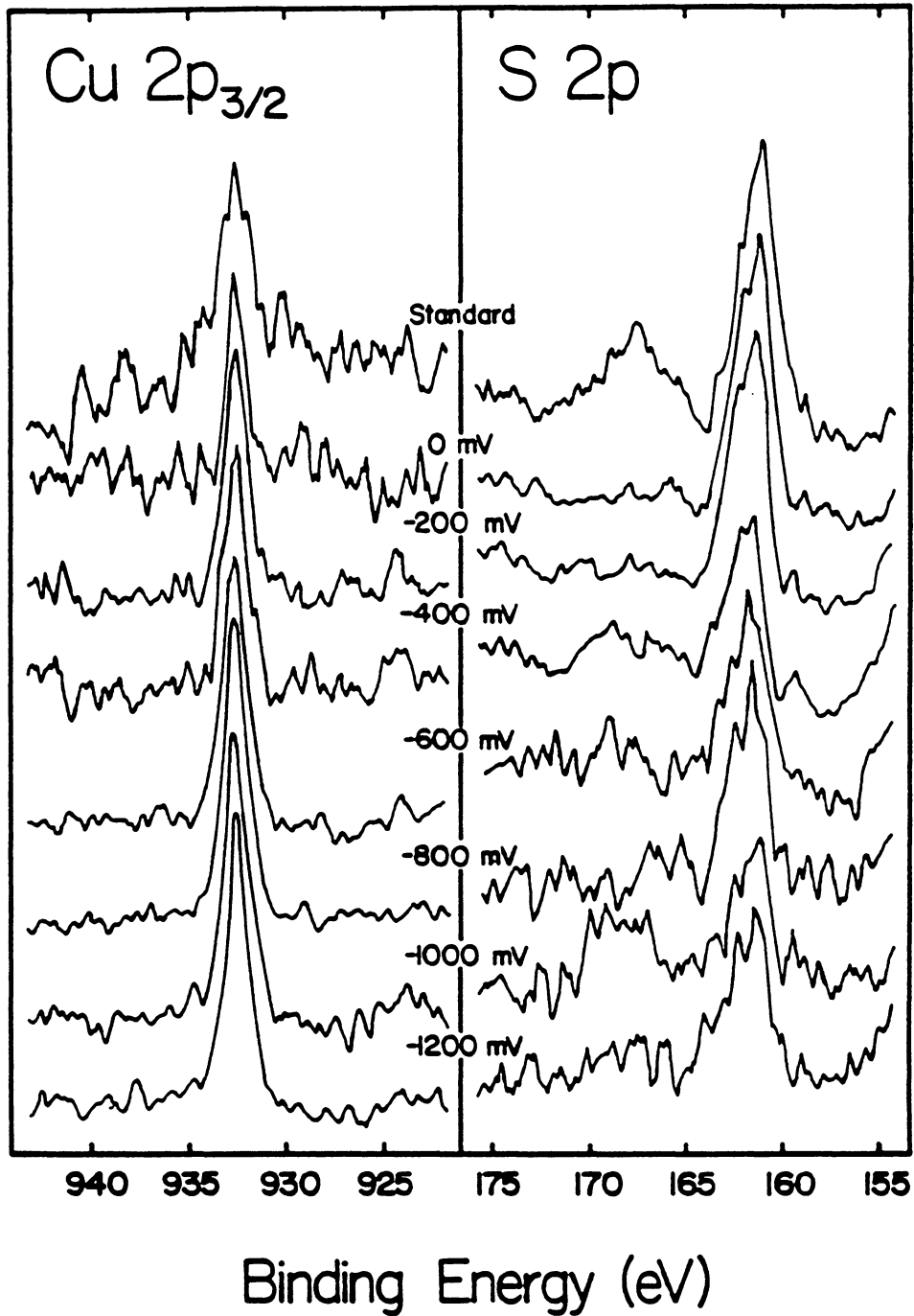
Figure 4.7   Narrow XPS scans of the Cu $2p_{3/2}$ and S 2p
photoelectrons after 5 minutes of applying the
indicated potentials to Cu_2S at pH 9.2 (0.05 M
$Na_2B_4O_7$) with stirring.

explained since it occurred sporadically.

Adding the binding energy of the Cu $2p_{3/2}$ peak, 932.7 eV, to the kinetic energy of the Cu L_3VV peak, 917.1 and 918.7 eV, gives Auger parameters of 1849.8 and 1851.4 eV for chalcocite and metallic copper, respectively. These results are quite comparable to the expected values of 1850 and 1851 eV (see Figure 3.4); however, the 0.4 eV difference between 1851 and 1851.4 eV for metallic copper suggests that the copper that formed was metastable. After all, the copper that formed was quite black in color and, most likely, would not have the same structure as the stable form. The Cu $2p_{3/2}$ binding energy of 932.7 eV is also comparable to the 932.3 eV determined by Mielczarski and Suoninen (1984) and the 932.6 eV determined by Nakai et al. (1978), Nefedov et al. (1980), and Ranta et al. (1981). These same authors also determined the binding energy of the S 2p peak to be 161.5, 162.0, 162.6, and 162.5 eV, respectively, which compare to the 161.5 eV determined in the present work.

To quantify the XPS results, intensities (i.e., the areas under each peak) were determined and substituted along with the sensitivity factors of 892.198 for the Cu $2p_{3/2}$ peak and 834.721 for the S 2p peak into Equation [3.4] to determine Cu/S ratios for the electrolyzed samples as well as the standard (see Table 4.1). As shown in Table 4.1, the surface Cu/S ratio increases from 0.147 (standard) to 5.027

Table 4.1

XPS Data Determined by the Cu $2p_{3/2}$ and S 2p Electrons
During the Reduction and Oxidation of Chalcocite

| Sample | Cu 2p3/2 | | S 2p | | Surface |
	Intensity	Scans	Intensity	Scans	Cu/S Ratio
Standard	6349	4	20262	2	0.147
0 mV	9075	3	23690	2	0.239
-200 mV	17653	3	28251	2	0.390
-400 mV	12393	2	13237	2	0.876
-600 mV	36337	2	8894	2	1.911
-800 mV	40391	2	12081	2	3.128
-1000 mV	22925	2	4952	2	4.331
-1200 mV	47265	2	8796	2	5.027
*Crushed	115495	2	99110	2	1.090
*+600 mV	10402	4	52997	2	0.092
*Sulfur	—	—	440888	2	—

* discussed later

(-1200 mV). The preferential orientation of sulfur (sulfide) atoms at the surface in the crystal structure of chalcocite (Kostov and Minceva-Stefanova, 1981) may cause the ratio to be less than the bulk ratio of two. Hurlbut and Klein (1977) stated single crystals of chalcocite are extremely rare (i.e., they are polycrystalline) so it is highly unlikely that the chalcocite was cut along a crystal face that preferentially allowed the sulfur atoms to be exposed at the surface.

The results are plotted in Figure 4.8 which shows that, as the potential decreased, the surface Cu/S ratio increased with a definite change in slope near -370 mV. Because IGP has shown that the reduction of djurleite occurred at -370 mV, the plot was correspondingly labeled with C_1 and C_2 which coincide with Reactions [4.1] and [4.2], respectively. Since each test was performed for five minutes, the rates of each reaction are shown to increase linearly with decreasing potentials. Below -1000 mV, Reaction [4.1] became mass-transport controlled. Prior to -370 mV, the sulfide-rich surface may react to form aqueous sulfide which diffuses away. Most likely, though, the sulfide-rich surface would react with copper atoms that migrate to the surface from underneath to produce a copper sulfide, possibly djurleite or one of similar stoichiometry (i.e., $Cu_{1.93}S$), which would further contaminate the chalcocite. In either case, the
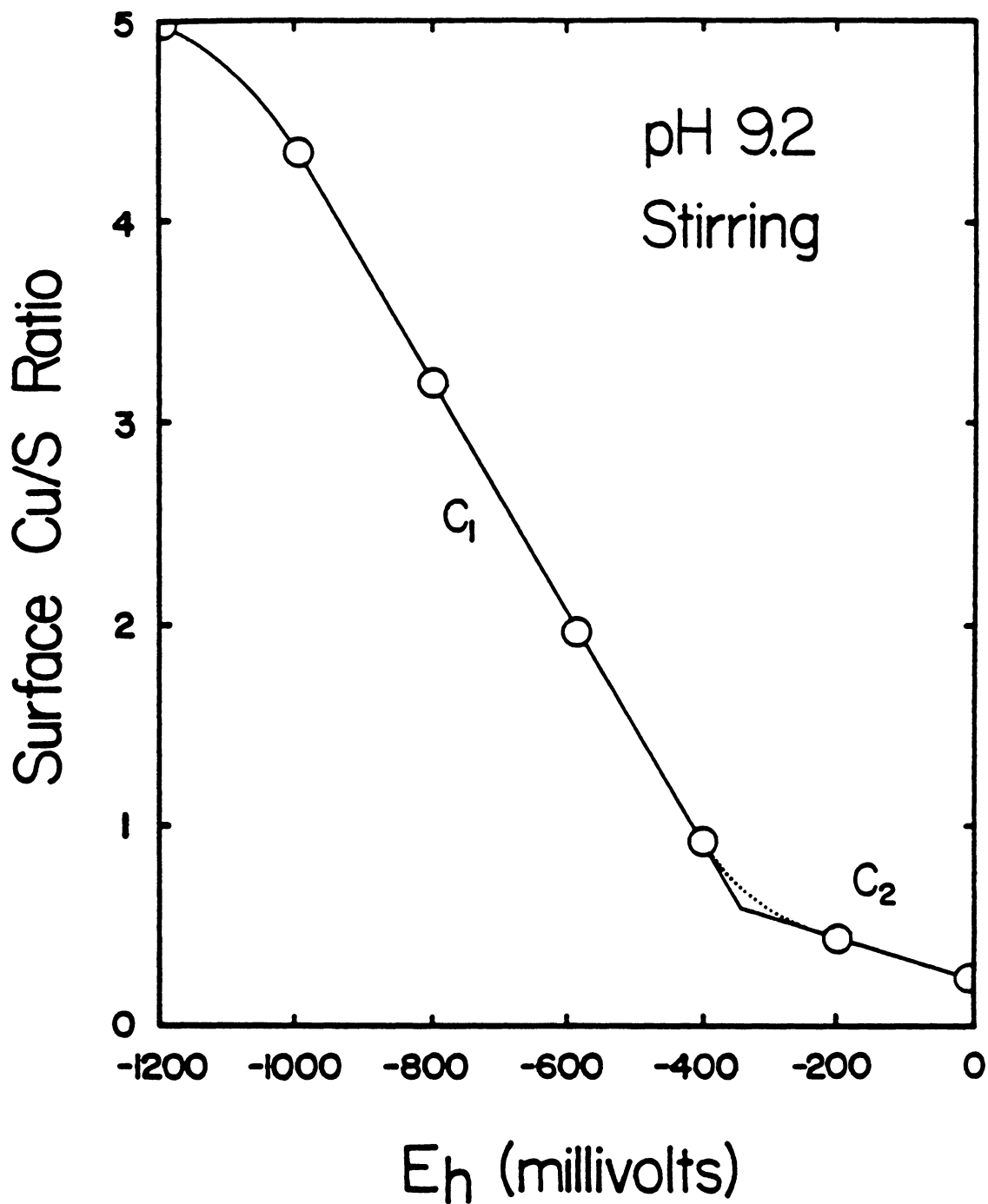
Figure 4.8 Surface Cu/S ratio as a function of applied potential after 5 minutes of polarization at pH 9.2 (0.05 M $Na_2B_4O_7$) with stirring.

surface Cu/S would increase.

In order to confirm these calculations, a sample of chalcocite was dry-ground with a porcelain mortar-and-pestle and immediately mounted on the sample holder with double-stick adhesive tape and placed in the sample chamber. As before, the sample was cooled and narrow scans of the Cu $2p_{3/2}$, Cu L_3VV, S $2p$ and C $1s$ peaks were taken. Since epoxy was absent, the carbon signal from adventitious carbon was not masked. Equating the C $1s$ peak to a binding energy of 284.8 eV resulted in a static charge of 0.1 eV. After referencing, as shown in Figure 4.9, the kinetic energy of the Cu L_3VV peak measured 917.1 eV and the binding energies of the Cu $2p_{3/2}$ and S $2p$ peaks were 932.8 and 161.5 eV, respectively. Except for the acceptable difference of 0.1 eV for the Cu $2p_{3/2}$ peak, these measurements match the earlier results. Adding the energies of the two copper peaks together gives 1849.9 eV which also concurs with Figure 3.4. Excellent agreement was therefore obtained for all calculations; however, the surface Cu/S ratio was determined to be 1.09 which does not compare to 0.147 obtained earlier (see Table 4.1). The difference can be credited to the sample preparation techniques: three stages of wet-polishing versus dry-grinding. Because a higher surface Cu/S ratio was obtained for dry-grinding, it appears that wet-polishing altered the surface of chalcocite by
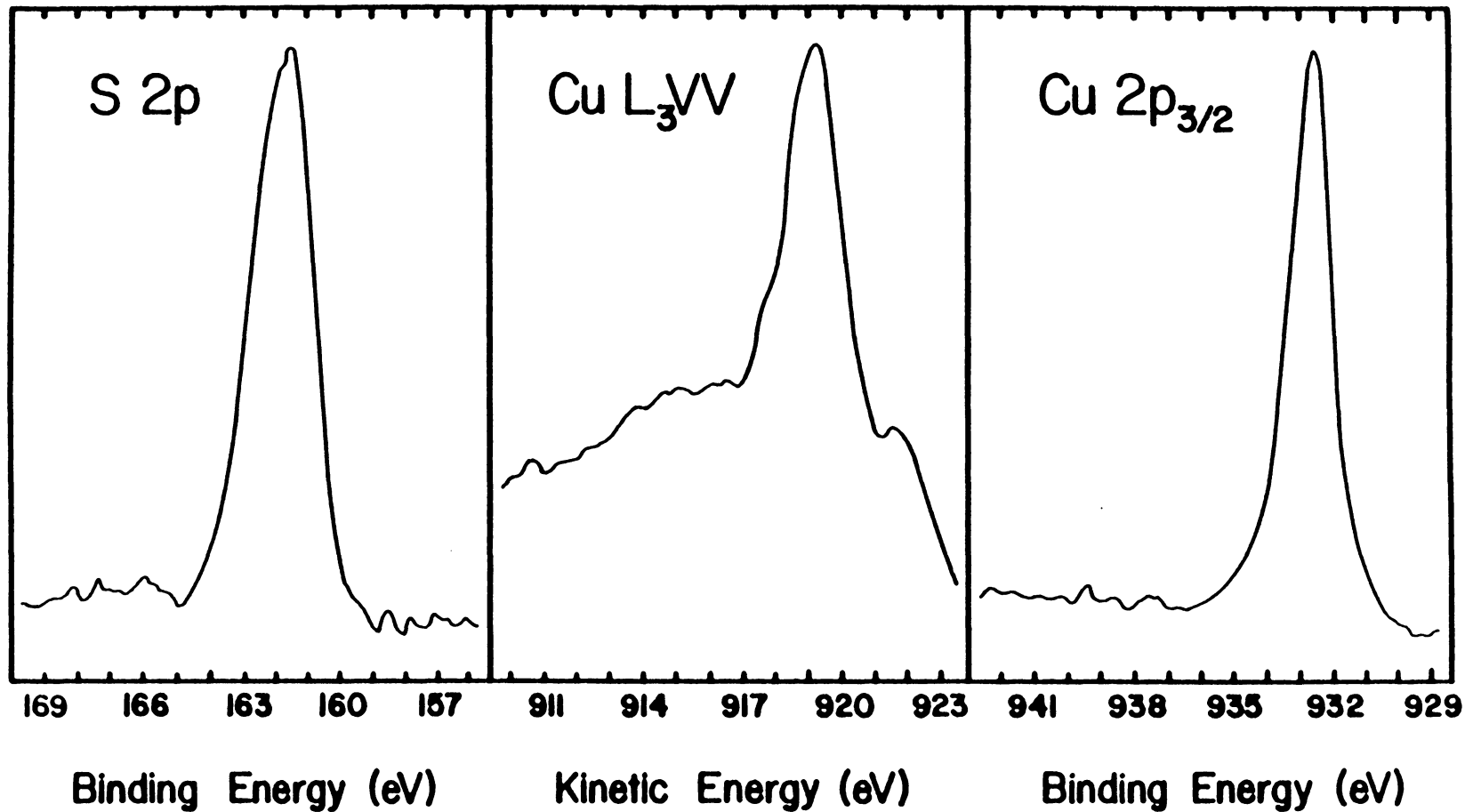
Figure 4.9   Narrow XPS scans of the S 2p, Cu L$_3$VV and Cu 2p$_{3/2}$ electrons for crushed Cu$_2$S.

specifically dissolving the copper. Therefore, wet-polishing, or at least three stages of it, should be avoided. Probably for the reason mentioned earlier, the surface Cu/S ratio was still not two.

Assuming the surface Cu/S ratio of chalcocite of 1.09 is correct, then metallic copper can only exist if the ratio is greater than 1.09. Because Table 4.1 and, hence, Figure 4.8 show that the surface Cu/S ratio for -400 mV was less than 1.09, metallic copper could not be present which, of course, contradicts the evidence illustrated by the Cu L_3VV Auger electrons. It is possible, although unlikely, that the somewhat large static charge that was present altered the shape of the peak.

Since chalcocite only contains copper and sulfur atoms in the form of cuprous sulfide, perfectly shaped Gaussian peaks for the Cu $2p_{3/2}$ and S 2p electrons should be produced provided the signal-to-noise ratio of each narrow scan is high. From Figure 4.9, this is evident for the Cu $2p_{3/2}$ peak but not for the S 2p peak. The asymmetry of the S 2p peak is not caused by the presence of a second sulfur species, but rather by the excellect resolution of the S 2p peak into its two components, the S $2p_{1/2}$ and S $2p_{3/2}$, often referred to as the S 2p doublet. Such resolution is not possible without the hemispherical analyzer.

4.2.2 Oxidation of Chalcocite

Since IGP experiments at pH 1.1 have shown covellite to be a product of chalcocite oxidation and since mass-balanced calculations of oxidation to elemental sulfur have shown covellite to be stable near 600 mV vs. SHE, a constant potential of 600 mV was applied to chalcocite for five minutes. Narrow scans of Cu $2p_{3/2}$, Cu L_3VV, S 2p, and C 1s peaks were then taken of the dark blue oxidation product that resulted. A static charge of 2.8 eV was determined and peak energies of 917.9 and 162.1 eV were subsequently calculated for the Cu L_3VV and S 2p electrons, respectively (see Figure 4.10). Because so little copper was on the surface (i.e., the Cu/S ratio was 0.092), the signal for the Cu $2p_{3/2}$ peak was weak and the binding energy could not be determined. Once again, the S 2p doublet was visible; however, two new peaks appear as shoulders with binding energies near 164 eV. Because elemental sulfur can form at 600 mV vs. SHE and has an S 2p binding energy near 164 eV (Wagner et al., 1979; Luttrell and Yoon, 1984) the shoulders may have been produced by elemental sulfur. Therefore, a standard of elemental sulfur of A.C.S. grade was analyzed and is compared to the S 2p peaks obtained from the crushed chalcocite sample and the oxidized chalcocite sample (see the dotted peaks in Figure 4.11). Some slight resolution of the doublet for the standard of elemental sulfur also

S 2p

Cu L₃VV

Cu 2p₃/₂

169 166 163 160 157
Binding Energy (eV)

911 914 917 920 923
Kinetic Energy (eV)

941 938 935 932 929
Binding Energy (eV)
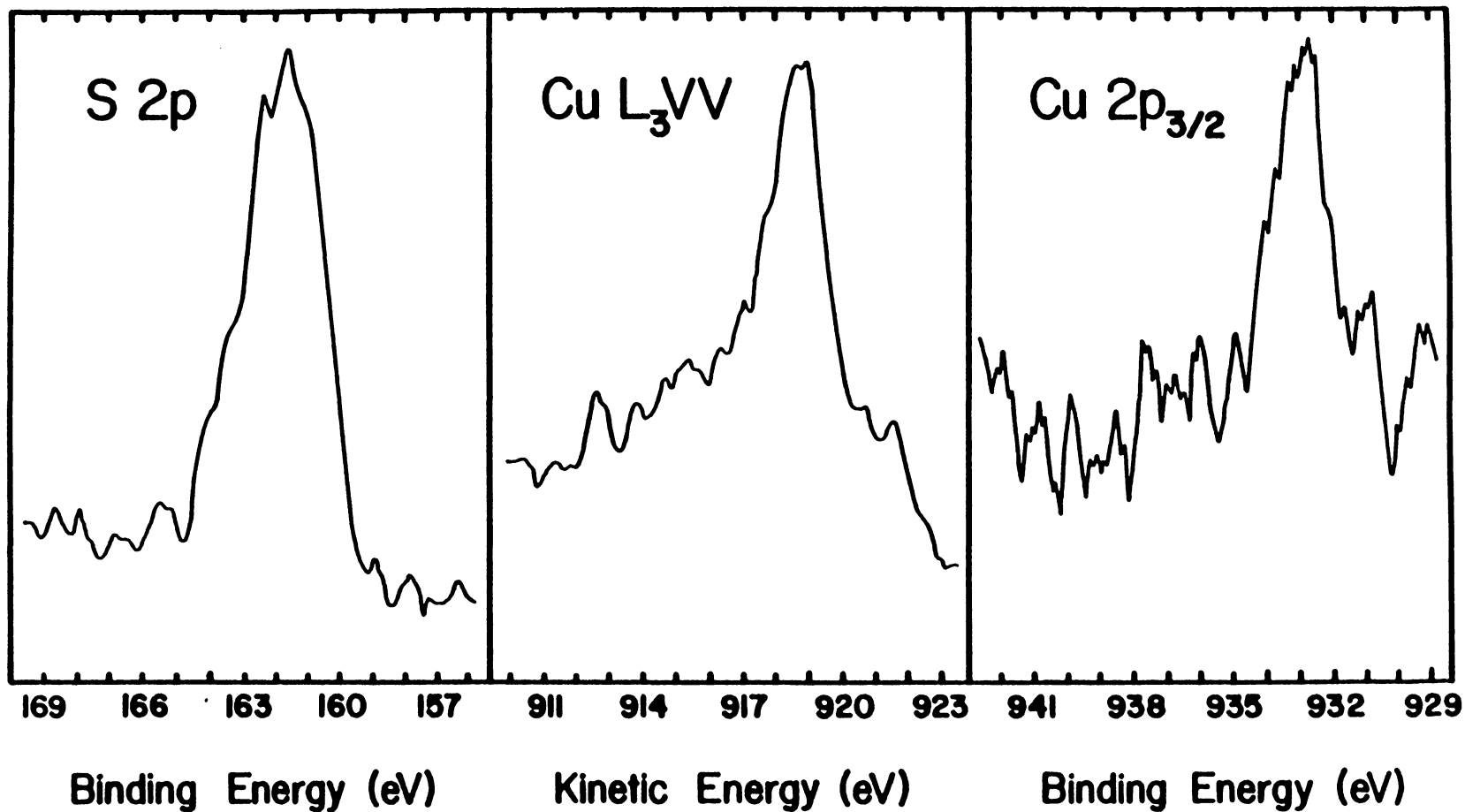
Figure 4.10   Narrow XPS scans of the S 2p, Cu L_3VV and Cu $2p_{3/2}$ electrons for Cu_2S after applying a potential of 600 mV for 5 minutes at pH 1.1 (0.1 M $HClO_4$) while stirring.

S 2p

······ Elemental Sulfur

— Crushed Cu_2S (top)

— Oxidized Cu_2S (bot.)

174   170   166   162   158   156

Binding Energy (eV)
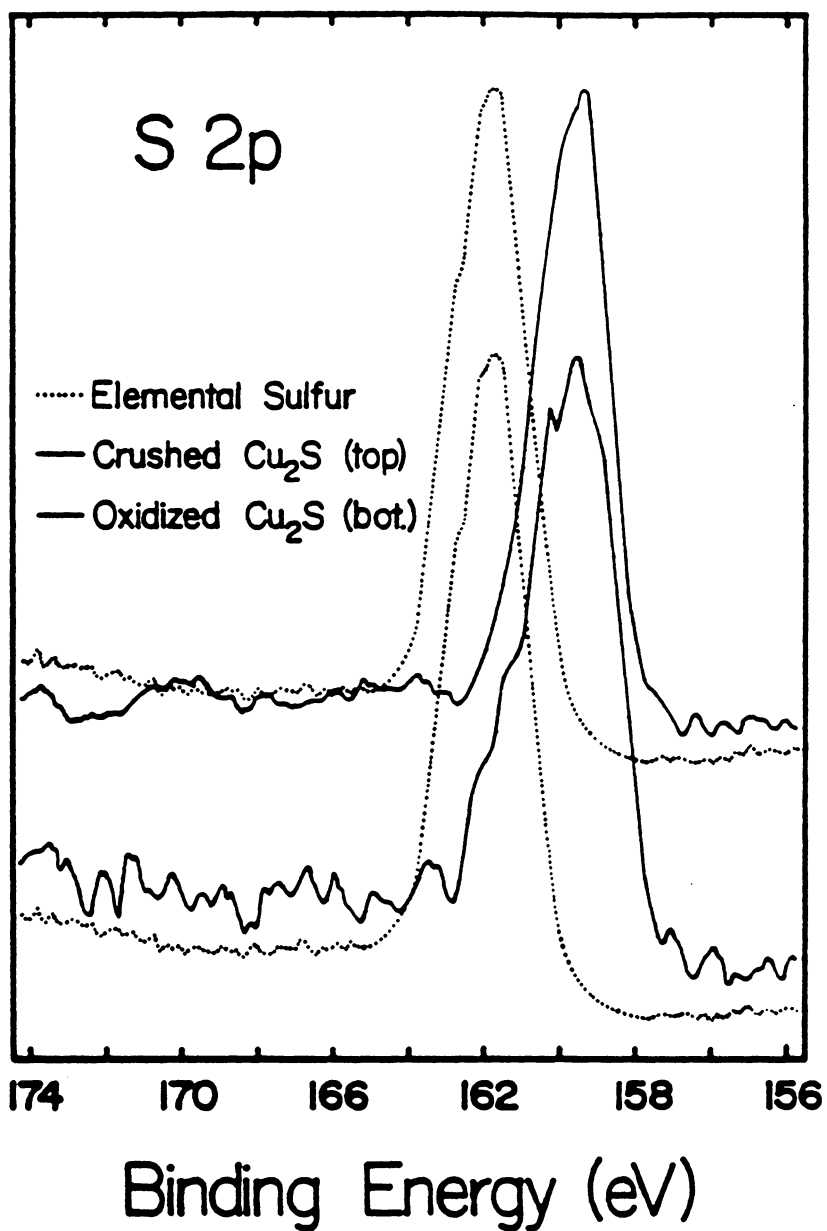
Figure 4.11   Narrow XPS scans of the S 2p electrons for elemental sulfur (dotted) compared to that of crushed chalcocite (top) and chalcocite oxidized at 600 mV for 5 minutes at pH 1.1 (0.1 M $HClO_4$) while stirring (bottom).

occurred. After referencing, the binding energy of the S 2p electron was 163.9 eV for elemental sulfur but no definite conclusion could be drawn as to what sulfur species was responsible for the formation of the two shoulders.

To determine what accounted for the formation of the two shoulders, each of the S 2p doublets were resolved with the computer. A best fit was obtained by minimizing the square of the difference between calculated and experimental peaks. For the crushed chalcocite sample, the only constraint was to keep the intensity of the S $2p_{3/2}$ twice that of the S $2p_{1/2}$ since the intensities or peak areas of any $p_{3/2}$ peak is always twice that of its respective $p_{1/2}$ peak. Binding energies of 161.5 and 162.7 eV and peak widths at half height (PWHH) of 1.53 and 1.40 eV resulted for the S $2p_{3/2}$ and S $2p_{1/2}$ electrons, respectively (see Figure 4.12a). Further constraints were then placed on the remaining peaks to be resolved: the difference between the binding energies of the S $2p_{3/2}$ and S $2p_{1/2}$ had to be kept at 1.2 eV and their respective peak widths at half height had to be kept constant at 1.53 and 1.40 eV, respectively. Some slight deviation was tolerated. Binding energies of 163.7 and 164.9 were resolved for the S $2p_{3/2}$ and S $2p_{1/2}$ peaks of elemental sulfur, respectively, and are quite comparable to the 163.8 and 164.7 eV determined by Pritzker et al. (1980) and exactly match those of Leppinen (1987)
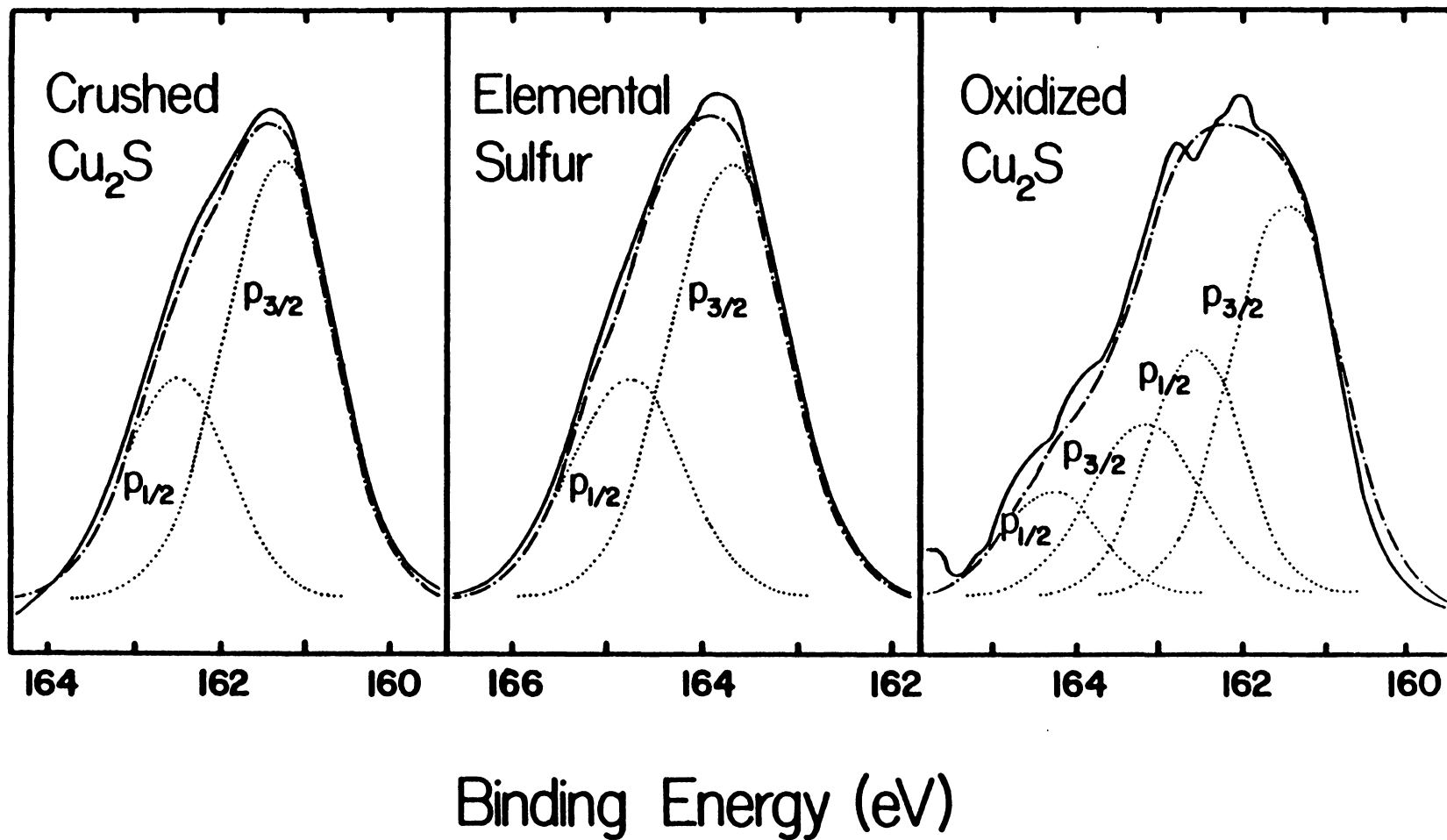
Figure 4.12   Curve-resolved spectrum of the S $2p_{1/2}$ and S $2p_{3/2}$ electrons for crushed Cu_2S, elemental sulfur and Cu_2S oxidized at 600 mV for 5 minutes at pH 1.1 (0.1 M $HClO_4$) while stirring.

(see Figure 4.12b). The four peaks in Figure 4.12c were resolved from the oxidized sample and had binding energies of 161.5, 162.6, 163.2 and 164.3 eV. The results are listed in Table 4.2.

The doublet represented by the 161.5 and 162.6 eV binding energies match that of chalcocite; however, the remaining doublet of 163.2 and 164.3 eV do not correspond to that of elemental sulfur. In fact, the binding energies are between those of chalcocite and elemental sulfur implying that the shoulders are caused by a polysulfide. Because Oftedal (1932), Berry (1954) and Sugiura (1971) showed that naturally-occurring covellite contained equivalent amounts of chalcocite and copper disulfide, $Cu_2S \cdot CuS_2$, than the metastable covellite produced during chalcocite oxidation probably also contains disulfide which, of course, is a polysulfide. Although two oxidation states of copper are present, neither the Cu L_3VV nor the Cu $2p_{3/2}$ electrons could distinguish them.

Since covellite contains a combination of disulfide and sulfide, it is possible that the nonstoichiometric copper sulfides do as well. The nonstoichiometric copper sulfides can then be represented by $Cu_2S \cdot xCuS_2$, where 'x' ranges from 0 for chalcocite to 1 for covellite. For example, 'x' for djurleite ($Cu_{1.96}S$) and anilite ($Cu_{1.75}S$) would be 0.0137 and 0.1, respectively. This further suggests that the

Table 4.2

XPS Data for the Curve Resolution of S 2p Electrons

	Binding Energy (eV)	Peak Height	PWHH	Intensity
Crushed Chalcocite:				
S $2p_{3/2}$	161.5	3605	1.53	68113
S $2p_{1/2}$	162.7	1802	1.40	30997
			*Total:	99110
Elemental Sulfur:				
S $2p_{3/2}$	163.7	15646	1.65	297873
S $2p_{1/2}$	164.9	8001	1.55	143015
			*Total:	440888
Oxidized Chalcocite:				
1. S $2p_{3/2}$	161.5	1550	1.55	24380
S $2p_{1/2}$	162.6	969	1.30	12777
2. S $2p_{3/2}$	163.2	678	1.55	10647
S $2p_{1/2}$	164.3	407	1.30	5193
			*Total:	52997

* See Table 4.1

nonstoichiometric copper sulfides are not copper-deficient but rather copper polysulfides. This has been a subject of great debate (Craig, 1987). On the other hand, Goble (1985) seemingly took the middle ground. His mathematical approach with atom-sizes and bond-distances showed that each copper sulfide, except chalcocite, contained various amounts of cupric and cuprous atoms but only the covellites, both normal and blue-remaining, contained disulfide.

4.3 Cyclic Voltammetry

Voltammetry experiments on chalcocite have been performed at pH 1.1 (0.1 M $HClO_4$), pH 4.6 (0.5 M CH_3COOH/ 0.5 M CH_3COONa), pH 6.8 (0.1 M KH_2PO_4/0.1 M NaOH), and pH 9.2 (0.05 M $Na_2B_4O_7$). However, the voltammetry experiments with xanthate were conducted by Basilio (1985) in a similar study. Although the saturated calomel electrode (SCE) was used, all potentials are referenced to the standard hydrogen electrode (SHE).

4.3.1 Without Xanthate

a. pH 1.1: In the first series of experiments, the effect of the starting potential was examined as single scans were cycled between an upper limit of 450 mV and a lower limit of -500 mV at a rate of 20 mV/sec. No stirring was allowed. Scans first proceeded in the anodic direction

from starting potentials of 0, -350, -400, and -500 mV (see Figure 4.13).

At the starting potential of 0 mV, small cathodic current initially developed. Because mass-balanced calculations suggest there should be no reaction, the cathodic current indicates the reaction of oxidation products that formed while the electrode was being polished and transferred to the cell. Anodic current starts to flow upon increasing the potential to 250 mV and corresponds to chalcocite oxidation (A_1) to cupric ions in combination with nonstoichiometric copper sulfides, elemental sulfur, or both. After switching the scan direction, cathodic peaks C_1 and C_3 appear at 300 and -100 mV, respectively. This implies that two oxidation products were produced at A_1, neither of which could be the reduction of elemental sulfur which would take place at a reversible potential of 257 mV with 10^{-6} M H_2S(aq). Furthermore, this is confirmed by XPS which showed that, at an even higher potential of 600 mV, no elemental sulfur was detected. Therefore, the oxidation reaction at A_1 must produce nonstoichiometric copper sulfides. As to which one or ones are produced cannot be determined although at such a high scan rate only one appears to be produced:

$$Cu_2S = Cu_{2-x}S + xCu^{2+} + 2xe. \qquad [4.4]$$
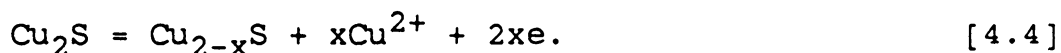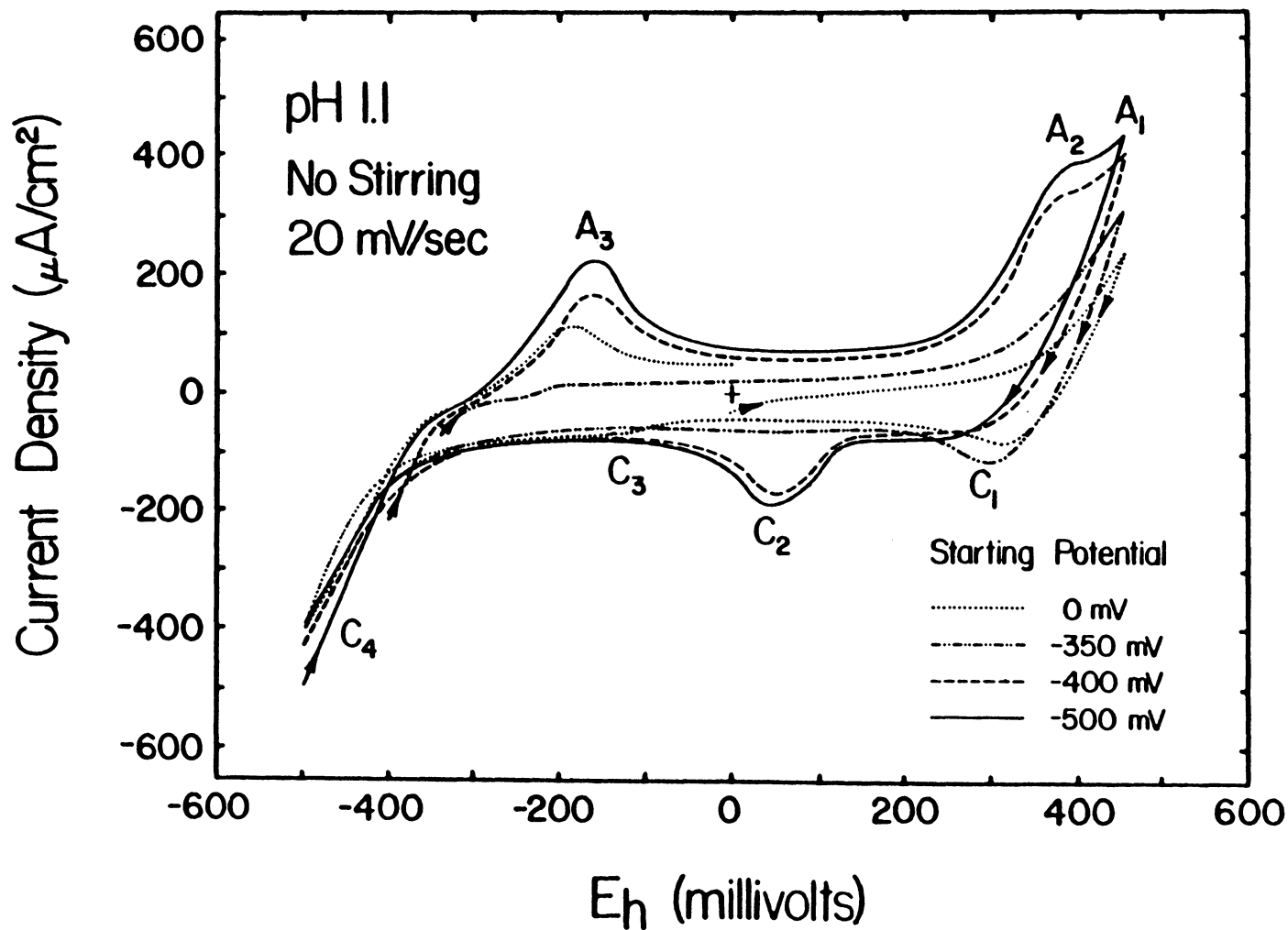
Figure 4.13 Cyclic voltammograms of chalcocite at pH 1.1 (0.1 M HClO$_4$) for different starting potentials. Scans cycled between -500 and 450 mV. No stirring. Scan rate = 20 mV/sec.

The reaction at C_1 would then be the opposite of Reaction [4.4] but cannot go to completion since some cupric ions will have diffused away. The diffusion of cupric ions explains why the charge passed at A_1 is greater than that at C_1. Hence, some of the nonstoichiometric copper sulfide remained on the surface until it reacted at C_3:

$$2Cu_{2-x}S + 2xH^+ + 2xe = (2-x)Cu_2S + xH_2S(aq). \qquad [4.5]$$
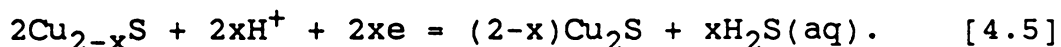
Chalcocite oxidation at A_1 and reduction at C_1 are confirmed by the E_h-pH diagrams in Figures 2.6 and 2.18. However, the loss of cupric ions permitted Reaction [4.5] to occur at C_3 implying the electrode behaved like djurleite (see Figure 2.7). Undoubtedly, the current at C_4 is caused by the reduction of chalcocite,

$$Cu_2S + 2H^+ + 2e = 2Cu^o + H_2S(aq). \qquad [4.6]$$
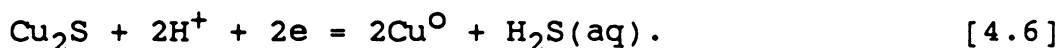
Upon switching the scan direction, the reverse of Reaction [4.6] is observed as A_3 at -300 mV which agrees with all E_h-pH diagrams. Because aqueous hydrogen sulfide diffused away from the surface, some metallic copper did not react at A_3 as is evidenced by the larger charge that is passed at C_4. Then by starting the scans below the reversible potential of -300 mV for Reaction [4.6], metallic copper will be produced at C_4 and will not totally react at A_3.

With a starting potential of -350 mV, the current at A_1

was increased signifying that unreacted metallic copper from the small A_3 peak oxidized to give the additional current:

$$Cu^0 = Cu^{2+} + 2e. \qquad\qquad [4.7]$$

The cupric ions produced by Reaction [4.7] offset the cupric ions that diffused away, enabling the reverse of Reaction [4.4] to go to completion. Therefore, the peak at C_1 increased and the peak at C_3 disappeared.

Lowering the starting potential to -400 and -500 mV increased the rate of chalcocite reduction and, hence, the amount of metallic copper production; new peaks at A_2 and C_2 grew correspondingly. Reaction [4.7] is responsible for A_2. The appearance of both peaks at 150 mV suggests the reverse of Reaction [4.7] caused C_2. Although it looks as if the peak at C_1 vanished, the large current flow indicates otherwise.

In the second set of tests, the effect that scan rate has on the system was investigated. Single cycles between the same two potential limits were employed. Again, the system was not stirred. With a starting potential of -400 mV, scans proceeded in the anodic direction at rates of 20, 10, 5, and 1 mV/sec and are shown in Figure 4.14. Results indicate that, as the scan rate is slowed, the cathodic peak C_2 disappears which allows for the peaks at C_1 and C_3 to be better observed. Furthermore, the anodic peaks A_1 and A_2
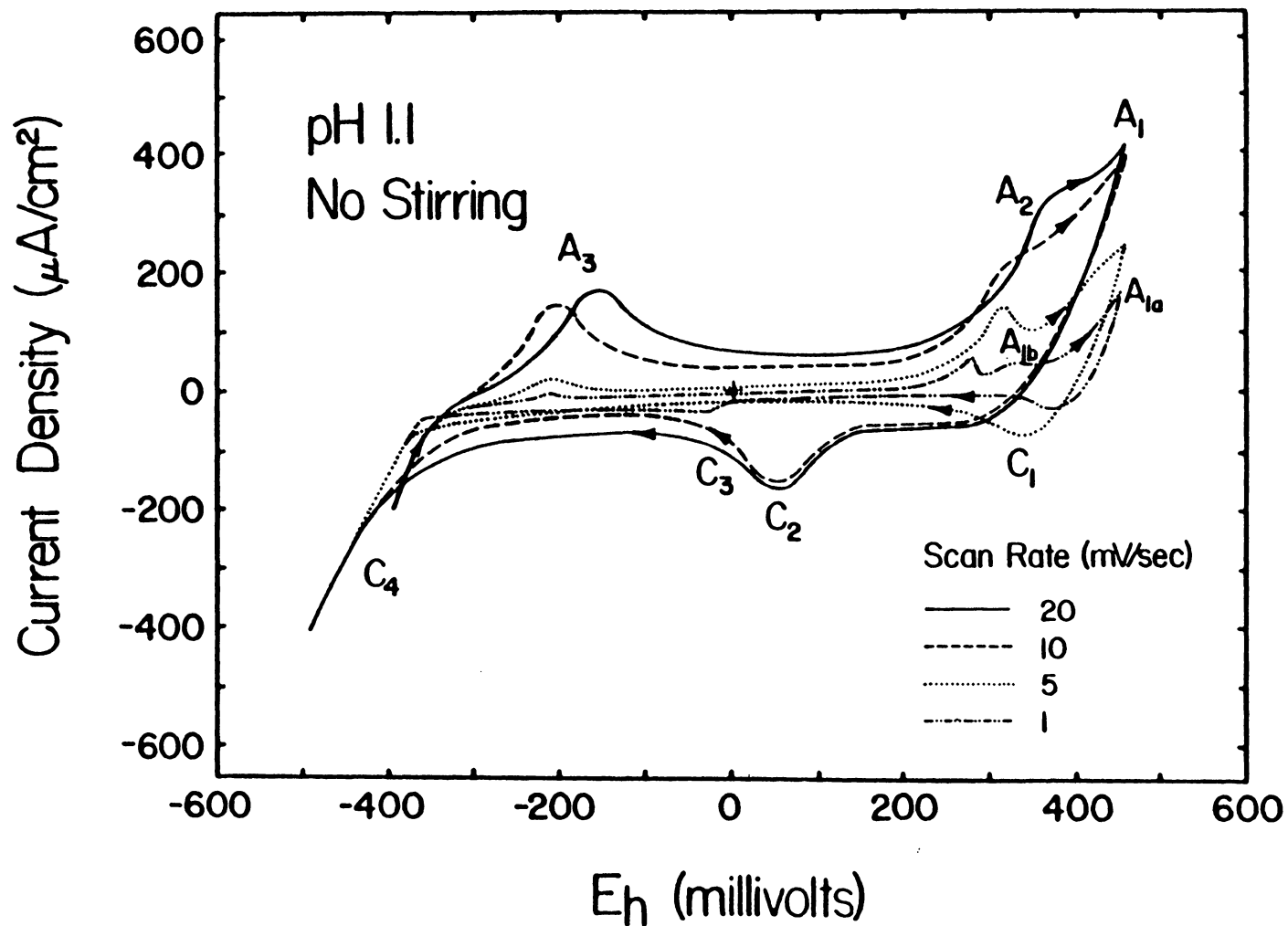
Figure 4.14 Cyclic voltammograms of chalcocite at pH 1.1 (0.1 M HClO$_4$)
for different scanning rates. Scans cycled between -500 and
450 mV from a starting potential of -400 mV. No stirring.

are more distinguishable, especially the A_1 peak which resolved into two noticeable peaks, A_{1a} and A_{1b}, which represent the formation of two nonstoichiometric copper sulfides.

Slowing the scan rate permits cupric ions produced at A_1 and A_2 to diffuse away from the surface before they react at C_1 and C_2. Because cupric ions are consumed at C_1 before they are at C_2, the peak at C_2 disappears as the scan rate is slowed. Further lessening of the scan rate causes the peak at C_2 to diminish to such a point that the peak at C_3 reappears once again. As explained earlier, C_3 is formed via Reaction [4.5] and suspected of being caused by djurleite. However, the anodic peak A_{1b} at 325 mV is in agreement with Koch and McIntyre (1976), Brage et. al. (1979), Gerlach and Kuzeci (1983), and the mass-balanced calculations in Figures 2.6 and 2.18 all of which showed a nonstoichiometric copper sulfide to be stable at that potential.

In the final set of experiments, the effect of stirring was investigated at a scan rate of 10 mV/sec. Scans first proceeded in the anodic direction from a starting potential of -400 mV and were cycled between potential limits of 450 and -500 mV only once. Results shown in Figure 4.15 reveal that, when the system was stirred, cathodic peaks at C_1 and C_2 disappear as does the anodic peak at A_3. Therefore, at
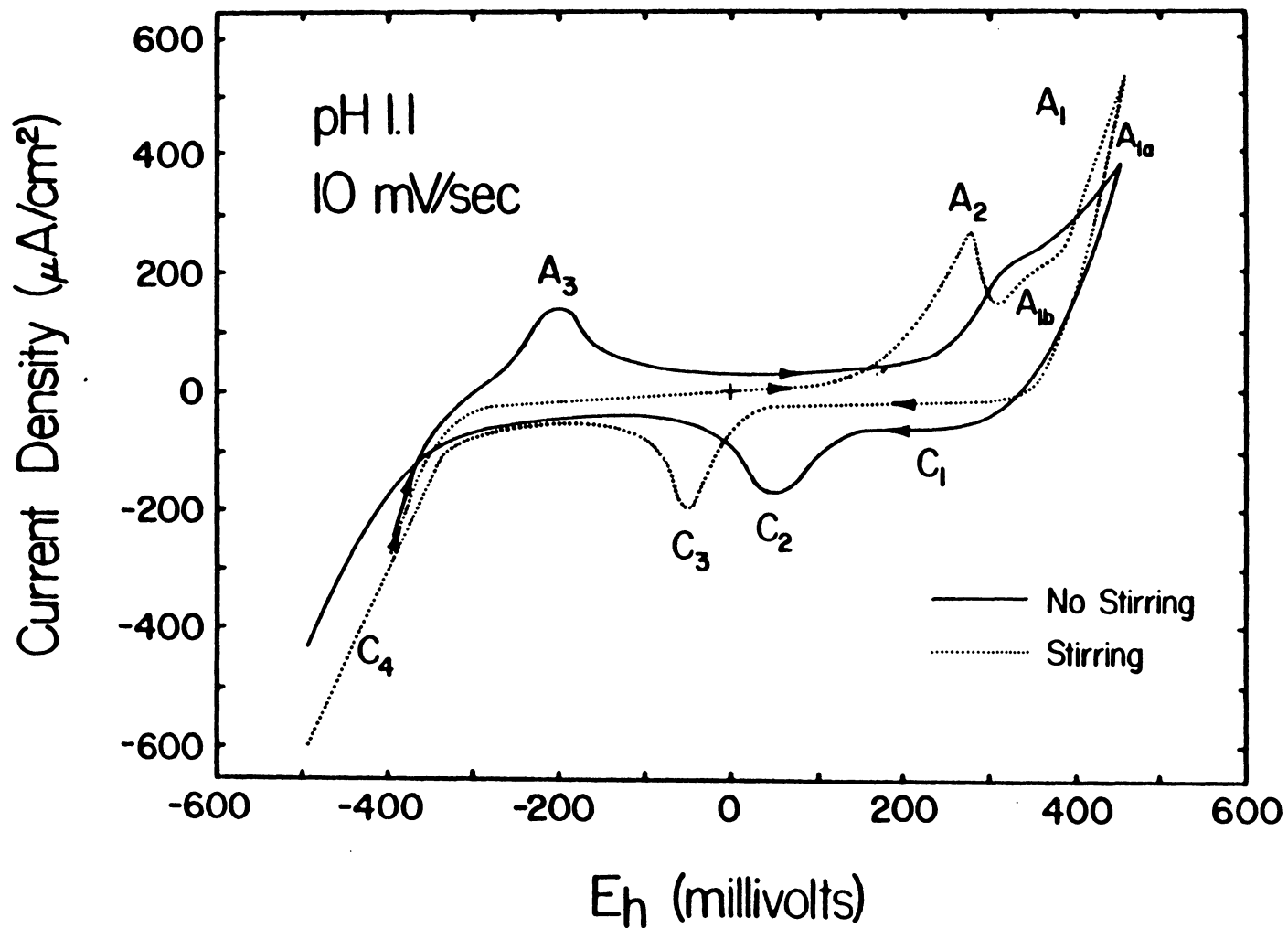
Figure 4.15 Cyclic voltammograms of chalcocite at pH 1.1 (0.1 M HClO$_4$) for stirred and unstirred cases. Scans cycled between -500 and 450 mV from a starting potential of -400 mV. Scan rate = 10 mV/sec.

Table 4.3

Electrochemical Reactions of Chalcocite at pH 1.1

Peak	Proposed Reaction	Number
A_1	$Cu_{2-x}S = Cu_{2-x-y}S + yCu^{2+} + 2ye$	[4.4]
A_2	$Cu^{o} = Cu^{2+} + 2e$	[4.7]
A_3	$2Cu^{o} + H_2S(aq) = Cu_2S + 2H^+ + 2e$	[4.6]
C_1	$Cu_{2-x}S + xCu^{2+} + 2xe = Cu_2S$	[4.4]
C_2	$Cu^{2+} + 2e = Cu^{o}$	[4.7]
C_3	$2Cu_{2-x}S + 2xH^+ + 2xe = 2-xCu_2S + xH_2S(aq)$	[4.5]
C_4	$Cu_2S + 2H^+ + 2e = 2Cu^{o} + H_2S(aq)$	[4.6]

least one reactant in the reactions which give rise to the peaks must have been aqueous. For the peaks which remain, all reactants must be solid. Stirring removes aqueous hydrogen sulfide and, hence, peak A_3, but causes peaks at A_1 and A_2 to be more pronounced. Since oxidation produces cupric ions which are also stirred away, corresponding peaks at C_1 and C_2 vanished which greatly enhanced the C_3 peak. The reactions mentioned earlier are confirmed and are listed in Table 4.3.

b. pH 4.6: Initially scanning anodically from 0 mV at 20 mV/sec, the effect of stirring was examined as scans between 400 and -750 mV were repeated on the chalcocite electrode (see Figure 4.16). Comparing to the results obtained at pH 1.1 indicated that the peaks A_1, A_2, C_1, and C_2 occurred at the same potentials where peaks A_3, C_3, and C_4 shifted to lower potentials. Referring to Table 4.3 shows that the reactions at A_1, A_2, C_1, and C_2 are pH-independent and should therefore occur at the same potentials. Likewise, the reactions at A_3, C_3, and C_4 are pH-dependent and should shift to lower potentials. All E_h-pH diagrams indicate that chalcocite reduction, C_4, and its reverse, A_3, should occur near -500 mV which is close to the -450 mV in the voltammograms. In Figure 2.7, djurleite reduction to chalcocite, Reaction [4.5] at C_3, takes place near -300 mV which also fits the voltammetry.
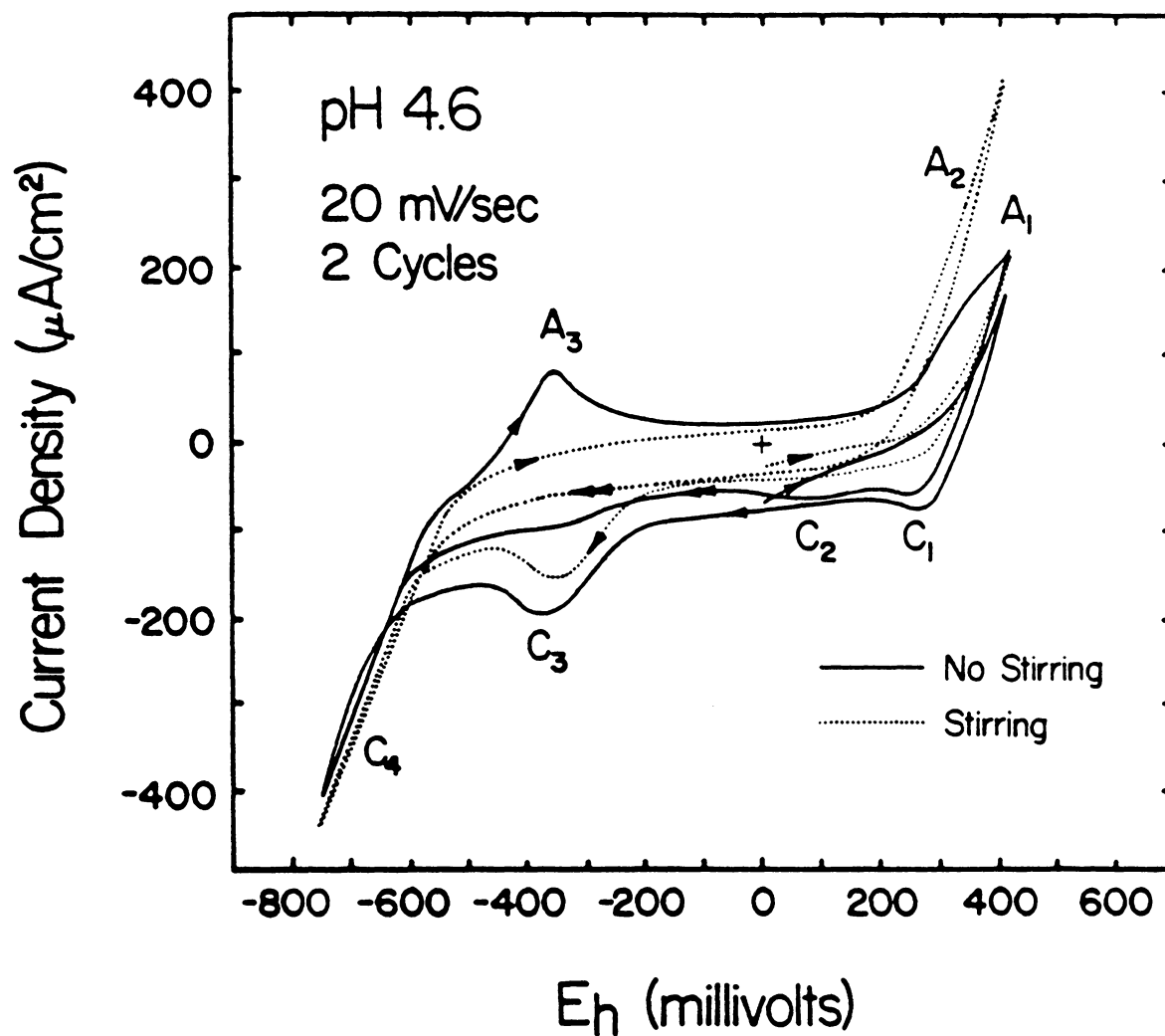
Figure 4.16 Cyclic voltammograms of chalcocite at pH 4.6
(0.5 M CH_3COOH/0.5 M CH_3COONa) for stirred and
unstirred cases. Scans cycled between -750 and
400 mV from a starting potential of 0 mV. Scan
rate = 20 mV/sec.

During the second scan of the stirred system in Figure 4.16, the peak at C_3 disappeared because so much metallic copper was produced at C_4 that chalcocite oxidation to a nonstoichiometric copper sulfide at A_1 was prevented. Therefore, because the chalcocite electrode was covered with metallic copper, it behaved totally like a copper electrode. Comparing to the voltammogram of a copper electrode with stirring implies this to be true (see Figure 4.17).

Although the cathodic peak at 150 mV for the unstirred voltammogram in Figure 4.17 indicated that the C_2 peak in the other voltammograms was caused by metallic copper formation from cupric ions, a unique approach was taken to verify it. With a scan rate of 20 mV/sec and a starting potential of 0 mV, three cycles between 400 and -750 mV were completed; however, the system was stirred only between -550 and 150 mV on the anodic scan. This effectively removed the A_3 peak (see Figure 4.18). On the third cycle, a cupric ion concentration of 10^{-4} M was added to the system at -550 mV. Results exhibit the growth of the C_2 peak, thereby verifying that the reverse of Reaction [4.7] takes place there. Also, with the addition of 10^{-4} M cupric ions, cathodic current began to flow at 230 mV which compares to the reversible potential of 222 mV for Reaction [4.7] at the specified concentration. Peaks at A_2 and C_4 were repeated when the system was stirred throughout the voltammetry experiment.
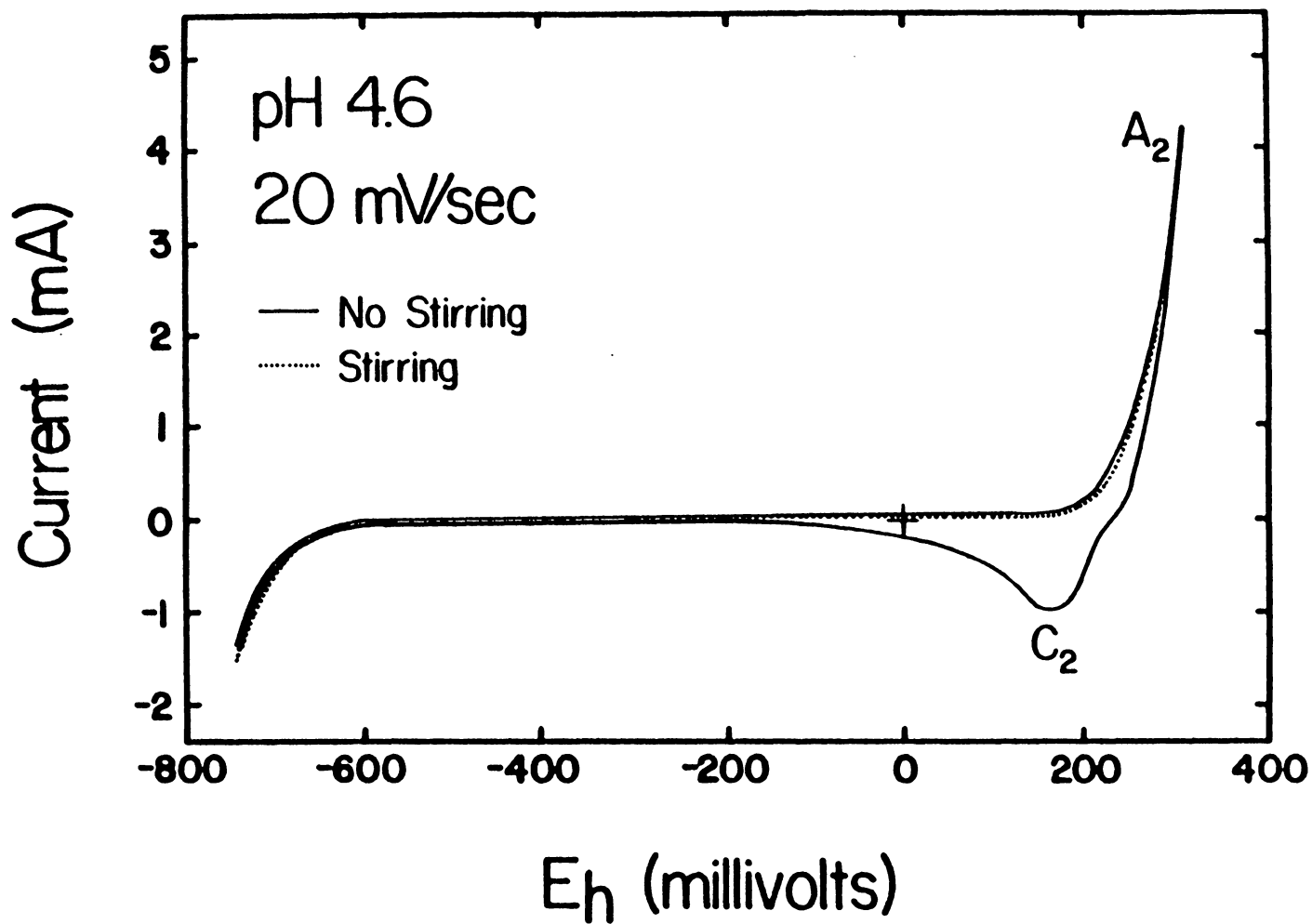
Figure 4.17   Cyclic voltammograms of metallic copper at pH 4.6 (0.5 M
CH3COOH/0.5 M CH3COONa) for stirred and unstirred cases.
Scans cycled between -750 and 400 mV from a starting
potential of 0 mV.   Scan rate = 20 mV/sec.
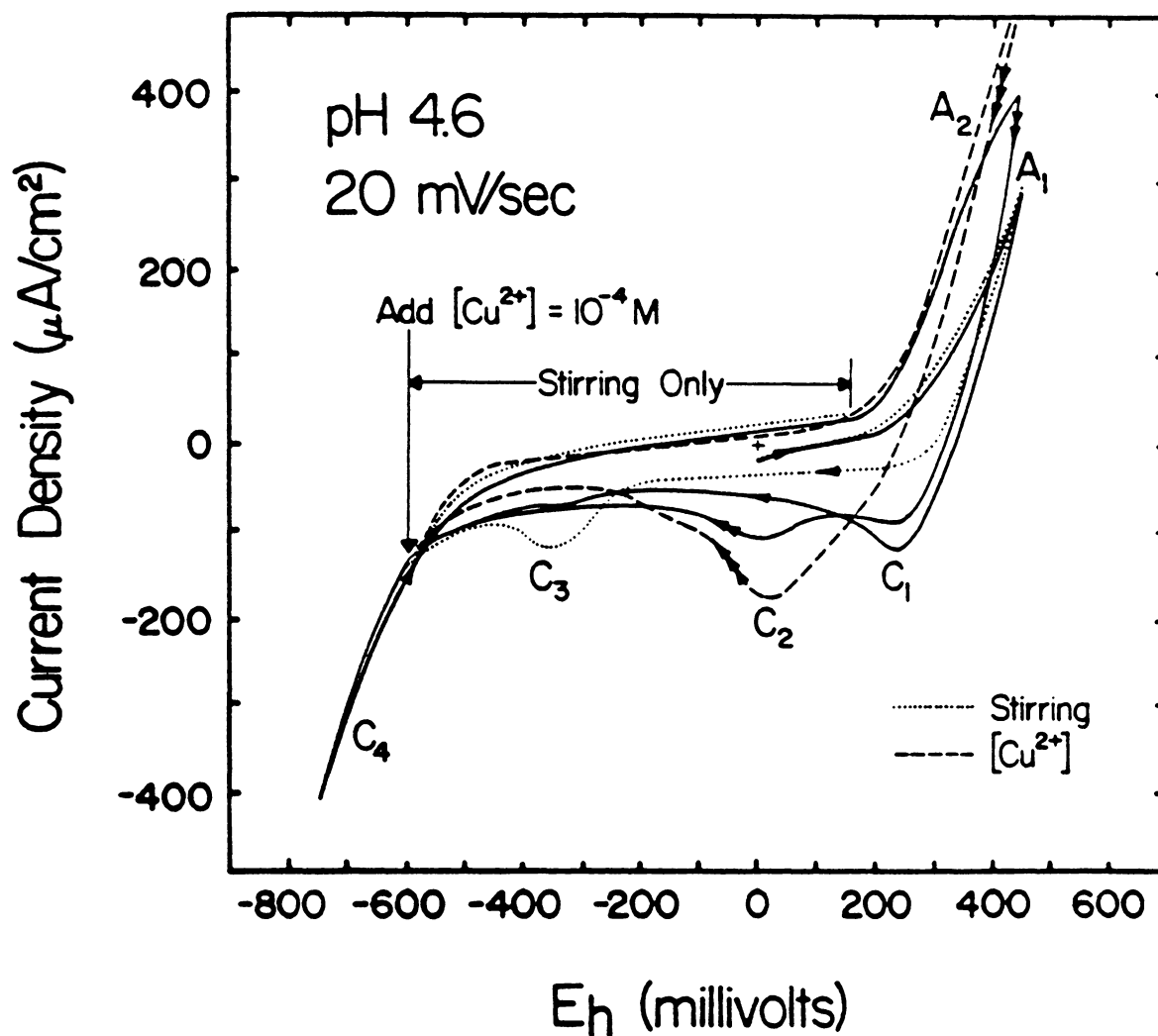
Figure 4.18   Cyclic voltammograms of chalcocite at pH 4.6
(0.5 M CH_3COOH/0.5 M CH_3COONa) with stirring on
the anodic scan between -550 and 150 mV. Scans
cycled between -750 and 400 mV from a starting
potential of 0 mV. Scan rate = 20 mV/sec.
$[Cu^{2+}]$ = 10^{-4} added on the third scan.

c. pH 6.8: Repetitive cycling of the potential between -775 and 400 mV produced the voltammograms shown in Figure 4.19. With no stirring and a scan rate of 10 mV/sec, the potential was initiated from -50 mV in the anodic direction. The same peaks as before were observed, but each at lower potentials. Therefore, in order for the reactions at A_1, A_2, C_1, and C_2 to be pH dependent, they must have involved the formation of cupric oxide instead of cupric ions; hence, Reactions [4.4] and [4.7] respectively become

$$Cu_2S + xH_2O = Cu_{2-x}S + xCuO + 2xH^+ + 2xe \qquad [4.8]$$

$$\text{and} \quad Cu^o + H_2O = CuO + 2H^+ + 2e. \qquad [4.9]$$
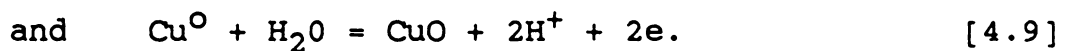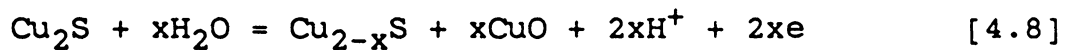
Cupric oxide, CuO, is used in the above reactions instead of copper hydroxides because it is the stable form as depicted in the E_h-pH diagrams.

On the first scan, Reaction [4.8] occurred at A_1 and its reverse at C_1. However, the reverse reaction did not go to completion because unreacted cupric oxide reacted to develop a small peak at C_2 corresponding to the reverse of Reaction [4.9]. Since unreacted cupric oxide existed, an unreacted nonstoichiometric copper sulfide must also have as evidenced by the cathodic peak, C_3, which started at -400 mV. Figure 2.7 shows djurleite reduction to chalcocite occurs at that same potential. Reducing the potential further produced metallic copper and hydrogen sulfide (C_4),

The graph shows cyclic voltammograms with axes:
- Y-axis: Current Density ($\mu A/cm^2$), ranging from -300 to 200
- X-axis: E_h (millivolts), ranging from -800 to 400

Labels on graph: pH 6.8, No Stirring, 10 mV/sec, peaks labeled A_1, A_2, A_3, C_1, C_2, C_3, C_4

Cycle No.
——— 1
------ 2
········ 3
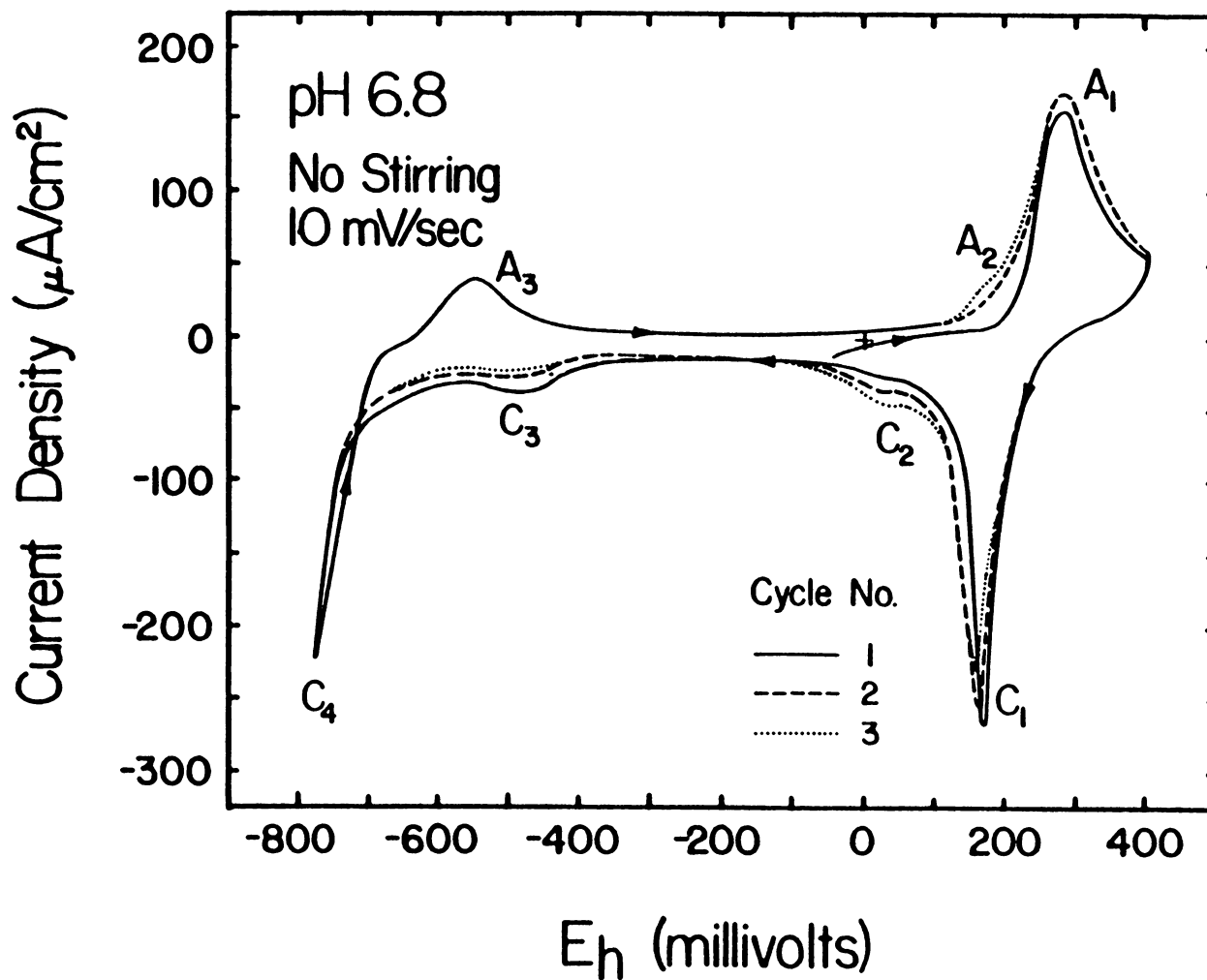
Figure 4.19   Cyclic voltammograms of chalcocite at pH 6.8 (0.1 M
KH_2PO_4/0.1 M NaOH) without stirring. Scans cycled between
-775 and 400 mV from a starting potential of 0 mV. No
stirring. Scan rate = 10 mV/sec.

of which a majority is brought back as chalcocite (A_3). However, some metallic copper did not react at A_3 due to the diffusion of hydrogen sulfide. This unreacted metallic copper oxidizes at A_2 to form cupric oxide according to Reaction [4.9].

With continuous cycling, excess copper built-up and peaks at A_2 and C_2 therefore increased. However, a corresponding decrease in the peak at C_3 was observed and can be explained in a number of ways. First, the metallic copper produced at C_2 coated the electrode surface and blocked the reaction at C_3. Second, excess cupric oxide produced at A_2 allowed the reverse of Reaction [4.8] to go further to completion so that less djurleite would be available to react at C_3. Third, the formation of cupric oxide at A_2 began passivating the surface and thereby hindering Reaction [4.8] at A_1 and producing less of the nonstoichiometric copper sulfide. The steady decrease in the current at C_1 implies this to be true. Fourth, any combination of the above explanations is highly probable.

Additional experiments were also carried out to examine the effect that changing the lower limit has on the anodic peak A_3 in which chalcocite is reformed. Lower limits of -450, -500, -550, -650, -725, and -775 mV were used. Results in Figure 4.20 show the formation of a very shallow peak at A_4 due to the reverse of the reaction at C_3. The
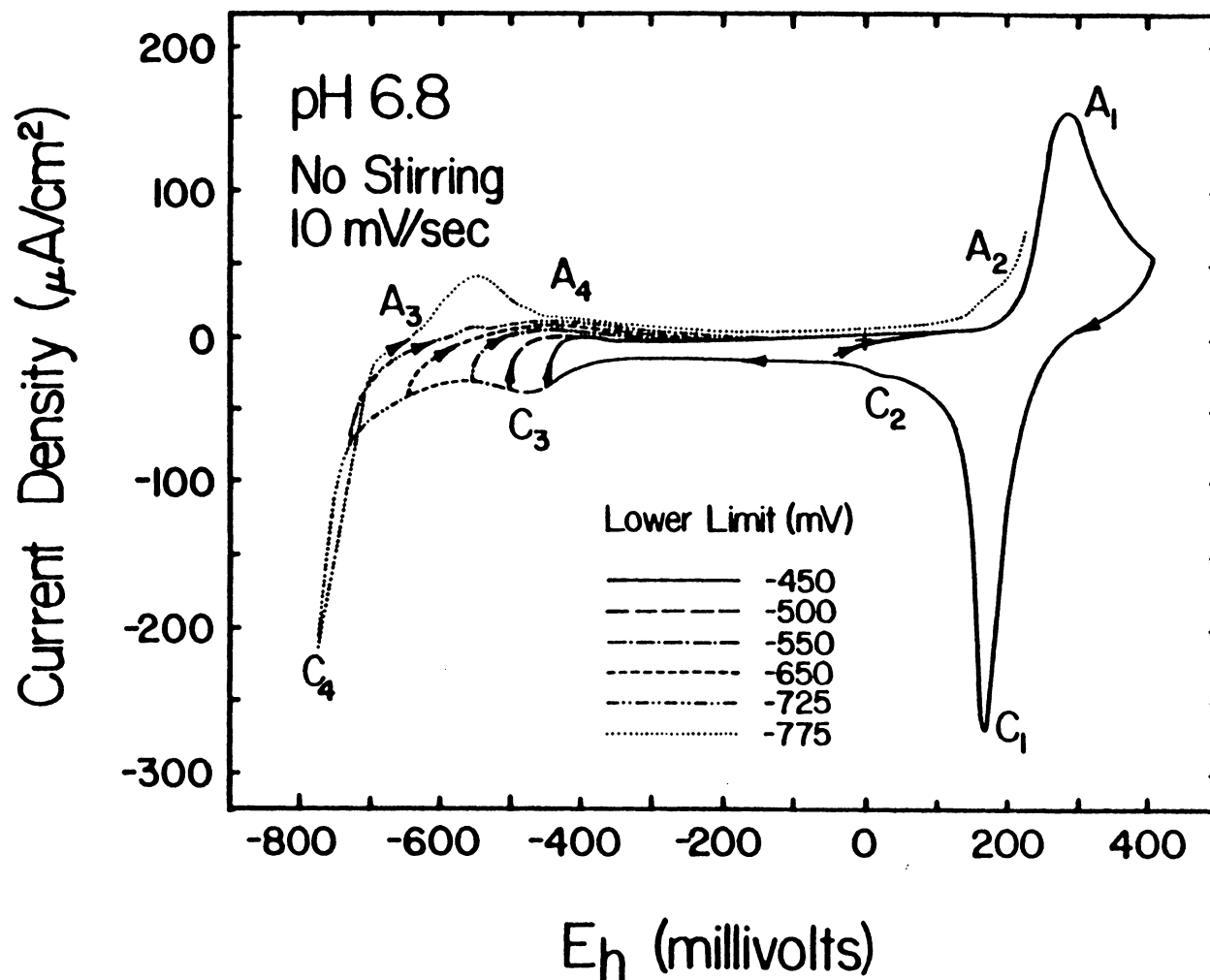
Figure 4.20   Cyclic voltammograms of chalcocite at pH 6.8 (0.1 M
KH$_2$PO$_4$/0.1 M NaOH) for different lower potentials.   Scans
cycled to 400 mV from a starting potential of 0 mV.   No
stirring.   Scan rate = 10 mV/sec.

peak is shallow because some hydrogen sulfide produced at C_3 is lost to diffusion. However, the peak continued to grow because hydrogen sulfide was being replenished due to chalcocite reduction to metallic copper at C_4. Furthermore, the shallowness of the peak indicates that chalcocite was indeed being formed at C_3. When the lower limit was -725 mV, an extremely small peak was observed at A_3.

d. pH 9.2: Because the series of metastable nonstoichiometric copper sulfides produced during the oxidation of chalcocite had not yet been observed, the upper limit was set at -200, 250, 350, 400, and 450 mV so that oxidation would proceed to various copper sulfides. Single scans were performed from a starting potential of -200 mV at 10 mV/sec. A lower limit of -925 mV was used. Results shown in Figure 4.21 clearly revealed the envelope of a number of cathodic peaks that represent reactions involving various nonstoichiometric copper sulfides. Increasing the upper limit increased the number of peaks.

Scanning cathodically from -200 mV produced C_3 at 525 mV which corresponds to djurleite reduction to chalcocite. Because prior oxidation did not take place, the reaction at C_3 verifies the presence of djurleite-contamination. Numerous investigators (Walker et al., 1984 and 1986; O'Dell et al., 1984 and 1986; Basilio, 1985) observed much larger current flows at C_3 and subsequently misidentified the
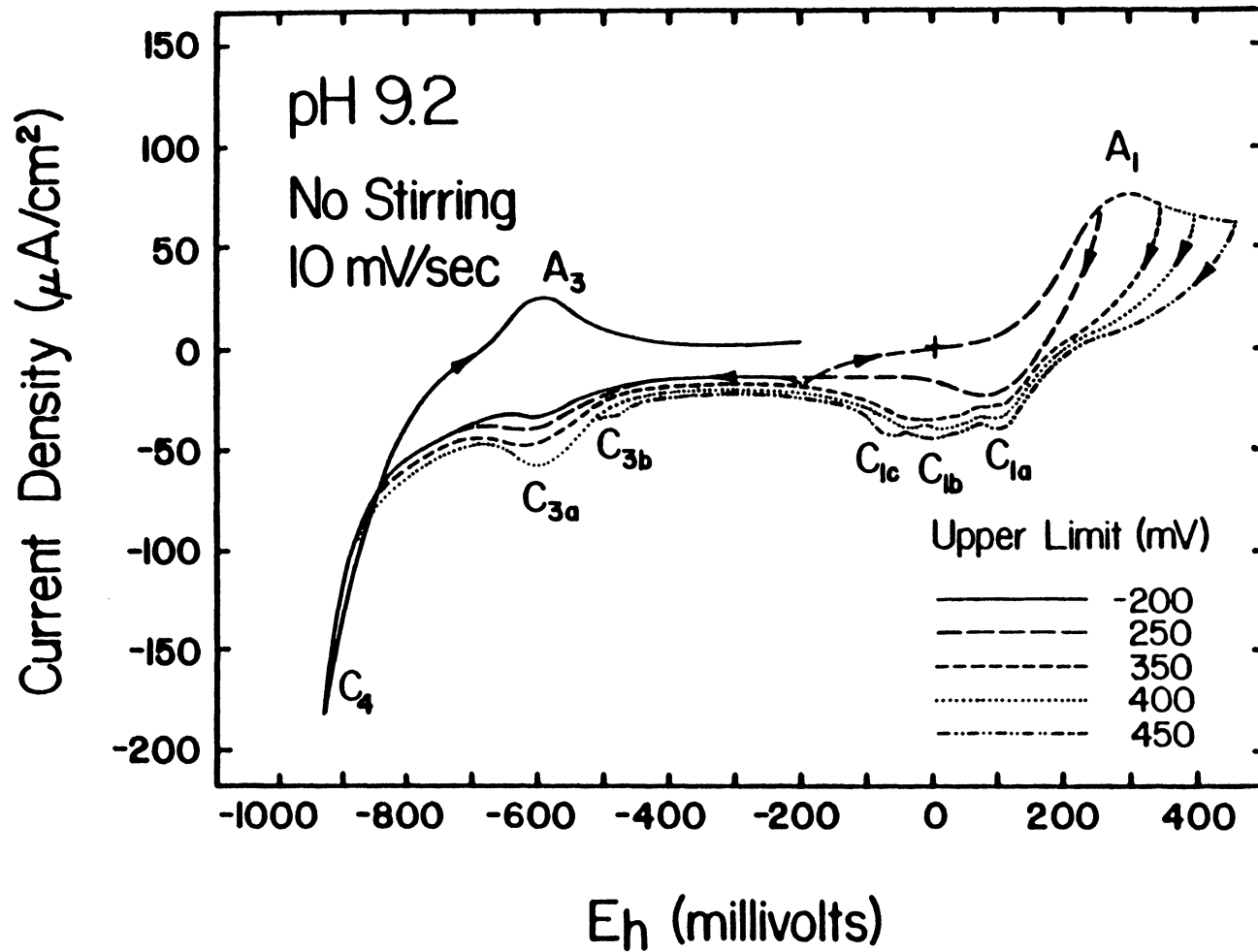
Figure 4.21 Cyclic voltammograms of chalcocite at pH 9.2 (0.05 M
Na₂B₄O₇) for different upper potentials. Scans cycled to
-925 mV from a starting potential of -200 mV. No stirring.
Scan rate = 10 mV/sec.

reaction as chalcocite reduction to metallic copper.
Therefore, their chalcocite samples most likely contained
much larger amounts of djurleite. Continued scanning
produced a cathodic peak at C_4 and an anodic peak at A_3
which are the same as before except they occur near -700 mV,
in agreement with the E_h-pH diagrams, IGP and the
chronoamperometry tests conducted for XPS.

With an upper limit of 250 mV, peaks at A_1 and C_{1a}
developed via Reaction [4.8] at A_1 and its reverse at C_{1a}.
However, along with the copper hydroxides and oxides,
soluble copper complexes form in borate solutions (Walker et
al., 1984) and are lost due to diffusion. Some of the
nonstoichiometric copper sulfide produced at A_1, therefore,
could not react at C_{1a} but could at C_{3a} according to
Reaction [4.5]. Hence the current at C_3 increased as
compared to the previously mentioned voltammogram.
Increasing the upper limit also produced corresponding
increases in the current at C_3.

The higher the upper potential limit reached, the more
cathodic peaks that developed. In addition to C_{1a}, C_{1b}
formed when the upper limit was 350 mV. With upper limits
set at 400 and 450 mV, additional peaks at C_{1c} and C_{3b} were
produced, respectively. Because the C_1 peaks are grouped
around the potential where copper hydroxides or oxides
react:

$$Cu_{2-x-y}S + CuO + 2yH^+ + 2ye = Cu_{2-x}S + yH_2O. \quad [4.10]$$

Products of Reaction [4.10] can become reactants for the same reaction or can undergo the reaction at C_3 where the two peaks that are grouped together, C_{3a} and C_{3b}, appear to be the reduction of one copper sulfide to another:

$$xCu_yS + (x-y)H^+ + 2(x-y)e = yCu_xS + (x-y)HS^-. \quad [4.11]$$
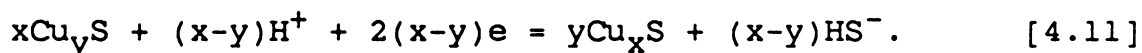
Based on earlier conclusions, the product of Reaction [4.11] at C_{3b} looks to be djurleite or a similar copper sulfide (e.g., $Cu_{1.93}S$) which undergoes the same reaction to produce chalcocite at C_{3a}. Furthermore, the products of the other peaks may also conform to the results of Koch and McIntyre (1976) as illustrated in Table 4.4. It is interesting to note that the reduction reaction at C_{1a} occurred at the same potential, independent of the copper sulfides that were obtained by adjusting the upper limit. Although this appears to be in accordance with the E_h-pH diagrams in Figures 2.6 to 2.9 (i.e., reduction reactions involving CuO and any copper sulfide occur close to the same potentials), the phenomena is probably caused by the passivation of the surface with copper oxides or hydroxides.

Walker et al. (1984) demonstrated that soluble copper complexes form in borate solutions and the loss of copper due to diffusion has just been illustrated. In order to explore this further, the effect of stirring on the system

Table 4.4

Reaction Products of Cathodic Peaks Formed From Cyclic
Voltammetry With Various Upper Limits at pH 9.2

Upper Limit	Cathodic Peak	Reaction Product
-200 mV	C_{3a}	Cu_2S
250 mV	C_{1a}	$Cu_{1.93}S$
	C_{3a}	Cu_2S
350 mV	C_{1a}	$Cu_{1.83}S$
	C_{1b}	$Cu_{1.93}S$
	C_{3a}	Cu_2S
400 mV	C_{1a}	$Cu_{1.67}S$
	C_{1b}	$Cu_{1.83}S$
	C_{1c}	$Cu_{1.93}S$
	C_{3a}	Cu_2S
450 mV	C_{1a}	$Cu_{1.38}S$
	C_{1b}	$Cu_{1.67}S$
	C_{1c}	$Cu_{1.83}S$
	C_{3b}	$Cu_{1.93}S$
	C_{3a}	Cu_2S

was investigated. Starting the potential from -200 mV and cycling between 400 and -925 mV at 10 mV/sec. Comparing the first cycles between stirred and unstirred cases showed no difference except for the disappearance of the anodic peak at A_3. However, on the second cycles, the cathodic peak at C_{1c} shifted from -75 to -325 mV (see Figures 4.21 and 4.22). Therefore, when the system is stirred, Reaction [4.10] no longer occurs because the copper oxide layer has been removed as is evidenced by the difference between C_1 peaks.

Because the A_2 peak in Figure 4.22 has been identified as the oxidation of metallic copper, the contradiction about the co-existence of metallic copper and chalcocite at pH 9.2 and -400 mV that resulted from chronoamperometry experiments in the XPS study could be finalized. Therefore, in order to confirm the presence of metallic copper at -400 mV, the chronoamperometry experiments were duplicated. After holding the potential at 0, -200, -400, -600 and -800 mV for 5 minutes while stirring, voltammograms of the chalcocite electrode were initiated from the holding potential and scanned to an upper limit of 350 mV. Stirring was stopped prior to each scan. Results are shown in Figure 4.23 along with a voltammogram that was completed immediately after immersing the electrode in solution. This would correspond to the standard of the XPS samples. Scan rates were set at 20 mV/sec.
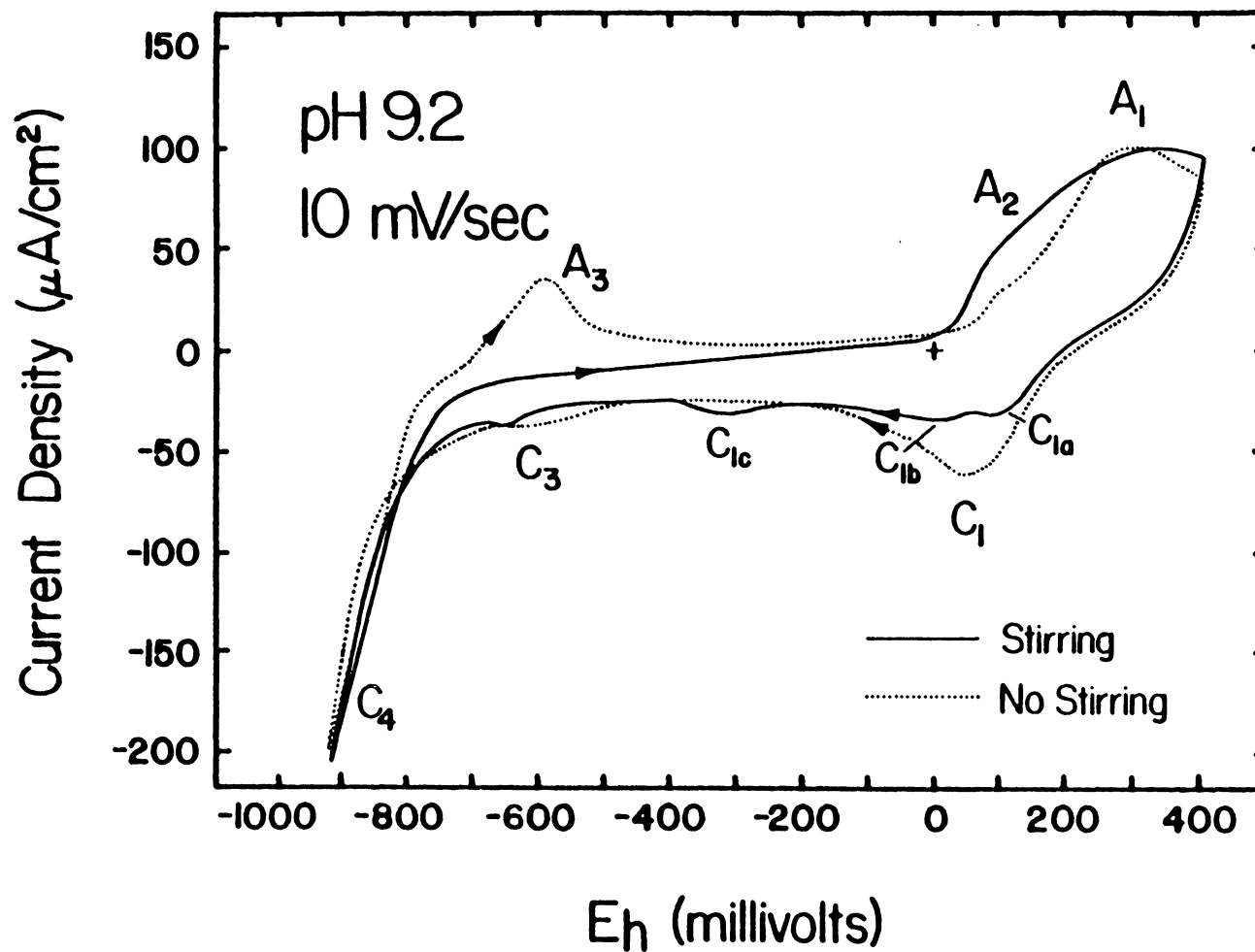
Figure 4.22 Cyclic voltammograms of chalcocite at pH 9.2 (0.05 M
Na$_2$B$_4$O$_7$) for stirred and unstirred cases. Scans cycled
between -925 and 400 mV. Scan rate = 10 mV/sec.
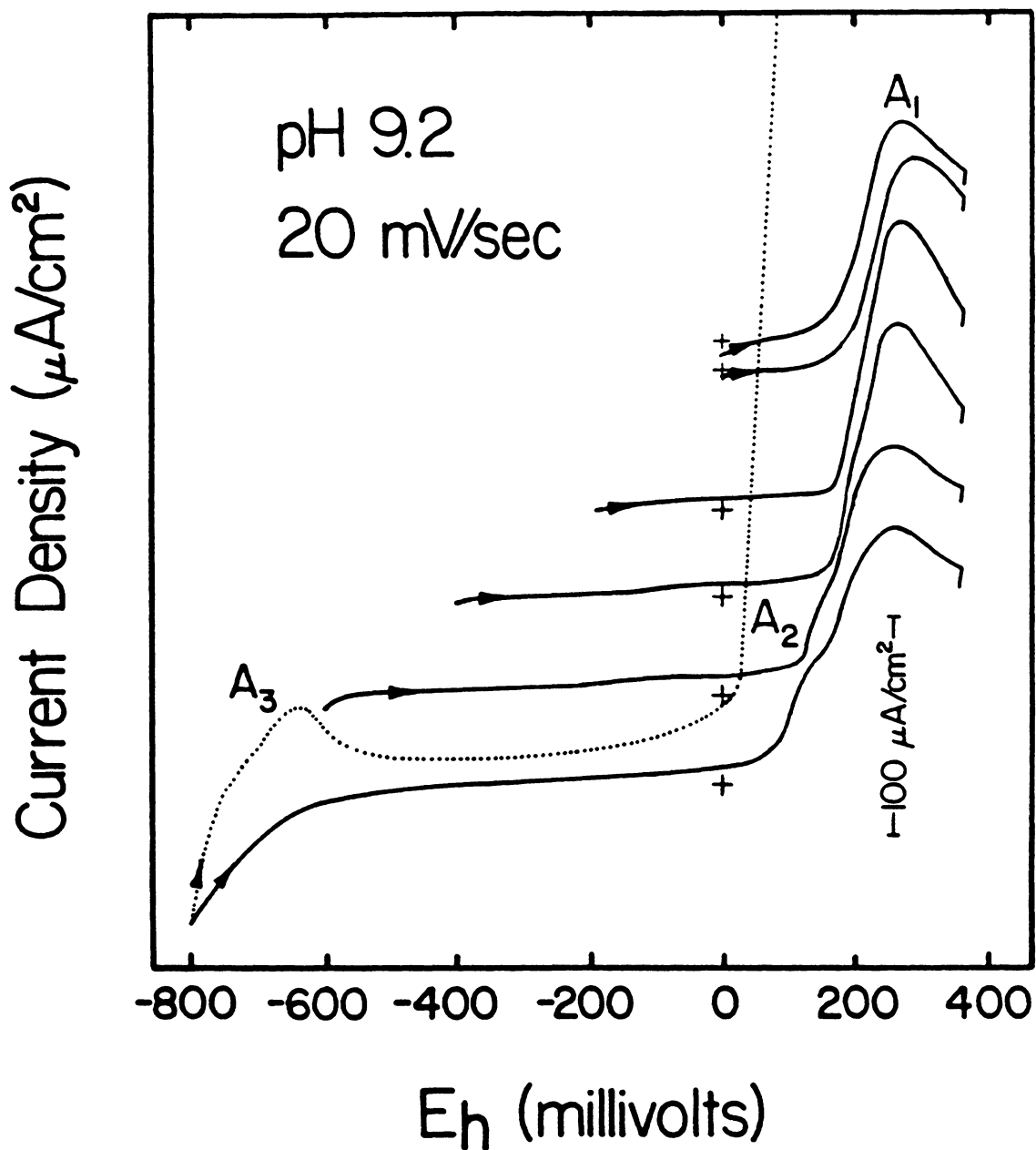
Figure 4.23   Voltammograms of chalcocite at pH 9.2 (0.05 M
              Na$_2$B$_4$O$_7$) for various starting potentials.
              Potential held at the starting potential for 5
              minutes. Stirring was stopped when scan was
              started. Scans stopped after being reversed at
              350 mV. Scan rate = 20 mV/sec.

The voltammograms for the holding potentials of 0 and -200 mV as well as the standard indicate that oxidation to cupric oxide began slightly greater than 150 mV. Assuming the nonstoichiometric copper sulfide in Reaction [4.8] is $Cu_{1.93}S$, chalcocite oxidation should begin at 165 mV. Decreasing the holding potential to -400 mV caused a shoulder to develop; however, oxidation still occurred at 150 mV so it looks as if metallic copper is not present at -400 mV. The appearance of this shoulder is intriguing and will be discussed later.

Applying a potential of -600 mV caused the ensuing voltammogram to begin oxidation at 100 mV. This implies that the formation of A_2 at 100 mV was caused by metallic copper oxidizing which should occur at 22 mV. Analyzing the charge passed at A_2 indicates that a monolayer of metallic copper was produced which would be in agreement with the E_h-pH diagrams of chalcocite. With an applied potential of -800 mV, the peak at A_3 is observed but, because so much metallic copper was produced, the subsequent oxidation at A_2 went off-scale; however, the peak was registered at 0 mV which is close to the 22 mV just mentioned. Since the current went off-scale, a seventh voltammogram is also shown in Figure 4.23: a potential of -800 mV was applied for 5 seconds. To insure that metallic copper would be present, stirring was not stopped until a potential of -400 mV was

reached. Hence, the peak at A_3 was removed and the peaks at A_2 and A_1 were noticed. A_2 is shown to start near 50 mV which is close to the 22 mV.

Because holding the potential at -400 mV caused the shoulder to appear, the effect of holding time was examined. Furthermore, the production of metallic copper could be time-dependent. Therefore, a potential of -400 mV was held for 1, 10, 100, 1000, and 10000 seconds and ensuing voltammograms were recorded at 20 mV/sec (see Figure 4.24). Each voltammogram showed that oxidation started near 150 mV which means metallic copper does not co-exist with chalcocite at pH 9.2 and -400 mV. The shoulder that appeared after 5 minutes of oxidation also appeared at 1000 seconds (i.e., 16 minutes and 40 seconds). Increasing the time to 10000 seconds allowed 2 more shoulders to form. A total of four peaks were thus revealed, each at approximately 170, 200, 220 and 255 mV. Assuming the four peaks correspond to the nonstoichiometric copper sulfides from Koch and McIntyre (1976), $Cu_{1.93}S$, $Cu_{1.83}S$, $Cu_{1.67}S$ and $Cu_{1.38}S$ should have respectively been observed at 164, 196, 222 and 244 mV (see Reaction [4.10]). These values are remarkably close to the experimental values just determined.

An explanation for the appearance of the shoulders follows. First of all, djurleite reduction, according to Reaction [4.2] with a hydrogen sulfide ion concentration of

193
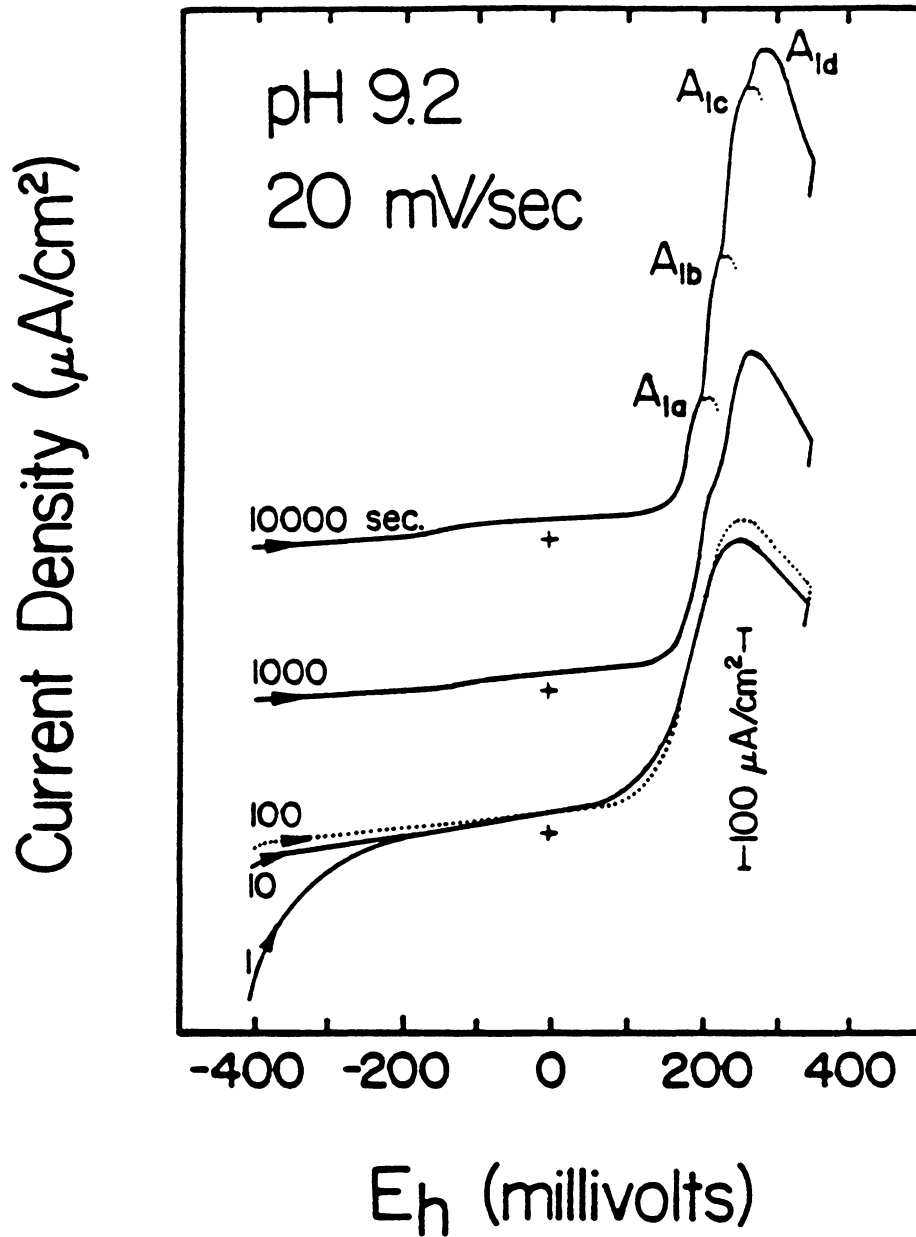
Figure 4.24 Voltammograms of chalcocite at pH 9.2 (0.05 M Na$_2$B$_4$O$_7$) for a starting potential of -400 mV. Potential held at -400 mV for various times. Stirring was stopped when scan was started. Scans reversed at 350 mV and stopped. Scan rate = 20 mV/sec.

10^{-6} M, will occur at -362 mV which agrees with the -370 mV
discussed for IGP and XPS (see Figures 4.1a and 4.8). Thus,
voltammograms initiated from potentials above -370 mV (e.g.,
0 and -200 mV) witnessed the simultaneous oxidation of both
djurleite and chalcocite. Holding the potential at -400 mV
converted the djurleite to chalcocite explaining why the
subsequent voltammetry looked more like chalcocite
oxidation. The longer the potential was held at -400 mV,
the more djurleite that reacted to form chalcocite.
Apparently, 10000 seconds was long enough to convert all of
the djurleite to chalcocite. The oxidation of the metallic
copper that formed from holding potentials at -600 mV or
lower obscured the oxidation of chalcocite to the
nonstoichiometric copper sulfides. Therefore, the presence
of either djurleite or metallic copper will obscure the
oxidation of chalcocite. At pH 9.2, pure chalcocite can be
obtained by holding the potential at -400 mV, a potential
which is just low enough to change djurleite into
chalcocite.

4.3.2 With Xanthate

a. pH 6.8: Voltammograms of chalcocite produced by
Basilio (1985), both in the absence and presence of
xanthate, are shown in Figure 4.25 in which the potential
was cycled between 455 and -555 mV at 10 mV/sec from a
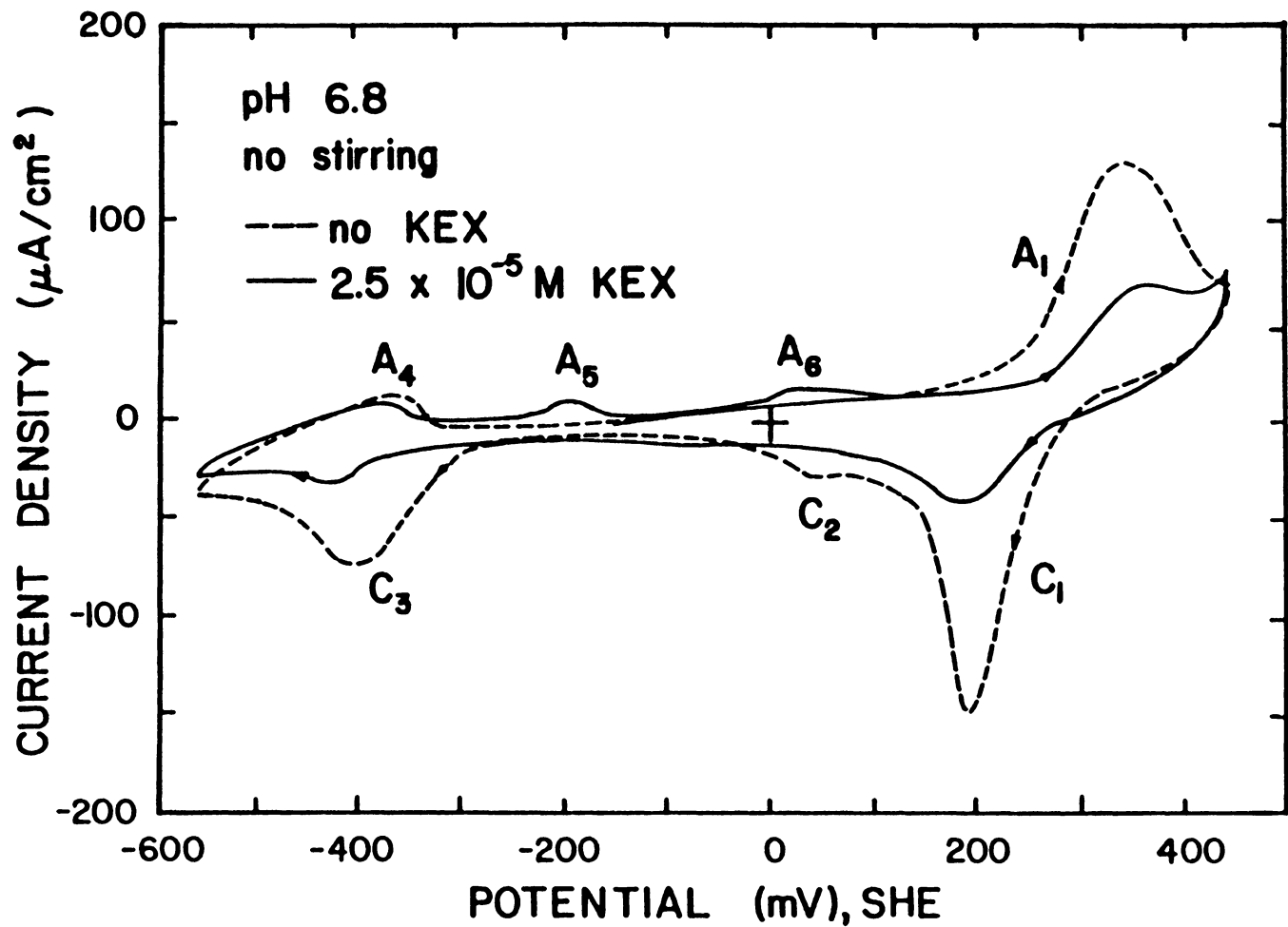
Figure 4.25   Voltammograms of chalcocite at pH 6.8 (0.1 M KH_2PO_4/0.1 M NaOH) with (——) and without (---) 2.5 x 10^{-5} M xanthate. Scans cycled between 455 and -555 mV from a starting potential of -155 mV. No stirring. Scan rate = 10 mV/sec (from Basilio, 1985).

starting potential of -155 mV. The only difference between the voltammogram without xanthate and those shown in Figures 4.19 and 4.20 is the amount of current passed at C_1, C_2 and C_3. This difference was probably caused by the presence of more djurleite than before as evidenced by the larger C_3 peak in Figure 4.25. However, in the presence of xanthate, two new peaks, A_5 and A_6, appear near -200 and 0 mV, respectively, and all other peaks decreased because of the xanthate species which formed at A_5 and A_6 passivated the surface.

Since all previous voltammograms have shown chalcocite oxidation proceeded to nonstoichiometric copper sulfides, oxidation in the presence of xanthate must as well. Additionally, the passivation of the surface would also prevent oxidation from proceeding any further. Hence, the E_h-pH diagrams with xanthate in Figures 2.22 and 2.23 should apply as should the corresponding $[S^{2-}]$ contour plot in Figure 2.29 and the % CuX and CuX_2 formation plots in Figures 2.32 and 2.36. Comparing the voltammogram to these figures indicates that, because the peak at A_6 is close to 0 mV, A_6 is caused by the reaction

$$Cu_2S + .07X^- = Cu_{1.93}S + .07CuX + .07e \qquad [4.12]$$
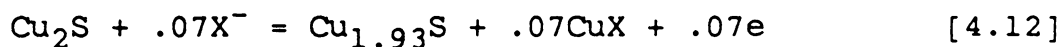
which thermodynamically calculates to have a reversible potential at -59 mV at 2.5×10^{-5} M xanthate. Richardson et

al. (1984) first suggested such a reaction occurred but did not specify which nonstoichiometric copper sulfide would form since it was obvious that $Cu_{1.93}S$ would form first. Because Figure 4.20 shows metallic copper cannot be produced until -725 mV and the lower limit in the presence of xanthate was only -555 mV, the peak at A_5 cannot involve metallic copper. However, as explained in Chapter 1, A_5 could be caused by dixanthogen formation,

$$2X^- = X_2(aq) + 2e, \qquad\qquad [4.13]$$

or by the direct chemisorption of xanthate,

$$X^- = X_{ads} + e. \qquad\qquad [4.14]$$
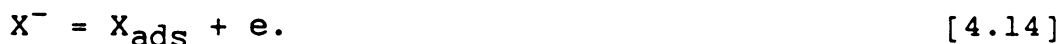
At 2.5×10^{-5} M xanthate, the reversible potential for dixanthogen formation is 357 mV, much too high for the A_5 peak observed at approximately -200 mV. Therefore, Reaction [4.14] is most likely responsible for the formation of A_5 which has been concluded by numerous investigators.

Basilio (1985) produced the voltammograms shown in Figure 4.26 by increasing the scan rate to 20 mV/sec and narrowing the potential range to 205 and -355 mV. As before, anodic peaks A_5 and A_6 are observed at approximately -220 mV and -30 mV, respectively; however, an additional peak at C_5 developed near -100 mV and continued to develop to -200 mV, thereby, suggesting that C_5 encompasses the
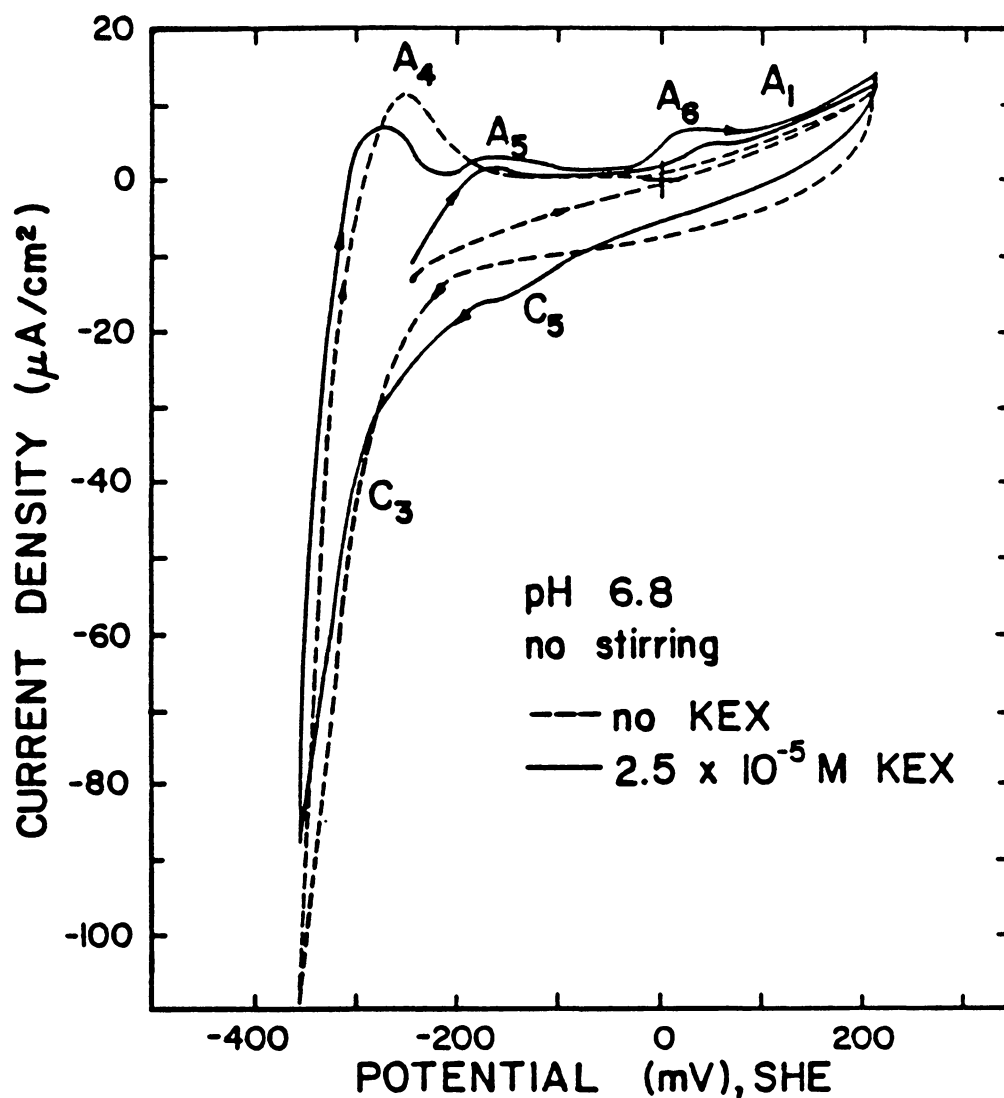
Figure 4.26 Voltammograms of chalcocite at pH 6.8 (0.1 M
KH_2PO_4/0.1 M NaOH) with (——) and without (---)
2.5×10^{-5} M xanthate. Scans cycled between
205 and -355 mV from a starting potential of
-255 mV. No stirring. Scan rate = 20 mV/sec
(from Basilio, 1985).

reverse of both Reactions [4.12] and [4.14]. Remaining peaks of A_1, A_4 and C_3 were repeated, each larger than before because of the increased scan rate. The increase of the C_3 peak, however, may have resulted from a larger amount of djurleite contamination.

b. pH 9.2: At a scan rate of 20 mV/sec, voltammograms of chalcocite, both with and without 2.5×10^{-5} M xanthate, are shown in Figure 4.27 (from Basilio, 1985). Because the upper and lower limits were respectively restricted to 105 and -415 mV only peaks at C_3, djurleite reduction to chalcocite, and A_4, chalcocite oxidation to djurleite, were observed without xanthate. In the presence of xanthate, however, peaks at C_5, A_{5a}, A_{5b} and A_6 were produced. Comparing to the voltammogram at pH 6.8 shows that C_5, A_5 and A_6 occurred at the same potentials as C_5, A_{5a} and A_6, respectively. This would be expected since the reactions which represent them, Reactions [4.12] and [4.14], are pH-independent. The additional peak at A_{5b} is probably caused by additional chemisorption of xanthate; however, this additional chemisorption occurs at a different potential because xanthate has already chemisorbed onto the surface at A_{5a}. In other words, the chemisorption of xanthate is dependent on the surface to which it is chemisorbing to. Woods (1971) and Pritzker (1985) have shown xanthate chemisorbs on galena near 0 mV.
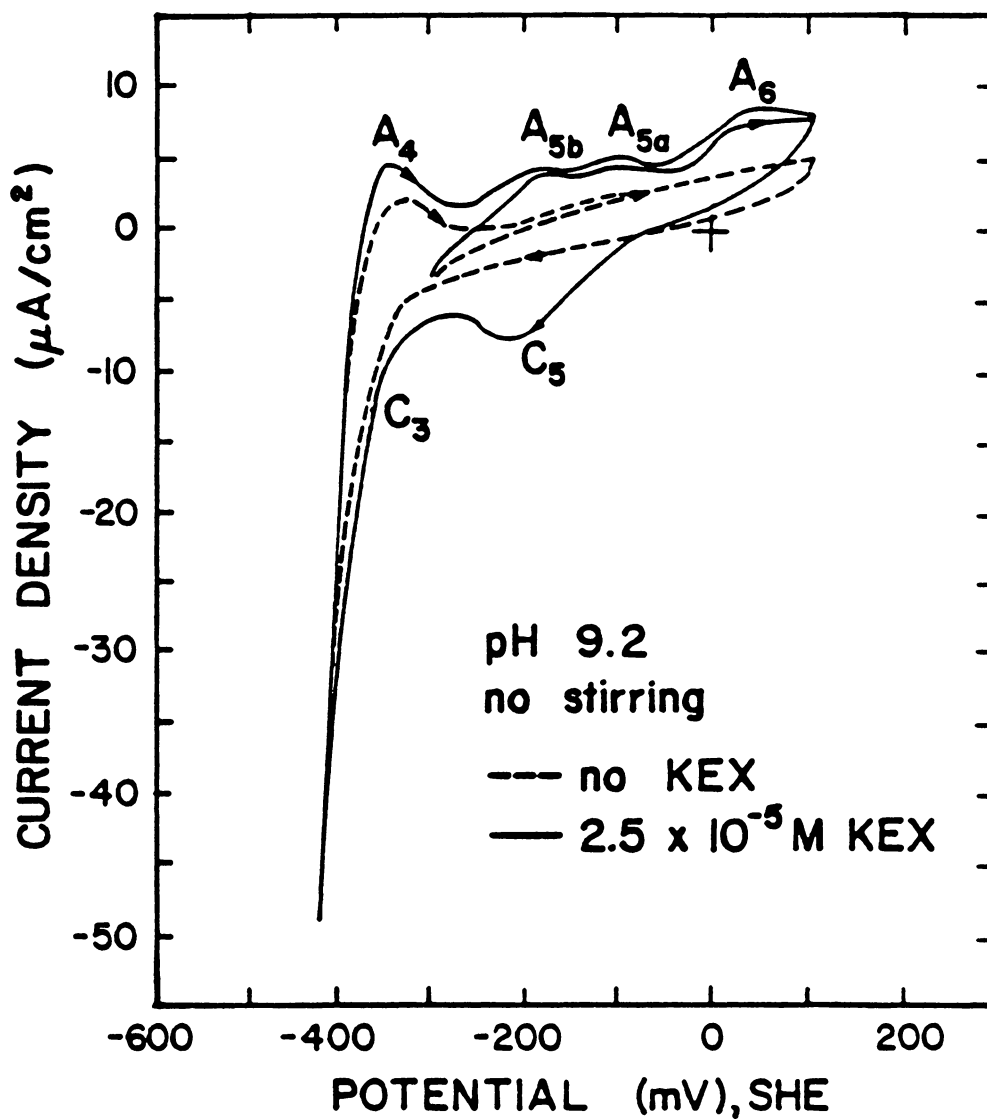
Figure 4.27   Voltammograms of chalcocite at pH 9.2 (0.05 M
Na$_2$B$_4$O$_7$) with (——) and without (---) 2.5 x 10^{-5}
M xanthate. Scans cycled between 105 and -415
mV from a starting potential of -295 mV. No
stirring. Scan rate = 20 mV/sec (from Basilio,
1985).
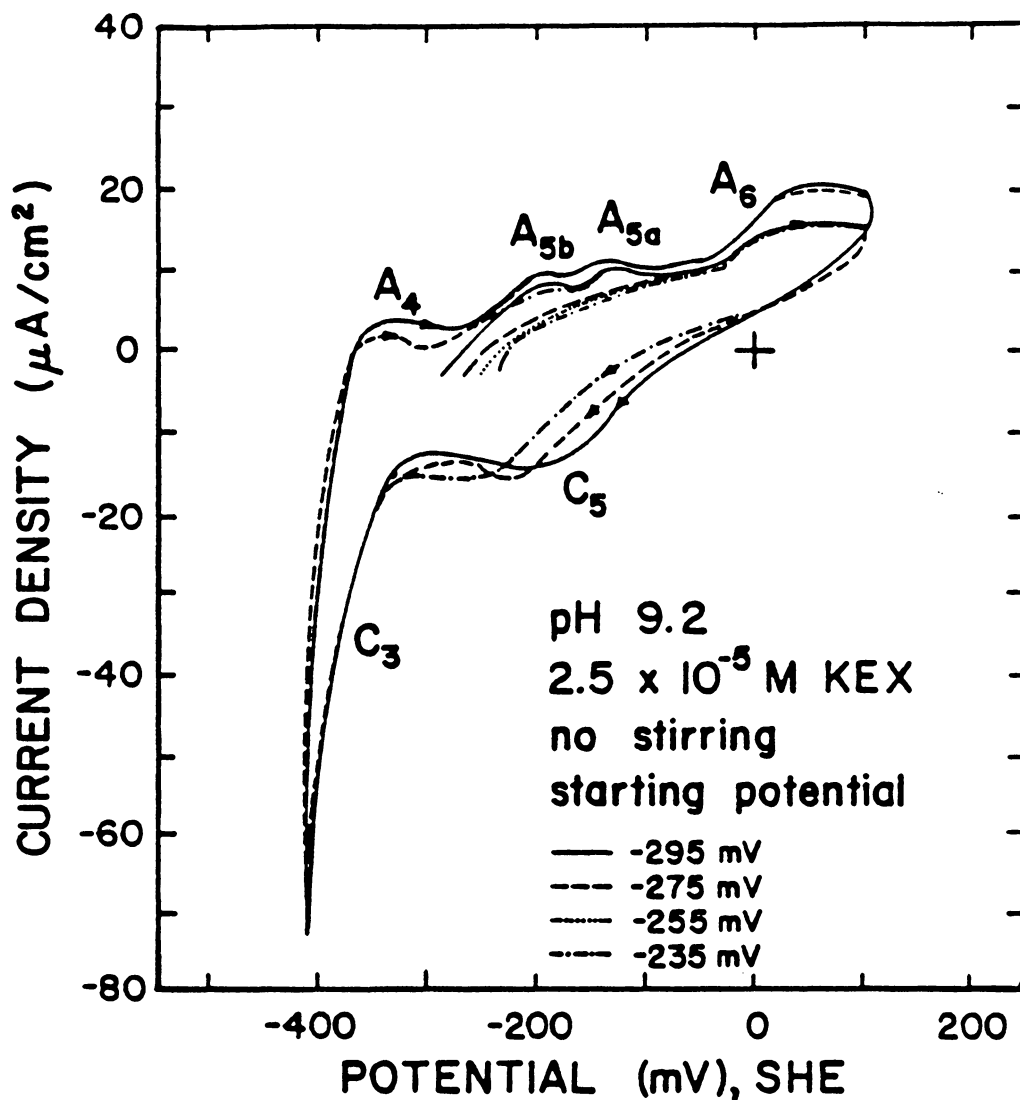
Figure 4.28 Voltammograms of chalcocite at pH 9.2 (0.05 M
Na$_2$B$_4$O$_7$) with 2.5 x 10^{-5} M xanthate. Scans
cycled between 105 and -415 mV from various
starting potentials at 20 mV/sec. No stirring
(from Basilio, 1985).

Kowal and Pomianowski (1973) originally observed the xanthate chemisorption peaks on chalcocite at A_{5a} and A_{5b} and referred to them as 'prepeaks.' They also calculated thermodynamic data based on the peak position and the assumption that the reactions which caused the peaks to form were one-electron transfer reactions, but they neglected to take the concentration of the xanthate ion into account. From Figure 4.28 in which Basilio (1985) investigated the effect that the starting potential had on the prepeak formation, the standard free energy of chemisorbed xanthate on Cu_2S was determined to be -13.08 kcal/mole. In the calculations, a xanthate concentration of 2.5×10^{-5} M was used as was a reversible potential of -295 mV. This potential was chosen since the xanthate chemisorption peaks at A_{5a} and A_{5b} were not observed at the higher potentials because chemisorption had already occurred.

4.4 Microflotation

Microflotation experiments on chalcocite that were performed by Basilio (1985) at pH 5, 8 and 11 with 10^{-5} M xanthate have shown that the lower flotation edge was pH-independent but was dependent on when the xanthate was added. Adjusting the potential with hydrazine after xanthate addition (Method I) created a lower flotation edge near -400 mV and adjusting the potential beforehand (Method

II) created one near -200 mV. Since the tests were carried out in the open atmosphere, this phenomena may have been caused by oxygen eventhough efforts were made to deoxygenate the solutions. Microflotation tests were therefore conducted at pH 9.2 (0.05 M $Na_2B_4O_7$) in a glove box purged with nitrogen gas. Results duplicated those of Basilio (1985) as shown in Figure 4.29, thereby indicating that oxygen was not the cause.

Additional investigation into these phenomena revealed that hydrazine-produced reducing potentials on a platinum electrode were 200 mV more negative than on a chalcocite electrode when Method II was employed. The relevant potential should be that established at the mineral surface, especially in mixed-potential systems (Rand and Woods, 1984). However, the platinum electrode developed the same potential as the chalcocite electrode when it was pressed into a bed of chalcocite particles treated by Method II. When Method I was used, xanthate probably chemisorbed on both the platinum and chalcocite electrodes at open-circuit and thereby caused the same potential to be measured. Woods (1971) showed xanthate chemisorbed on platinum without charge transfer at potentials lower than 0 mV. Therefore, the true lower flotation edge of chalcocite is at -200 mV which agrees with the flotation results of Heyes and Trahar (1979) and Richardson et al. (1984) as illustrated by Figure
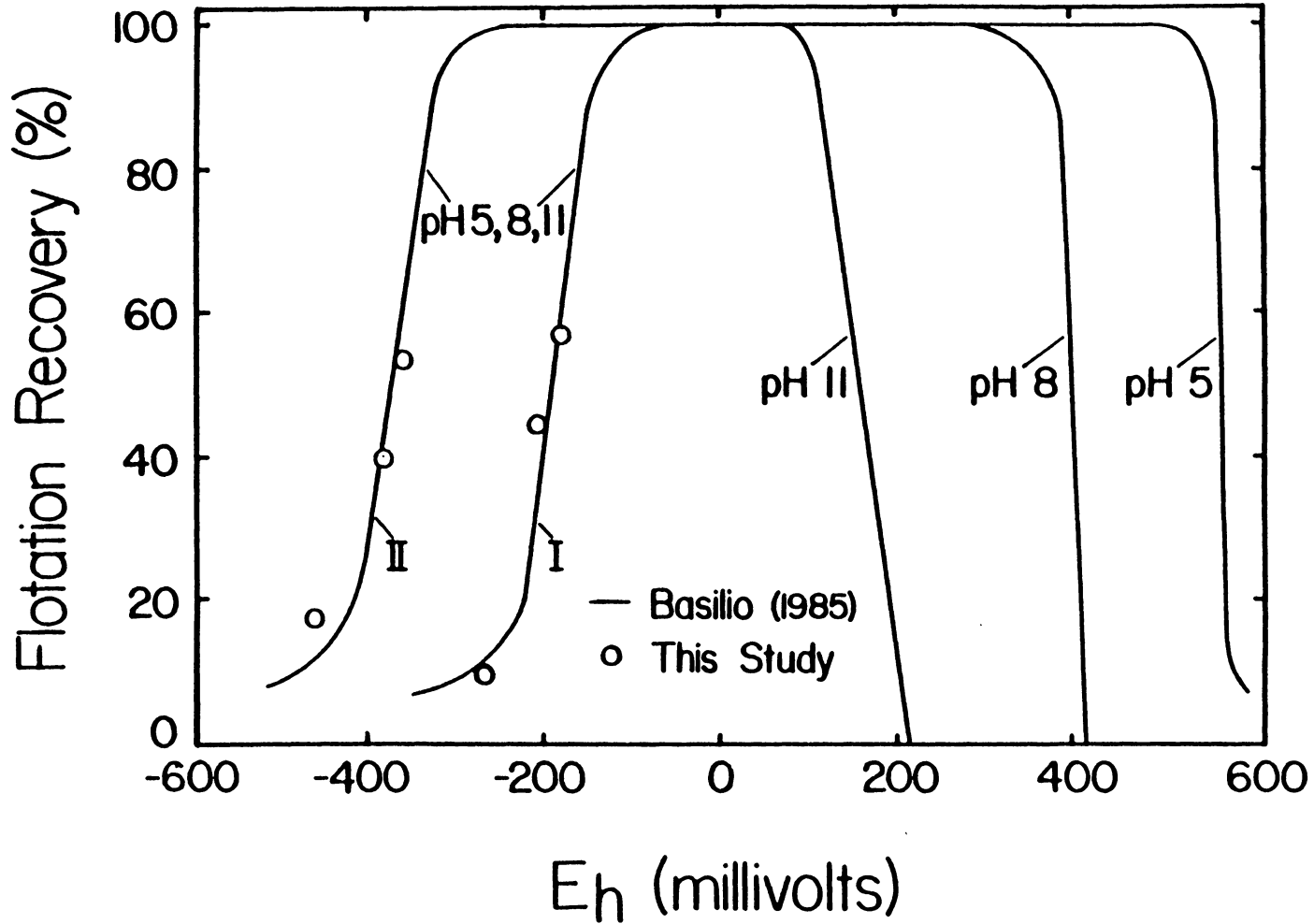
Figure 4.29   Microflotation of chalcocite at pH 5, 8 and 11 at 10^{-5} M xanthate added before (I) and after (II) potential control (from Basilio, 1985) as compared to this study (o).
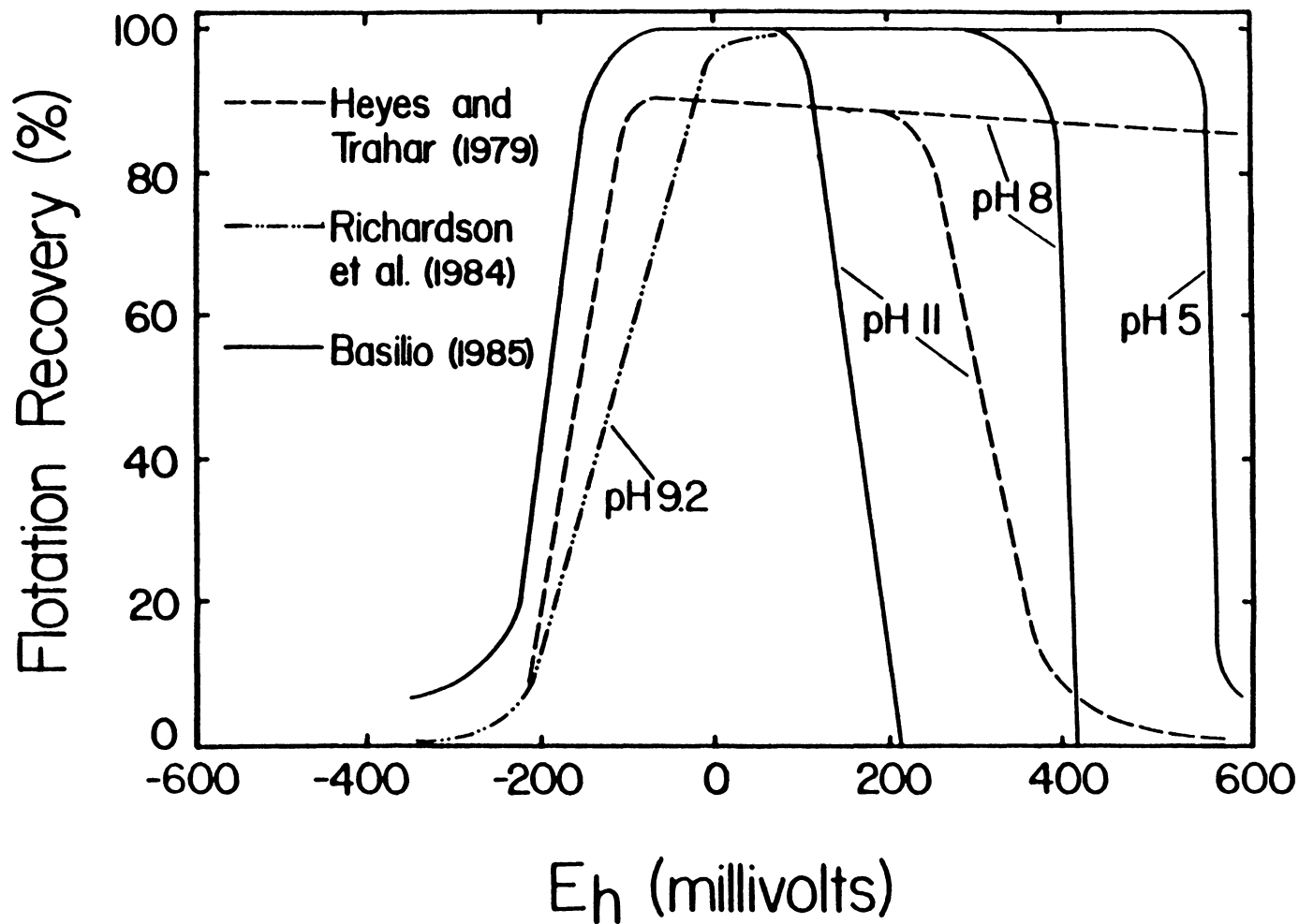
Figure 4.30 Comparison of chalcocite flotation data obtained by Heyes and Trahar (1979) at pH 8 and 11 with 4.7 x 10^{-5} M xanthate, Richardson et al. (1984) at pH 9.2 with 1.44 x 10^{-5} M xanthate, and Basilio (1985) at pH 5, 8 and 11 with 10^{-5} M xanthate.

4.30. Heyes and Trahar conducted flotation tests in a 3-liter modified Denver D1 cell using 4.7×10^{-5} M xanthate at pH 8 and 11. They used either sodium dithionite or sodium hypochlorite to adjust the potential. On the other hand, Richardson et al. electrically applied the potential to a packed-bed of chalcocite in a microflotation-electrochemical cell at pH 8 in the presence of 1.44×10^{-5} M xanthate. After applying the potential, the bed was released and flotation was started.

Voltammetry experiments have shown xanthate chemisorption, Reaction [4.14], begins at -295 mV but does not reach monolayer coverage until -200 mV is obtained. This fits quite well with the flotation results but, because thermodynamic data for chemisorbed xanthate was not available at the time, does not match the lower flotation edge of -35 mV shown in Figures 2.22, 2.23 and 2.32. Obviously, the difference between -35 mV and -200 mV is caused by chemisorbed xanthate which Woods (1971) has stated can render a surface slightly hydrophobic.

Further comparisons of Figure 2.32 with the works of Basilio (1985) shown in Figures 4.29 and 4.30 indicate nearly exact matches at the upper flotation edge for each pH. He used hydrogen peroxide to produce the oxidizing potentials. At these oxidizing potentials, no differences between the results of Method I and II were recorded.

CHAPTER V

SUMMARY AND CONCLUSIONS

5.1 Introduction

Since its inception, the xanthate flotation of sulfides has been controlled by adjusting the pH of the mineral slurry. However, past investigations have shown that E_h, the potential, also plays an important role. Not only is xanthate affected by E_h and pH changes, but the sulfide minerals themselves are. More specifically, chalcocite (Cu_2S) is known to produce nonstoichiometric copper sulfides when oxidized. Therefore, the effects of E_h and pH on chalcocite, both with and without xanthate, were studied. Mass-balanced, thermodynamic calculations were performed to construct E_h-pH diagrams and then verified using several experimental techniques: intermittent galvanostatic polarization (IGP), X-ray photoelectron spectroscopy (XPS), cyclic voltammetry, and microflotation.

5.2 Computer Calculations

The results of the computer calculations both with and without xanthate are summarized in the following sections.

5.2.1 Without Xanthate

Mass-balanced E_h-pH diagrams have been constructed from computer calculations for the copper-sulfur-water system involving Cu/S ratios that pertain to each of the stable copper sulfides: chalcocite (Cu_2S), djurleite ($Cu_{1.96}S$), anilite ($Cu_{1.75}S$) and covellite (CuS). Each mineral was allowed to oxidize to elemental sulfur, thiosulfate, sulfate, and sulfate destabilized by 75 kcal/mole. Never before have such calculations involved destabilized sulfate, let alone the oxidation of each copper sulfide mineral.

The diagrams reveal that the stability regions for each copper sulfide are dependent on both the Cu/S ratio in the system and the final oxidation state of the sulfur. From a geological point-of-view, this is important because it explains why a single ore body can have a variety of stable copper sulfides present. Furthermore, the only time oxidation of a copper sulfide produced a sulfide of less copper content (i.e., copper-deficient) was when oxidation proceeded to elemental sulfur.

Under no condition did more than two solid phases exist at the same time. This co-existence has been explained using both Gibbs' phase rule and the definition of solubility. The most commonly observed co-existence was that between chalcocite and metallic copper.

E_h-pH digrams involving oxidation to destabilized

sulfate demonstrated elemental sulfur to be the primary oxidation product in acid conditions and sulfate in neutral. However, without including the destabilization of other sulfur-oxy species such as thiosulfate and thionates in the mass-balanced calculations, it was difficult to assess whether the approach was realistic or not.

E_h-pH diagrams representing chalcocite oxidation to metastable copper sulfides are consistent with previous investigations in which experiments were conducted under acidic conditions to prevent copper oxides from forming and thereby passivating the mineral surface.

5.2.2 With Xanthate

Mass-balanced E_h-pH diagrams have been constructed from computer calculations for chalcocite and metallic copper in the presence of 10^{-5} M xanthate. Chalcocite oxidation was allowed to form metastable copper sulfides when oxidation proceeded to elemental sulfur or thiosulfate but not to sulfate. Destabilized sulfate was not considered.

Except under acidic conditions where various aqueous copper-sulfur-oxy species are predominant, the cupric xanthate stability region remained unaffected by the final oxidation state of the sulfur. Reactions involving cupric xanthate were therefore sulfur-independent. For the most part, the upper flotation edge was defined by cupric

xanthate formation.

On the other hand, cuprous xanthate, which is responsible for the lower flotation edge, was shown to be dependent on the sulfur oxidation state. As oxidation proceeded from elemental sulfur to sulfate, the lower flotation edge was observed to decrease from an equilibrium potential of -35 mV established by

$$Cu_2S + .07X^- = Cu_{1.93}S + .07CuX + .07e \qquad [5.1]$$
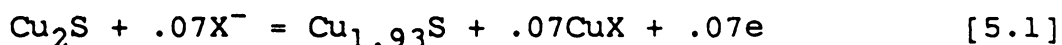
to an equilibrium potential of -320 mV predicted by

$$Cu^O + X^- = CuX + e. \qquad [5.2]$$

No matter what sulfur oxidation state is produced, the lower flotation edge corresponded exactly with a $10^{-19.2}$ M sulfide ion concentration which is thermodynamically calculated from

$$Cu_2S + 2X^- = 2CuX + S^{2-} \qquad [5.3]$$

when 10^{-5} M xanthate concentration is used. Protonation and oxidation reactions must therefore control the sulfide ion concentration.

Gibbs' phase rule was again used to explain why the co-existence of three solid phases occurred. These three phases were predominantly cuprous xanthate and chalcocite with either $Cu_{1.93}S$ or metallic copper.

5.3 Experimental Studies Without Xanthate

The results of the experimental studies for the reduction and oxidation of chalcocite without xanthate are summarized in the following sections.

5.3.1 Reduction of Chalcocite

In the IGP experiments, djurleite contamination of the chalcocite was discovered which, thereby, prevented the verification of the co-existence between chalcocite and metallic copper. X-ray diffraction patterns of the chalcocite confirmed djurleite was present. Further confirmation was achieved with the chronoamperometry tests used for the XPS study and with cyclic voltammetry. Each of the electrochemical experiments showed that djurleite reduced to chalcocite at -370 mV which agreed with the computer calculations:

$$2Cu_{1.96}S + .04H^+ + .08e = 1.96Cu_2S + .04HS^-. \qquad [5.4]$$
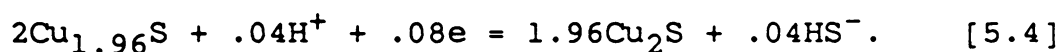
Previous investigators using cyclic voltammetry have misidentified the djurleite reduction peak at -370 mV as chalcocite reduction to metallic copper,

$$Cu_2S + H^+ + 2e = 2Cu^0 + HS^-, \qquad [5.5]$$
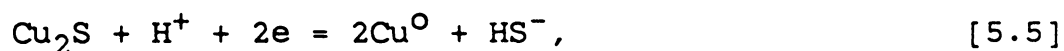
which was experimentally determined and thermodynamically calculated to occur at a reversible potential of -700 mV.

Cyclic voltammetry has shown Reaction [5.5] did not occur at -400 mV but did produce a monolayer of metallic copper at -600 mV. The monolayer coverage was in agreement with the computer calculations but the absence of metallic copper production at -400 mV disagreed with the XPS results that showed the beginnings of a Cu L_3VV peak corresponding to metallic copper. Further quantification of the XPS results by calculating surface Cu/S ratios seemingly discredited the presence of metallic copper at -400 mV.

XPS has also shown that the wet-polishing of a chalcocite electrode specifically allowed copper to dissolve and, hence, leave behind a sulfide-rich surface. The transportation of copper from inside the solid to the surface set up a reaction in which djurleite was produced causing further contamination.

5.3.2 Oxidation of Chalcocite

IGP experiments successfully showed chalcocite oxidation produced a series of copper sulfides confirming the work of several investigators:

$$Cu_{2-x}S = Cu_{2-x-y}S + yCu^{2+} + 2ye. \qquad [5.6]$$
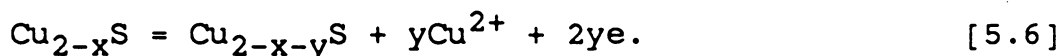
However, the resulting plateaus, although evident, were not very distinguishable possibly for two reasons. First, each plateau may have been produced by a solid solution of copper

sulfides rather than a copper sulfide of specific stoichiometry. Second, the production of cupric ions and their subsequent loss due to diffusion would affect the potential at which the plateaus occur.

The single chronoamperometry experiment that was carried out at 600 mV and analyzed with XPS resulted in the appearance of a new oxidation state of sulfur. Since the S 2p binding energy of the new state was between that of chalcocite and elemental sulfur, the new state was a polysulfide. Because covellite is actually a one-to-one mixture of chalcocite and copper disulfide, the most likely polysulfide would be disulfide. All copper sulfides could then be represented by $Cu_2S \cdot xCuS_2$, where 'x' would range from 0 for chalcocite to 1 for covellite.

Cyclic voltammetry has shown that chalcocite oxidation produces nonstoichiometric copper sulfides at each pH. Under basic conditions, Reaction [5.6] becomes

$$Cu_2S + xH_2O = Cu_{2-x}S + xCuO + 2xH^+ + 2xe. \qquad [5.7]$$
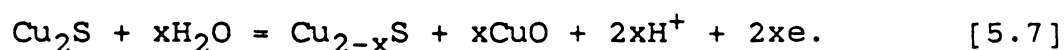
In sodium borate solutions (pH 9.2), however, copper oxides are readily soluble making nonstoiciometric copper sulfide reactions very distinguishable.

5.4 Experimental Studies With Xanthate

Cyclic voltammograms in the presence of xanthate have

shown that two oxidation reactions, both pH-independent, occurred on chalcocite:

$$Cu_2S + .07X^- = Cu_{1.93}S + .07CuX + .07e \qquad [5.8]$$

$$\text{and} \qquad X^- = X_{ads} + e. \qquad [5.9]$$
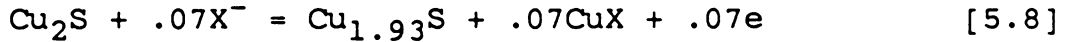
Reaction [5.8] occurred near 0 mV which is in agreement with the thermodynamically calculated equilibrium potential of -59 mV. Reaction [5.9] was shown to occur at -295 mV which gave rise to a standard free energy of -13.08 kcal/mole for X_{ads} assuming that the standard free energy of the xanthate ion was 0 kcal/mole. Reaction [5.9] was observed to have occurred twice: the chemisorption of xanthate on chalcocite at -295 mV followed by subsequent xanthate chemisorption on top of the previously chemisorbed xanthate.

Microflotation tests have shown that reducing the potential of the slurry after and before xanthate addition respectively produced lower flotation edges at -400 and -200 mV. The difference between the two flotation edges was not caused by dissolved oxygen but, rather, by how the mixed-potential system was established. Adjusting the potential after xanthate addition allowed xanthate adsorption to take place on both platinum and chalcocite; however, adjusting the potential before xanthate addition only allowed xanthate adsorption on chalcocite. Therefore, the true lower flotation edge was that established at -200 mV which is in

agreement with other investigators.

Because thermodynamic data for X_{ads} was lacking, computer calculations revealed a lower flotation edge at -35 mV. Therefore, X_{ads} must have caused the surface to become hydrophobic in order for the lower flotation edge to be at -200 mV. On the other hand, computer calculations exactly match the upper flotation edges shown for each pH.

5.5 Future Recommendations

The following suggestions are offered as possibilities for future research with various copper-sulfur systems:

1. Although chalcocite is known to oxidize only as far as elemental sulfur in the time frame encountered in mineral processing, its oxidation and that of djurleite, anilite and covellite could proceed to sulfite which has never before been considerd in mass-balanced calculations of this kind. Similiarly, other sulfur-oxy species such as thionates could be considered. Although experimental results would be needed to determine the overpotential required for the formation of sulfur-oxy species, destabilization of the species could also be considered.

2. Because chalcocite oxidation produces metastable copper sulfides, electrochemical reactions of djurleite, anilite and covellite may produce them as well.

Thermodynamic data would therefore have to be determined to construct E_h-pH diagrams.

3. E_h-pH diagrams could be constructed for djurleite, anilite, and covellite in the presence of xanthate. The effect of Cu/S ratio on the copper xanthate stability regions would be observed. The effects of the final sulfur oxidation state and amount of xanthate addition could also be investigated.

4. As could now be accomplished for chalcocite, E_h-pH diagrams could be constructed with X_{ads} considered as a species. Experimental studies such as cyclic voltammtry or potentiometric titration would have to be performed to determine free energy values for X_{ads} on the other copper sulfides.

5. Thermodynamic calculations of this sort could also be performed on each copper sulfide in the presence of other reagents including dithiophosphates, thionocarbamates, and even cyanide. These calculations have never been done.

6. Confirmation of any of the E_h-pH diagrams suggested above could be accomplished with the techniques used in this study: IGP, XPS, cyclic voltammetry and microflotation. Other techniques include infrared (IR) and ultraviolet (UV) spectroscopy. Both of these spectroscopic techniques have

the advantage of being performed in situ as do Raman and electrochemical modulation spectroscopy.

7. Several of the techniques could also be used to investigate the disulfide theory in which all of the copper sulfides, except chalcocite, are suspected of containing various mixtures of chalcocite and copper disulfide, $Cu_2S \cdot xCuS_2$. These techniques could also be used to study the effect that dissolved oxygen had on the system.

8. Because XPS has shown that wet-polishing affects the Cu/S ratios, the results of cyclic voltammetry may have been affected since the chalcocite electrode was wet-polished. The effect of wet-polishing on voltammetry could be explored by mounting freshly ground chalcocite on carbon paste electrodes and comparing the resulting voltammograms to those produced by wet-polished chalcocite electrodes.

REFERENCES

Ahmed, S. M., 1978. Electrochemical studies of sulphides:
II. Measurement of the galvanic currents in galena
and the general mechanism of oxygen reduction and
xanthate adsorption on sulphides in relation to
flotation. Int. J. Miner. Process., 5:175-182.

Basilio, C. I., 1985. Thermodynamics and Electrochemistry
of the Chalcocite-Potassium Ethyl Xanthate System. MS
Thesis, Virginia Polytechnic Institute and State
University, Blacksburg, Virginia.

Basilio, C. I., Pritzker, M. D. and Yoon, R. H., 1985.
Thermodynamics, electrochemistry and flotation of the
chalcocite-potassium ethyl xanthate system. 114th AIME
annual meeting, New York, New York, Preprint No. 85-86.

Berry, L. A., 1954. The crystal structure of covellite,
CuS, and klockmannite, CuSe. Am. Mineral., 39:504-509.

Bethke, C. M., 1978. Program SOLUPLOT--a FORTRAN program to
calculate and plot equilibrium Eh-pH and aO_2-pH
diagrams for chemical systems, considering speciation
of ligands from free energy and thermodynamic activity
data. Pennsylvania State Computation Center,
University Park, Pennsylvania 16802.

Bilinski, H., Sjoberg, S., Kezic, S. and Brnicevic, N.,
1985. Precipitation and hydrolysis of thorium in
aqueous solution. VI. Determination of formation
constants for mixed thorium-maleate-hydroxo complexes
and characterization of solids. Acta Chem. Scand.,
39:317-325.

Brage, M. C., Lamache, M. and Bauer, D., 1979. Contribution
a l'etude des sulfres de cuivre non stoichiometriques.
Electrochim. Acta, 24:25-30.

Briggs, D. and Seah, M. P., 1983. Practical Surface
Analysis by Auger and X-ray Photoelectron Spectroscopy.
John Wiley and Sons, New York, New York.

Brook, P. A., 1971. A computer method of calculating
potential-pH diagrams. Corr. Sci., 11:371-377.

Buckley, A. N., Hamilton, I. C. and Woods, R., 1984. Investigation of the surface oxidation of bornite by linear potential sweep voltammetry and x-ray photoelectron spectroscopy. J Appl. Elecrochem., 14:63-74.

Buerger, N. W., 1942. X-ray evidence of the existence of the mineral digenite Cu_9S_5. Amer. Mineral., 27:712-716.

Chander, S. and Fuerstenau, D. W., 1975. Electrochemical reaction control of contact angles on copper and synthetic chalcocite in aqueous potassium diethyl-dithiophosphate solutions. Int. J. Miner. Process, 2:333-352.

Chen, K. Y. and Gupta, S. K., 1973. Formation of Polysulfides in Aqueous Chemistry. Environmental Letters, 4:187-200.

Clark, A. H., 1972. A natural occurence of hexagonal $Cu_{1.83}S$ in Rancagua, Chile. Nature Phys. Sci., 238:123-124.

Cook, M. A. and Nixon, J. C., 1950. Theory of water-repellent films on solids formed by adsorption from aqueous solutions of heteropolar compounds. J. Phys. Colloid Chem., 54:445-459.

Craig, J., 1987. Personal Communication.

Craynon, J. R., 1985. The Collectorless Flotation of Sphalerite. MS Thesis, Virginia Polytechnic Institute and State University, Blacksburg, Virginia.

Crerar, D. A., 1975. A method for computing multicomponent chemical equilibria based on equilibrium constants. Geochim. Cosmochim. Acta, 39:1375-1384.

Cutting, D. E., Womack, R. A. and MacGuffie, J. V., 1975. U. S. Patent 3,883,421.

Djurle, S., 1958. An x-ray study on the system Cu-S. Acta Chem. Scand., 12:1415-1426.

Duby, P., 1977. The thermodynamic properties of aqueous inorganic copper systems. International Copper Research Association (INCRA) Monograph IV, Library of Congress catalogue card No. 77-71709.

DuRietz, C., 1976. Chemisorption of collectors in flotation. Proc. 11th Int. Miner. Process. Congr., Cagliari, 1975, 375-403.

Eadington, P. and Prosser, A. P., 1969. Oxidation of Lead Sulphide in Aqueous Suspensions. Trans. IMM, 78:C74-82.

Eriksson, G., 1971. Thermodynamic studies of high temperature equilibria. III. SOLGAS, a computer program for calculating the composition and heat condition of an equilibrium mixture. Acta Chem. Scand., 25:2651-58.

Eriksson, G., 1979. An algorithm for the computation of aqueous multicomponent, multiphase equilibria. Anal. Chim. Acta, 112:375-383.

Etienne, A. and Peters, E., 1972. Thermodynamic measurements in the Cu-S system in the temperature range $40-80^{\circ}C$. IMM Trans. Sect. C, 81:176-181.

Finkelstein, N. P., 1970. Quantitative aspects of the role of oxygen in the interaction between xanthate and galena. Sep. Sci., 5:227-256.

Forssberg, K. S. E., Antti, B. M. and Palsson, B. I., 1984. Computer-assisted calculations of thermodynamic equilibria in the chalcopyrite-ethyl xanthate system. In: Reagents in the Minerals Industry. Institution of Mining and Metallurgy (IMM), London, 251-264.

Frenzel, G., 1959. Idait und "blaubleibender covellin". Neues Jahrb. Mineral. Abh., 93:87-132.

Frenzel, G., 1961. Der Cu-ubeschuss des blaubleibenden covellins. Neues Jahrb. Mineral. Monatsh., 199-204.

Froning, M. H., Shanley, M. E. and Verink, E. D., 1976. An improved method for calculation of potential-pH diagrams of metal-ion-water systems by computer. Corr. Sci., 16:371-377.

Fuerstenau, D. W., 1962. Preface to froth flotation. In: D.W. Fuerstenau (Editor), Froth Flotation. SME/AIME, New York, New York.

Gardner, J. R. and Woods, R., 1979. A study of the surface oxidation of galena using cyclic voltammetry. J. Electroanal. Chem., 100:447-459.

Garrels, R. M. and Christ, C. L., 1965. Solutions, Minerals and Equilibria. Harper and Row, New York, New York.

Gaudin, A. M., 1927. Flotation mechanism, a discussion of the functions of flotation reagents. AIME Tech. Publ., 4:27-42.

Gaudin, A. M., Dewey, F., Duncan, W. E., Johnson, R. A. and Tangel, O. F., 1934. Reactions of xanthates with sulfide minerals. Trans. AIME, 112:319-347.

Gaudin, A. M. and Finkelstein, N. P., 1965. Interactions in the system galena-potassium ethyl xanthate-oxygen. Nature, 207:389-391.

Gautam, R. and Seider, W. D., 1979. Computation of phase and chemical equilibrium. AIChE J., 25:991-1015.

Gerlach, J. and Kuzeci, E., 1983. Application of carbon paste electrodes to elucidate hydrometallurgical dissolution processes with special regard to chalcocite and covellite. Hydrometallurgy, 11:345-361.

Goble, R. J., 1980. Copper sulfides from Alberta: yarrowite Cu_9S_8 and spionkopite $Cu_{39}S_{28}$. Can. Mineral., 18:511-518.

Goble, R. J., 1981. The leaching of copper from anilite and the production of a metastable copper sulfide structure. Can. Mineral., 19:583-591.

Goble, R. J. and Robinson, G., 1980. Geerite, $Cu_{1.60}S$, a new copper sulfide from Dekalb Township, New York. Can. Mineral., 18:519-523.

Goble, R. J., 1985. The relationship between crystal structure, bonding and cell dimensions in the copper sulfides. Can. Mineral., 23:61-76.

Harris, P. J. and Finkelstein, N. P., 1975. Interactions between sulfide minerals and xanthates. I. The formation of monothiocarbonate at galena and pyrite surfaces. Int. J. Miner. Process., 2:77-100.

Hepel, T. and Pomianowski, A., 1977. Diagrams of electrochemical equilibria of the system copper-potassium ethyl xanthate-water at $25^{\circ}C$. Int. J. Miner. Process., 4:345-361.

Hillrichs, E. and Bertram, R., 1983a. Anodic dissolution of copper sulfides in sulfuric acid solution. I. The anodic decomposition of $Cu_{2-x}S$. Hydrometallurgy, 11:181-193.

Hillrichs, E. and Bertram, R., 1983b. Anodic dissolution of copper sulfides in sulfuric acid solution. II. The anodic decomposition of CuS. Hydrometallurgy, 11:181-193.

Hopstock, D. M., 1968. Chemical Properties of Xanthates and Dithiocarbamates. M.Sc. Thesis, University of Minnesota, Minneapolis, Minnesota.

Horvath, J. and Hackl, L., 1965. Check of the potential/pH equilibrium diagrams of different metal-sulphur-water ternary systems by intermittent galvanostatic polarization method. Corr. Sci., 5:525-538.

Hurlbut, C. S., Jr. and Klein, C., 1977. Manual of Mineralogy, 19th Ed. John Wiley and Sons, New York, New York.

Ingri, N., Kakolowicz, W. and Sillen, L. G., 1967. High-speed computers as a supplement to graphical methods. V. HALTAFALL, a general program for calculating the composition of equilibrium mixtures. Talanta, 14:1261-1286.

Iwasaki, I. and Cooke, S. R. B., 1958. The decomposition of xanthate in acid solution. J. Am. Chem. Soc., 80:285-288.

Johnson, N., 1987. Unpubl. work and pers. comm.

Jones, M. H. and Woodcock, J. T., 1978. Perxanthates - A new factor in the theory and practice of flotation. Int. J. Miner. Process., 5:285-296.

Jones, M. H. and Woodcock, J. T., 1984. Applications of pulp chemistry to regulation of chemical environment in sulphide mineral flotation. In: M.H. Jones and J.T. Woodcock (Editors), Principles of Mineral Flotation. The Wark Symposium. Aust. Inst. Min. Met., Parkville, Victoria, Australia, pp. 91-115.

Kakovskii, I. A., 1957. Physiochemical properties of some flotation reagents and their salts with ions of heavy non-ferrous metals. Proceedings, Second Int. Congr. Surf. Act., 225-441.

Karpov, I. K. and Kaz'min, L. A., 1972. Calculation of geochemical equilibria in heterogeneous multicomponent systems. Geokhimiya, 4:252-262 and 402-414.

Keller, C. H., 1925. U. S. Patent 1,554,216.

Kitchener, J. A., 1984. The froth flotation process: past, present and future- in brief. In: K.J. Ives (Editor), The Scientific Basis of Flotation, NATO ASI Series, No. 75(E).

Koch, D. F. A. and McIntyre, R., 1976. The application of reflectance spectroscopy to a study of the anodic oxidation of cuprous sulphide. J. Electroanal. Chem., 71:285-296.

Kostov, I. and Minceva-Stefanova, J., 1981. Sulphide Minerals: Crystal, Chemistry, Parageneses, and Systematics. Publishing House of the Bulgarian Academy of Sciences, Sofia, Bulgaria.

Kowal, A. and Pomianowski, A., 1973. Cyclic voltammetry of ethyl xanthate on a natural copper sulfide electrode. Electroanal. Chem. Interfacial. Electrochem., 46:411-420.

Lajunen, L. H. J. and Sjoberg, S., 1985. A potentiometric study of the Cu2+ - 4(5)-hydroxy-methylimidazole system in 0.1M NaClO4 medium. Acta Chem. Scand., 39:341-346.

Lawson, G. E., 1984. Computer data file of the sensitivity factors for the X-SAM 800 Spectrometer. Virginia Polytechnic Institute and State University, Blacksburg, Virginia.

Leja, J., Little, L. H. and Poling, G., 1963. Xanthate adsorption using infrared spectroscopy. 1 - Oxidized and sulphidized copper substrates. 2 - Evaporated lead sulfide, galena and metallic lead substrates. Trans. IMM, 72:407-423.

Leja, J., 1982. Surface Chemistry and Froth Flotation. Plenum Press, New York, New York.

Leppinen, J., 1987. Unpublished results.

Linkson, P. B., Phillips, B. D. and Rowles, C. D., 1979. Computer methods for the generation of Eh-pH diagrams. Minerals Sci. Engng., 11:65-79.

Luttrell, G.H. and Yoon, R. H., 1984. Surface Studies of the Collectorless Flotation of Chalcopyrite. Colloids and Surfaces, 12:239-254.

Majima, H., 1961. Fundamental studies on the collection of sulphide minerals with xanthic acid. Sci. Rep. Res. Inst. Tohuku Univ., Ser. A., 13:433-447.

Marcantonio, P., 1976. Chalcocite Dissolution in Acidic Ferric Sulfate Solutions. Ph.D. Dissertation, University of Utah, Salt Lake City, Utah.

Mathieu, H.J. and Rickert, H., 1972. Electrochemical-thermodynamic studies on the copper-sulfur systems at 15-90°. Z. Phys. Chem. (Frankfurt am Main), 79:315-330.

Mielczarski, J. and Suoninen, E., 1984. XPS study of ethyl xanthate adsorbed onto cuprous sulphide. Surf. Interface Anal., 6:34-39.

Moh, G. H., 1971. Blue-remaining covellite and its relations to phases in the sulfur rich portion of the copper-sulfur system at low temperatures. Mineral. Soc. Japan Spec. Pap., 1:226-232.

Morimoto, N., 1962. Djurleite, a new copper sulfide mineral. Mineral. J., 3:338-344.

Morimoto, N., Koto, K. and Shimazaki, Y., 1969. Anilite, Cu_7S_4, a new mineral. Amer. Mineral., 54:1256-1268.

Nagel, K., Ohse, R. and Lange, E., 1957. Z. Electrochem, 61:75.

Nakai, I., Sugitani, Y., Nagashima, K. and Niwa, Y., 1978. X-ray photoelectron spectroscopic study of copper minerals. J. Inorg. Nucl. Chem., 40:789-791.

Nefedov, V. I., Salyn, Y. V., Solozhenkin, P. M. and Pulatov, G. Y., 1980. X-ray photoelectron study of surface compounds formed during flotation of minerals. Surf. Interface Anal., 5:170-172.

Nowak, P., Barzyk, W. and Pomianowski, A., 1984. The applicability of EMF measurements to evaluation of thermodynamic properties of the Cu-S system. J. Electroanal. Chem., 171:355-358.

O'Dell, C. S., Dooley, R. K., Walker, G. W. and Richardson,
    P. E., 1984. Chemical and electrochemical reactions in
    the chalcocite-xanthate system. In: P.E. Richardson,
    S. Srinivasan and R. Woods (Editors), Proceedings of
    the International Symposium on Electrochemistry in
    Mineral and Metal Processing. The Electrochemical
    Society, Pennington, NJ, 84-10:81-95.

O'Dell, C. S., Walker, G. W. and Richardson, P. E., 1986.
    Electrochemistry of the chalcocite-xanthate system.
    J. Appl. Electrochem., 16:544-554.

Oftedal, I., 1932. Die kristallstrukture des covelline
    (CuS). Z. Kristallogr., 83:9-25.

Osseo-Asare, K., 1981. Application of activity-activity
    diagrams to ammonia hydrometallurgy. II. The copper-,
    nickel-, cobalt-ammonia-water systems at elevated
    temperatures. In: M.C. Kuhn (Editor), Process and
    Fundamental Considerations of Selected
    Hydrometallurgical Systems. SME/AIME, New York,
    359-369.

Palsson, B. I. and Forssberg, K. S. E., 1986. Computer-
    assisted calculations of thermodynamic equilibriua in
    the galena-ethyl xanthate system. Int. J. Miner.
    Process., in press.

Partridge, A. C. and Smith, G. W., 1971. Small-sample
    flotation testing: a new cell. Trans. IMM, 80:C199.

Paterson, J. G. and Salman, T., 1968. Interaction of
    xanthate with chalcocite. CIM Bulletin, 61:74-78.

Peters, E., 1984. Electrochemical mechanisms for
    decomposing sulfide minerals. In: P.E. Richardson, S.
    Srinivasan and R. Woods (Editors), Proceedings of the
    International Symposium on Electrochemistry in Mineral
    and Metal Processing. The Electrochemical Society,
    Pennington, NJ, 84-10:343-361.

Peters, E., 1986. Leaching of sulfides. In: P.
    Somasundaran (Editor), Advances in Mineral Processing.
    SME/AIME, Littleton, CO, 445-462.

Pettersson, L., Andersson, I. and Ohman, L. O., 1985a.
    Multicomponent polyanions. 35. A P-NMR study of
    aqueous molbdophosphates. Acta Chem. Scand., 39:53-58.

Pettersson, L., Hedman, B., Nenner, A. M. and Andersson, I., 1985b. Multicomponent polyanions. 36. A complimentary potentiometric and V-NMR study at low concentrations in acid solution. Acta Chem. Scand., 39:499-506.

Phillip, B. and Fichte, C., 1960. Kinetic studies on the decomposition of xanthate. Fraserforsch Text-Tech., 11:118-124; 172-179.

Plaksin, I. N. and Bessonov, S. V., 1957. Role of gases in flotation reactions. Proc. 2nd Int. Congr. Surface Act., Butterworths, London, 3:361-367.

Plaksin, I. N., 1959. Interaction of minerals with gases and reagents in flotation. Trans. AIME, 214:319-324.

Poling, G. W. and Leja, J., 1963. Infrared study of xanthate adsorption on vacuum deposited films of lead sulfide and metallic copper under conditions of controlled oxidation. J. Phys. Chem., 67:2121-2126.

Pomianowski, A. and Czarnecki, J., 1974. Mixed potentials and local cells in flotation systems. J. Colloid Interface Sci., 47:315-321.

Potter, R. W., 1977. An electrochemical investigation of the system copper-sulfur. Econ. Geol., 72:1524-1542.

Pourbaix, M., 1963. Atlas of Electrochemical Equilibria. Gauthiers-Villars, Paris, France.

Pritzker, M. D., Yoon, R. H. and Dwight, D. W., 1980. An ESCA study of the chalcopyrite concentrate produced by collectorless flotation. 54th Colloid and Surface Sci., Lehigh University.

Pritzker, M. D. and Yoon, R. H., 1984a. Thermodynamic calculations on sulfide flotation systems. I. Galena-ethyl xanthate system in the absence of metastable species. Int. J. Miner. Process., 12:95-125.

Pritzker, M. D. and Yoon, R. H., 1984b. Thermodynamic calculations and electrochemical studies on the galena-ethyl xanthate system. In: P.E. Richardson, S. Srinivasan and R. Woods (Editors), Proceedings of the International Symposium on Electrochemistry in Mineral and Metal Processing. The Electrochemical Society, Pennington, NJ, 84-10:26-53.

Pritzker, M. D., 1985. Thermodynamic and Kinetic Studies of Galena in the Presence and Absence of Potassium Ethyl Xanthate. Ph.D. Dissertation, Virginia Polytechnic Institute and State University, Blacksburg, Virginia.

Pritzker, M. D., Yoon, R. H., Basilio, C. I. and Choi, W. Z. 1985. Solution and flotation chemistry of sulfide minerals. Can. Metall. Quarterly, 24:27-38.

Ramdohr, P., 1943. Die mineralien im system Cu_2S-CuS. Z. prakt Geol., 51:1-9.

Rand, D. A. J. and Woods, R., 1984. E_h measurements in sulfide mineral slurries. Int. J. Miner. Process., 13:29-42.

Ranta, L., Minni, E., Suoninen, E., Heimala, S., Hintikka, V., Saari, M. and Rastas, J., 1981. XPS studies of adsorption of xanthate on sulfide minerals. App. of Surf. Sci., 7:393-401.

Richardson, P. E., Stout, J. V., Proctor, C. L. and Walker, G. W., 1984. Electrochemical flotation of sulfides: Chalcocite-ethylxanthate interactions. Int. J. Miner. Process., 12:73-93.

Rickard, D. T., 1972. Covellite formation in low temperature aqueous solutions. Mineral. Deposita, 7:180-188.

Rolia, E., 1977. Methods of analyses for sulphate, for individual thiosalts, and for elemental sulpher produced during the oxidation od sulphide ores. CANMET Mineral Sciences Laboratories Report MRP/MSL 77-21.

Roseboom, E. H., 1962. Djurleite, $Cu_{1.96}S$, a new mineral. Amer. Mineral., 47:1181-1184.

Roseboom, E. H., 1966. An investigation of the system Cu-S and some natural copper sulfides between 25° and $700^{\circ}C$. Econ. Geol., 61:641-672.

Sadanaga, R., Morimoto, N. and Ohmasa, M., 1963. X-ray study of djureite. Proceedings, 16th annual meeting of Mineral. Soc. of Japan.

Salamy, S. G. and Nixon, J. C., 1953. The application of electrochemical methods to flotation research. In: Recent Developments in Mineral Dressing. IMM, p. 503.

Shannon, L. K. and Trahar, W. J., 1986. The role of collector in sulphide ore flotation. In: P. Somasundaran (Editor), Advances in Mineral Processing. SME, Littleton, Colorado, 408-425.

Sjoberg, S., Ingri, N., Nenner, A. M. and Ohman, L. O., 1985. Equilibrium and structural studies of silicon (IV) and aluminum (III) in aqueous solution. 12. A potentiometric and Si-NMR study of silicon tropolonates. J. Inorg. Biochem., 24:267-277.

Sjoberg, S. and Ohman, L. O., 1985. Equilibrium and structural studies of silicon (IV) and Aluminum (III) in aqueous solution. Part 13. A potentiometric and Al-Nuclear Magnetic Resonance study of speciation and equilibria in the aluminum(III)-oxalic acid-hydroxide system. J. Chem. Soc. Dalton Trans., 2665-2669.

Slanina, P., Frech, W., Ekstrom, L. G., Loof, L., Slorach, S. and Cedergren, A., 1986. Dietary citric acid enhances absorption of aluminum in antacids. Clin. Chem., 32/3:539-541.

Smith, W. R., 1980. The computation of chemical equilibria in complex systems. Ind. Eng. Chem. Fundam., 19:1-10.

Sohn, H. J. and Wadsworth, M. E., 1984. Chemical conversion of chalcopyrite to copper sulfides. 113th AIME Annual Meeting, Los Angelos, California, Preprint No. 84-112.

Sparrow, G., Pomianowski, A. and Leja, J., 1977. Soluble copper xanthate complexes. Separation Sci., 12:87-102.

Sugiura, C., 1971. X-ray emission and K adsorption spectra of sulfur in some metallic sulfides. Japan J. Appl. Phys., 10:1120-1121.

Sutherland, K. L. and Wark, I. W., 1955. Principles of Flotation. Aust. Inst. Min. Met., Melbourne, Aust.

Swift, P., 1982. Adventitious carbon-the panacea for energy referencing? Surf. Interface Anal., 2:47-51.

Taggart, A. F., Taylor, T. C. and Knoll, A. F., 1930. Chemical reactions in flotation. AIME Tech. Publ.

Takeda, H. and Donnay, J. D. H., 1964. Twinning interpretation of super-lattice reflections of copper sulfides. Proceedings, annual metting of the Amer. Crystal. Assoc., Bozeman, Montana.

Takeda, H., Donnay, J. D. H. and Appleman, D. E., 1967. Djurleite twinning. Z. Kristallogr., 125:414-422.

Termes, S. C., Buckley, A. N. and Gillard, R. D., 1987. 2p electron binding energies for the sulfur atoms in metal polysulfides. Inorg. Chim. Acta., 126:79-82.

Thomas, G., Ingraham, T. R. and MacDonald, R. J. C., 1967. Kinetics of dissolution of synthetic digenite and chalcocite in aqueous acidic ferric sulphate solution. Can. Met. Quart., 6:281-292.

Thornber, M. R., 1982. Mineralogical and electrochemical stability of the nickel-iron sulfides- pentlandite and violorarite. J. App. Electrochem., 13:253-267.

Ting Po I and Nancollas, G. H., 1972. EQUIL - a general computational method for the the calculation of solution equibrium. Anal. Chem., 44:1940-1950.

Tipman, R. N. and Leja, J., 1975. Reactivity of xanthate and dixanthogen in aqueous solutions at different pH. Colloid Polym. Sci., 253:1-12.

Tolun, R. and Kitchener, J. A., 1964. Electrochemical study of the galena-xanthate-oxygen flotation system. Trans. IMM, 73:313-322.

Toperi, D. and Tolun, R., 1969. Electrochemical study and thermodynamic equilibria of the galena-oxygen-xanthate flotation system. Trans. IMM, 78:C191-C197.

Tornell, B., 1966. Svensk Papperstidning, 69(19):658-663.

Vaughan, D. J. and Craig, J. R., 1978. Mineral Chemistry of Metal Sulfides. Cambridge University Press, New York.

Verhulst, D. and Duby, P. 1977. A computer program for calculating and plotting potential-pH diagrams. In: P. Duby, 1977. The thermodynamic properties of aqueous inorganic copper systems. International Copper Research Association (INCRA), Monograph IV, Library of Congress Catalogue Card No. 77-71709.

Wagner, C. D., Riggs, W. M., Davis, L. E. and Moulder, J. F., 1979. Handbook of X-ray Photoelectron Spectroscopy, a Reference Book of Standard Data For use in X-ray Photoelectron Spectroscopy. G.E. Muilenberg (Editor).

Walker, G. W., Stout, J. V. and Richardson, P. E., 1984.
    Electrochemical flotation of sulfides: Reactions of
    chalcocite in aqueous solution. Int. J. Miner.
    Process., 12:55-72.

Walker, G. W., Walters, C. P. and Richardson, P. E., 1986.
    Hydrophobic effects of sulfur and xanthate on metal and
    mineral surfaces. Int. J. Miner. Process., 18:119-137.

Walsh, C. A. and Rimstidt, J. D., 1986. Rates of reaction
    covellite and blaubliebender covellite with ferric iron
    at pH 2.0. Can. Mineral., 24:35-44.

Warren, G. W., 1978. The Electrochemical Oxidation of
    $CuFeS_2$. Ph.D. Dissertation, University of Utah, Salt
    Lake City, Utah.

White, W. B., Johnson, S. M. and Dantzig, G. B., 1958.
    Chemical equilibria in complex mixtures.
    J. Chem. Phys., 28:751-755.

Whiteside, L. S. and Goble, R. J., 1986. Structural and
    compositional changes in copper sulfides during
    leaching and dissolution. Can. Mineral., 24:247-258.

Williams, B. G. and Patrick, W. H. Jr., 1977. A computer
    method for the construction of Eh-pH diagrams.
    J. Chem. Educ., 54:107.

Wolery, T. J. and Walters, L. J. Jr., 1975. Calculation of
    equilibrium distributions of chemical species in
    aqueous solutions by means of monotone sequences.
    J. Int. Assoc. Math. Geol., 7:99-115.

Woods, R., 1971. The oxidation of ethyl xanthate on
    platinum, gold, copper and galena electrodes. Relation
    to the mechanism of mineral flotation. J. Phys. Chem.,
    75:354-362.

Woods, R., 1984. Electrochemistry of sulphide flotation.
    In: M.H. Jones and J.T. Woodcock (Editors), Principles
    of Mineral Flotation. The Wark Symposium. Aust. Inst.
    Min. Met., Parkville, Victoria, Australia, pp. 91-115.

Woods, R., 1985. Personal Communication.

Woods, R. and Yoon, R. H., 1986. Personal Communications.

APPENDIX I

The Relationship Between E_h and Log [e]

Although Forssberg et al. (1984) showed the electron concentration to be logarithmically related to the redox potential, they did not show how the formula was derived. The following explanation is, therefore, offered:

To consider the electron as a distinct and separate species, the phases the electron goes through must be identified:

1) e^* is the deignation for an electron in the captured state (ie. Cu has two e^*'s compared to Cu^{2+}), and

2) e is the symbol for an electron in the free state.

The phase transition for n electrons then becomes

$$ne^* = ne. \qquad [1]$$

The free energy of the above reaction is zero by definition. Therefore, E^o is zero which reduces the Nernst equation to

$$E_h = (2.303RT/nF)\log\{[e]/[e^*]\}^n. \qquad [2]$$

If free electrons have activity coefficients of one and captured electrons have unit activity, Equation [2] becomes

$$E_h = (2.303RT/F)\log[e], \qquad [3]$$

which reveals the logarithmic relationship between [e] and E_h. Substituting R = 8.314 Joul/mol-K, T = 298.15K, and

F = 96,485 coul/mol in Equation [3] yields

$$\log[e] = E_h/59.16mV. \qquad [4]$$

Equation [4] was not previously incorporated in the SOLGASWATER program. However, comment statements in the program now reveal where it has been added (see Appendix II).

APPENDIX II

The Computer Program SOLGASWATER

```
C     SOLGASWATER, A COMPUTER PROGRAM FOR THE MASS BALANCE CALCULATION
C                     OF THERMODYNAMIC SYSTEMS
C
C
C
C
C         As indicated below, the SOLGASWATER program was developed by
C         Gunnar Eriksson, The Department of Inorganic Chemistry, Umea
C         University, Umea, Sweden.
C
C
C         After adaptation, this program can calculate the equilibrium
C         composition of an Eh-pH diagram in any thermodynamic system.
C         This equilibrium composition includes the following:
C
C             1) concentrations of all aqueous species, and
C             2) amounts of all solid species.
C
C
C         To indicate which lines have been changed, added, or omitted
C         in the program, comment statements were provided.   Comments
C         were also added to further document the program.
C
C
C
C              +---------------------------------------------+
C              |                                             |
C              |   SOLGASWATER (INTERACTIVE VERSION)         |
C              +---------------------------------------------+
C              |   GUNNAR ERIKSSON                           |
C              |   UMES UNIVERSITY                           |
C              |   DEPARTMENT OF INORGANIC CHEMISTRY         |
C              |   S-901 87  UMES, SWEDEN                    |
C              |   TELEPHONE: 46 - 90 16 52 64               |
C              +---------------------------------------------+
C
C
      IMPLICIT REAL*8(A-H,O-Z)
      COMMON /SGGA/ ASS(80), RLMAX, IFLG, IPOT(48), LKH(24), MX, N1(80)
      COMMON /SGGP/ B(12,99), B0(12), H, POTM, Y(80), IEL(12), KH(12),
     *MG, MS, MSOL, M1, NP
      COMMON /SGLN/ A(80,12), G(80), PI(24), L
      COMMON /SGNS/ NG, NSUM(250)
      COMMON /SGRD/ STEP, STOP, VER, IN, IND, IOUT, IRE, IUT, IXT,
     *KVALM, KVAL1, MCO, MV, NCFN
      COMMON /TALR/ TAL(99), ITAL(99)
      COMMON /TEXT/ IDENT(80)
      COMMON /TXT1/ INDFIL, ITEXT
      DIMENSION AT(12), A0(12), BLG(80), COL(80,99), JH(12), MF(10),
     *ML(10), MN(10), NL(80), NPR(80), NR(80), NY(99), TOT(12), VT(99)
      CHARACTER ICHR*1,IDENT*10,INDFIL*9,INBL*1,ITEXT*80,I1*119,I2*57
      LOGICAL LKH, N1, STEP, STOP, VER
      PARAMETER(EP1 = 1.E1,RN0 = 0.E0,RNA = 174.673E0,RT = 8.3144126E0*298.15E0,
     *INBL = ' ')
C
C     The two lines below have been added to the program. Whenever IOUT
C     is 6, WRITE statements will print to the screen.  READ statements
C     will always read on 5 since IN will always be 5.
C
      IN = 5
      IOUT = 6
C
C     The two lines below have been omitted from the program.
```

```
C
C     OPEN(IN,FILE = 'INPUT',STATUS = 'UNKNOWN')
C     OPEN(IOUT,FILE = 'OUTPUT',STATUS = 'UNKNOWN')
C
C     To execute or edit a file, the name of the file is entered,
C     but to create a file, a carriage return is required.
C
      WRITE (IOUT,597)
  597 FORMAT(' SOLGASWATER (INTERACTIVE VERSION)'/ 1X, 33('-')/ ' ENTER
     *THE NAME FOR THE FILE FROM WHICH DATA IS TO BE READ (OR CARRIAGE R
     *ETURN)')
      GO TO 805
  575 CALL READUT(-1,0)
      CLOSE(IND,ERR = 805)
  805 INDFIL(:1) = ' '
      READ (IN,104,END = 776) INDFIL
  104 FORMAT(A)
  776 IF (INDFIL(:1) .EQ. ' ') THEN
      REWIND IN
      STEP = .FALSE.
      ELSE
      NCFN = 8
C
C     Files are identified with names of a maximum of 7 characters.
C     A carriage return will be equivalent to '       '.
C
  803 NCFN = NCFN - 1
      IF (INDFIL(NCFN:NCFN) .EQ. ' ') GO TO 803
      IND = 10
      OPEN(IND,FILE = INDFIL(:NCFN),STATUS = 'OLD',ERR = 575)
      REWIND IND
      STEP = .TRUE.
      END IF
      IUT = 11
      OPEN(IUT,FILE = 'SGWNEW',STATUS = 'UNKNOWN')
      REWIND IUT
      IXT = 12
      H = LOG(EP1)
      KVAL1 = 10
      MPOT = 48
C
C     The real constant range is defaulted to exp(+/- 174.673),
C     which is the overflow/underflow limits of the computer.
C
      POTM = RNA
      RLMAX = EXP(POTM)
      I2 = '(8H A0 FOR ,A,3H = ,1PE12.5, X,8H AT FOR ,A,3H = ,E12.5)'
C
C     The two following WRITE-FORMAT statements can be executed any-
C     time during the running of the program: SUBROUTINE READIN will
C     then be called upon.
C
      WRITE (IOUT,740)
  740 FORMAT(' AT EACH INPUT OCCASION, ENTER EITHER DATA OR 1 OF THE FOL
     *LOWING:'/ ' H = HELP INSTRUCTIONS'/ ' Q = QUIT THE PROGRAM'/ '
     * SN = IDENTIFICATION FOR SPECIES N'/ ' RN = RETURN TO THE N P
     *REVIOUS STOP')
C
C     To execute a file, heading is is to be entered as 'XF99'.
C     To edit a file, heading is to be 'FN or XFN', where N < 99.
```

```
C     To create a file, heading can be anything < = 80 characters.
C
      IF (STEP) WRITE (IOUT,741) INDFIL(:NCFN), INDFIL(:NCFN)
741 FORMAT(' FN = FORWARD N LINES IN ', A/ ' XFN = FORWARD N LINES IN
   * ', A, ' WITH SUPPRESSED VERIFICATION')
615 STOP = .TRUE.
564 IF (STOP) WRITE (IOUT,742)
742 FORMAT(' ENTER HEADING')
      CALL READIN(-4,1,1,0,0)
      IF (IRE) 615,586,505
C
C     Anytime data is entered, SUBROUTINE READUT is called upon to
C     make sure the data is entered correctly. In this case, READUT
C     is called to make sure the HEADING is entered correctly.
C
580 CALL READUT(-3,0)
      GO TO 564
505 READ (IND,104,END = 580) ITEXT
      IF (VER) WRITE (IOUT,105) ITEXT
105 FORMAT(1X, A)
586 WRITE (IUT,104) ITEXT
C
C     The total # of components, L, is the number of atoms and/or
C     molecules used in defining the formation of all species. For
C     instance, in the Cu-S-X-H2O System, there are 5 components:
C     the copper atom, the sulfur atom, the xanthate molecule, the
C     proton, H +; and the electron, e-. However, even though H2O
C     takes part in some reactions, it is not considered to be a
C     component because it is the solvent and has unit activity.
C
565 IF (STOP) WRITE (IOUT,743)
743 FORMAT(' ENTER THE TOTAL NO. OF COMPONENTS (< = 12)')
      CALL READIN(-1,0,1,1,12)
      IF (IRE) 564,704,611
704 L = ITAL(1)
C
C     The total number of fluids, MP, is usually 1: H2O.
C
566 IF (STOP) WRITE (IOUT,744)
744 FORMAT(' ENTER THE TOTAL NO. OF FLUIDS (< = 9)')
      CALL READIN(0,0,1,1,9)
      IF (IRE) 565,705,566
705 MP = ITAL(1)
C
C     The total number of species in each fluid, MN(MP), is the
C     number of gases and solutes dissolved in each fluid, MP.
C
567 IF (STOP) WRITE (IOUT,745)
745 FORMAT(' ENTER THE TOTAL NO. OF SPECIES IN EACH FLUID (< = 80)')
      CALL READIN(1,0,MP,1,80)
      IF (IRE) 566,706,567
706 DO 799 M = 1, MP
799 MN(M) = ITAL(M)
800 MSOL = 80
      DO 548 M = 1, MP
548 MSOL = MSOL - MN(M)
      IF (MSOL) 543,653,679
543 CALL READUT(-1,0)
      GO TO 567
653 IF (IRE) 567,515,515
```

238

```
  679 ITEMP = MIN(MSOL,MPOT)
C
C     Because the program can handle only 80 species, the total number
C     of solids, MSOL, becomes a variable as calculated by ITEMP.  But
C     only a maximum of 48 solids can be considered at once.
C
  569 IF (STOP) WRITE (IOUT,746) ITEMP
  746 FORMAT(' ENTER THE TOTAL NO. OF SOLIDS (< =', I2, ')')
      CALL READIN(0,1,1,0,ITEMP)
      IF (IRE) 567,516,569
  516 MSOL = ITAL(1)
      GO TO 515
  680 CALL READUT(-3,0)
      GO TO 565
  611 READ (IND,*,END=680) L, MP, (MN(M), M = 1, MP), MSOL
      IF (VER) WRITE (IOUT,307) L, MP, (MN(M), M = 1, MP), MSOL
  307 FORMAT(20I4)
  515 WRITE (IUT,307) L, MP, (MN(M), M = 1, MP), MSOL
      MCO = MIN(9,L)
      MF(1) = 1
      ML(1) = MN(1)
      MV = MP + 1
      MN(MV) = MSOL
      DO 132 M = 2, MV
      ITEMP = ML(M-1)
      MF(M) = ITEMP + 1
  132 ML(M) = ITEMP + MN(M)
      MG = ML(MP)
      M1 = MF(MV)
      MS = ML(MV)
      IF (MSOL .EQ. 0) MV = MP
      IPOT(1) = 1
      IF (MSOL .GT. 1) THEN
      MX = 1
      DO 193 M = 2, MSOL
      IPOT(M) = 2*IPOT(M-1)
  193 MX = MX + IPOT(M)
      ELSE
      MX = MSOL
      END IF
      DO 48 J = L+1, 2*L
   48 LKH(J) = .TRUE.
      I = 1
      M = 1
  550 IF (.NOT. STOP) GO TO 528
C
C     Fluid species, solutes (ie. gaseous and aqueous species), are
C     identified first.  Solids (and, if any, liquids) are last.
C
      IF (M .LE. MP) THEN
      WRITE (IOUT,748) M
  748 FORMAT(' FLUID', I2)
      ELSE
      WRITE (IOUT,735)
  735 FORMAT(' SOLIDS')
      END IF
C
C     Identification of all species follows (ie. CU2S,CU + 2,S3-2,etc.).
C
  572 IF (STOP) WRITE (IOUT,749) I
```

```
 749 FORMAT(' ENTER IDENTIFICATION FOR SPECIES', I3)
 528 CALL READIN(-4,0,1,0,0)
     IF (IRE) 574,708,520
 574 IF (I .EQ. 1) THEN
     CALL READUT(1,1)
     GO TO 800
     END IF
     I = I - 1
     IF (I .LT. MF(M)) M = M - 1
     CALL READUT(L/10 + 1,L/10 + 1)
     GO TO 570
 708 IDENT(I) = ITEXT(:10)
C
C     The amounts of components, J, in a species, I, are known as the
C     formula units, A(I,J).  For example, if the components for the
C     CU-S-X-H2O system were CU +, S-2, X-, H +, and e-, CU2S would be
C     identified with the reaction  2CU +  + S-2 = CU2S.  Stoichiometry
C     of the reaction reveals the formula units 2,1,0,0,0.  However,
C     if the components were CU + 2, HS-, X-, H +, and e-, the reaction
C     would be  2CU + 2 + HS- + 2e = CU2S + H +  so the formula units
C     become 2,1,0,-1,2.  The formula unit for H + is negative since
C     it appears on the right side of the equation.
C
 568 IF (STOP) WRITE (IOUT,750) IDENT(I)
 750 FORMAT(' ENTER THE FORMULA UNITS FOR ', A)
     CALL READIN(2,0,L,-99,999)
     IF (IRE) 572,709,568
 709 DO 512 J = 1, L
 512 A(I,J) = TAL(J)
C
C     The logarithm (base 10) of the reaction constant, BLG(I), is
C     calculated from the free energies of species involved. Therefore
C     the log term can be changed if the components are changed.
C
 570 IF (STOP) WRITE (IOUT,751) IDENT(I)
 751 FORMAT(' ENTER LOG KF FOR ', A)
     CALL READIN(3,L/10 + 1,1,-300,300)
     IF (IRE) 568,531,570
 531 BLG(I) = TAL(1)
     GO TO 509
 796 CALL READUT(-3,0)
     GO TO 572
 520 READ (IND,*,END = 796) IDENT(I), BLG(I), (A(I,J), J = 1, L)
C
C     INTEGER*119 FUNCTION I1(I) is called to arrange and order the
C     data being stored in SGWNEW.
C
     IF (VER) WRITE (IOUT,I1(I)) IDENT(I), BLG(I), (A(I,J), J = 1, L)
 509 WRITE (IUT,I1(I)) IDENT(I), BLG(I), (A(I,J), J = 1, L)
     NL(I) = 11
  81 NL(I) = NL(I) - 1
     IF (NL(I) .GT. 1 .AND. IDENT(I)(NL(I):NL(I)) .EQ. ' ') GO TO 81
     G(I) = -H*BLG(I)
     I = I + 1
     IF (I .LE. ML(M)) GO TO 572
     M = M + 1
     IF (I - MS) 550,550,813
C
C     Species (and therefore components) are identified in a numerical
```

```
C      order which determines the specie number of a component, IEL(J).
C
 813 IF (STOP) WRITE (IOUT,752)
 752 FORMAT(' ENTER THE SPECIES NO. FOR EACH COMPONENT IN COMPONENT ORD
    *ER')
     CALL READIN(0,1,L,1,MS)
     IF (IRE) 556,710,563
 556 I = MS
     M = MV
     CALL READUT(L/10+1,L/10+1)
     GO TO 570
 710 DO 669 J = 1, L
     IF (A(ITAL(J),J) .EQ. RN0) THEN
     CALL READUT(-1,0)
     GO TO 813
     END IF
 669 IEL(J) = ITAL(J)
     GO TO 587
 681 CALL READUT(-3,0)
 563 IF (IRE .EQ. 2) GO TO 813
     READ (IND,*,END=681) (IEL(J), J = 1, L)
     IF (VER) WRITE (IOUT,307) (IEL(J), J = 1, L)
 587 WRITE (IUT,307) (IEL(J), J = 1, L)
     DO 167 I = 1, MG
 167 Y(I) = RLMAX
     IF (MSOL .GT. 0) THEN
     DO 215 I = M1, MS
     Y(I) = RN0
     ASS(I) = RN0
     DO 215 J = 1, L
 215 ASS(I) = ASS(I) + ABS(A(I,J))
     END IF
C
C      SUBROUTINE PLOTT is called upon to prepare a plot or a variety
C      of plots.  Parameters for NF, NH, NB, NZ, and NY are selected.
C
C      NF is 0  =   No plot of anykind
C      NH is 0  =   No N-Bar/Z plot (NB and NZ are 0 if NH is)
C      NY is 0  =   No Distribution, Logarithmic, or ETA plots
C
 502 CALL PLOTT
     IF (IRE) 813,8,8
   8 KVALM = KVAL1
C
C      IOUT is changed back to 6 once all the calculations have been
C      performed and the results printed to a disk file.  Information
C      is then printed back to the terminal.
C
C
C
C      The EXECUTION OPTION, KVAL1, controls execution of the program
C      by offering 10 commands to edit the input.  However, if KVAL1
C      is less than 7, then plotting can be considered as well.
C
 664 IOUT = 6
     IF (STOP) WRITE (IOUT,754)
 754 FORMAT(' ENTER EXECUTION OPTION')
 815 CALL READIN(4,1,1,1,40+L)
     IF (IRE) 663,718,585
 718 KVAL1 = ITAL(1)
```

```
      IF (KVAL1 .LE. 10 .OR. KVAL1. GT. 40) GO TO 645
      CALL READUT(-1,0)
      GO TO 815
  687 CALL READUT(-3,0)
      GO TO 664
  585 READ (IND,*,END=687) KVAL1
      IF (VER) WRITE (IOUT,307) KVAL1
  645 WRITE (IUT,307) KVAL1
      IF (KVAL1 .EQ. 2) GO TO 546
      IF (KVAL1 - 4) 519,532,503
  663 IF (KVALM .EQ. 0) THEN
      STOP = .TRUE.
      GO TO 664
      END IF
      KVAL1 = KVALM
      KVALM = 0
  659 IF (KVAL1 .GT. 5 .AND. KVAL1 .LE. 10) THEN
      CALL READUT(1,1)
      IF (KVAL1 .EQ. 6 .OR. KVAL1 .EQ. 8) GO TO 664
      IF (KVAL1 - 9) 503,503,502
      ELSE IF (KVAL1 .LT. 5) THEN
      J = L
      GO TO 603
      END IF
  503 IF (KVAL1 .EQ. 5 .OR. KVAL1 .EQ. 7) THEN
C
C     If a plot is to be prepared (ie. NF or NH and NY are not 0 and
C     KVAL1 is less than 7), SUBROUTINE PLOTT is called to enter the
C     dependent or independent variable, the number of curves in the
C     plot, the values to be plotted, and the grid parameters.
C
      CALL PLOTT
      IF (IRE .EQ. -1) GO TO 664
C
C     When KVAL1 is 8, specie identifications, log reaction constants,
C     and formula units will be printed to the screen or terminal.
C
      ELSE IF (IRE .EQ. 0 .AND. KVAL1 .EQ. 8) THEN
      WRITE (IOUT,106)
  106 FORMAT(/15X, 'LOG KF', 8X, 'STOICHIOMETRY MATRIX')
      DO 4 I = 1, MS
    4 WRITE (IOUT,I1(I)) IDENT(I), BLG(I), (A(I,J), J = 1, L)
C
C     When KVAL1 is 9, a starred specie (a specie which is excluded
C     from the mass balance) will be unstarred or vice-versa.  NSTAR
C     is the specie number which is being starred or unstarred.
C
      ELSE IF (KVAL1 .EQ. 9) THEN
  514 IF (STOP) WRITE (IOUT,702)
  702 FORMAT(' ENTER THE NO. FOR A SPECIES TO BE STARRED (+) OR UNSTARRE
     *D (-)')
  654 CALL READIN(-1,1,1,-MS,MS)
      IF (IRE) 664,504,523
  504 IF (ITAL(1) .NE. 0) GO TO 802
      CALL READUT(-1,0)
      GO TO 654
  544 CALL READUT(-3,0)
      GO TO 514
  523 READ (IND,*,END=544) ITAL(1)
      IF (VER) WRITE (IOUT,307) ITAL(1)
```

```
  802 WRITE (IUT,307) ITAL(1)
      IF (ITAL(1) .GT. 0) THEN
      IDENT(ITAL(1))(10:) = '*'
      ELSE
      IDENT(-ITAL(1))(10:) = ' '
      END IF
      ELSE IF (KVAL1 .EQ. 10) THEN
      CALL READUT(-4,0)
      ELSE IF (KVAL1 .GT. 40) THEN
      J = KVAL1 - 40
      IF (IRE) 603,161,161
      END IF
      GO TO 8
C
C      When KVAL1 is 2, the type of output, NPR(N), for a species,
C      NR(N), is selected.  The output will be in columns numbering
C      from 1 to NPRINT which is the total number of columns needed.
C
  546 N = 1
  648 IF (STOP) WRITE (IOUT,510) N
  510 FORMAT(' ENTER THE CONTENTS OF COLUMN', I3)
      CALL READIN(5,0,2,0,0)
      IF (N .EQ. 1) THEN
      IF (IRE) 522,714,571
      END IF
      IF (IRE) 591,714,648
  522 CALL READUT(1,1)
      GO TO 664
  591 N = N - 1
      GO TO 648
  714 IF (N .EQ. 1 .OR. ITAL(1) .NE. 99 .OR. ITAL(2) .NE. 99) THEN
      NPR(N) = ITAL(1)
      NR(N) = ITAL(2)
      IF (NPR(N) .EQ. 0 .AND. NR(N) .EQ. 0) GO TO 650
      IF (NPR(N).LT.-L.OR.NPR(N).EQ.0.OR.NPR(N).GT.11*MCO) THEN
      ELSE IF (NR(N) .GE. 0 .AND. NR(N) .LE. MS) THEN
      IF (NPR(N) .LT. 6) THEN
      IF (NR(N) .GT. 0) GO TO 650
      ELSE IF (NPR(N) .LT. 11) THEN
      IF (NR(N) .GT. 0 .AND. NR(N) .LE. L) GO TO 650
      ELSE
      IF (MOD(NPR(N),10) .LE. MCO .AND. NR(N) .LE. MV) GO TO 650
      END IF
      END IF
      CALL READUT(-1,0)
      GO TO 648
  650 N = N + 1
      IF (N .LE. 80) GO TO 648
      END IF
      NPRINT = N - 1
      IF (.NOT. STEP) GO TO 807
      READ (IND,*,END=683,ERR=807) JPRINT
      IF (JPRINT .GT. 9) CALL READUT(-2,JPRINT/10)
      GO TO 646
  683 CALL READUT(-3,0)
  571 IF (IRE - 1) 807,592,546
  592 READ (IND,*,END=683) NPRINT, (NPR(N), NR(N), N = 1, NPRINT)
      IF (VER) WRITE (IOUT,307) NPRINT, (NPR(N), NR(N), N = 1, NPRINT)
  807 JPRINT = NPRINT
```

```
646 WRITE (IUT,307) NPRINT, (NPR(N), NR(N), N = 1, NPRINT)
C
C     The number of equilibriums to be calculated, NPKT, is entered
C     but must be less than or equal to 99.
C
519 IF (STOP) WRITE (IOUT,757)
757 FORMAT(' ENTER THE TOTAL NO. OF EQUILS. TO BE CALCD. (< = 99)')
    CALL READIN(6,0,1,1,99)
    IF (IRE) 672,719,511
672 IF (KVAL1 .NE. 2) GO TO 522
    N = NPRINT
    CALL READUT(NPRINT/10 + 1,JPRINT/10 + 1)
    GO TO 648
719 NPKT = ITAL(1)
C
C     The number of groups in a predominance diagram plot, NPKY. If
C     NPKY is 0 then no diagram will be plotted.  In running the
C     program, NPKY was set equal to 0 since plots were not needed.
C
579 IF (STOP) WRITE (IOUT,578)
578 FORMAT(' ENTER THE TOTAL NO. OF GROUPS IN THE PREDOMINANCE DIAGRAM
    * (< = 99)')
    CALL READIN(0,0,1,0,99)
    IF (IRE) 519,715,579
715 NPKY = ITAL(1)
    IF (.NOT. STEP) GO TO 674
    READ (IND,*,END = 688,ERR = 674) JPKT
    GO TO 539
688 CALL READUT(-3,0)
    IF (IRE) 674,674,519
511 READ (IND,*,END = 688) NPKT, NPKY
    IF (VER) WRITE (IOUT,307) NPKT, NPKY
674 JPKT = NPKT
539 WRITE (IUT,307) NPKT, NPKY
C
C     The initial and subsequent (after each equilibrium calculation)
C     amounts of components, J, are controlled in 11 ways: KH(J).
C
661 IF (STOP) WRITE (IOUT,755)
755 FORMAT(' ENTER THE VARIATION IN TC OR LOG A FOR EACH COMPONENT IN
    *COMPONENT ORDER')
    CALL READIN(10,0,L,1,11)
    IF (IRE) 579,671,613
671 DO 670 J = 1, L
670 KH(J) = ITAL(J)
    IF (.NOT. STEP) GO TO 673
    READ (IND,*,END = 689,ERR = 673) (JH(J), J = 1, L)
    GO TO 537
689 CALL READUT(-3,0)
613 IF (IRE - 1) 673,525,661
525 READ (IND,*,END = 689) (KH(J), J = 1, L)
    IF (VER) WRITE (IOUT,307) (KH(J), J = 1, L)
673 DO 660 J = 1, L
660 JH(J) = KH(J)
537 WRITE (IUT,307) (KH(J), J = 1, L)
    IF (KVAL1 .EQ. 1) NPRINT = 0
    ITIT = 0
    JTIT = 0
    DO 131 J = 1, L
    IF (JH(J) .EQ. 1 .OR. JH(J) .EQ. 8) THEN
```

```
      JH(J) = (JPKT + 5)/6
      ELSE
      IF (JH(J) .EQ. 4 .OR. JH(J) .EQ. 5) JTIT = JH(J)
      JH(J) = 1
      END IF
      IF (KH(J) .LT. 8) THEN
      LKH(J) = .TRUE.
      IF (KH(J) .EQ. 4 .OR. KH(J) .EQ. 5) ITIT = KH(J)
      ELSE
      LKH(J) = .FALSE.
      END IF
  131 CONTINUE
  532 NS = 0
      IF (ITIT - 4) 533,535,538
  684 CALL READUT(-3,0)
C
C     If KH(J) is 4, volumetric titrations vary the concentration
C     of a component, J. The initial titration volume, V0, and the
C     subsequent titration volumes, VT(N), vary.
C
  535 IF (STOP) WRITE (IOUT,760)
  760 FORMAT(' ENTER THE INITIAL VOL.')
      CALL READIN(-3,0,1,0,0)
      IF (IRE) 527,724,557
  724 V0 = TAL(1)
  626 IF (STOP) WRITE (IOUT,761) NPKT
  761 FORMAT(' ENTER THE TOTAL VOLS. ADDED (', I2, ' VALUES)')
      CALL READIN(-2,0,NPKT,0,0)
      IF (IRE) 535,725,626
  725 DO 716 N = 1, NPKT
  716 VT(N) = TAL(N)
      GO TO 530
  557 READ (IND,*,END=684) V0, (VT(N), N = 1, NPKT)
      IF (VER) WRITE (IOUT,314) V0, (VT(N), N = 1, NPKT)
  314 FORMAT(6(1X, G12.6))
  530 WRITE (IUT,314) V0, (VT(N), N = 1, NPKT)
      IF (IRE) 533,533,576
C
C     If KH(J) is 5, volumetric titrations vary the concentration
C     of a component, J. The initial volume, V0, and the subsequent
C     and constant titration volumes, VT(N), are entered.
C
  538 IF (STOP) WRITE (IOUT,762)
  762 FORMAT(' ENTER THE INITIAL VOL. AND THE CONST. VOL. ADDN.')
      CALL READIN(-3,0,2,0,0)
      IF (IRE) 527,726,666
  726 V0 = TAL(1)
  533 IF (STEP) THEN
      IF (JTIT .EQ. 4) CALL READUT(-2,JPKT/6+1)
      IF (JTIT .EQ. 5) CALL READUT(-2,1)
      END IF
      IF (ITIT - 4) 576,576,508
  690 CALL READUT(-3,0)
  666 IF (IRE .EQ. 2) GO TO 538
      READ (IND,*,END=690) V0, TAL(2)
      IF (VER) WRITE (IOUT,314) V0, TAL(2)
  508 WRITE (IUT,314) V0, TAL(2)
      VT(1) = RN0
      DO 18 N = 2, NPKT
   18 VT(N) = VT(N-1) + TAL(2)
```

```
576 J = 1
161 IF (.NOT. STOP) THEN
C
C      If KH(J) is 1, the total concentration varies irregularly.
C
       ELSE IF (KH(J) .EQ. 1) THEN
       WRITE (IOUT,756) IDENT(IEL(J))(:NL(IEL(J))), NPKT
756 FORMAT(' ENTER TC FOR ', A, ' (', I2, ' VALUES)')
C
C      If KH(J) is 2, the total concentration is always constant.
C
       ELSE IF (KH(J) .EQ. 2) THEN
       WRITE (IOUT,758) IDENT(IEL(J))
758 FORMAT(' ENTER TC FOR ', A)
C
C      If KH(J) is 3, the concentration varies by a constant increment.
C
       ELSE IF (KH(J) .EQ. 3) THEN
       WRITE (IOUT,766) IDENT(IEL(J))
766 FORMAT(' ENTER THE INITIAL TC VALUE AND THE CONST. INCREMENT FOR '
     *, A)
       ELSE IF (KH(J) .LT. 6) THEN
       WRITE (IOUT,768) IDENT(IEL(J))
768 FORMAT(' ENTER THE TC VALUES IN TITRANT AND TITRATOR FOR ', A)
C
C      If KH(J) is 6, log of concentration varies by constant increment.
C
       ELSE IF (KH(J) .LT. 8) THEN
       WRITE (IOUT,534) IDENT(IEL(J))
534 FORMAT(' ENTER THE INITIAL LOG TC VALUE AND THE CONST. INCREMENT F
     *OR ', A)
C
C      If KH(J) is 8, the log of total concentration varies irregularly.
C
       ELSE IF (KH(J) .EQ. 8) THEN
       WRITE (IOUT,536) IDENT(IEL(J))(:NL(IEL(J))), NPKT
536 FORMAT(' ENTER LOG A FOR ', A, ' (', I2, ' VALUES)')
C
C      If KH(J) is 9, the log of total concentration is always constant.
C
       ELSE IF (KH(J) .EQ. 9) THEN
       WRITE (IOUT,764) IDENT(IEL(J))
764 FORMAT(' ENTER LOG A FOR ', A)
       ELSE
C
C      If KH(J) is 10, log of concentration has a constant increment.
C
       WRITE (IOUT,767) IDENT(IEL(J))
767 FORMAT(' ENTER THE INITIAL LOG A VALUE AND THE CONST. INCREMENT FO
     *R ', A)
       END IF
       IF (KH(J) .EQ. 1 .OR. KH(J) .EQ. 8) THEN
       CALL READIN(-2,JH(J),NPKT,0,0)
       IF (IRE) 582,720,617
720 DO 545 N = 1, NPKT
545 B(J,N) = TAL(N)
       GO TO 577
617 IF (IRE .EQ. 2) GO TO 161
       READ (IND,*,END=676) (B(J,N), N = 1, NPKT)
       IF (VER) WRITE (IOUT,314) (B(J,N), N = 1, NPKT)
```

```
577 WRITE (IUT,314) (B(J,N), N = 1, NPKT)
    ELSE IF (KH(J) .EQ. 2 .OR. KH(J) .EQ. 9) THEN
    CALL READIN(-2,JH(J),1,0,0)
    IF (IRE) 582,542,618
618 READ (IND,*,END=676) TAL(1)
    IF (VER) WRITE (IOUT,314) TAL(1)
542 WRITE (IUT,314) TAL(1)
    DO 160 N = 1, NPKT
160 B(J,N) = TAL(1)
    ELSE IF (KH(J) .EQ. 3 .OR. KH(J) .EQ. 6 .OR. KH(J) .EQ. 10) THEN
    CALL READIN(-2,JH(J),2,0,0)
    IF (IRE) 582,722,621
722 B(J,1) = TAL(1)
    GO TO 529
621 IF (IRE .EQ. 2) GO TO 161
    READ (IND,*,END=676) B(J,1), TAL(2)
    IF (VER) WRITE (IOUT,314) B(J,1), TAL(2)
529 WRITE (IUT,314) B(J,1), TAL(2)
    DO 165 N = 2, NPKT
165 B(J,N) = B(J,N-1) + TAL(2)
    ELSE IF (KH(J) .LT. 6) THEN
    CALL READIN(-2,JH(J),2,0,0)
    IF (IRE) 582,723,622
723 A0(J) = TAL(1)
    AT(J) = TAL(2)
    GO TO 642
622 IF (IRE .EQ. 2) GO TO 161
    READ (IND,*,END=676) A0(J), AT(J)
    IF (VER) WRITE (IOUT,314) A0(J), AT(J)
642 WRITE (IUT,314) A0(J), AT(J)
    TEMP = A0(J)*V0
    DO 32 N = 1, NPKT
 32 B(J,N) = (AT(J)*VT(N) + TEMP)/(V0 + VT(N))
    ELSE
    CALL READIN(-2,JH(J),2,0,0)
    IF (IRE) 582,727,624
727 STEPY = TAL(2)
    GO TO 649
624 IF (IRE .EQ. 2) GO TO 161
    READ (IND,*,END=676) TAL(1), STEPY
    IF (VER) WRITE (IOUT,314) TAL(1), STEPY
649 WRITE (IUT,314) TAL(1), STEPY
    KHJ = J
    DO 191 N = 1, NPKT
191 B(J,N) = TAL(1)
    END IF
    IF (KVAL1 .GT. 40) GO TO 555
    J = J + 1
    IF (J - L) 161,161,555
582 IF (KVAL1 .GT. 40) GO TO 522
    IF (J .EQ. 1) THEN
    IF (ITIT - 4) 678,703,667
    END IF
    J = J - 1
603 IF (KH(J) .EQ. 1 .OR. KH(J) .EQ. 8) THEN
    CALL READUT((NPKT+5)/6,JH(J))
    ELSE
    CALL READUT(1,JH(J))
    END IF
    GO TO 161
```

```
678 IF (STEP) THEN
    IF (JTIT .EQ. 4) CALL READUT(0,JPKT/6 + 1)
    IF (JTIT .EQ. 5) CALL READUT(0,1)
    END IF
    CALL READUT(1,1)
527 IF (KVAL1 - 4) 661,664,664
703 IF (NPKT .GT. 5) CALL READUT(NPKT/6,0)
667 IF (STEP.AND.JPKT.GT.5.AND.JTIT.EQ.4) CALL READUT(0,JPKT/6)
    CALL READUT(1,1)
    IF (ITIT - 4) 626,626,538
676 CALL READUT(-3,0)
    GO TO 161
555 STOP = .TRUE.
C
C     Because the program was editted so that the output would print
C     to a disk file, the following line had to be changed. It used to
C     to read 'RESULTS ON THE TERMINAL?'
C
    WRITE (IOUT,770)
770 FORMAT(' RESULTS SENT TO THE DISK FILE? (Y OR N OR R)')
595 READ (IN,104,END = 693) ICHR
    IF (ICHR .EQ. 'N') GO TO 8
    IF (ICHR .EQ. 'R') GO TO 659
    IF (ICHR .EQ. 'Y') GO TO 34
693 CALL READUT(-1,0)
    GO TO 595
 34 NP = 0
C
C     IOUT is changed to 10 when all user information has been printed
C     to the terminal and all data has been entered. The results of
C     the calculations can then be stored on a disk file.
C
C     The following statement, IOUT = 10, was added to the program.
C
    IOUT = 10
    NS = NS + 1
 27 NP = NP + 1
C
C     SUBROUTINE GASOL is called to minimize the free energy.
C
    CALL GASOL
    IF (NG .LT. 251) THEN
    DO 17 J = 1, L
    IF (LKH(J) .AND. MSOL .EQ. 0) THEN
    TOT(J) = B0(J)
    ELSE
    TOT(J) = RN0
    DO 50 I = 1, MG
 50 TOT(J) = TOT(J) + A(I,J)*Y(I)
    B0(J) = TOT(J)
    IF (MSOL .GT. 0) THEN
    DO 133 I = M1, MS
133 B0(J) = B0(J) + A(I,J)*Y(I)
    END IF
    END IF
 17 CONTINUE
    IF (NPRINT .GT. 0) THEN
    DO 150 N = 1, NPRINT
    COL(N,NP) = RN0
    J = NPR(N)
```

```
      IF (J .LT. 0) THEN
      I = NR(N)
      J = -J
C
C     Manipulation of the completed calculations into desired results
C     and storing those results into the specified columns follows.
C
      IF (I.LT.M1.AND.TOT(J).NE.RN0) COL(N,NP)=A(I,J)*Y(I)/TOT(J)
      ELSE IF (J .EQ. 0) THEN
      COL(N,NP) = VT(NP)
      ELSE IF (J .EQ. 1) THEN
      COL(N,NP) = Y(NR(N))
      ELSE IF (J .EQ. 2) THEN
      IF (Y(NR(N)) .GT. RN0) COL(N,NP) = LOG10(Y(NR(N)))
      ELSE IF (J .EQ. 3) THEN
      IF (.NOT. N1(NR(N))) THEN
      TEMP = ALN(NR(N))
      IF (ABS(TEMP) .LT. POTM) COL(N,NP) = EXP(TEMP)
      END IF
      ELSE IF (J .EQ. 4) THEN
      IF (.NOT. N1(NR(N))) COL(N,NP) = ALN(NR(N))/H
      ELSE IF (J .EQ. 5) THEN
      IF (Y(NR(N)) .GT. RN0) COL(N,NP) = LOG10(RT*Y(NR(N)))
      ELSE IF (J .EQ. 6) THEN
      IF (TOT(NR(N)) .NE. RN0) COL(N,NP) = LOG10(ABS(TOT(NR(N))))
      ELSE IF (J .EQ. 7) THEN
      COL(N,NP) = TOT(NR(N))
      ELSE IF (J .EQ. 8) THEN
      IF (B0(NR(N)) .NE. RN0) COL(N,NP) = LOG10(ABS(B0(NR(N))))
      ELSE IF (J .EQ. 9) THEN
      COL(N,NP) = B0(NR(N))
      ELSE IF (J .EQ. 10) THEN
      IF (TOT(NR(N)).GT.RN0) COL(N,NP)=LOG10(TOT(NR(N))/Y(IEL(NR(N))))
      ELSE
      K = J/10
      J = J - 10*K
      IF (NR(N) .EQ. 0) THEN
      IF (B0(J) .NE. RN0) COL(N,NP) = (B0(K) - Y(IEL(K)))/B0(J)
      ELSE
      TEMP = RN0
      TEMP1 = RN0
      DO 145 I = MF(NR(N)), ML(NR(N))
      IF (I .NE. IEL(K) .AND. A(I,J) .NE. RN0) TEMP = TEMP + A(I,K)*Y(I)
  145 TEMP1 = TEMP1 + A(I,J)*Y(I)
      IF (TEMP1 .NE. RN0) COL(N,NP) = TEMP/TEMP1
      END IF
      END IF
  150 CONTINUE
      END IF
      IF (IFLG .EQ. 2) THEN
      NY(NP) = -1
      ELSE
      NY(NP) = 0
      END IF
      ELSE
      NY(NP) = NG - 250
      END IF
      IF (NP .LT. NPKT) GO TO 27
      IF (NPRINT .GT. 0) THEN
      WRITE (IOUT,104) INBL
```

```
      DO 144 N = 1, NPRINT
      J = NPR(N)
      IF (J .LT. 0) THEN
      I = IEL(-J)
C
C     A list of column number vs the quantity calculated is printed.
C
      WRITE (IOUT,251) N, IDENT(I)(:NL(I)), IDENT(NR(N))
  251 FORMAT(' COL', I3, '   FRACTION OF ', A, ' PRESENT IN ', A)
      ELSE IF (J .EQ. 0) THEN
      WRITE (IOUT,113) N
  113 FORMAT(' COL', I3, '   TOTAL VOLUME ADDED IN TITRATION')
      ELSE IF (J .EQ. 1) THEN
      WRITE (IOUT,103) N, IDENT(NR(N))
  103 FORMAT(' COL', I3, '   C FOR ', A)
      ELSE IF (J .EQ. 2) THEN
      WRITE (IOUT,125) N, IDENT(NR(N))
  125 FORMAT(' COL', I3, '   LOG C FOR ', A)
      ELSE IF (J .EQ. 3) THEN
      WRITE (IOUT,124) N, IDENT(NR(N))
  124 FORMAT(' COL', I3, '   A FOR ', A)
      ELSE IF (J .EQ. 4) THEN
      WRITE (IOUT,120) N, IDENT(NR(N))
  120 FORMAT(' COL', I3, '   LOG A FOR ', A)
      ELSE IF (J .EQ. 5) THEN
      WRITE (IOUT,107) N, IDENT(NR(N))
  107 FORMAT(' COL', I3, '   LOG (P/KPA) FOR ', A)
      ELSE IF (J .EQ. 6) THEN
      WRITE (IOUT,116) N, IDENT(IEL(NR(N)))
  116 FORMAT(' COL', I3, '   LOG ABS(TF) FOR ', A)
      ELSE IF (J .EQ. 7) THEN
      WRITE (IOUT,114) N, IDENT(IEL(NR(N)))
  114 FORMAT(' COL', I3, '   TF FOR ', A)
      ELSE IF (J .EQ. 8) THEN
      WRITE (IOUT,108) N, IDENT(IEL(NR(N)))
  108 FORMAT(' COL', I3, '   LOG ABS(TC) FOR ', A)
      ELSE IF (J .EQ. 9) THEN
      WRITE (IOUT,109) N, IDENT(IEL(NR(N)))
  109 FORMAT(' COL', I3, '   TC FOR ', A)
      ELSE IF (J .EQ. 10) THEN
      WRITE (IOUT,123) N, IDENT(IEL(NR(N)))
  123 FORMAT(' COL', I3, '   ETA FOR ', A)
      ELSE
      K = J/10
      I = IEL(J-10*K)
      IF (NR(N) .EQ. 0) THEN
      WRITE (IOUT,252) N, IDENT(IEL(K))(:NL(IEL(K))), IDENT(I)(:NL(I))
  252 FORMAT(' COL',I3,'   AVERAGE NUMBER OF ',A,' BOUND PER ',A,' (Z)')
      ELSE
      WRITE (IOUT,101) N, IDENT(IEL(K))(:NL(IEL(K))), IDENT(I)(:NL(I)),
     *NR(N)
  101 FORMAT(' COL', I3, '   AVERAGE NUMBER OF ', A, ' BOUND PER ', A,
     *' IN FLUID', I2, ' (N-BAR)')
      END IF
      END IF
  144 CONTINUE
      WRITE (IOUT,104) INBL
      IF (ITIT .GT. 0) WRITE (IOUT,110) V0
  110 FORMAT(' V0 =', 1PE12.5)
      DO 24 J = 1, L
```

```fortran
      IF (KH(J) .EQ. 2) THEN
      WRITE (IOUT,253) IDENT(IEL(J))(:NL(IEL(J))), B(J,1)
  253 FORMAT(' TC FOR ', A, ' = ', 1PE12.5)
      ELSE IF (KH(J) .EQ. 4 .OR. KH(J) .EQ. 5) THEN
      I = IEL(J)
      WRITE (I2(29:30),102) 11-NL(I)
  102 FORMAT(I2)
      WRITE (IOUT,I2) IDENT(I)(:NL(I)), A0(J), IDENT(I)(:NL(I)), AT(J)
      ELSE IF (KH(J) .EQ. 9 .OR. KH(J) .EQ. 11) THEN
      WRITE (IOUT,112) IDENT(IEL(J))(:NL(IEL(J))), B(J,1)
  112 FORMAT(' LOG A FOR ', A, ' = ', 1PE12.5)
      END IF
   24 CONTINUE
C
C     The following 7 statements were added to the program to convert
C     electron concentration to volts vs. standard hydrogen electrode.
C     To do that, the identification of the electron must be E-.  The
C     number -.0591562617 comes from -RT(ln10)/F where R is the gas
C     constant (8.314 J/mole-K), T is temperature (298.15 K), and F is
C     Faraday's constant (96,485 Coul/mole). Recall that Volt = J/Coul.
C
      DO 998 J = 1, NPRINT
      IF (INDEX(IDENT(NR(J)),'E-') .GT. 0) THEN
      DO 997 N = 1, NPKT
      COL(J,N) = COL(J,N)*(-.0591562617)
  997 CONTINUE
      END IF
  998 CONTINUE
      NPR1 = 1
    2 NPR2 = NPR1 + 7
      IF (NPR2 .GT. NPRINT) NPR2 = NPRINT
C
C     The next two lines print out the column number above each column.
C
      WRITE (IOUT,119) (N, N = NPR1, NPR2)
  119 FORMAT(/8('    COL', I3, :))
C
C     The following two lines were added to the program to print out
C     the identification of a species at the top of the column which
C     will contain the calculated quantity of that species.
C
      WRITE (IOUT,999) (IDENT(NR(N)), N = NPR1, NPR2)
  999 FORMAT(8(A, :))
C
C     The results are printed out according to the following:
C
C     1) If NY(N) .LE. 0 and .NE. -1 then results are printed.
C     2) If NY(N) .EQ. -1 then results are printed as well but
C        the composition was numerically unstable.
C     3) Otherwise, no equilibrium composition was obtained.
C
      DO 184 N = 1, NPKT
      IF (NY(N) .LE. 0) THEN
      IF (NY(N) .EQ. -1) WRITE (IOUT,121)
  121 FORMAT(' THE COMPOSITION GIVEN BELOW IS NUMERICALLY UNSTABLE')
      WRITE (IOUT,111) (COL(J,N), J = NPR1, NPR2)
  111 FORMAT(8F10.5)
      ELSE
      WRITE (IOUT,118)
  118 FORMAT(' THE EQUILIBRIUM COMPOSITION HAS NOT BEEN OBTAINED')
```

```
      IF (NY(N) .EQ. 1) THEN
      WRITE (IOUT,122)
  122 FORMAT(' 250 DIFFERENT PHASE COMBINATIONS HAVE BEEN CONSIDERED')
      ELSE
      WRITE (IOUT,117)
  117 FORMAT(' ALL POSSIBLE PHASE COMBINATIONS HAVE BEEN CONSIDERED')
      END IF
      END IF
  184 CONTINUE
      IF (NPR2 .LT. NPRINT) THEN
      NPR1 = NPR1 + 8
C
C     Return to statement 2 to continue printing results in columns.
C
      GO TO 2
      END IF
      END IF
C
C     If NS > NPKY, return to statement 8 to enter EXECUTION OPTION
C     where NS is a counter for the number of data groups calculated
C     and NPKY is the total number of groups to be calculated. The
C     calculations will be finished when this statement is true.
C
      IF (NS .GE. NPKY) GO TO 8
      TEMP = B(KHJ,1) + STEPY
      DO 43 N = 1, NPKT
   43 B(KHJ,N) = TEMP
C
C
C     Return to statement 34 to execute another data group which must
C     be in the same data file that was called on in the start.
C
      GO TO 34
      END
C
C
C     INTEGER*119 FUNCTION I1(I) is called to order the data in SGWNEW.
C
C     " """"",A,""""""  =  the specie identification
C               G12.6  =  log of reaction constant
C     F5.1,..........,F5.1  =  formula units
C
C
      CHARACTER*119 FUNCTION I1(I)
      IMPLICIT REAL*8(A-H,O-Z)
      COMMON /SGLN/ A(80,12), G(80), PI(24), L
      PARAMETER(EP1 = 1.E1,EP2 = 1.E2,RN0 = 0.E0,RN1 = 1.E0)
      I1 = '(" """"",A,"""""",1X,G12.6,1X,F5.1,1X,F5.1,1X,F5.1,1X,F5.1
     *,1X,F5.1,1X,F5.1,1X,F5.1,1X,F5.1,1X,F5.1/1X,F5.1,1X,F5.1,1X,F5.1)'
      DO 227 J = 1, L
      IF (A(I,J).EQ.INT(A(I,J)).OR.A(I,J).LT.-EP1.OR.A(I,J).GT.EP2) THEN
      ELSE IF (A(I,J) .GT. RN0 .AND. A(I,J) .LT. RN1) THEN
      ITEMP = 8*J + 22
      I1(ITEMP:ITEMP) = '4'
      ELSE IF (A(I,J) .GT. -RN1 .AND. A(I,J) .LT. EP1) THEN
      ITEMP = 8*J + 22
      I1(ITEMP:ITEMP) = '3'
      ELSE
      ITEMP = 8*J + 22
      I1(ITEMP:ITEMP) = '2'
```

```
      END IF
  227 CONTINUE
      RETURN
      END
C
C
C
C
C     SUBROUTINE GASOL is the free energy minimization routine.
C
C
C
      SUBROUTINE GASOL
      IMPLICIT REAL*8(A-H,O-Z)
      COMMON /GAYB/ YMIN, ISOL(13), LJ(12), MSA
      COMMON /SGGA/ ASS(80), RLMAX, IFLG, IPOT(48), LKH(24), MX, N1(80)
      COMMON /SGGP/ B(12,99), B0(12), H, POTM, Y(80), IEL(12), KH(12),
     *MG, MS, MSOL, M1, NP
      COMMON /SGLN/ A(80,12), G(80), PI(24), L
      COMMON /SGNS/ NG, NSUM(250)
      COMMON /TALR/ YMAX(99), INR(99)
      COMMON /TEXT/ IDENT(80)
      DIMENSION AKT(80),MNR(80),NRI(80),N0(80),OPI(24),R(24,25),YF(80)
      CHARACTER*10 IDENT
      LOGICAL LJ,LJ0(12),LKH,LSGN(12),NEG,N0,N00(80),N1,N10(80),SLAM
      PARAMETER(EM1 = 1.E-1,EP2 = 1.E2,EM5 = 1.E-5,EM6 = 1.E-6,EM8 = 1.E-8,EP8 =
     *1.E8,RN0 = 0.E0,RN1 = 1.E0,RN2 = 2.E0,RN8 = 8.E0)
C
C     The equilibrium composition is calculated.
C
      MS1 = MG
      DO 1 J = 1, L
      B0(J) = B(J,NP)
      IF (KH(J) .GT. 5) THEN
      TEMP = H*B0(J)
      IF (LKH(J)) THEN
      B0(J) = EXP(TEMP)
      ELSE
      PI(J) = TEMP/A(IEL(J),J)
      END IF
      END IF
    1 LJ0(J) = .TRUE.
C
C     The species in the system are considered for mass balancing:
C
C     1) A starred specie will not take part in mass balance, and
C     2) A solute withdrawn from consideration will not either.
C
      DO 75 I = 1, MS
   75 N10(I) = .FALSE.
   72 L0 = 0
      DO 22 J = 1, L
      LSGN(J) = .FALSE.
      IF (LJ0(J) .AND. LKH(J)) THEN
      L0 = L0 + 1
      TEMP = RN0
      DO 49 I = 1, MS
      IF (N10(I) .OR. IDENT(I)(10:) .EQ. '*' .OR. A(I,J) .EQ. RN0) THEN
      ELSE IF (TEMP*A(I,J) .EQ. RN0) THEN
      TEMP = A(I,J)
      ELSE IF (TEMP*A(I,J) .LT. RN0) THEN
```

```
     LSGN(J) = .TRUE.
     GO TO 22
     END IF
 49 CONTINUE
     IF (B0(J) .EQ. RN0) THEN
     DO 30 I = 1, MS
 30 IF (A(I,J) .NE. RN0) N10(I) = .TRUE.
     LJ0(J) = .FALSE.
     GO TO 72
     END IF
     END IF
 22 CONTINUE
     DO 225 I = 1, MS
     IF (N10(I) .OR. IDENT(I)(10:) .EQ. '*') THEN
     Y(I) = RN0
     N00(I) = .TRUE.
     ELSE
     YMAX(I) = RLMAX
     DO 204 J = 1, L
     IF (LKH(J) .AND. .NOT. LSGN(J) .AND. A(I,J) .NE. RN0) THEN
     TEMP = B0(J)/A(I,J)
     IF (TEMP .LT. YMAX(I)) YMAX(I) = TEMP
     END IF
204 CONTINUE
     N00(I) = .FALSE.
     END IF
225 CONTINUE
     DO 175 J = 1, L
     IF (LSGN(J)) THEN
     TEMP1 = B0(J)
     TEMP = -TEMP1
     DO 178 I = 1, MS
     IF (A(I,J) .GT. RN0 .AND. TEMP .LT. RLMAX) THEN
     IF (YMAX(I) .LT. RLMAX) THEN
     TEMP = TEMP + A(I,J)*YMAX(I)
     ELSE
     TEMP = RLMAX
     END IF
     ELSE IF (A(I,J) .LT. RN0 .AND. TEMP1 .LT. RLMAX) THEN
     IF (YMAX(I) .LT. RLMAX) THEN
     TEMP1 = TEMP1 - A(I,J)*YMAX(I)
     ELSE
     TEMP1 = RLMAX
     END IF
     END IF
178 CONTINUE
     IF (TEMP .LT. RLMAX) THEN
     DO 179 I = 1, MS
     IF (A(I,J) .LT. RN0) THEN
     TEMP2 = -TEMP/A(I,J)
     IF (TEMP2 .LT. YMAX(I)) YMAX(I) = TEMP2
     END IF
179 CONTINUE
     END IF
     IF (TEMP1 .LT. RLMAX) THEN
     DO 187 I = 1, MS
     IF (A(I,J) .GT. RN0) THEN
     TEMP2 = TEMP1/A(I,J)
     IF (TEMP2 .LT. YMAX(I)) YMAX(I) = TEMP2
     END IF
```

```
187 CONTINUE
    END IF
    END IF
175 CONTINUE
    IF (MSOL .GT. 0) THEN
    DO 183 I = M1, MS
    INR(I) = I
    IF (.NOT. N00(I)) THEN
    DO 189 J = 1, L
    IF (LKH(J) .AND. A(I,J) .NE. RN0) GO TO 183
189 CONTINUE
    Y(I) = RN0
    N00(I) = .TRUE.
    END IF
183 NRI(I) = I - MG
    END IF
    I = 1
 87 IF (N00(I)) THEN
    ELSE IF (YMAX(I) .EQ. RLMAX) THEN
    DO 195 J = 1, L
    IF (LKH(J) .AND. A(I,J) .NE. RN0) THEN
    IF (Y(I) .EQ. RLMAX) Y(I) = RN0
    GO TO 199
    END IF
195 CONTINUE
    TEMP = -G(I)
    DO 99 J = 1, L
 99 IF (.NOT. LKH(J)) TEMP = TEMP + A(I,J)*PI(J)
    Y(I) = EXP(MAX(MIN(TEMP,POTM),-POTM))
    END IF
199 I = I + 1
    IF (I .LE. MG) GO TO 87
    IS = -1
    NG = 0
C
C      A number specifying the solid phase combination is calculated.
C      (Solid 1 = 1, Solid 2 = 2,....Solid MPOT = 2**(MPOT - 1)).
C
 55 NG = NG + 1
    IF (NG .EQ. 251) RETURN
    MSA = 0
    NSUM(NG) = 0
    IF (MSOL .GT. 0) THEN
    DO 52 K = M1, MS
    IF (Y(INR(K)) .NE. RN0) THEN
    MSA = MSA + 1
    ISOL(MSA) = INR(K)
    NSUM(NG) = NSUM(NG) + IPOT(K-MG)
    END IF
 52 CONTINUE
    END IF
    IF (NSUM(NG) .LE. IS) GO TO 86
    IF (MSA .LE. L0) THEN
    IF (NSUMCH(NSUM(NG)) - NG) 86,129,129
    END IF
216 IF (MSA .GT. 0) THEN
    ITEMP = 0
    DO 243 N = 1, MSA
    IF (NSUMCH(NSUM(NG)-IPOT(NRI(ISOL(N)))) .GE. NG) THEN
    ITEMP = ISOL(N)
```

```
      IF (Y(ITEMP)) 137,137,243
      END IF
243 CONTINUE
      IF (ITEMP) 59,59,137
137 DO 281 N = 1, MSA
281 Y(ISOL(N)) = RN1
      Y(ITEMP) = RN0
      GO TO 55
      END IF
C
C      The solids are ranked and a solid or solid phase combination
C      which has not been previously considered is chosen.
C
  59 NG = NG + 1
      IF (NG .EQ. 251) RETURN
  86 IF (MSOL .EQ. 1 .OR. MS1 .EQ. MG) GO TO 66
      DO 206 K = M1, MS
206 MNR(K) = INR(K)
212 N = M1 + 1
      DO 211 K = M1, MS1
      IF (AKT(K) .LT. AKT(K+1)) THEN
      N = K + 1
      TEMP = AKT(K)
      AKT(K) = AKT(N)
      AKT(N) = TEMP
      ITEMP = INR(K)
      INR(K) = INR(N)
      INR(N) = ITEMP
      END IF
211 CONTINUE
      MS1 = N - 2
      IF (MS1 .GT. MG) GO TO 212
      DO 207 K = M1, MS
207 NRI(INR(K)) = K - MG
      IS = -1
      N = 0
151 N = N + 1
      IF (N .EQ. NG) GO TO 66
      IF (NSUM(N) .EQ. 0) GO TO 151
      ITEMP1 = NSUM(N)
      NSUM(N) = 0
      M = 0
  25 M = M + 1
      ITEMP = ITEMP1/IPOT(M)
      IF (ITEMP/2*2 .EQ. ITEMP) GO TO 25
      NSUM(N) = NSUM(N) + IPOT(NRI(MNR(M+MG)))
      IF (ITEMP - 1) 151,151,25
  76 IS = IS + IPOT(M) - 1
  66 IF (IS .EQ. MX) THEN
      NG = 252
      RETURN
      END IF
      IS = IS + 1
      IF (NSUMCH(IS) .LT. NG) GO TO 66
      IF (MSA .GT. 0) THEN
      DO 68 N = 1, MSA
  68 Y(ISOL(N)) = RN0
      MSA = 0
      END IF
      IF (IS .GT. 0) THEN
```

```
      M = 0
 71 M = M + 1
    ITEMP = IS/IPOT(M)
    IF (ITEMP/2*2 .EQ. ITEMP) GO TO 71
    I = INR(M+MG)
    IF (N00(I)) GO TO 76
    IF (MSA .EQ. L0) GO TO 66
    MSA = MSA + 1
    ISOL(MSA) = I
    Y(I) = RN1
    IF (ITEMP .GT. 1) GO TO 71
    END IF
    NSUM(NG) = IS
C
C     The components are checked for the last time.
C
129 DO 51 I = 1, MS
    N0(I) = N00(I)
 51 N1(I) = N10(I)
    DO 156 J = 1, L
156 LJ(J) = LJ0(J)
 13 DO 62 J = 1, L
    IF (LJ(J) .AND. LSGN(J) .AND. B0(J) .EQ. RN0) THEN
    TEMP = RN0
    DO 7 I = 1, MG
    IF (.NOT. N0(I) .AND. A(I,J) .NE. RN0) THEN
    IF (TEMP*A(I,J)) 62,162,7
162 TEMP = A(I,J)
    END IF
  7 CONTINUE
    IF (MSA .GT. 0) THEN
    DO 36 N = 1, MSA
    I = ISOL(N)
    IF (.NOT. N0(I) .AND. A(I,J) .NE. RN0) THEN
    IF (TEMP*A(I,J)) 62,57,36
 57 TEMP = A(I,J)
    END IF
 36 CONTINUE
    END IF
    DO 82 I = 1, MS
    IF (.NOT. N1(I) .AND. A(I,J) .NE. RN0) THEN
    Y(I) = RN0
    N0(I) = .TRUE.
    N1(I) = .TRUE.
    END IF
 82 CONTINUE
    LJ(J) = .FALSE.
    GO TO 13
    END IF
 62 CONTINUE
    DO 45 I = 1, MG
    IF (.NOT. N0(I) .AND. Y(I) .GT. YMAX(I)) Y(I) = EM1*YMAX(I)
 45 MNR(I) = 0
C
C     SUBROUTINE YBER(NO) is called to reconsider if a species should
C     be involved in the mass balance. Otherwise, the concentration
C     of the species is kept equal to the lower limit, exp(-174.673).
C
    CALL YBER(1)
    ITEMP = MSA
```

```
      DO 219 J = 1, L
      IF (LJ(J)) THEN
      DO 220 I = 1, MS
      IF (A(I,J) .NE. RN0 .AND. Y(I) .NE. RN0) GO TO 219
220   CONTINUE
      IF (MSA .EQ. L0) GO TO 86
      I = MG
205   I = I + 1
      IF (I .GT. MS) GO TO 86
      IF (N0(INR(I)) .OR. A(INR(I),J) .EQ. RN0) GO TO 205
      K = I
      IF (MSA - L0 + 1) 136,155,155
155   IF (NSUMCH(NSUM(NG) + IPOT(I-MG)) - NG) 205,228,228
136   K = K + 1
      IF (K .GT. MS) GO TO 155
      IF (N0(INR(K)) .OR. A(INR(K),J) .EQ. RN0) GO TO 136
      IF (NSUMCH(NSUM(NG) + IPOT(I-MG) + IPOT(K-MG)) - NG) 136,228,228
222   I = K
228   MSA = MSA + 1
      ISOL(MSA) = INR(I)
      Y(INR(I)) = RN1
      NSUM(NG) = NSUM(NG) + IPOT(I-MG)
      IF (K .GT. I .AND. K .LE. MS) GO TO 222
      END IF
219   CONTINUE
      IF (ITEMP .LT. MSA) THEN
      NG = NG - 1
      GO TO 55
      END IF
      LS1 = L + MSA
      LS = LS1 - 1
      LS2 = LS + 2
134   IFLGM = 0
      IVAR = 0
      IVARJ = -MX
      Q = RN8
C
C     The coefficients in the linear system of equations are computed.
C
16    DO 6 J = 1, LS1
      DO 6 K = J, LS2
6     R(J,K) = RN0
      DO 5 I = 1, MG
      IF (Y(I) .GT. RN0) THEN
      AKT(I) = LOG(Y(I))
      TEMP1 = AKT(I) + G(I) - RN1
      DO 77 J = 1, L
      IF (A(I,J) .NE. RN0) THEN
      TEMP = A(I,J)*Y(I)
      R(J,LS2) = R(J,LS2) + TEMP*TEMP1
      DO 80 K = J, L
80    R(J,K) = R(J,K) + TEMP*A(I,K)
      END IF
77    CONTINUE
      END IF
5     CONTINUE
      DO 9 J = 1, L
9     R(J,LS2) = R(J,LS2) + B0(J)
      IF (MSA .GT. 0) THEN
      DO 67 N = 1, MSA
```

```
      I = ISOL(N)
      K = L + N
      R(K,LS2) = G(I)
      DO 67 J = 1, L
   67 R(J,K) = A(I,J)
      DO 31 K = 2, LS1
      DO 31 J = 1, K-1
   31 R(K,J) = R(J,K)
      DO 44 K = 1, L
      IF (.NOT. LKH(K)) THEN
      DO 83 J = 1, LS1
   83 R(J,LS2) = R(J,LS2) - PI(K)*R(J,K)
      END IF
   44 CONTINUE
C
C     The Gaussian elimination is prepared for by pivoting.
C
      DO 10 K = 1, LS
      IF (LKH(K)) THEN
      TEMP = RN0
      DO 11 J = K, LS1
      IF (LKH(J) .AND. ABS(R(J,K)) .GT. TEMP) THEN
      ITEMP = J
      TEMP = ABS(R(J,K))
      END IF
   11 CONTINUE
      IF (TEMP .EQ. RN0) THEN
      IF (K .GT. L) GO TO 10
      IF (B0(K) .EQ. RN0) GO TO 10
      IF (MSOL .GT. 0) THEN
      DO 74 I = M1, MS
      IF (N0(INR(I)) .OR. A(INR(I),K) .EQ. RN0) THEN
      ELSE IF (NSUMCH(NSUM(NG)+IPOT(I-MG)) .GE. NG) THEN
      Y(INR(I)) = RN1
      GO TO 55
      END IF
   74 CONTINUE
      END IF
      GO TO 216
      ELSE IF (ITEMP .GT. K) THEN
      DO 15 N = K, LS2
      TEMP = R(ITEMP,N)
      R(ITEMP,N) = R(K,N)
   15 R(K,N) = TEMP
      END IF
      ITEMP = K + 1
      DO 46 J = ITEMP, LS1
      TEMP = -R(J,K)/R(K,K)
      DO 46 N = ITEMP, LS2
   46 R(J,N) = R(J,N) + TEMP*R(K,N)
      END IF
   10 CONTINUE
      ELSE
C
C     The Gaussian elimination is prepared for by Choleski's method.
C
      DO 85 K = 1, L
      IF (.NOT. LKH(K)) THEN
      DO 93 J = 1, K
   93 R(J,LS2) = R(J,LS2) - PI(K)*R(J,K)
```

```
      IF (K .LT. L) THEN
      DO 23 J = K+1, L
23 R(J,LS2) = R(J,LS2) - PI(K)*R(K,J)
      END IF
      END IF
85 CONTINUE
      DO 95 J = 2, LS1
      IF (LKH(J) .AND. R(J,J) .NE. RN0) THEN
      DO 79 K = 1, J-1
      IF (LKH(K) .AND. R(K,K) .NE. RN0) THEN
      TEMP = -R(K,J)/R(K,K)
      DO 96 N = J, LS2
96 R(J,N) = R(J,N) + TEMP*R(K,N)
      END IF
79 CONTINUE
      END IF
95 CONTINUE
      END IF
C
C     Gaussian elimination is carried out.
C
      DO 20 K = LS1, 1, -1
      IF (.NOT. LKH(K)) THEN
      ELSE IF (R(K,K) .EQ. RN0 .OR. R(K,LS2) .EQ. RN0) THEN
      PI(K) = RN0
      ELSE
      PI(K) = R(K,LS2)/R(K,K)
      IF (K .GT. 1) THEN
      DO 58 J = 1, K-1
58 R(J,LS2) = R(J,LS2) - PI(K)*R(J,K)
      END IF
      END IF
20 CONTINUE
      IF (IVARJ .GE. 0) GO TO 91
      IF (IVAR .EQ. 0) GO TO 65
      DO 89 J = 1, LS1
      IF (ABS(OPI(J)) .GT. EP8 .AND. ABS(PI(J)) .GT. EP8) THEN
      IF (.NOT. SLAM .OR. SIGN(OPI(J),PI(J)) .EQ. -OPI(J)) GO TO 216
      END IF
89 CONTINUE
      IF (SLAM) GO TO 65
      DO 70 J = 1, L
      IF (ABS(PI(J)) .GT. EM8) THEN
      IF (ABS(OPI(J)/PI(J) - RN1) - EM5) 70,70,65
      END IF
70 CONTINUE
      TEMP1 = YMIN
      DO 176 I = 1, MG
      IF (.NOT. N0(I) .AND. Y(I) .EQ. RN0) THEN
      YF(I) = EXP(MAX(MIN(ALN(I),POTM),-POTM))
      IF (MNR(I) .EQ. 0 .AND. YF(I) .GT. TEMP1) THEN
      ITEMP = I
      TEMP1 = YF(I)
      END IF
      END IF
176 CONTINUE
      IF (TEMP1 - YMIN) 159,159,135
135 Y(ITEMP) = MIN(YF(ITEMP),YMAX(ITEMP))
      MNR(ITEMP) = 1
      GO TO 134
```

```
  159 IF (NEG) GO TO 216
C
C     The solids are ranked once again and a check is made to lower
C     the total free energy by including solids not involved.
C
      MS1 = MS - 1
      TEMP = EM5
      DO 54 K = M1, MS
      I = INR(K)
      IF (Y(I) .NE. RN0) THEN
      AKT(K) = RN0
      ELSE IF (N0(I)) THEN
      AKT(K) = -RLMAX
      ELSE
      TEMP1 = ALN(I)
      TEMP2 = TEMP1/ASS(I)
      IF (TEMP2 .GT. EM5) THEN
      AKT(K) = TEMP2
      ELSE
      AKT(K) = TEMP1
      END IF
      IF (AKT(K) .GT. TEMP) THEN
      ITEMP = I
      TEMP = AKT(K)
      END IF
      END IF
   54 CONTINUE
      IF (TEMP .GT. EM5) THEN
      Y(ITEMP) = RN1
      GO TO 55
      END IF
      IVARJ = 0
      GO TO 91
   65 DO 60 J = 1, LS1
   60 OPI(J) = PI(J)
C
C     Negative concentrations are checked for and eliminated by
C     calculating new positive starting estimates.
C
   91 IFLG = 0
      FLAM = RN1
      QQ = Q/(Q + RN1)
      SLAM = .FALSE.
      I = 1
  285 IF (Y(I) .GT. RN0) THEN
      YF(I) = AKT(I) - ALN(I)
      IF (ABS(YF(I)) .LE. EM6) THEN
      ELSE IF (YF(I) .GT. RN0 .OR. Y(I) .LT. YMAX(I)) THEN
      IF (YF(I) .GT. RN1) SLAM = .TRUE.
      TEMP1 = MAX(-Q/YF(I),QQ/YF(I))
      IF (TEMP1 .LT. FLAM) FLAM = TEMP1
      IF (IFLG .LT. 2 .AND. IVAR .GT. 0) THEN
      IFLG = 1
      IF (SIGN(ASS(I),YF(I)) .EQ. -ASS(I)) IFLG = 2
      END IF
      END IF
      ASS(I) = YF(I)
      END IF
      I = I + 1
      IF (I .LE. MG) GO TO 285
```

```
      DO 29 I = 1, MG
   29 IF (Y(I) .GT. RN0) Y(I)  =  MIN(Y(I)*(RN1-FLAM*YF(I)),YMAX(I))
C
C      SUBROUTINE YBER(NO) is called to possibly withdraw a species
C      from the mass balance. If so, the concentration of the species
C      will be set equal to the lower limit, exp(-174.673).
C
      CALL YBER(2)
      NEG = .FALSE.
      IF (MSA .GT. 0) THEN
      DO 53 N = 1, MSA
      TEMP = PI(L+N)
      IF (TEMP .EQ. RN0 .OR. TEMP .LE. -YMIN) NEG = .TRUE.
      IF (IFLG .EQ. 0 .AND. IFLGM .GT. 0 .AND. ABS(TEMP) .GE. YMIN) THEN
      IF (ABS(TEMP/Y(ISOL(N)) - RN1) .GT. EM6) IFLG = 2
      END IF
   53 Y(ISOL(N)) = TEMP
      END IF
      IF (IFLG .EQ. 2) Q = Q/RN2
      IF (IFLG .EQ. 1 .AND. IFLGM .EQ. 1) Q = MIN(RN2*Q,RN8)
      IFLGM = IFLG
      IVAR = IVAR + 1
      IF (IVAR .GT. 99 .AND. IVARJ .LT. 0) GO TO 216
      IF (SLAM .OR. IVAR .EQ. 1 .OR. IVARJ .LT. 0) GO TO 16
      IF (IFLG .EQ. 1 .AND. IVARJ .EQ. 0) GO TO 16
      IVARJ = IVARJ + 1
      IF (IFLG .EQ. 1 .OR. IFLG .EQ. 2 .AND. IVARJ .LT. 50) GO TO 16
C
C      Concentrations for previously withdrawn species are computed.
C
      DO 149 ITEMP = 1, MG
      IF (.NOT. N0(ITEMP) .AND. Y(ITEMP) .EQ. RN0) THEN
      YF(ITEMP) = EXP(MAX(MIN(ALN(ITEMP),POTM),-POTM))
      IF (MNR(ITEMP) .EQ. 0 .AND. YF(ITEMP) .GT. YMIN) GO TO 135
      IF (MNR(ITEMP) .EQ. 1 .AND. YF(ITEMP) .GT. EP2*YMIN) GO TO 216
      END IF
  149 CONTINUE
      IF (NEG) GO TO 216
      DO 210 I = 1, MG
  210 IF (.NOT. N0(I) .AND. Y(I) .EQ. RN0) Y(I) = YF(I)
      IF (MSA .EQ. 0) RETURN
      DO 61 N = 1, MSA
   61 IF (Y(ISOL(N)) .LT. YMIN) Y(ISOL(N)) = RN0
      RETURN
      END
C
C
C
C      SUBROUTINE YBER(NO) is called upon to reconsider including a
C      species (NO = 1) in or possibly withdraw a species (NO = 2)
C      from the mass balance calculations. Depending on the case,
C      the concentration of the species is either set at or taken
C      off the lower limit of the computer which is exp(-174.673).
C      The specie must therefore be aqueous or gaseous.
C
C
C
      SUBROUTINE YBER(NO)
      IMPLICIT REAL*8(A-H,O-Z)
      COMMON /GAPL/ YF(80), YMAX(80), INR(80), N0(80)
```

```
      COMMON /GAYB/ YMIN, ISOL(13), LJ(12), MSA
      COMMON /SGGA/ ASS(80), RLMAX, IFLG, IPOT(48), LKH(24), MX, N1(80)
      COMMON /SGGP/ B(12,99), B0(12), H, POTM, Y(80), IEL(12), KH(12),
     *MG, MS, MSOL, M1, NP
      COMMON /SGLN/ A(80,12), G(80), PI(24), L
      LOGICAL LJ, LKH, N0, N1
      PARAMETER(EM6 = 1.E-6,RN0 = 0.E0)
      YMIN = RLMAX
      DO 171 J = 1, L
      IF (LJ(J)) THEN
      TEMP = RN0
      DO 201 I = 1, MG
  201 IF (A(I,J) .NE. RN0 .AND. Y(I) .GT. TEMP) TEMP = Y(I)
      IF (MSA .GT. 0) THEN
      DO 213 N = 1, MSA
      IF (A(ISOL(N),J) .EQ. RN0) THEN
      ELSE IF (N0 .EQ. 1) THEN
      IF (Y(ISOL(N)) .GT. TEMP) TEMP = Y(ISOL(N))
      ELSE
      IF (PI(L + N) .GT. TEMP) TEMP = PI(L + N)
      END IF
  213 CONTINUE
      END IF
      TEMP = EM6*TEMP
      IF (TEMP .LT. YMIN) YMIN = TEMP
      END IF
  171 CONTINUE
      IF (N0 .EQ. 1) THEN
      DO 208 I = 1, MG
  208 IF (.NOT. N0(I) .AND. Y(I) .LT. YMIN) Y(I) = YMIN
      RETURN
      END IF
      DO 209 I = 1, MG
  209 IF (Y(I) .GT. RN0 .AND. Y(I) .LT. YMIN) Y(I) = RN0
      RETURN
      END
C
C
C
C     FUNCTION NSUMCH(N) keeps track of which solid phase combination
C     (none, one, or more solids at the same time) has minimized the
C     free energy by keeping track of the number specifying the solid
C     phase combination.
C
C     NG = # of phase combinations considered (maximum of 250 allowed).
C
C
C
      FUNCTION NSUMCH(N)
      COMMON /SGNS/ NG, NSUM(250)
      NSUMCH = 1
  148 IF (NSUM(NSUMCH) .EQ. N) RETURN
      NSUMCH = NSUMCH + 1
      IF (NSUMCH .LT. NG) GO TO 148
      RETURN
      END
C
C
C     FUNCTION ALN(I) calculates the log of the activity for species.
```

```
C
C
      FUNCTION ALN(I)
      IMPLICIT REAL*8(A-H,O-Z)
      COMMON /SGLN/ A(80,12), G(80), PI(24), L
      PARAMETER(RN0 = 0.E0)
      TEMP = RN0
      DO 19 J = 1, L
   19 TEMP = TEMP + A(I,J)*PI(J)
      ALN = TEMP - G(I)
      RETURN
      END
C
C
C
C      SUBROUTINE PLOTT is used to see if a plot is desired.
C      If so, plotting parameters will then be entered.
C
C
C
      SUBROUTINE PLOTT
      IMPLICIT REAL*8(A-H,O-Z)
      COMMON /SGGP/ B(12,99), B0(12), H, POTM, Y(80), IEL(12), KH(12),
     *MG, MS, MSOL, M1, NP
      COMMON /SGLN/ A(80,12), G(80), PI(24), L
      COMMON /SGRD/ STEP, STOP, VER, IN, IND, IOUT, IRE, IUT, IXT,
     *KVALM, KVAL1, MCO, MV, NCFN
      COMMON /TALR/ TAL(99), ITAL(99)
      LOGICAL STEP, STOP, VER
      IF (IRE .GE. 0) THEN
      IF (KVAL1 - 7) 427,429,429
      ELSE IF (KVAL1 .EQ. 5) THEN
      CALL READUT(2,2)
      GO TO 558
      END IF
      IF (NF.EQ.0.OR.NH.GT.0.OR.NB.GT.0.OR.NZ.GT.0) GO TO 599
      IF (NT - 5) 639,429,429
  695 CALL READUT(-3,0)
  429 IF (STOP) WRITE (IOUT,771)
  771 FORMAT(' DIAGRAMS'/ ' ENTER THE DEPENDENT VARIABLE')
  517 CALL READIN(11,0,1,0,60+MCO)
      IF (IRE .EQ. 1) GO TO 677
      IF (IRE .EQ. -1) RETURN
      NF = ITAL(1)
      IF (NF .LE. MCO .OR. NF .EQ. 20 .OR. NF .EQ. 30) GO TO 599
      IF (NF .GT. 10 .AND. NF .LE. 10 + MCO) GO TO 599
      IF (NF .GT. 50 .AND. NF .LE. 50 + MCO .OR. NF .GT. 60) THEN
      ELSE IF (NF .LE. 40 .OR. NF .GT. 40 + MCO) THEN
      CALL READUT(-1,0)
      GO TO 517
      END IF
      NB = 0
      NH = 0
      NY = 0
      NZ = 0
      IF (STEP) CALL READUT(-2,1)
      GO TO 651
  694 CALL READUT(-1,0)
  599 IF (STOP) WRITE (IOUT,772)
  772 FORMAT(' N-BAR OR Z DEPENDENT VARIABLE? (I,J,K OR 3*0)')
```

```
      CALL READIN(7,0,3,0,0)
      IF (IRE) 429,729,599
729 NH = ITAL(1)
      NB = ITAL(2)
      NZ = ITAL(3)
      IF (NH .EQ. 0 .AND. NB .EQ. 0 .AND. NZ .EQ. 0) THEN
      IF (NF .GT. 0) GO TO 639
      ELSE
      IF (NH .LE. 0 .OR. NB .LE. 0 .OR. NZ .LT. 0) GO TO 694
      IF (NH .GT. L .OR. NB .GT. L .OR. NZ .GT. MV) GO TO 694
      END IF
      NY = 0
      IF (STEP) CALL READUT(-2,1)
      GO TO 651
639 IF (STOP) WRITE (IOUT,773)
773 FORMAT(' LOG C FOR SPECIES I INDEPENDENT VARIABLE? (I OR 0)')
      CALL READIN(0,1,1,0,MS)
      IF (IRE) 599,730,639
730 NY = ITAL(1)
      GO TO 651
677 READ (IND,*,END=695) NF, NH, NB, NZ, NY
      IF (VER) WRITE (IOUT,811) NF, NH, NB, NZ, NY
811 FORMAT(20I4)
651 WRITE (IUT,811) NF, NH, NB, NZ, NY
      IF (NF .GT. 0 .OR. NH .GT. 0) NT = NF/10 + 1
      RETURN
427 IF (STOP) WRITE (IOUT,809)
809 FORMAT(' DIAGRAMS'/' ENTER THE INDEPENDENT VARIABLE')
518 CALL READIN(12,0,1,-MCO,10)
      IF (IRE .EQ. 1) GO TO 631
      IF (IRE .EQ. -1) RETURN
      NPL = ITAL(1)
      IF (NPL .LE. MCO .OR. NPL .EQ. 10) THEN
      IF (NT - 4) 640,640,600
      END IF
      CALL READUT(-1,0)
      GO TO 518
640 IF (STOP) WRITE (IOUT,810)
810 FORMAT(' ENTER THE TOTAL NO. OF CURVES (< =80) (= 0 N-BAR OR Z DEPE
     *NDENT VARIABLE)')
      CALL READIN(0,0,1,0,80)
      IF (IRE) 427,808,640
600 IF (STOP) WRITE (IOUT,728)
728 FORMAT(' ENTER THE DEPENDENT VARIABLE')
521 CALL READIN(8,0,1,-MCO,MCO)
      IF (IRE) 427,733,600
733 LPL = ITAL(1)
      MPL = 0
      IF (LPL .NE. 0) GO TO 524
      CALL READUT(-1,0)
      GO TO 521
808 MPL = ITAL(1)
      LPL = 0
524 IF (.NOT. STEP) GO TO 573
      READ (IND,*,END=697,ERR=573) JPL
      GO TO 628
697 CALL READUT(-3,0)
      IF (IRE) 573,573,427
631 READ (IND,*,END=697) MPL, NPL, LPL
      IF (VER) WRITE (IOUT,811) MPL, NPL, LPL
```

```
573 JPL = MPL
628 WRITE (IUT,811) MPL, NPL, LPL
    IF (MPL) 607,607,620
540 IF (MPL .EQ. 0) THEN
    CALL READUT(1,1)
    IF (NT - 4) 640,640,600
    END IF
    CALL READUT((MPL + 19)/20,(JPL + 19)/20)
620 IF (.NOT. STOP) THEN
    ELSE IF (NT .LT. 3) THEN
    WRITE (IOUT,700) MPL
700 FORMAT(' ENTER THE F VALUES TO BE PLOTTED (',I2,' SPECIES NOS.)')
    ELSE IF (NT .EQ. 3) THEN
    WRITE (IOUT,778) MPL
778 FORMAT(' ENTER THE LOG C VALUES TO BE PLOTTED (', I2, ' SPECIES NO
   *S.)')
    ELSE
    WRITE (IOUT,779) MPL
779 FORMAT(' ENTER THE ETA VALUES TO BE PLOTTED (', I2, ' COMPONENT NO
   *S.)')
    END IF
    IF (NT .LT. 4) THEN
    CALL READIN(-1,(JPL + 19)/20,MPL,1,MS)
    ELSE
    CALL READIN(-1,(JPL + 19)/20,MPL,1,L)
    END IF
    IF (IRE) 640,559,632
698 CALL READUT(-3,0)
632 IF (IRE .EQ. 2) GO TO 620
    READ (IND,*,END=698) (ITAL(N), N = 1, MPL)
    IF (VER) WRITE (IOUT,811) (ITAL(N), N = 1, MPL)
559 WRITE (IUT,811) (ITAL(N), N = 1, MPL)
607 IF (STOP) WRITE (IOUT,780)
780 FORMAT(' ENTER THE LENGTH OF THE X AXIS/CM (5 < = LENGTH < = 75)')
    CALL READIN(-2,0,1,5,75)
    IF (IRE) 540,736,731
736 XAXL = TAL(1)
623 IF (STOP) WRITE (IOUT,781)
781 FORMAT(' ENTER THE LOWEST VALUE ON THE X AXIS')
    CALL READIN(-2,0,1,0,0)
    IF (IRE) 607,737,623
737 XLOW = TAL(1)
625 IF (STOP) WRITE (IOUT,782)
782 FORMAT(' ENTER THE HIGHEST VALUE ON THE X AXIS')
801 CALL READIN(-2,0,1,0,0)
    IF (IRE) 623,738,625
738 XHIGH = TAL(1)
    IF (XHIGH .LE. XLOW) THEN
    CALL READUT(-1,0)
    GO TO 801
    END IF
627 IF (STOP) WRITE (IOUT,783)
783 FORMAT(' ENTER THE LENGTH OF THE Y AXIS/CM (5 < = LENGTH < = 75)')
    CALL READIN(-2,0,1,5,75)
    IF (IRE) 625,739,627
739 YAXL = TAL(1)
629 IF (STOP) WRITE (IOUT,784)
784 FORMAT(' ENTER THE LOWEST VALUE ON THE Y AXIS')
    CALL READIN(-2,0,1,0,0)
    IF (IRE) 627,685,629
```

```
685 YLOW = TAL(1)
630 IF (STOP) WRITE (IOUT,785)
785 FORMAT(' ENTER THE HIGHEST VALUE ON THE Y AXIS')
560 CALL READIN(-2,0,1,0,0)
    IF (IRE) 629,691,630
691 YHIGH = TAL(1)
    IF (YHIGH .LE. YLOW) THEN
    CALL READUT(-1,0)
    GO TO 560
    END IF
558 IF (STOP) WRITE (IOUT,786)
786 FORMAT(' ENTER THE Y VALUE TO BE ATTAINED FOR A CURVE TO BE PLOTTE
    *D (Y OR 0)')
    CALL READIN(9,2,1,0,0)
    IF (IRE) 630,526,558
712 CALL READUT(-3,0)
    GO TO 607
731 READ (IND,*,END=712) XAXL, XLOW, XHIGH, YAXL, YLOW, YHIGH, TAL(1)
    IF (VER) WRITE (IOUT,616) XAXL,XLOW,XHIGH,YAXL,YLOW,YHIGH,TAL(1)
616 FORMAT(6(1X, G12.6))
526 WRITE (IUT,616) XAXL, XLOW, XHIGH, YAXL, YLOW, YHIGH, TAL(1)
    RETURN
    END
C
C
C
C      SUBROUTINE READIN is called upon whenever special instructions
C      are requested. These instructions include HELP,(H); RETURN TO
C      PREVIOUS STEPS,(RN); FORWARD N STEPS WITH or WITHOUT SUPPRESSED
C      VERIFICATION,(FN or XFN); QUIT THE PROGRAM,(Q); or IDENTIFYING
C      SPECIES N,(SN).
C
C
C
    SUBROUTINE READIN(NR,NS,NTAL,LL,LH)
    IMPLICIT REAL*8(A-H,O-Z)
    COMMON /SGGP/ B(12,99), B0(12), H, POTM, Y(80), IEL(12), KH(12),
    *MG, MS, MSOL, M1, NP
    COMMON /SGRD/ STEP, STOP, VER, IN, IND, IOUT, IRE, IUT, IXT,
    *KVALM, KVAL1, MCO, MV, NCFN
    COMMON /TALR/ TAL(99), ITAL(99)
    COMMON /TEXT/ IDENT(80)
    COMMON /TXT1/ INDFIL, ITEXT
    CHARACTER IDENT*10, INDFIL*9, ITEXT*80
    LOGICAL STEP, STOP, VER
    DATA BLANK/1H /, IBLANK/1H /
    IF (.NOT. STOP) THEN
    NSTEP = NSTEP - 1
    IF (NSTEP .EQ. 1) STOP = .TRUE.
    GO TO 549
    END IF
    N0 = 1
    DO 552 N = 1, NTAL
    ITAL(N) = IBLANK
552 TAL(N) = BLANK
    GO TO 547
699 CALL READUT(-1,0)
    IF (NTAL .GT. 1) THEN
    IRE = 2
    RETURN
```

```
     END IF
547 READ (IN,506,END = 699) ITEXT
506 FORMAT(A)
    IF (NR .GT. -4) THEN
    IF (ITEXT(:1) .EQ. 'H') THEN
    IF (NR .EQ. 1) THEN
    WRITE (IOUT,789)
789 FORMAT(' THE TOTAL NO. OF SPECIES MUST BE < = 80')
    ELSE IF (NR .EQ. 2) THEN
    WRITE (IOUT,790)
790 FORMAT(' ENTER THE COEFFS. OF THE STOICHIOMETRY MATRIX IN COMPONEN
   *T ORDER')
    ELSE IF (NR .EQ. 3) THEN
    WRITE (IOUT,791)
791 FORMAT(' KF = EQUIL. CONST. OF FORMATION'/' SUBTRACT LOG RT (=1.39
   * AT 298 K) FROM LOG KF FOR GASES WITH ATM IN THE UNIT'/' FOR KF')
    ELSE IF (NR .EQ. 4) THEN
    WRITE (IOUT,792)
792 FORMAT('  1 NO OUTPUT'/' 2  DEFINE OR CHANGE THE OUTPUT'/' 3
   * CHANGE NO. OF EQUILS. TO BE CALCD. AND VARIATION IN INPUT CONCNS.
   *'/' 4  CHANGE INPUT CONCNS. (A SINGLE CONCN. IS CHANGED BY ENTER
   *ING'/'    40 + A COMPONENT NO.)'/' 5  DEFINE OR CHANGE DIAGRAM D
   *IMENSIONS AND PLOT'/' 6  PLOT WITH UNCHANGED DIAGRAM DIMENSIONS'
   */' 7  CHANGE DEPENDENT VARIABLE'/' 8  PRINT OUT INPUT THERMODN
   *. DATA'/' 9  CHANGE IDENTIFICATION (STAR OR BLANK IN COLUMN 10)'
   */' 10  FINISH THE CALCNS.'/' RESULTS FROM MAX. 15 GROUPS OF CALC
   *D. EQUILS. WILL BE PLOTTED IN A N-BAR/Z'/' DIAGRAM, RESULTS FROM
   *1 GROUP IN THE OTHER')
    IF (KVALM .EQ. 0) WRITE (IOUT,793)
793 FORMAT(' RETURN NOT ALLOWED')
    ELSE IF (NR .EQ. 5) THEN
    WRITE (IOUT,794)
794 FORMAT('   0,0  TOTAL VOL. ADDED IN TITRN.'/'   1,I  C FOR SP
   *ECIES I (C = CONCN./MOL.DM-3)'/'   2,I  LOG C FOR SPECIES I'/'
   *  3,I  A FOR SPECIES I (A = ACTIVITY)'/'   4,I  LOG A FOR SPECIE
   *S I'/'   5,I  LOG (P/KPA) FOR SPECIES I (298.15 K, 1 DM3)'/'
   *  6,J  LOG ABS(TF) FOR COMPONENT J (TF = TOTAL CONCN. IN THE FLUIDS
   *)'/'   7,J  TF FOR COMPONENT J'/'   8,J  LOG ABS(TC) FOR COM
   *PONENT J (TC = TOTAL CONCN.)'/'   9,J  TC FOR COMPONENT J'/'
   *10,J  ETA FOR COMPONENT J'/'   -J,I  FRACTION OF COMPONENT J PRE
   *SENT IN SPECIES I'/' 10I + J,K  AV. NO. OF COMP. I BOUND PER COMP.
   *J IN FLUID K (N-BAR) (I,J < = 9)'/' 10I + J,0  AV. NO. OF COMPONENT I
   *BOUND PER COMPONENT J (Z) (I,J < = 9)'/'   99,99 END OF INPUT')
    ELSE IF (NR .EQ. 6) THEN
    WRITE (IOUT,581)
581 FORMAT(' THE VARIATION IN INPUT CONCNS. FOR EACH COMPONENT WILL BE
   * DEFINED')
    ELSE IF (NR .EQ. 7) THEN
    WRITE (IOUT,707)
707 FORMAT(' N-BAR  AV. NO. OF COMPONENT I BOUND PER COMPONENT J IN FL
   *UID K'/'    Z  (TC(I) - C(I))/TC(J), TC = TOTAL CONCN., C = FREE COM
   *PONENT CONCN. (K = 0)')
    IF (MSOL .GT. 0) WRITE (IOUT,747) MV
747 FORMAT(' THE SOLIDS ARE CONSIDERED AS BEING PRESENT IN FLUID', I2)
    ELSE IF (NR .EQ. 8) THEN
    WRITE (IOUT,696)
696 FORMAT('  J  INPUT VALUES OF LOG TC OR LOG A FOR COMPONENT J (J < = 9
   *)'/' -J  INPUT VALUES OF -LOG TC OR -LOG A FOR COMPONENT J (J < = 9)
   *')
    ELSE IF (NR .EQ. 9) THEN
```

```
      WRITE (IOUT,721)
721 FORMAT(' 0 THE VALUE AT 1 % OF THE LENGTH OF THE Y AXIS')
      ELSE IF (NR .EQ. 10) THEN
      WRITE (IOUT,593)
593 FORMAT(' 1 TC VARIES IRREGULARLY'/' 2 TC IS CONST.'/' 3 TC
   * VARIES BY A CONST. INCREMENT'/' 4 TC VARIES BY TITRN. WITH VAR
   *YING VOL. ADDNS.'/' 5 TC VARIES BY TITRN. WITH CONST. VOL. ADDN
   *S.'/' 6 LOG TC VARIES BY A CONST. INCREMENT'/' 7 LOG TC IS D
   *EPENDENT VARIABLE IN THE PREDOMINANCE DIAGRAM'/' 8 LOG A VARIES
   * IRREGULARLY'/' 9 LOG A IS CONST.'/' 10 LOG A VARIES BY A CON
   *ST. INCREMENT'/' 11 LOG A IS DEPENDENT VARIABLE IN THE PREDOMINA
   *NCE DIAGRAM')
      ELSE IF (NR .EQ. 11) THEN
      WRITE (IOUT,734)
734 FORMAT('    0 NONE OF THE VARIABLES BELOW'/'   J FRACTION (F) O
   *F COMPONENT J IN A SOLUTE OR A GAS, 0 < = F < = 1 (J < = 9)'/' 10 + J ACCUMU
   *LATED SUM OF F FOR COMPONENT J (J < = 9)'/'  20 LOG C (C = CONCN. FOR
   * SOLUTES AND GASES AND AMT. OF SUBSTANCE FOR SOLIDS)'/'  30 ETA
   *( = LOG(TF/C), TF = TOTAL CONCN. IN THE FLUIDS, C = FREE COMPONENT CONCN
   *.)'/' 40 + J PREDOMINANCE DIAGRAM WITH SOLIDS OR SOLUTES CONTG. COM
   *PONENT J (J < = 9)'/' 50 + J PREDOMINANCE DIAGRAM WITH SOLIDS CONTG. C
   *OMPONENT J OR SOLUTES CONTG.'/'     COMPONENT J (J < = 9)'/' 60 + J P
   *REDOMINANCE DIAGRAM WITH SOLUTES CONTG. COMPONENT J (J < = 9)')
      IF (KVAL1 .EQ. 7) WRITE (IOUT,795)
795 FORMAT(' NEXT OPTION MUST BE < 5 IF THE NEW OR OLD VALUE AT THIS PO
   *INT IS 20 OR > 40')
      ELSE IF (NR .EQ. 12) THEN
      WRITE (IOUT,513)
513 FORMAT(' 0 TOTAL VOL. ADDED IN TITRN.'/' J INPUT VALUES OF TC
   *, LOG TC, OR LOG A FOR COMPONENT J (J < = 9)'/' -J INPUT VALUES OF
   *-TC, -LOG TC, OR -LOG A FOR COMPONENT J (J < = 9)'/' 10 CALCD. LOG
   *C VALUES')
      ELSE
      WRITE (IOUT,788)
788 FORMAT(' HELP NOT AVAILABLE')
      END IF
      GO TO 547
      ELSE IF (ITEXT(:1) .EQ. 'Q') THEN
      CALL READUT(-4,0)
      ELSE IF (ITEXT(:1) .EQ. 'S') THEN
      IBEG = 2
      GO TO 507
      END IF
      END IF
      IF (STEP .AND. ITEXT(:1) .EQ. 'F') THEN
      IBEG = 2
      VER = .TRUE.
      ELSE IF (STEP .AND. ITEXT(:2) .EQ. 'XF') THEN
      IBEG = 3
      VER = .FALSE.
      ELSE IF (ITEXT(:1) .EQ. 'R') THEN
      IBEG = 2
      VER = .FALSE.
      ELSE
      IF (NR .EQ. -4) GO TO 541
      REWIND IXT
      WRITE (IXT,506) ITEXT
      REWIND IXT
      IF (NR .LT. -1 .OR. NR .EQ. 2 .OR. NR .EQ. 3 .OR. NR .EQ. 9) THEN
      READ (IXT,*,END = 614,ERR = 699) (TAL(N), N = N0, NTAL)
```

```
614 DO 551 N = N0, NTAL
    IF (TAL(N) .EQ. BLANK) THEN
    N0 = N
    GO TO 547
    ELSE IF (LH .GT. 0) THEN
    ITAL(N) = TAL(N)
    IF (ITAL(N) .LT. LL .OR. ITAL(N) .GT. LH) GO TO 699
    END IF
551 CONTINUE
    ELSE
    READ (IXT,*,END = 598,ERR = 699) (ITAL(N), N = N0, NTAL)
598 DO 562 N = N0, NTAL
    IF (ITAL(N) .EQ. IBLANK) THEN
    N0 = N
    GO TO 547
    ELSE IF (LH .GT. 0) THEN
    IF (ITAL(N) .LT. LL .OR. ITAL(N) .GT. LH) GO TO 699
    END IF
562 CONTINUE
    END IF
    GO TO 541
    END IF
507 I = 80
638 IF (ITEXT(I:I) .EQ. ' ') THEN
    I = I - 1
    GO TO 638
    ELSE IF (I .EQ. IBEG - 1) THEN
    NSTEP = 1
    ELSE
    REWIND IXT
    WRITE (IXT,506) ITEXT(IBEG:I)
    REWIND IXT
    READ (IXT,*,ERR = 501) NSTEP
    IF (NSTEP .LT. 1) GO TO 501
    END IF
    IF (ITEXT(:1) .EQ. 'S') THEN
    IF (NSTEP .GT. MS) GO TO 699
    WRITE (IOUT,787) NSTEP, IDENT(NSTEP)
787 FORMAT(' SPECIES', I3, ' = ', A)
    GO TO 547
    END IF
    IF (NSTEP .GT. 1) STOP = .FALSE.
549 IF (VER .OR. IBEG .EQ. 3) THEN
    IRE = 1
    ELSE
    IF (NR .EQ. -3 .OR. NR .EQ. -1 .OR. NR .GT. 9) CALL READUT(1,1)
    IRE = -1
    END IF
    RETURN
501 IF (NR + 4) 541,541,699
541 IF (STEP .AND. NS .GT. 0) CALL READUT(-2,NS)
    IRE = 0
    RETURN
    END
C
C
C
C
C    SUBROUTINE READUT is called upon to insure data has been entered
C    correctly and to indicate that a file SGWNEW has been created.
C    SGWNEW is formed at all times; even if a file is only executed.
```

```
C
C
C
      SUBROUTINE READUT(NR,NS)
      IMPLICIT REAL*8(A-H,O-Z)
      COMMON /SGRD/ STEP, STOP, VER, IN, IND, IOUT, IRE, IUT, IXT,
     *KVALM, KVAL1, MCO, MV, NCFN
      COMMON /TXT1/ INDFIL, ITEXT
      CHARACTER ICHR*1, INDFIL*9, ITEXT*80
      LOGICAL STEP, STOP, VER
      IF (NR .EQ. -4) THEN
      WRITE (IOUT,775)
775   FORMAT(/' *** THE DATA FILE CREATED HAS THE NAME SGWNEW ***')
      STOP
      ELSE IF (NR .LT. -1) THEN
      IF (NR .EQ. -2) THEN
      READ (IND,604,END=605) (ICHR, N = 1, NS)
604   FORMAT(A)
      RETURN
      END IF
605   STEP = .FALSE.
      STOP = .TRUE.
      WRITE (IOUT,769) INDFIL(:NCFN)
769   FORMAT(' *** END-OF-FILE ENCOUNTERED ON ', A, ', FORWARD NOT ALLOW
     *ED ***')
      IF (IRE .EQ. 1) IRE = 2
      RETURN
      ELSE IF (NR .EQ. -1) THEN
      WRITE (IOUT,656)
656   FORMAT(' *** ILLEGAL INPUT, TRY AGAIN| ***')
      REWIND IN
      RETURN
      ELSE IF (NR .GT. 0) THEN
      DO 606 N = 1, NR
606   BACKSPACE IUT
      END IF
      IF (.NOT. STEP .OR. NS .EQ. 0) RETURN
      DO 561 N = 1, NS
561   BACKSPACE IND
      RETURN
      END
```

APPENDIX III

The Mathematical Model for SOLGASWATER

The following model derivation is the basis for the SOLGASWATER program. It is a combination of the models described and developed by White et al. (1958) and Eriksson (1979); however, it is presented here in much more detail. The model is based on the thermodynamic fact that a system in equilibrium is a system with a minimum free energy.

The free energy, F(X), of a mixture is equivalent to the sum of the free energies, f, of individual species, i, in the mixture which is at constant temperature and pressure:

$$F(X) = \sum f_i, \quad i = 1 \text{ to } n \qquad [1]$$

where,

$$f_i = x_i[(F^o/RT)_i + \ln P + \ln(x_i/\bar{x})], \qquad [2]$$

x_i = unknown equilibrium composition of species i,

$(F^o/RT)_i$ = standard free energy function of species i,

P = total pressure in atmospheres,

n = total number of species, and

$$\bar{x} = \sum x_i, \quad i = 1 \text{ to } n \text{ by definition.} \qquad [3]$$

Substituting C_i for the constant $[(F^o/RT)_i + \ln P]$ gives

$$F(X) = \sum x_i[C_i + \ln(x_i/\bar{x})]. \qquad [4]$$

Obviously, x_i should satisfy the mass balance constraint

$$b_j = \sum a_{ij}x_i, \quad i = 1 \text{ to } n \text{ and } j = 1 \text{ to } m \qquad [5]$$

where,

b$_j$ = total weight of component j in the mixture,

a$_{ij}$ = stoichiometry of j in species i, and

m = total number of components in the mixture.

Therefore, x$_i$ must be non-negative. Assuming non-negative values of y$_i$ satisfy the mass balance constraint, then the free energy function becomes

$$F(Y) = \sum[C_i y_i + y_i \ln(y_i/\bar{y})], \quad i = 1 \text{ to } n, \quad [6]$$

where the following terms are defined for i = 1 to n,

$$\bar{y} = \sum y_i, \quad [7]$$

$$\Delta_i = x_i - y_i, \text{ and} \quad [8]$$

$$\bar{\Delta} = \bar{x} - \bar{y}. \quad [9]$$

If the terms beyond the quadratic are considered negligible, a Taylor's expansion about Y is, by definition, equivalent to the following:

$$Q(X) = F(Y) + \left.\sum\frac{dF}{dy_i}\right|_{X=Y} \Delta_i + 1/2\sum\sum\left.\frac{d^2F}{dy_i dy_k}\right|_{X=Y} \Delta_i \Delta_k \quad [10]$$

$$[10a] \qquad\qquad\qquad [10b]$$

where, dF is the first partial of F(Y) with respect to y$_i$ and d^{2}F is the second. Solving the first partial, Equation [10a], and the second partial, Equation [10b], yields:

a. $dF/dy_i = d/dy_i\sum[C_i y_i + y_i \ln(y_i/\bar{y})]$

$$= \sum[d/dy_i(C_iy_i) + d/dy_i\{y_i\ln(y_i/\overline{y})\}]$$

$$= \sum[C_i + \ln(y_i/\overline{y}) + y_i(\overline{y}/y_i)\cdot d/dy_i(y_i/\overline{y})]$$

$$= \sum[C_i + \ln(y_i/\overline{y}) + \overline{y}(\overline{y} - y_i)/\overline{y}^2]$$

$$= \sum[C_i + \ln(y_i/\overline{y}) + (\overline{y} - y_i)/\overline{y}]$$

$$= \sum[C_i + \ln(y_i/\overline{y})]. \tag{11}$$

Substituting Equations [8] and [11] into Equation [10a]:

$$\sum\left.\frac{dF}{dy_i}\right|_{X=Y}\Delta_i = \sum[(C_i + \ln(y_i/\overline{y}))(x_i - y_i)]. \tag{12}$$

b. $$d^2F/dy_i^2 = d/dy_i\sum[C_i + \ln(y_i/\overline{y})]$$

$$= \sum[d/dy_i\ln(y_i/\overline{y})]$$

$$= \sum[(y/y_i)\{(\overline{y} - y_i)/\overline{y}^2\}]$$

$$= \sum[(\overline{y} - y_i)/y_i\overline{y}]$$

$$= \sum[1/y_i - 1/\overline{y}] \quad \text{when } i = k; \tag{13}$$

$$= -1/\overline{y} \quad \text{when } i \neq k. \tag{14}$$

Substituting Equations [13] and [14] into Equation [10b] and noting, because $k = i$, $\sum\Delta_k = \overline{\Delta}_k = (\overline{x} - x_i) - (\overline{y} - y_i)$:

$$1/2\sum\sum\left.\frac{d^2F}{dy_idy_k}\right|_{X=Y}\Delta_i\Delta_k = 1/2\sum[(-\Delta_i/\overline{y})\{(\overline{x} - \overline{y}) - (x_i - y_i)\}$$
$$+ (\Delta_i^2/y_i - \Delta_i^2/\overline{y})] \tag{15}$$

$$= 1/2\sum[(-\Delta_i/\overline{y})(\overline{\Delta} - \Delta_i) + (\Delta_i^2/y_i - \Delta_i^2/\overline{y})]$$

$$= 1/2\sum[\Delta_i^2/y_i - \overline{\Delta}\Delta_i/y]$$

$$= 1/2\sum[\Delta_i(\Delta_i/y_i - \overline{\Delta}/\overline{y}]$$

$$= 1/2\sum(x_i-y_i)[(x_i-y_i)/y_i - (\overline{x}-\overline{y})/\overline{y}]$$

$$= 1/2\sum(x_i - y_i)[x_i/y_i - \bar{x}/\bar{y}]$$

$$= 1/2\sum[x_i^2/y_i - x_i\bar{x}/\bar{y} + y_i\bar{x}/\bar{y} - x_i]. \quad [16]$$

Substituting A(Y) and B(Y) for Equations [12] and [16] in [10]:

$$Q(X) = F(Y) + A(Y) + B(Y), \quad [17]$$

where,

$$F(Y) = \sum[C_iy_i + y_i\ln(y_i/\bar{y})] \quad [18]$$

$$A(Y) = \sum[(C_i + \ln(y_i/\bar{y}))(x_i - y_i)] \quad [19]$$

$$B(Y) = 1/2\sum[x_i^2/y_i - x_i\bar{x}/\bar{y} + y_i\bar{x}/\bar{y} - x_i]. \quad [20]$$

Rewriting the mass balance constraint:

$$-\sum a_{ij}x_i + b_j = 0. \quad [21]$$

Using the method of Lagrange multipliers to solve Equation [17] subject to Equation [21] gives, where π_j are the Lagrange multipliers and G(X) is a new function:

$$G(X) = Q(X) + \sum_{j=1}^{m}\pi_j(-\sum_{i=1}^{n}a_{ij}x_i + b_j). \quad [22]$$

Since the free energy is to be minimized and the x_i values are to be solved, the derivative of Equation [22] is taken with respect to x_i and set equal to zero:

$$dG/dx_i = dQ/dx_i + d/dx_i[\sum\pi_j(-\sum a_{ij}x_i + b_j)]$$

$$= dF/dx_i + dA/dx_i + dB/dx_i - \sum\pi a_{ij};$$

$$dF/dx_i = d/dx_i[C_iy_i + y_i\ln(y_i/\overline{y})]$$
$$= 0,$$

$$dA/dx_i = d/dx_i[(C_i + \ln(y_i/\overline{y}))(x_i - y_i)]$$
$$= C_i + \ln(y_i/\overline{y}), \text{ and}$$

$$dB/dx_i = d/dx_i \ [1/2(x_i^2/y_i - x_i\overline{x}/\overline{y} + y_i\overline{x}/\overline{y} - x_i)]$$
$$= 1/2[2x_i/y_i - \overline{x}/\overline{y} - 1]$$
$$= 1/2[2x_i/y_i - 2\overline{x}/\overline{y}] \quad (\text{* see note})$$
$$= x_i/y_i - \overline{x}/\overline{y}.$$

* Note: At the desired minimum, X = Y. Hence, $\overline{x}/\overline{y} = 1$.

$$dG/dx_i = C_i + \ln(y_i/\overline{y}) + x_i/y_i - \overline{x}/\overline{y} - \sum\pi_j a_{ij} \qquad [23]$$

Setting Equation [23] to zero and solving for x_i:

$$x_i = -y_i[C_i + \ln(y_i/\overline{y})] + y_i\sum\pi_j a_{ij} + \overline{x}y_i/\overline{y}$$
$$x_i = -f_i + y_i\sum\pi_j a_{ij} + \overline{x}y_i/\overline{y}, \qquad [24]$$

where f_i comes from Equation [2]. Summing Equation [24]:

$$\overline{x} = -\sum f_i + \sum\pi_j\sum a_{ij}y_i + (\sum y_i/\overline{y})\overline{x}$$
$$\overline{x} = -\sum f_i + \sum\pi_j b_j + \overline{x}$$
$$\sum f_i = \sum\pi_j b_j. \qquad [25]$$

The free energy function, F, is therefore related to the
Lagrange multipliers, π, for each component, j, and the
total weight, b, of each component in the system. However,
a system of aqueous species employs the following common

free energy function:

$$F = F^O + RT\ln K, \qquad [26]$$

where, F^O is the standard free energy function, R is the gas constant, T is the temperature and K is the equilibrium constant for the system. Therefore, Equation [26] is the sum of the free energies of all species, n, in the system. The free energy for an individual species is, however,

$$f_i = (F_i{}^O + RT\ln z_i)x_i, \qquad [27]$$

where $F_i{}^O$ is the standard free energy of species i and z_i is the activity of species i. Substituting Equations [1], [5], and [25]:

$$[(F_i{}^O + RT\ln z_i)x_i] = RT\sum\pi_j\sum a_{ij}x_i. \qquad [28]$$

Factoring out common terms and rearranging Equation [28]:

$$F_i{}^O/RT + \ln z_i = \sum\pi_j a_{ij}. \qquad [29]$$

Replacing z_i with $c_i x_i$ where c_i is the activity coefficient:

$$F_i{}^O/RT + \ln c_i + \ln x_i = \sum\pi_j a_{ij}$$
$$\sum\pi_j a_{ij} - F_i{}^O/RT - \ln c_i - \ln x_i = 0. \qquad [30]$$

Assuming values of y_i satisfy the mass balance constraint, then the free energy function, F, becomes

$$F(Y) = \sum\pi_j a_{ij} - F_i{}^O/RT - \ln c_i - \ln y_i. \qquad [31]$$

Employing another Taylor's expansion about Y:

$$G(X) = F(Y) + \sum \frac{dF}{dy_i}\Big|_{X=Y} \Delta_i + 1/2 \sum \sum \frac{d^2F}{dy_i dy_k}\Big|_{X=Y} \Delta_i \Delta_k. \quad [32]$$

Solving the derivatives as before:

$$dF/dy_i = d/dy_i [\sum \pi_j a_{ij} - F_i^o/RT - \ln c_i - \ln x_i]$$

$$= -1/y_i; \quad [33]$$

$$d^2F/dy_i^2 = d/dy_i(-1/y_i)$$

$$= 1/y_i^2 \quad \text{for } k = i; \quad [34]$$

$$d^2F/dy_i dy_k = d/dy_k(-1/y_i)$$

$$= 0 \quad \text{for } k \neq i. \quad [35]$$

Substituting Equations [33], [34] and [35] in Equation [32] and summing over i:

$$G(X) = F(Y) - \Delta_i/y_i + \Delta_i^2/2y_i^2 \quad [36]$$

Equation [36] is, however, equivalent to zero:

$$F(Y) - \Delta_i/y_i + \Delta_i^2/2y_i^2 = 0$$

$$y_i^2[F(Y)] - y_i(x_i - y_i) + 1/2(x_i - y_i)^2 = 0$$

$$y_i^2[F(Y)] + 1/2x_i^2 - 2x_i y_i + 3/2y_i^2 = 0. \quad [37]$$

Substituting Equation [31]:

$$y_i^2[\sum \pi_j a_{ij} - F_i^o/RT - \ln c_i - \ln y_i] + 1/2x_i^2 - 2x_i y_i + 3/2y_i^2 = 0$$

$$y_i^2[\sum \pi_j a_{ij} - F_i^o/RT - \ln c_i] - y_i^2 \ln y_i + 1/2x_i^2 - 2x_i y_i + 3/2y_i^2 = 0.$$

Taking the derivative with respect to y_i:

$$2y_i[\sum \pi_j a_{ij} - F_i^o/RT - \ln c_i] - [2y_i \ln y_i + y_i] - 2x_i + 3y_i = 0$$

$$y_i[\sum \pi_j a_{ij} - F_i^o/RT - \ln c_i] - y_i \ln y_i - x_i + y_i = 0.$$

Solving for x_i:

$$x_i = y_i[\sum \pi_j a_{ij} - F_i^o/RT - \ln c_i - \ln y_i + 1]$$

$$x_i = y_i[\sum \pi_j a_{ij}] - y_i[F_i^o/RT + \ln c_i + \ln y_i - 1].$$

Substituting Ψ_i for $-y_i[F_i^o/RT + \ln c_i + \ln y_i - 1]$:

$$x_i = y_i[\sum \pi_j a_{ij}] + \Psi_i. \qquad [38]$$

Substituting back into the mass balance equation:

$$b_j = \sum a_{ij}[y_i \sum \pi_k a_{ik} + \Psi_i]$$

$$b_j = \sum a_{ij}\Psi_i + \sum\sum a_{ij} a_{ik} y_i \pi_k.$$

Substituting r_{jk} for $\sum a_{ij} a_{ik} y_i$:

$$b_j = \sum a_{ij}\Psi_i + \sum r_{jk}\pi_k. \qquad [39]$$

However, if species i is a solid, Equation [31] becomes

$$\sum \pi_j a_{ij} - F_i^o/RT = 0. \qquad [40]$$

Substituting in the mass balance equation:

$$\sum \pi_j b_j/x_i = F_i^o/RT$$

$$\sum \pi_j b_j = x_i F_i^o/RT. \qquad [41]$$

From Equation [41], the free energy contribution of a solid

is directly proportional to the amount of the solid present. Hence, Equation [39] becomes

$$b_j = \sum r_{jk}\pi_k + \sum a_{ij}\Psi_i + \sum a_{ij}x_i. \qquad [42]$$

Rearranging and showing the bounds on the summations:

$$\sum_{k=1}^{m} r_{jk}\pi_k + \sum_{i=n+1}^{nt} a_{ij}x_i = b_j - \sum_{i=1}^{n} a_{ij}\Psi_i, \quad j = 1 \text{ to } m \qquad [43]$$

where,

m = total number of components in the system,

nt = total number of species in the system, and

n = total number of aqueous species in the system.

Equations [40] and [43] are solved simultaneously by Gaussian Elimination for the π_k values. Equation [38] is then used to solve for the x_i values.

APPENDIX IV

The Derivation of Log K_f Values for Gases

Free energy data is presented to SOLGASWATER as logarithms of formation (ie. reaction) constants, K_f, based based on the Gibbs' free energy change equation:

$$\Delta G^O = -2.303RTlogK_f. \qquad [1]$$

However, the following derivation shows that the log K_f of reactions involving gases are also dependent on the log of the product between the temperature, T, and gas constant, R.

Assuming a reaction, Reactants = Products + Gas, occurs, then, by definition, the K_f for the reaction is

$$K_f = P_{gas}\Pi[Products]/\Pi[Reactants], \qquad [2]$$

where,

P_{gas} = Pressure of the gaseous product in atmospheres,

$\Pi[Products]$ = multiplication of product concentrations, and

$\Pi[Reactants]$ = multiplication of reactant concentrations.

Letting $Y = \Pi[Products]/\Pi[Reactants]$, Equation [2] becomes

$$K_f = P_{gas}Y. \qquad [3]$$

Assuming the gas behaves ideally then, from PV = nRT:

$$P_{gas} = nRT/V. \qquad [4]$$

From the definition of concentration, n/V is replaced by C:

$$P_{gas} = CRT. \qquad [5]$$

Substituting Equation [5] into Equation [3] gives

$$K_f = CRTY. \qquad [6]$$

Taking the log of both sides, expanding, and rearranging:

$$\log CY = \log K_f - \log RT. \qquad [7]$$

Substituting R = .082 l·atm/mol·K and T = 298.15K yields

$$\log CY = \log K_f - 1.3882. \qquad [8]$$

Therefore, log CY is entered into SOLGASWATER and log K_f is calculated from Equation [1].

APPENDIX V

The Minimization of Log K_f Values

Using Cu^{2+}, HS^-, H^+ and e as the components in the copper-sulfur-ethyl xanthate-water system, the following reactions and log formation constants were determined for $H_2S(aq)$, $H_2SO_4(aq)$, Cu_2S and Cu_2O:

Reaction	Log K_f
1) $HS^- + H^+ = H_2S(aq)$	6.99
2) $HS^- + H_2O = H_2SO_4(aq) + 7H^+ + 8e$	-33.65
3) $2Cu^{2+} + HS^- + 2e = Cu_2S + H^+$	40.12
4) $2Cu^{2+} + H_2O + 2e = Cu_2O + 2H^+$	7.38

Some of the log K_f values shown are small or large enough to cause the SOLGASWATER program to have underflow or overflow problems. However a technique has been developed to help overcome them. This scheme has been used throughout this investigation.

Because a species identified with an asterisk in the tenth column will not be considered in the mass balance, a component can be invented strictly to minmize the log K_f values and, thereby, ease the underflow/overflow problems. The components for the above system could then become Cu^*, S^*, H^+ and e. However, the standard free energies for each of the invented species must be determined. This can be accomplished by using the largest and smallest formation constants for each component. For example, $H_2SO_4(aq)$ has the largest and $H_2S(aq)$ has the smallest formation constant

for the HS$^-$ component. In doing this, new reactions are determined as are the free energies of those reactions:

Invented Reaction	Free Energy
1) $S^* + 2H^+ + 2e = H_2S(aq)$	$48.778 - F_S^*$
2) $S^* + 4H_2O = H_2SO_4(aq) + 6H^+ + 6e$	$-6.66 - F_S^*$
3) $2Cu^* + S^* = Cu_2S$	$-20.45 - F_S^* - 2F_{Cu}^*$
4) $2Cu^* + H_2O = Cu_2O + 2H^+ + 2e$	$21.337 - 2F_{Cu}^*$

where F_S^* and F_{Cu}^* are the unknown standard free energies. Setting one free energy term equal to the opposite of the other for the same component and solving will yield the standard free energy of the invented species:

$$48.778 - F_S^* = 6.66 + F_S^*$$

$$F_S^* = 21.059$$

$$20.45 + F_S^* + 2F_{Cu}^* = 21.337 - 2F_{Cu}^*$$

$$41.509 + 2F_{Cu}^* = 21.337 - 2F_{Cu}^*$$

$$F_{Cu}^* = -5.043$$

This procedure is equivalent to subtracting one reaction from the other to form a reaction absent of invented species. Then the free energy of this reaction is divided by the total number of invented species deleted from the two original reactions to yield the standard free energy of the invented species. In either case, the following log K_f values result:

	Invented Reaction	Log K_f
1)	$S^* + 2H^+ + 2e = H_2S(aq)$	20.32
2)	$S^* + 4H_2O = H_2SO_4(aq) + 6H^+ + 6e$	-20.32
3)	$2Cu^* + S^* = Cu_2S$	23.04
4)	$2Cu^* + H_2O = Cu_2O + 2H^+ + 2e$	-23.04

Comparing the log K_f values, the large and small values are better; but other values were sacrificed. Nevertheless, the the underflow/overflow problems were nearly eliminated.

APPENDIX VI

The Input and Output of SOLGASWATER

CHALCOCITE OXIDATION TO METASTABLE SPECIES WITH XANTHATE

5	1	23	13					

' E- '	0.000000E+00	1.0	0.0	0.0	0.0	0.0
' H+ '	0.000000E+00	0.0	1.0	0.0	0.0	0.0
' CU TOTAL* '	0.000000E+00	0.0	0.0	1.0	0.0	0.0
' S TOTAL* '	0.000000E+00	0.0	0.0	0.0	1.0	0.0
' X TOTAL* '	0.000000E+00	0.0	0.0	0.0	0.0	1.0
' CU+ '	-8.95971	-1.0	0.0	1.0	0.0	0.0
' CU+2 '	-11.5988	-2.0	0.0	1.0	0.0	0.0
' CUOH+ '	-18.9201	-2.0	-1.0	1.0	0.0	0.0
' CU2OH2+2 '	-34.1747	-4.0	-2.0	2.0	0.0	0.0
' CUOH2 AQ '	-25.8308	-2.0	-2.0	1.0	0.0	0.0
' CUOH3-1 '	-37.8878	-2.0	-3.0	1.0	0.0	0.0
' CUOH4-2 '	-51.0004	-2.0	-4.0	1.0	0.0	0.0
' H2S AQ '	9.30499	2.0	2.0	0.0	1.0	0.0
' HS- '	2.31140	2.0	1.0	0.0	1.0	0.0
' S-2 '	-10.6055	2.0	0.0	0.0	1.0	0.0
' S2-2 '	-5.08318	2.0	0.0	0.0	2.0	0.0
' S3-2 '	0.36581	2.0	0.0	0.0	3.0	0.0
' S4-2 '	5.59587	2.0	0.0	0.0	4.0	0.0
' S5-2 '	10.6040	2.0	0.0	0.0	5.0	0.0
' H2S G '	8.91378	2.0	2.0	0.0	1.0	0.0
' X- '	-2.48221	1.0	0.0	0.0	0.0	1.0
' HX '	-0.84011	1.0	1.0	0.0	0.0	1.0
' X2 AQ '	-7.83810	0.0	0.0	0.0	0.0	2.0
' X2 L '	-2.93379	0.0	0.0	0.0	0.0	2.0
' CUX '	7.83810	0.0	0.0	1.0	0.0	1.0
' CUX2 '	7.63577	0.0	0.0	1.0	0.0	2.0
' CU '	-0.08944	0.0	0.0	1.0	0.0	0.0
' CU2S '	19.2353	0.0	0.0	2.0	1.0	0.0
' CU1.93S '	18.9043	0.0	0.0	1.93	1.0	0.0
' CU1.83S '	18.3268	0.0	0.0	1.83	1.0	0.0
' CU1.67S '	17.3148	0.0	0.0	1.67	1.0	0.0
' CU1.38S '	15.3614	0.0	0.0	1.38	1.0	0.0
' CUS '	12.5731	0.0	0.0	1.0	1.0	0.0
' S '	4.42267	0.0	0.0	0.0	1.0	0.0
' CUO '	-19.2353	-2.0	-2.0	1.0	0.0	0.0
' CU2O '	-15.8206	-2.0	-2.0	2.0	0.0	0.0

1	2	3	4	5								
20	0	0	0	0								

8
2

40	2	1	2	6	2	7	2	8	2	9	2	10	2
11	2	12	2	1	2	13	2	14	2	15	2	16	2
17	2	18	2	19	2	1	2	20	2	21	2	22	2
23	2	24	2	25	2	26	2	21	2	27	2	28	2
29	2	30	2	31	2	32	2	33	2	1	2	34	2
35	2	36	6	3	6	4	6	5	2	2			
36	1												

10	9	2	2	2

0.676176E+00   -0.169044E+00
-9.500000E+00
0.118000E+00
0.590000E-01
0.100000E-04
10

```
COL  1    LOG C FOR   E-
COL  2    LOG C FOR   CU+
COL  3    LOG C FOR   CU+2
COL  4    LOG C FOR   CUOH+
COL  5    LOG C FOR   CU2OH2+2
COL  6    LOG C FOR   CUOH2 AQ
COL  7    LOG C FOR   CUOH3-1
COL  8    LOG C FOR   CUOH4-2

COL  9    LOG C FOR   E-
COL 10    LOG C FOR   H2S AQ
COL 11    LOG C FOR   HS-
COL 12    LOG C FOR   S-2
COL 13    LOG C FOR   S2-2
COL 14    LOG C FOR   S3-2
COL 15    LOG C FOR   S4-2
COL 16    LOG C FOR   S5-2

COL 17    LOG C FOR   E-
COL 18    LOG C FOR   H2S G
COL 19    LOG C FOR   X-
COL 20    LOG C FOR   HX
COL 21    LOG C FOR   X2 AQ
COL 22    LOG C FOR   X2 L
COL 23    LOG C FOR   CUX
COL 24    LOG C FOR   CUX2

COL 25    LOG C FOR   E-
COL 26    LOG C FOR   CU
COL 27    LOG C FOR   CU2S
COL 28    LOG C FOR   CU1.93S
COL 29    LOG C FOR   CU1.83S
COL 30    LOG C FOR   CU1.67S
COL 31    LOG C FOR   CU1.38S
COL 32    LOG C FOR   CUS

COL 33    LOG C FOR   E-
COL 34    LOG C FOR   S
COL 35    LOG C FOR   CUO
COL 36    LOG C FOR   CU2O
COL 37    LOG ABS(TF) FOR CU TOTAL*
COL 38    LOG ABS(TF) FOR  S TOTAL*
COL 39    LOG ABS(TF) FOR  X TOTAL*
COL 40    LOG C FOR   H+

LOG A FOR H+         =  -9.50000E+00
TC FOR CU TOTAL* =   1.18000E-01
TC FOR   S TOTAL* =   5.90000E-02
TC FOR   X TOTAL* =   1.00000E-05
```

COL 1	COL 2	COL 3	COL 4	COL 5	COL 6	COL 7	COL 8
E-	CU+	CU+2	CUOH+	CU2OH2+2	CUOH2 AQ	CUOH3-1	CUOH4-2
-0.04000	-14.36446	-17.67972	-15.50102	-27.33655	-12.91172	-15.46872	-19.08132
-0.03000	-14.19541	-17.34164	-15.16294	-26.66037	-12.57364	-15.13064	-18.74324
-0.02000	-14.02637	-17.00355	-14.82485	-25.98419	-12.23555	-14.79255	-18.40515
-0.01000	-13.85733	-16.66546	-14.48676	-25.30802	-11.89746	-14.45446	-18.06706
0.00000	-13.68828	-16.32737	-14.14867	-24.63184	-11.55937	-14.11637	-17.72897
0.01000	-13.51924	-15.98928	-13.81058	-23.95567	-11.22128	-13.77828	-17.39088
0.02000	-13.35019	-15.65120	-13.47250	-23.27949	-10.88320	-13.44020	-17.05280
0.03000	-13.18115	-15.31311	-13.13441	-22.60331	-10.54511	-13.10211	-16.71471
0.04000	-13.01211	-14.97502	-12.79632	-21.92714	-10.20702	-12.76402	-16.37662
0.05000	-12.84306	-14.63693	-12.45823	-21.25096	-9.86893	-12.42593	-16.03853
0.06000	-12.67402	-14.29884	-12.12014	-20.57479	-9.53084	-12.08784	-15.70044
0.07000	-12.50497	-13.96076	-11.78206	-19.89861	-9.19276	-11.74976	-15.36236
0.08000	-12.33593	-13.62267	-11.44397	-19.22243	-8.85467	-11.41167	-15.02427
0.09000	-12.16689	-13.28458	-11.10588	-18.54626	-8.51658	-11.07358	-14.68618
0.10000	-11.99784	-12.94649	-10.76779	-17.87008	-8.17849	-10.73549	-14.34809
0.11000	-11.82880	-12.60840	-10.42970	-17.19391	-7.84040	-10.39740	-14.01000
0.12000	-11.65975	-12.27032	-10.09162	-16.51773	-7.50232	-10.05932	-13.67192
0.13000	-11.49071	-11.93223	-9.75353	-15.84155	-7.16423	-9.72123	-13.33383
0.14000	-11.32167	-11.59414	-9.41544	-15.16538	-6.82614	-9.38314	-12.99574
0.15000	-11.26007	-11.36350	-9.18480	-14.70410	-6.59550	-9.15250	-12.76510
0.16000	-11.42911	-11.36350	-9.18480	-14.70410	-6.59550	-9.15250	-12.76510
0.17000	-11.59816	-11.36350	-9.18480	-14.70410	-6.59550	-9.15250	-12.76510
0.18000	-11.76720	-11.36350	-9.18480	-14.70410	-6.59550	-9.15250	-12.76510
0.19000	-11.93625	-11.36350	-9.18480	-14.70410	-6.59550	-9.15250	-12.76510
0.20000	-12.10529	-11.36350	-9.18480	-14.70410	-6.59550	-9.15250	-12.76510
0.21000	-12.27433	-11.36350	-9.18480	-14.70410	-6.59550	-9.15250	-12.76510
0.22000	-12.44338	-11.36350	-9.18480	-14.70410	-6.59550	-9.15250	-12.76510
0.23000	-12.61242	-11.36350	-9.18480	-14.70410	-6.59550	-9.15250	-12.76510
0.24000	-12.78147	-11.36350	-9.18480	-14.70410	-6.59550	-9.15250	-12.76510
0.25000	-12.95051	-11.36350	-9.18480	-14.70410	-6.59550	-9.15250	-12.76510
0.26000	-13.11955	-11.36350	-9.18480	-14.70410	-6.59550	-9.15250	-12.76510
0.27000	-13.28860	-11.36350	-9.18480	-14.70410	-6.59550	-9.15250	-12.76510
0.28000	-13.45764	-11.36350	-9.18480	-14.70410	-6.59550	-9.15250	-12.76510
0.29000	-13.62669	-11.36350	-9.18480	-14.70410	-6.59550	-9.15250	-12.76510
0.30000	-13.79573	-11.36350	-9.18480	-14.70410	-6.59550	-9.15250	-12.76510
0.31000	-13.96477	-11.36350	-9.18480	-14.70410	-6.59550	-9.15250	-12.76510

COL 9 E-	COL 10 H2S AQ	COL 11 HS-	COL 12 S-2	COL 13 S2-2	COL 14 S3-2	COL 15 S4-2	COL 16 S5-2
-0.04000	-18.12082	-15.61441	-19.03131	-23.28714	-27.61631	-32.16441	-36.93443
-0.03000	-18.45890	-15.95249	-19.36939	-23.62523	-27.95440	-32.50249	-37.27252
-0.02000	-18.79699	-16.29058	-19.70748	-23.96332	-28.29249	-32.84058	-37.61061
-0.01000	-19.13508	-16.62867	-20.04557	-24.30141	-28.63057	-33.17867	-37.94870
0.00000	-19.47317	-16.96676	-20.38366	-24.63949	-28.96866	-33.51676	-38.28679
0.01000	-19.81126	-17.30485	-20.72175	-24.97758	-29.30675	-33.85485	-38.62487
0.02000	-20.14934	-17.64293	-21.05983	-25.31567	-29.64484	-34.19293	-38.96296
0.03000	-20.48743	-17.98102	-21.39792	-25.65376	-29.98293	-34.53102	-39.30105
0.04000	-20.82552	-18.31911	-21.73601	-25.99185	-30.32101	-34.86911	-39.63914
0.05000	-21.16361	-18.65720	-22.07410	-26.32993	-30.65910	-35.20720	-39.97723
0.06000	-21.50170	-18.99529	-22.41219	-26.66802	-30.99719	-35.54529	-40.31531
0.07000	-21.83978	-19.33337	-22.75027	-27.00611	-31.33528	-35.88337	-40.65340
0.08000	-22.17787	-19.67146	-23.08836	-27.34420	-31.67337	-36.22146	-40.99149
0.09000	-22.51596	-20.00955	-23.42645	-27.68229	-32.01145	-36.55955	-41.32958
0.10000	-22.85405	-20.34764	-23.76454	-28.02037	-32.34954	-36.89764	-41.66767
0.11000	-23.19214	-20.68573	-24.10263	-28.35846	-32.68763	-37.23573	-42.00575
0.12000	-23.53022	-21.02381	-24.44071	-28.69655	-33.02572	-37.57381	-42.34384
0.13000	-23.86831	-21.36190	-24.77880	-29.03464	-33.36381	-37.91190	-42.68193
0.14000	-24.20640	-21.69999	-25.11689	-29.37273	-33.70189	-38.24999	-43.02002
0.15000	-24.33711	-21.83070	-25.24760	-29.29606	-33.41785	-37.75858	-42.32123
0.16000	-24.02269	-21.51628	-24.93318	-28.32913	-31.79841	-35.48662	-39.39677
0.17000	-23.70827	-21.20186	-24.61876	-27.36220	-30.17897	-33.21467	-36.47230
0.18000	-23.40137	-20.89496	-24.31186	-26.41032	-28.58211	-30.97284	-33.58549
0.19000	-23.12076	-20.61435	-24.03125	-25.51101	-27.06410	-28.83612	-30.83007
0.20000	-22.87238	-20.36597	-23.78287	-24.67616	-25.64279	-26.82834	-28.23582
0.21000	-22.68318	-20.17677	-23.59367	-23.95968	-24.39901	-25.05727	-25.93747
0.22000	-22.55471	-20.04830	-23.46520	-23.36464	-23.33741	-23.52912	-23.94275
0.23000	-22.50341	-19.99700	-23.41390	-22.92396	-22.50734	-22.30966	-22.33390
0.24000	-22.50341	-19.99700	-23.41390	-22.58587	-21.83117	-21.29539	-20.98155
0.25000	-22.56988	-20.06347	-23.48037	-22.38072	-21.35440	-20.54701	-19.96155
0.26000	-22.90797	-20.40156	-23.81846	-22.71881	-21.69249	-20.88510	-20.29964
0.27000	-23.24606	-20.73965	-24.15655	-23.05690	-22.03058	-21.22319	-20.63773
0.28000	-23.58414	-21.07773	-24.49463	-23.39498	-22.36866	-21.56127	-20.97581
0.29000	-23.92223	-21.41582	-24.83272	-23.73307	-22.70675	-21.89936	-21.31390
0.30000	-24.26032	-21.75391	-25.17081	-24.07116	-23.04484	-22.23745	-21.65199
0.31000	-24.59841	-22.09200	-25.50890	-24.40925	-23.38293	-22.57554	-21.99008

COL 17 E-	COL 18 H2S G	COL 19 X-	COL 20 HX	COL 21 X2 AQ	COL 22 X2 L	COL 23 CUX	COL 24 CUX2
-0.04000	-18.51203	-5.00000	-12.85790	-14.22603	0.00000	0.00000	0.00000
-0.03000	-18.85011	-5.08461	-12.94251	-14.05716	0.00000	-5.75200	0.00000
-0.02000	-19.18820	-5.25365	-13.11155	-14.05716	0.00000	-5.35422	0.00000
-0.01000	-19.52629	-5.42269	-13.28059	-14.05716	0.00000	-5.20610	0.00000
0.00000	-19.86438	-5.59174	-13.44964	-14.05716	0.00000	-5.12843	0.00000
0.01000	-20.20247	-5.76078	-13.61868	-14.05716	0.00000	-5.08274	0.00000
0.02000	-20.54055	-5.92983	-13.78773	-14.05716	0.00000	-5.05430	0.00000
0.03000	-20.87864	-6.09887	-13.95677	-14.05716	0.00000	-5.03604	0.00000
0.04000	-21.21673	-6.26791	-14.12581	-14.05716	0.00000	-5.02409	0.00000
0.05000	-21.55482	-6.43696	-14.29486	-14.05716	0.00000	-5.01618	0.00000
0.06000	-21.89291	-6.60600	-14.46390	-14.05716	0.00000	-5.01089	0.00000
0.07000	-22.23099	-6.77505	-14.63295	-14.05716	0.00000	-5.00735	0.00000
0.08000	-22.56908	-6.94409	-14.80199	-14.05716	0.00000	-5.00497	0.00000
0.09000	-22.90717	-7.11313	-14.97103	-14.05716	0.00000	-5.00336	0.00000
0.10000	-23.24526	-7.28218	-15.14008	-14.05716	0.00000	-5.00227	0.00000
0.11000	-23.58335	-7.45122	-15.30912	-14.05716	0.00000	-5.00154	0.00000
0.12000	-23.92143	-7.62027	-15.47817	-14.05716	0.00000	-5.00104	0.00000
0.13000	-24.25952	-7.78931	-15.64721	-14.05716	0.00000	-5.00071	0.00000
0.14000	-24.59761	-7.95835	-15.81625	-14.05716	0.00000	-5.00048	0.00000
0.15000	-24.72832	-8.01995	-15.87785	-13.84226	0.00000	-5.00041	0.00000
0.16000	-24.41390	-7.85091	-15.70881	-13.16608	0.00000	-5.00061	0.00000
0.17000	-24.09948	-7.68186	-15.53976	-12.48991	0.00000	-5.00090	0.00000
0.18000	-23.79258	-7.51282	-15.37072	-11.81373	0.00000	-5.00134	0.00000
0.19000	-23.51197	-7.34377	-15.20167	-11.13756	0.00000	-5.00197	0.00000
0.20000	-23.26359	-7.17473	-15.03263	-10.46138	0.00000	-5.00292	0.00000
0.21000	-23.07439	-7.00569	-14.86359	-9.78520	0.00000	-5.00432	0.00000
0.22000	-22.94592	-6.83664	-14.69454	-9.10903	0.00000	-5.00644	0.00000
0.23000	-22.89462	-6.66760	-14.52550	-8.43285	0.00000	-5.00977	0.00000
0.24000	-22.89462	-6.49855	-14.35645	-7.75668	0.00000	-5.01558	0.00000
0.25000	-22.96109	-6.41775	-14.27564	-7.25697	0.00000	0.00000	-5.32298
0.26000	-23.29918	-6.41774	-14.27564	-6.91888	0.00000	0.00000	-5.32898
0.27000	-23.63727	-6.41775	-14.27564	-6.58079	0.00000	0.00000	-5.34234
0.28000	-23.97535	-6.41774	-14.27564	-6.24271	0.00000	0.00000	-5.37294
0.29000	-24.31344	-6.41775	-14.27564	-5.90462	0.00000	0.00000	-5.44815
0.30000	-24.65153	-6.41775	-14.27564	-5.56653	0.00000	0.00000	-5.67865
0.31000	-24.98962	-6.46167	-14.31957	-5.31630	0.00000	0.00000	0.00000

| COL 25 | COL 26 | COL 27 | COL 28 | COL 29 | COL 30 | COL 31 | COL 32 |
E-	CU	CU2S	CU1.93S	CU1.83S	CU1.67S	CU1.38S	CUS
-0.04000	0.00000	-1.22915	-11.74048	0.00000	0.00000	0.00000	0.00000
-0.03000	0.00000	-1.22933	-4.59709	0.00000	0.00000	0.00000	0.00000
-0.02000	0.00000	-1.22961	-4.19932	0.00000	0.00000	0.00000	0.00000
-0.01000	0.00000	-1.22980	-4.05119	0.00000	0.00000	0.00000	0.00000
0.00000	0.00000	-1.22993	-3.97353	0.00000	0.00000	0.00000	0.00000
0.01000	0.00000	-1.23002	-3.92784	0.00000	0.00000	0.00000	0.00000
0.02000	0.00000	-1.23008	-3.89940	0.00000	0.00000	0.00000	0.00000
0.03000	0.00000	-1.23012	-3.88114	0.00000	0.00000	0.00000	0.00000
0.04000	0.00000	-1.23014	-3.86919	0.00000	0.00000	0.00000	0.00000
0.05000	0.00000	-1.23016	-3.86127	0.00000	0.00000	0.00000	0.00000
0.06000	0.00000	-1.23017	-3.85598	0.00000	0.00000	0.00000	0.00000
0.07000	0.00000	-1.23018	-3.85242	0.00000	0.00000	0.00000	0.00000
0.08000	0.00000	-1.23019	-3.85000	0.00000	0.00000	0.00000	0.00000
0.09000	0.00000	-1.23019	-3.84832	0.00000	0.00000	0.00000	0.00000
0.10000	0.00000	-1.23020	-3.84708	0.00000	0.00000	0.00000	0.00000
0.11000	0.00000	-1.23020	-3.84600	0.00000	0.00000	0.00000	0.00000
0.12000	0.00000	-1.23020	-3.84477	0.00000	0.00000	0.00000	0.00000
0.13000	0.00000	-1.23021	-3.84282	0.00000	0.00000	0.00000	0.00000
0.14000	0.00000	-1.23022	-3.83910	0.00000	0.00000	0.00000	0.00000
0.15000	0.00000	0.00000	-1.22915	0.00000	0.00000	0.00000	0.00000
0.16000	0.00000	0.00000	-1.22915	0.00000	0.00000	0.00000	0.00000
0.17000	0.00000	0.00000	-1.22915	0.00000	0.00000	0.00000	0.00000
0.18000	0.00000	0.00000	0.00000	-1.22915	0.00000	0.00000	0.00000
0.19000	0.00000	0.00000	0.00000	-1.22915	0.00000	0.00000	0.00000
0.20000	0.00000	0.00000	0.00000	0.00000	-1.22915	0.00000	0.00000
0.21000	0.00000	0.00000	0.00000	0.00000	0.00000	-1.22915	0.00000
0.22000	0.00000	0.00000	0.00000	0.00000	0.00000	-1.22915	0.00000
0.23000	0.00000	0.00000	0.00000	0.00000	0.00000	0.00000	-1.22915
0.24000	0.00000	0.00000	0.00000	0.00000	0.00000	0.00000	-1.22915
0.25000	0.00000	0.00000	0.00000	0.00000	0.00000	0.00000	0.00000
0.26000	0.00000	0.00000	0.00000	0.00000	0.00000	0.00000	0.00000
0.27000	0.00000	0.00000	0.00000	0.00000	0.00000	0.00000	0.00000
0.28000	0.00000	0.00000	0.00000	0.00000	0.00000	0.00000	0.00000
0.29000	0.00000	0.00000	0.00000	0.00000	0.00000	0.00000	0.00000
0.30000	0.00000	0.00000	0.00000	0.00000	0.00000	0.00000	0.00000
0.31000	0.00000	0.00000	0.00000	0.00000	0.00000	0.00000	0.00000

COL 33 E-	COL 34 S	COL 35 CUO	COL 36 CU2O	COL 37 CU TOTAL*	COL 38 S TOTAL*	COL 39 X TOTAL*	COL 40 H +
-0.04000	0.00000	0.00000	0.00000	-12.89443	-15.61234	-5.00000	-9.50000
-0.03000	0.00000	0.00000	0.00000	-12.56111	-15.95043	-5.08461	-9.50000
-0.02000	0.00000	0.00000	0.00000	-12.22629	-16.28852	-5.25365	-9.50000
-0.01000	0.00000	0.00000	0.00000	-11.89042	-16.62660	-5.42269	-9.50000
0.00000	0.00000	0.00000	0.00000	-11.55385	-16.96469	-5.59174	-9.50000
0.01000	0.00000	0.00000	0.00000	-11.21679	-17.30278	-5.76078	-9.50000
0.02000	0.00000	0.00000	0.00000	-10.87940	-17.64087	-5.92983	-9.50000
0.03000	0.00000	0.00000	0.00000	-10.54179	-17.97896	-6.09887	-9.50000
0.04000	0.00000	0.00000	0.00000	-10.20402	-18.31704	-6.26791	-9.50000
0.05000	0.00000	0.00000	0.00000	-9.86615	-18.65513	-6.43696	-9.50000
0.06000	0.00000	0.00000	0.00000	-9.52821	-18.99322	-6.60600	-9.50000
0.07000	0.00000	0.00000	0.00000	-9.19022	-19.33131	-6.77505	-9.50000
0.08000	0.00000	0.00000	0.00000	-8.85220	-19.66940	-6.94409	-9.50000
0.09000	0.00000	0.00000	0.00000	-8.51416	-20.00748	-7.11313	-9.50000
0.10000	0.00000	0.00000	0.00000	-8.17610	-20.34557	-7.28218	-9.50000
0.11000	0.00000	0.00000	0.00000	-7.83804	-20.68366	-7.45122	-9.50000
0.12000	0.00000	0.00000	0.00000	-7.49996	-21.02175	-7.62027	-9.50000
0.13000	0.00000	0.00000	0.00000	-7.16188	-21.35984	-7.78931	-9.50000
0.14000	0.00000	0.00000	0.00000	-6.82380	-21.69792	-7.95835	-9.50000
0.15000	0.00000	-2.38513	0.00000	-6.59317	-21.82864	-8.01995	-9.50000
0.16000	0.00000	-2.38513	0.00000	-6.59317	-21.51422	-7.85090	-9.50000
0.17000	0.00000	-2.38513	0.00000	-6.59317	-21.19979	-7.68185	-9.50000
0.18000	0.00000	-1.99914	0.00000	-6.59317	-20.89290	-7.51277	-9.50000
0.19000	0.00000	-1.99914	0.00000	-6.59317	-20.61228	-7.34363	-9.50000
0.20000	0.00000	-1.71086	0.00000	-6.59317	-20.36386	-7.17428	-9.50000
0.21000	0.00000	-1.43688	0.00000	-6.59318	-20.17446	-7.00425	-9.50000
0.22000	0.00000	-1.43688	0.00000	-6.59318	-20.04431	-6.83203	-9.50000
0.23000	0.00000	-1.22922	0.00000	-6.59318	-19.97215	-6.65294	-9.50000
0.24000	0.00000	-1.22922	0.00000	-6.59318	-19.74824	-6.45308	-9.50000
0.25000	-1.22915	-0.92814	0.00000	-6.59318	-19.11878	-6.30729	-9.50000
0.26000	-1.22915	-0.92814	0.00000	-6.59318	-19.45687	-6.20534	-9.50000
0.27000	-1.22915	-0.92814	0.00000	-6.59318	-19.79496	-6.04227	-9.50000
0.28000	-1.22915	-0.92813	0.00000	-6.59318	-20.13304	-5.81647	-9.50000
0.29000	-1.22915	-0.92813	0.00000	-6.59318	-20.47113	-5.54161	-9.50000
0.30000	-1.22915	-0.92813	0.00000	-6.59318	-20.80922	-5.23594	-9.50000
0.31000	-1.22915	-0.92812	0.00000	-6.59318	-21.14731	-5.00000	-9.50000